UNIVERSITY OF SOUTHAMPTON

FACULTY OF SOCIAL, HUMAN AND MATHEMATICAL SCIENCES

Mathematical Sciences

Applications of Holography and Entanglement

by

William Robert Woodhead

Thesis for the degree of Doctor of Philosophy

April 2017

UNIVERSITY OF SOUTHAMPTON

ABSTRACT

FACULTY OF SOCIAL, HUMAN AND MATHEMATICAL SCIENCES

Mathematical Sciences

Thesis for the degree of Doctor of Philosophy

APPLICATIONS OF HOLOGRAPHY AND ENTANGLEMENT

by William Robert Woodhead

In this thesis we will investigate a number of topics on the applications of the gauge-gravity duality to topics in condensed matter physics and quantum entanglement. This duality is a conjectured equivalence between type IIB string theory on asymptotically anti-de Sitter backgrounds with certain quantum field theories in one dimension less. Using this conjecture we can model strongly-coupled quantum systems using classical gravity duals which provide novel methods for calculating otherwise computationally inaccessible quantum properties. We will use this for the following applications:

- We study a novel method for introducing broken translational symmetry into a holographic model whilst retaining homogeneity in the field equations. We demonstrate that this leads to a finite DC conductivity and shows features of heavy fermion models in the AC conductivity.
- We explore the nature of real time scalar correlators in holographic models of critical systems that possess a non-relativistic scaling symmetry. Specifically we explore systems with dual Schrödinger or Lifshitz scaling symmetries, and discuss the problems that arise when trying to apply the standard framework of real time holography to these systems.
- We provide an explicit counterexample to the holographic F-theorem, and an analytic argument that shows that this violation is not specific to the model in consideration but is rather a more general property of a class of holographic systems.
- Finally we introduce a holographic renormalization scheme for the entanglement entropy based on the standard framework of holographic renormalization. We connect this to the field theory via the replica trick and use it to calculate a number of explicit examples both analytically and numerically.

Table of Contents

List of Figures

Declaration of Authorship

I, William Robert Woodhead, declare that the thesis entitled *Applications of Holography and Entanglement* and the work presented in the thesis are both my own, and have been generated by me as the result of my own original research. I confirm that:

- this work was done wholly or mainly while in candidature for a research degree at this University;
- where any part of this thesis has previously been submitted for a degree or any other qualification at this University or any other institution, this has been clearly stated;
- where I have consulted the published work of others, this is always clearly attributed;
- where I have quoted form the work of others, the source is always given. With the exception of such quotations, this thesis is entirely my own work;
- I have acknowledged all main sources of help;
- where the thesis is based on work done by myself jointly with others, I have made clear exactly what was done by others and what I have contributed myself;
- parts of this work have been published as:
  - M. Taylor and W. Woodhead, *Inhomogeneity simplified*, *The European Physical Journal C* **C74** (June, 2014) 3176, [1406.4870]
  - M. Taylor and W. Woodhead, *Renormalized entanglement entropy*, *Journal of High Energy Physics* **2016** (Aug., 2016) , [1604.06808]
  - M. Taylor and W. Woodhead, *The holographic F theorem*, 1604.06809

Signed: .....

Date: .....

Acknowledgements

Firstly I would like to thank my supervisor Marika Taylor for all her help over the course of my studies at Southampton. Thank you for all your patience, insight, effort, and guidance throughout my time here.

I also want to recognise the helpful discussions and support I have received from my officemates Ariana Stylianidi-Christodoulou, Stanislav Schmidt, and Joan Garcia i Tormo. This work was made possible through PhD studentship funding provided by the STFC.

Thank you to all the friends and colleagues I have had at the University of Southampton, there are far too many of you to list but special mentions must be made for John, Tim, Stu, Ariana, Stephanie, Christian, Vanessa, Greg, Kiki, Peter, Alice, Will, Charlie, Emma, Ramon, and Stefanos. You have all had to put up with far too many of my idiosyncarsies and ramblings than is fair.

I owe a great deal of thanks to the many friends that I have made in the London Gaymers especially to Rhys, Gareth, JB, Michael, Pompeo, Evan, and Jackie who have been fundamental in supporting me during my final year in Southampton.

Without all the new friends I have made recently in the Wessex Wyverns I would not be as healthy, happy, or sane as I am today. You have helped me enjoy a sport for the first time in my life, and made Southampton feel more like a home rather than just a campus.

Finally I would like to thank my family for their love and support, especially over the past eight years of my never ending studies. Without you I would not have made it this far.

CHAPTER 1

Introduction

1.1 Holography and the gauge-gravity duality

One of the most remarkable ideas to come out of modern theoretical physics in recent years is that of the *holographic principle*, which states that the number of possible states of a region of space is the same as that of a system of binary degrees of freedom distributed on the boundary of that region, and the number of such degrees of freedom is bounded by the area of the region in Planck units. The first such indications of this principle arose from the insights of Bekenstein [4] and Hawking [5] that black holes in general relativity are inherently thermodynamic objects to which one can prescribe an entropy:

$$S_{BH} = \frac{kc^3 A}{4\hbar G_N} \tag{1.1.1}$$

where A is the area of the event horizon, G_N is the Newton constant, c is the speed of light, $\hbar$ is the reduced Planck constant, and k is the Boltzmann constant. Note that we will work exclusively in units where $c = \hbar = k = 1$ throughout this thesis.

The surprising result here is that the entropy of the black hole is not proportional to its volume, as would be expected for an extensive property such as the entropy, but rather to its surface area. This seems to suggest that all the information contained in a $d+1$-dimensional gravitational theory can be equivalently described by a d-dimensional theory though of as "living" on some boundary of the spacetime like the event horizon.

This idea was further developed by 't Hooft [6] and Susskind [7] into the holographic principle.

The first direct realisation of the holographic principle came from Maldacena [8] in the form of a conjectured equivalence between seemingly unrelated theories, string theory on anti-de Sitter (AdS) backgrounds and a super Yang-Mills (SYM) theory, often called the *AdS/CFT correspondence* or the *gauge-gravity duality*. In its original formulation, the Maldacena conjecture claimed that $\mathcal{N} = 4$ SYM in 4-dimensions with gauge group $SU(N)$ is completely equivalent, or *dual*, to 10-dimensional type IIB superstring theory on an $AdS_5 \times S^5$ background where the parameters of the two theories are related in such a way that only the rank of the gauge group N and the string coupling constant g_s are left unfixed. In this formulation the superstring theory is referred to as the *bulk* theory and the SYM theory is referred to as the *dual* or *boundary* theory.

In the strongest form of the conjecture, these two theories are equivalent for general N and coupling constant g_s and the duality is at the level of the generating functionals for the two theories. A precise mapping between the states, operators, and global symmetries of the two theories has been well established in the so-called *holographic dictionary* which we will review later.

There exists two limits that can be taken that weaken the conjecture enough to make it more analytically tractable while still ensuring that the duality is non-trivial. The first such limit is the 't Hooft limit where $N \to \infty$ while keeping $\lambda = g_{YM}^2 N$ finite. In this form the bulk theory is classical string theory in a string loop expansion and the boundary theory is SYM in a large N expansion.

After taking this limit the only remaining free parameter is the 't Hooft coupling. On the boundary side the $\lambda \ll 1$ limit corresponds to a weakly coupled large N theory where standard quantum field theory perturbation theory applies. On the bulk side however it is more natural to take the $\lambda \gg 1$ which corresponds to the classical supergravity limit of string theory and the boundary side is strongly coupled. From this result we learn that the AdS/CFT correspondence is surprising not only by its very existence, but also by the fact that in this limit it allows us to learn about properties of a strongly coupled quantum field theory by working with a classical theory of supergravity.

Moreover, the Maldacena conjecture is not limited to this one compactification of string theory. A number of different compactifications over compact manifolds can be taken which result in a range of different holographic QFTs. Note that the compact manifold cannot be chosen arbitrarily. From this conjecture we can construct classical gravity theories that provide an analytic framework for understanding the physics of strongly coupled field theories.

1.2 Holographic dictionary

A consistent truncation of 10-dimensional supergravity compactified on a sphere gives holographic models known as *top-down* models. Much more is known about the dual theory in such cases, and the bulk gravitational theory is guaranteed to have a UV completion. Having such a truncation allows us to answer precise questions about the detailed dynamics of the dual theory. Once we have a basic understanding of the precise relations between bulk and boundary quantities we can then construct simplified models that we hope captures the universal results of the dynamics in question. Such models are called *bottom-up* models and are useful in gaining conceptual insights into strongly coupled physics. To construct such models we need to know some details of the holographic dictionary, which we will now review [9, 10].

The most fundamental building block of any bottom-up model of a d-dimensional dual theory is a $d+1$-dimensional gravitational theory on some manifold $\mathcal{M}$ with boundary $\partial\mathcal{M}$ and a negative cosmological constant:

$$S = \frac{1}{16\pi G_N}\int_{\mathcal{M}} \mathrm{d}^{d+1}x\,\sqrt{-g}\left(R + \frac{d(d-1)}{L^2}\right) + \frac{1}{8\pi G_N}\int_{\partial\mathcal{M}} \mathrm{d}^{d}x\,\sqrt{-h}K \tag{1.2.1}$$

where G_N is the $d+1$-dimensional Newton constant which is guaranteed to be small in the large λ limit as $G_N \sim N^{-2}$, $g_{\mu\nu}$ is the bulk metric, R is the Ricci scalar of g, L is some length scale usually called the *AdS radius*, and the boundary term is the Gibbons-Hawking-York term [11, 12] where K is the trace of the extrinsic curvature. This is always a consistent truncation of the 10-dimensional supergravity theory and is sufficient for understanding properties of the boundary stress tensor T_{ab} which is closed under the OPE. The bulk geometry is then dual to the boundary quantum state, with the conformal vacuum being represented by the vacuum anti-de Sitter AdS_{d+1}:

$$\mathrm{d}s^2 = \frac{L^2}{z^2}(\mathrm{d}z^2 - \mathrm{d}t^2 + \mathrm{d}\vec{x}^2) \tag{1.2.2}$$

where $(t, \vec{x})$ are the boundary $\mathbb{R}^{1,d-1}$ coordinates, and z is the new *holographic coordinate* with $z = 0$ representing the conformal boundary[1] [13].

The AdS geometry (1.2.2) possesses a clear scaling isometry:

$$z \to \lambda z, \qquad t \to \lambda t, \qquad \vec{x} \to \lambda\vec{x} \tag{1.2.3}$$

which encapsulates one of the most important aspects of the duality: the *renormalization group (RG) flow* of the dual theory is encapsulated in the geometry of the bulk

[1] This is not entirely correct as the $z \to 0$ limit does not yield the full conformal boundary. However this technical detail will not have any relevance to our discussion.

theory. This can be seen in the following way: consider a physical process with *proper* energy E_{loc} at some value of z in the bulk. This is measured in units of the local proper time $\mathrm{d}\tau = \frac{L}{z}\mathrm{d}t$ and so when viewed in terms of the boundary time t it corresponds to an excitation of energy

$$E = \frac{L}{z}E_{loc}. \tag{1.2.4}$$

Therefore physical processes in the bulk with identical proper energies but occurring at different holographic positions correspond to different field theory processes with energies that scale as $1/z$. This implies that z can be identified with as the RG scale of the boundary theory. The $z \to 0$ limit then corresponds to $E \to \infty$ which is the high-energy ultraviolet (UV) limit, and $z \to \infty$ is the low energy $E \to 0$ infrared (IR) region.

Away from the conformal vacuum we do not expect there to be excitations of arbitrarily small energies, this could be due to some effective IR cutoff such as a temperature, a conserved charge, or some mass gap. In all of these cases the dual geometry will not extend all the way to $z \to \infty$ but will instead have some sort of bulk cutoff either from an event horizon or from a smooth end to the geometry. Such states will not be dual to vacuum AdS but some more complicated geometry that preserves the UV properties of the CFTT·he negative cosmological constant ensures that any such geometry is asymptotically locally AdS, i.e. it admits a timelike conformal boundary. Such a constraint ensures that we can perform a *Fefferman-Graham* (FG) expansion of the bulk metric and all other bulk fields, which is a generalised power series expansion in terms of some holographic coordinate. Formally, the results of Fefferman and Graham [14, 15] imply that there always exists a coordinate chart near the conformal boundary such that:

$$\mathrm{d}s^2 = \frac{\mathrm{d}\rho^2}{4\rho^2} + \frac{1}{\rho}g_{\mu\nu}(\rho, x)\,\mathrm{d}x^\mu \mathrm{d}x^\nu \tag{1.2.5}$$

$$g(\rho, x) = g_{(0)} + \rho^2\, g_{(2)} + \cdots + \begin{cases} \rho^{(d-1)/2}\, g_{((d-1)/2)} + \cdots & \text{odd } d \\ \rho^{d/2}\,(g_{(d/2)} + \log\rho\, h_{(d/2)}) + \cdots & \text{even } d \end{cases} \tag{1.2.6}$$

where x^i is some coordinate chart on $\partial\mathcal{M}$ and ρ is the holographic coordinate with $\rho \to 0$ corresponding to the conformal boundary. The bulk field equations will always determine the coefficients $g_{(2)}, \ldots, g_{((d-2)/2)}, h_{(d/2)}$ and the trace and covariant derivative of $g_{(d/2)}$ *analytically* in terms of $g_{(0)}$. Hence the only free coefficients in the expansion are $g_{(0)}$ and either $g_{((d-1)/2)}$ or $g_{(d/2)}$ depending on whether d is odd or even. These remaining coefficients cannot be determined by a near boundary expansion of the field equations and must be found by other means. These coefficients are precisely the ones that are identified with field theory data: namely $g_{(0)}$ is interpreted as the field theory (non-dynamical) metric and $g_{(d/2)}$ (or equivalently $g_{((d-1)/2)}$) is directly related to the 1-point function of the dual stress energy tensor $\langle T_{\mu\nu}\rangle$.

Next we need to understand how boundary operators are mapped into the bulk. The

operators of interest in holographic models are the chiral conformal primary operators since these operators and their descendents are the lightest operators in the large λ large N limit and are thus the easiest to access. For each such conformal primary there is a massive field in the bulk with the same spin statistics. Consider for example a scalar operator $\mathcal{O}$, this is dual to a massive scalar field ϕ in the bulk whose action can be written as

$$S = -\frac{1}{2}\int_{\mathcal{M}} \mathrm{d}^{d+1}x\ \sqrt{-g}((\partial\phi)^2 + m^2\phi^2 + \cdots) \tag{1.2.7}$$

where the ellipses denote interaction terms. The field equations for this scalar field admit a FG expansion of the form

$$\phi(\rho, x) = \rho^{\Delta_-/2}\phi_{(0)}(x) + \cdots + \rho^{\Delta_+/2}\phi_{(\nu)}(x) + \cdots \tag{1.2.8}$$

where

$$\Delta_\pm = \frac{d}{2} \pm \nu, \qquad \nu = \frac{1}{2}\sqrt{d^2 + 4m^2L^2}. \tag{1.2.9}$$

The coefficient of the non-normalizable mode is then the source for the dual operator $\mathcal{O}$ and the normalizable mode is dual to the 1-point function $\langle\mathcal{O}\rangle$ in a way that we will make precise shortly. Note that reality of ν implies that we can have stable scalar fields in AdS_{d+1} with $m^2 < 0$ provided that the so-called Breitenlohner-Freedman (BF) bound is satisfied

$$m^2 \geq m^2_{BF} = -\frac{d^2}{4L^2} \tag{1.2.10}$$

The precise interpretation of which is the normalizable and non-normalizable mode depends on the value of ν, which leads to the concept of standard and alternate quantizations. The standard quantization is done by imposing Dirichlet boundary conditions on ϕ and is possible for all values of ν. In this case Δ_+ is the conformal dimension of $\mathcal{O}$, $\phi_{(0)}$ is the source for $\mathcal{O}$, and $\phi_{(\nu)}$ is related to $\langle\mathcal{O}\rangle$. The alternative quantization is available when $0 < \nu < 1$ and corresponds to imposing Neumann boundary conditions on ϕ, under which Δ_- is the conformal dimension, $\phi_{(\nu)}$ is the source and $\phi_{(0)}$ is related to the 1-point function. In this way, the same bulk solution can be dual to two different theories depending on the boundary conditions. The two theories are related by taking the Laplace transform of their respective generating functionals with respect to the operator sources[16, 17, 18].

Finally, in this thesis we will also be interested in the behaviour of boundary theories which possess a global symmetry under some matrix group such as $U(1)$. Such a global symmetry of the boundary theory is promoted to a *gauge* symmetry in the bulk theory, with the bulk gauge A_M field being dual to the conserved current J^μ. Boundary operators that are charged under this global symmetry are dual to bulk fields charged under

the gauge symmetry. The bulk action contains the standard terms for a gauge field:

$$S = -\frac{1}{4}\int_{\mathcal{M}} \mathrm{d}^{d+1}x\ \sqrt{-g}(F_{MN}F^{MN} + \cdots) \tag{1.2.11}$$

where $F = \mathrm{d}A$ is the gauge field strength tensor and the ellipses denote interactions and gauge couplings. We can once again perform a FG expansion of the gauge field A_M, note that since the FG expansion is effectively a pull back of the bulk fields onto the boundary there is no A_ρ component:

$$A_\mu = A_{(0)\mu} + \cdots + \rho^{(d-2)/2}A_{(d-2)\mu} + \cdots \tag{1.2.12}$$

where $A_{(0)\mu}$ is the source for the conserved current J^μ, and $A_{(d-2)\mu}$ is related to the 1-point function. At thermal equilibrium one can interpret $A_{(0)t}$ as the chemical potential for the dual theory.

Typically it is not enough to fully solve the bulk matter field equations based solely on Dirichlet or Neumann conditions on the conformal boundary. These must be supplemented with an additional boundary condition, which is usually in the form of a regularity condition in the deep interior of the geometry or on the horizon to ensure that the theory is well defined in the IR.

Using such boundary conditions the only free parameters in the bulk solutions are the source terms for the bulk fields and as such the on-shell gravitational action is a functional of these fields. By taking the large N and large 't Hooft coupling limits, the on-shell action is dual to the generating functional of connected graphs [19, 13]:

$$S_{on-shell}[\hat{g}_{(0)}, \phi_{(0)}, \ldots] = -W[\hat{g}_{(0)}, \phi_{(0)}, \ldots] \tag{1.2.13}$$

from which we can find the n-point functions using functional differentiation:

$$\begin{aligned}
\langle \mathcal{O}(x)\rangle &= \left.\frac{\delta S_{on-shell}}{\delta\phi_{(0)}(x)}\right|_{\phi_{(0)}=0} \\
\langle \mathcal{O}(x_1)\mathcal{O}(x_2)\rangle &= -\left.\frac{\delta^2 S_{on-shell}}{\delta\phi_{(0)}(x_1)\delta\phi_{(0)}(x_2)}\right|_{\phi_{(0)}=0} \\
\langle \mathcal{O}(x_1)\cdots\mathcal{O}(x_n)\rangle &= (-1)^{n+1}\left.\frac{\delta^n S_{on-shell}}{\delta\phi_{(0)}(x_1)\cdots\delta\phi_{(0)}(x_n)}\right|_{\phi_{(0)}=0}.
\end{aligned} \tag{1.2.14}$$

1.2.1 Holography in real time

The above discussion was implicitly in Euclidean signature, i.e. where the metric is positive definite which corresponds to taking the Wick rotation of the boundary theory. This

is often sufficient for practical applications as one can obtain real time correlators from their Euclidean counterparts by performing an analytic continuation. However there are situations where performing this continuation is technically difficult even though it is possible such as in the case of the thermal correlator or in states with non-trivial time dependence. On a more fundamental level the analytic continuation obscures the relation between the bulk and boundary dynamics, and the encoding of boundary causality by the bulk which manifests itself as the $i\epsilon$ insertions into correlators.

In the bulk geometry this change of signature poses a number of technical challenges. For example the bulk field equations change from elliptic equations to hyperbolic equations and so we must also consider initial conditions for the fields. Additionally there is the possibility that horizons can form in the bulk geometry which affects the types of regularity conditions that are possible. A purely holographic prescription for computing real time physics has been developed [20, 21, 22] which will be of importance to us in Chapter 3. The application of these results will be self contained to this chapter and so will not be discussed further here. An overview of real time QFT computations and the holographic prescription is presented in 3.2, with a more detailed review of the prescription available in [21].

1.3 Holographic renormalization

There is a a problem with the results of equation (1.2.13) in that both sides are plagued by divergences: on the gravitational side there are divergences arising from the infinite volume of the bulk geometry, and on the boundary side there are UV divergences of field theory. If we wish to make sense of equations (1.2.13) and (1.2.14) we must renormalize. Note that since the bulk geometry encodes the RG flow of the dual theory, these UV divergences of the boundary can be identified with the infinite volume divergences of the bulk.

A precise framework for performing renormalization holographically in terms of purely gravitational data has been developed [15, 23, 24, 25] called *holographic renormalization* which we now review. Holographic renormalization can be broken down into a three stage process:

1. Obtain general asymptotic solutions

2. Regularisation of on-shell action

3. Construct covariant counterterms

after which we can obtain renormalized n-point functions. We will outline these stages

and then give a concrete example in the form of a free massive scalar field in vacuum AdS_{d+1}, following closely the review of [25]. Note that more efficient methods of holographic renormalization exist however the method we will now review is the one that we will use in numerous places throughout the thesis.

1.3.1 Outline of the method

The first step in the holographic renormalization method is to obtain the most general solutions to the bulk field equations with given, but arbitrary, Dirichlet boundary conditions. Since the bulk geometry is asymptotically AdS then any such solution can be written as a FG expansion:

$$\begin{aligned} \mathrm{d}s^2 &= \frac{\mathrm{d}\rho^2}{4\rho^2} + \frac{1}{\rho} g_{\mu\nu}(\rho, x)\mathrm{d}x^\mu \mathrm{d}x^\nu \\ g(\rho, x) &= g_{(0)}(x) + \rho\, g_{(2)}(x) + \cdots \\ f(\rho, x) &= \rho^m f_{(0)} + \cdots + \rho^n (f_{(2(n-m))} + \log\rho\, \tilde{f}_{(2(n-m))}) + \cdots \end{aligned} \tag{1.3.1}$$

where f is some bulk matter field with spacetime and internal indices being suppressed. Note that the logarithmic term is only present if $n - m \in \mathbb{N}$. As discussed above the bulk field equations specify the sub-leading terms of the expansion, including the logarithmic coefficient in terms of $f_{(0)}$ but leave $f_{(2(n-m))}$ unspecified, which is to be expected as we have only specified one Dirichlet boundary condition on these solutions.

Once we have found such general asymptotic solutions for the bulk fields we can proceed to obtain the regularised on-shell action. We perform this regularisation by cutting off the holographic coordinate ρ such that $\rho \geq \epsilon$ where ϵ is some small cutoff parameter. This in effect transforms the bulk manifold $\mathcal{M}$ with conformal boundary $\partial\mathcal{M}$ to a regulated manifold $\mathcal{M}_\epsilon$ with boundary $\partial\mathcal{M}_\epsilon$. We can then evaluate the bulk action on this regulated manifold, and any boundary terms on the regulated boundary. Using the FG expansions the ρ integral can be performed explicitly:

$$S_{reg}[f_{(0)}; \epsilon] = \int_{\partial\mathcal{M}_\epsilon} \mathrm{d}^d x \sqrt{-g_{(0)}} [\epsilon^{-\nu} a_{(0)} + \epsilon^{1-\nu} a_{(2)} + \cdots + \log\epsilon\, a_{(2\nu)}] + O(\epsilon^0) \tag{1.3.2}$$

where ν is a positive number that only depends on the scaling dimensions of the dual operators, and the $a_{(k)}$ are local functions of the sources. The divergences do not depend on the unknown coefficient $f_{(2(n-m))}$, i.e. the terms that are not determined by the near boundary analysis.

The final step in the holographic renormalization method is to re-express these divergent terms as *covariant* quantities defined on the regulated boundary $\partial\mathcal{M}_\epsilon$, the induced metric there $\gamma_{\mu\nu} = g_{\mu\nu}(x, \epsilon)/\epsilon$, and the pull back of the bulk matter fields onto the bound-

ary. The requirement that these terms be covariant quantities is necessary to retain general co-variance in the renormalized theory. To actually find this re-expression one must invert the series expansions (1.3.1) to obtain $f_{(0)} = f_{(0)}(f(x,\epsilon),\epsilon)$ and consequentially $a_{(2k)}(f_{(0)}(x)) = a_{(2k)}(f(x,\epsilon),\epsilon)$ which can then be inserted back into (1.3.2). The counterterms action is then defined to be

$$S_{ct}[f(x,\epsilon);\epsilon] = -\text{divergent terms of } S_{reg}[f_{(0)};\epsilon] \tag{1.3.3}$$

from which we can define the subtracted S_{sub} and renormalized S_{ren} on-shell actions as

$$S_{sub}[f(x,\epsilon);\epsilon] = S_{reg}[f_{(0)};\epsilon] + S_{ct}[f(x,\epsilon);\epsilon] \tag{1.3.4}$$

$$S_{ren}[f_{(0)}] = \lim_{\epsilon\to 0} S_{sub}[f;\epsilon]. \tag{1.3.5}$$

With the subtracted and renormalized on-shell actions found, the renormalized 1-point functions can be found:

$$\langle \mathcal{O}(x)\rangle_s = \frac{1}{\sqrt{-g_{(0)}}}\frac{\delta S_{ren}}{\delta f_{(0)}(x)} = \lim_{\epsilon\to 0}\left(\frac{1}{\epsilon^{d/2-m}}\frac{1}{\sqrt{\gamma}}\frac{\delta S_{sub}}{\delta f(x,\epsilon)}\right) \tag{1.3.6}$$

where the s denotes the presence of sources, which is finite in the $\epsilon \to 0$ limit by construction. Explicit computation of this limit can be performed:

$$\langle \mathcal{O}(x)\rangle_s \sim f_{(2(n-m))} + C(f_{(0)}, \tilde{f}_{(2(n-m))}, g_{(m)}) \tag{1.3.7}$$

where C is a theory and scheme dependent function that depends locally on the sources. Similarly the coefficient in front of $f_{(2(n-m))}$ is theory dependent, but not scheme dependent. Once the renormalized 1-point functions have been found, higher point functions can be found via functional differentiation.

The scheme dependence of this renormalization method is captured by the ability to add finite counterterms to the counterterms action $S_{ct}[f(x,\epsilon);\epsilon]$. Such a counterterm is any analytic covariant counterterm defined on $\partial\mathcal{M}_\epsilon$ that is in and of itself finite and non-zero in the $\epsilon \to 0$ limit. If any such term can be constructed then it is a possible finite counterterms and must be considered in the scheme dependence of the result. Note that it is not always possible to construct such terms, in which case the resulting correlators are scheme independent.

1.3.2 Massive scalar

To illustrate the method described above we now consider the case of a probe massive free scalar ϕ in Euclidean AdS_{d+1}. The action for the scalar field is given by

$$S = \frac{1}{2}\int \mathrm{d}^{d+1}x\ \sqrt{g}((\partial\phi)^2 + m^2\phi^2) \tag{1.3.8}$$

where the bulk metric is

$$\mathrm{d}s^2 = g_{MN}\mathrm{d}x^M\mathrm{d}x^N = \frac{\mathrm{d}\rho^2}{4\rho^2} + \frac{1}{\rho}\mathrm{d}x^\mu\mathrm{d}x^\nu \tag{1.3.9}$$

and the Klein-Gordon equation is

$$\nabla^2\phi - m^2\phi = \frac{1}{\sqrt{g}}\partial_M(\sqrt{g}g^{MN}\partial_N\phi) - m^2\phi = 0 \tag{1.3.10}$$

which has an asymptotic solution of the form:

$$\phi(\rho, x) = \rho^{(d-\Delta)/2}\phi_{(0)} + \rho^{1+(d-\Delta)/2}\phi_{(2)} + \cdots + \rho^{\Delta/2}(\phi_{(2n)} + \psi_{(2n)}\log\rho) + \cdots \tag{1.3.11}$$

where $m^2 = \Delta(\Delta - d)$ and for simplicity we have assumed $\Delta = d/2 + n$ for some positive integer n. The sub-leading coefficients can be found algebraically:

$$\begin{aligned}\phi_{(2k)} &= \frac{1}{2(2\Delta - d - 2k)}\Box_0\phi_{(2(k-1))} \\ \psi_{(2n)} &= -\frac{1}{2^{2n}\Gamma(n)\Gamma(n+1)}(\Box_0)^k\phi_{(0)}\end{aligned} \tag{1.3.12}$$

where $\Box_0$ is the flat space D'Alembertian. Note that the sub-leading coefficients are determined analytically in terms of the boundary data as promised.

The regularised on-shell action can be computed:

$$\begin{aligned}S_{reg} &= -\frac{1}{2}\int_{\rho=\epsilon}\mathrm{d}^d x g^{\rho\rho}\phi\partial_\rho\phi \\ &= \int_{\rho=\epsilon}\mathrm{d}^d x(\epsilon^{-\Delta+\frac{d}{2}}a_{(0)} + \epsilon^{-\Delta+\frac{d}{2}+1}a_{(2)} + \cdots - \log\epsilon\ a_{(2\Delta-d)} + O(\epsilon^0))\end{aligned} \tag{1.3.13}$$

where

$$\begin{aligned}a_{(0)} &= -\frac{1}{2}(d-\Delta)\phi_{(0)}^2 \\ a_{(2)} &= -\frac{d-\Delta+1}{2(2\Delta-d-2)}\phi_{(0)}\Box_0\phi_{(0)} \\ a_{(2\Delta-d)} &= -\frac{d}{2^{2n}\Gamma(n)\Gamma(n+1)}(\Box_0)^n\phi_{(0)}.\end{aligned} \tag{1.3.14}$$

From this the subtracted and renormalized actions can be found and correlation functions can be found:

$$\langle \mathcal{O} \rangle_s = -(2\Delta - d)\phi_{(2\Delta-d)} + C(\phi_{(0)}, \psi_{(2n)}, g_{(n)}) \tag{1.3.15}$$

Note that the first term is the part of the asymptotic solution not determined by the near-boundary analysis, and the second term is a local function of the source $\phi_{(0)}$. Moreover this second term is scheme dependent and can be modified, or indeed removed in some cases, through the addition of appropriate finite counterterms. For example in the case of $n = 1$ a finite counterterms can be constructed:

$$S_{ct,fin} = \frac{1}{2}\int_{\partial\mathcal{M}_\epsilon} \mathrm{d}^d x\ \phi_{(0)}\Box_0\phi_{(0)} = \int_{\partial\mathcal{M}_\epsilon} \mathrm{d}^d x\ \sqrt{\gamma}\mathcal{A} \tag{1.3.16}$$

where $\mathcal{A}$ is the matter conformal anomaly, the anomalous variation of the action under a Weyl transformation.

1.4 Limitations and universality of holographic modelling

Now that we have reviewed the holographic dictionary and discussed how to obtain renormalized quantities we are in a position to start constructing holographic models of strongly coupled systems. Before doing so however we must discuss what kinds of systems we might be able to model holographically and what kind of questions we should hope to be able to answer.

It should come as no surprise that systems with a classical gravity description are not generic strongly coupled theories. Heuristically we can count the degrees of freedom holographically and compare it to the dual theory [9]. The holographic principle says that the maximum entropy of a state of a system with an Einstein gravity dual is the area of the boundary in Planck units. Considering AdS_{d+1} at fixed time with a UV cutoff $z > \epsilon$ and an IR cutoff $x \sim x + L$ the area of the boundary is

$$A = \left(\frac{L\ L_{AdS}}{\epsilon}\right)^{d-1}. \tag{1.4.1}$$

Comparing this to counting degrees of freedom in the boundary theory [9] we must identify

$$\frac{L_{AdS}^{d-1}}{G_N} = N^2 \tag{1.4.2}$$

from which we must conclude that the dual QFT has $N^2 \gg 1$ degrees of freedom per point. This result means that holographic models are not microscopically realistic models of any known materials or systems. Similarly the gauge-gravity duality in its most rigorous formulation is an equivalence between two theories which have a large number

of supersymmetries, whereas known physical systems do not have any supersymmetry.

With this in mind, our motivations for tackling problems with holography should not be to make contact with experiments rather they should be the more realistic goal of making contact with the phenomena of strongly coupled systems. Using holography to construct toy models we may hope to gain an understanding of the physics behind such phenomena and the general behaviour of strongly coupled systems.

Holography also promises a certain amount of universality to its results, that is the resulting physics is independent of the specific details of the theory in question. One example of this phenomenon is the calculation of the shear viscosity η in $\mathcal{N} = 4$ SYM in 4-dimensions. One can calculate this holographically by solving perturbations around the AdS_5 black brane metric to find

$$\frac{\eta}{s} = \frac{1}{4\pi} \tag{1.4.3}$$

where s is the entropy density [26, 27]. The holographic calculation of this result, which we will not cover here, is universal in the sense that it only relies on the pure gravity sector of the 5-dimensional bulk theory and arises from the universal properties of black hole horizons. The bulk matter content, nor the details of the 10-dimensional SUGRA completion were needed for this result. Moreover since the result depends only on the pure gravity sector, any holographic model with the same Einstein-Hilbert gravity sector and AdS asymptotics will have the same value for η/s. There is experimental evidence that the quark-gluon plasma created at RHIC has η/s close to this holographic value [28].

1.5 Applications

In this thesis we will explore various different topics that explore holography and its applications. These can be broadly categorised in three parts: holographic modelling of strongly coupled phases, holography with non-relativistic symmetries, and entanglement entropy. In this section we will review the background for these topics and the motivations for the corresponding chapters in the thesis. The subsequent chapters of this thesis can all be read independently of each other, except Chapter 6 which follows on directly from Chapter 5.

1.5.1 Holographic modelling of strongly coupled phases

Strongly coupled phases of matter exist across a whole range of temperatures and densities, from the quark-gluon plasma phase of QCD formed at the high temperature and density collisions inside the heavy ion colliders at the RHIC and the LHC, to ultra-cold metals at unitarity in condensed matter physics. For example there is a group of mate-

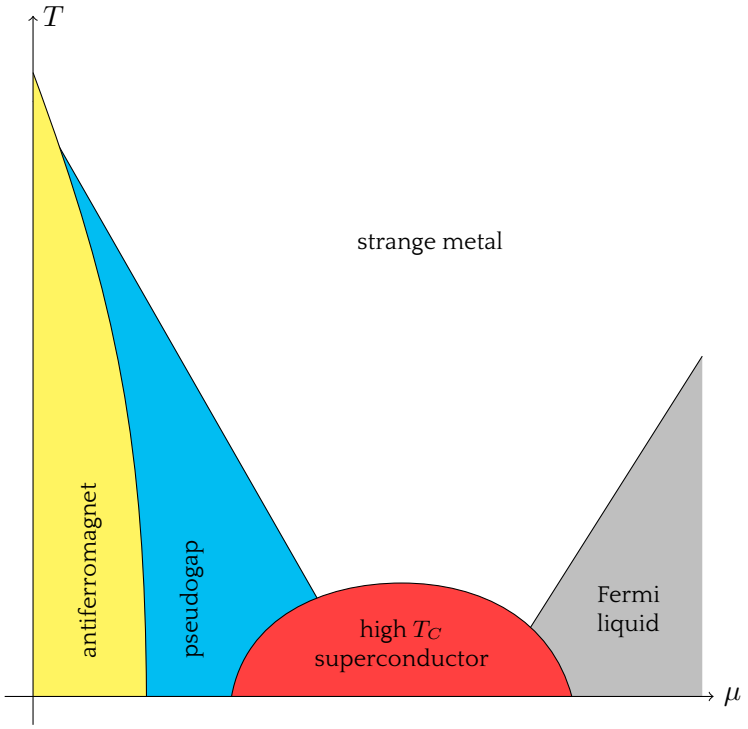

Figure 1.5.1: A sketch of the phase diagram of the cuprates.

rials called the *cuprates* which exhibit a very rich phase structure at low temperatures and doping, where they exhibit a superconducting phase, a strange metal phase, and a pseudo-gap phase as sketched in Figure 1.5.1 [29]. All of these phases have unique features that have so far escaped a satisfactory description in terms of conventional field theory, such as the high critical temperature T_C of the superconducting phase and the anomalous transport behaviour of the strange metal phase characterised most predominantly by a simple linear scaling of resistivity with temperature, and are thought to be the result of strongly coupled phenomena.

The weak coupling description of superconductivity is given by the BCS (Bardeen, Cooper, Schrieffer) model in which electron pairs with opposite spin interact with phonons to form charged bosonic *Cooper pair* quasi-particles which condense, i.e. they spontaneously acquire a non-zero expectation value, through a second order phase transition below the critical temperature. The BCS model does not accurately describe the behaviour seen in the cuprates however. There is evidence that electron pairs still form but the pairing mechanism is not understood [29] and potentially involves strong coupling phenomena.

We may thus hope to apply the gauge-gravity duality to understand the onset and properties of this new strongly coupled superconducting phase. A class of bottom-up holographic models have been constructed [30, 31, 32], the simplest of which is simply a charged massive complex scalar coupled to an Einstein-Maxwell theory with a nega-

tive cosmological constant. The standard solution to this system is an AdS-Reissner-Nördstrom black brane with zero scalar field. If the square mass of the scalar is sufficiently negative, but still above the BF bound, then the solution becomes unstable to spontaneous condensation of scalar hair as the black hole approaches extremality.

This is the simplest holographic model that could be written down to describe a dual superconductor[2] and it can be shown that it possesses a number of desirable features: it predicts that a charged scalar condensate forms below a critical temperature through a second order phase transition, and in this condensed phase the DC conductivity is infinite, and the optical conductivity develops a gap. The model can be extended to include non-trivial boundary magnetic fields without destroying the superconducting instability. Furthermore the London equation can be reproduced from the bulk dynamics, but the Meisner effect cannot be seen as the boundary Maxwell fields are non-dynamical. This system has spherical symmetry and so describes an s-wave superconductor, similarly holographic models of p-wave [33, 34, 35] and d-wave [36] superconductors can be found.

All of these models have a problem, however, as they all possess an infinite DC conductivity in their non-superconducting phases. This infinite DC conductivity is not superconductivity and is to be expected from the lack of momentum dissipation. Applying a constant electric field to a system will cause any charge carrying modes to accelerate uniformly producing an infinite DC conductivity unless these charge carriers can lose momentum. This is a symptom of the fact that we have neglected an important part of the physics in question, specifically we have ignored the fact that such phases occur in materials with explicitly broken translation invariance which can come from lattice effects and impurities.

On the gravitational side, the diffeomorphism Ward identity for an Einstein-Maxwell-scalar system is

$$\nabla^i \langle T_{ij} \rangle - \langle J^i \rangle F_{ij} + \langle \mathcal{O} \rangle \partial_j \phi = 0, \tag{1.5.1}$$

from which we can deduce that we can maintain energy conservation but break momentum conservation by introducing spatially dependent sources for the scalar field. Generically adding such sources will result in the bulk field equations being PDEs rather than ODEs which makes finding analytic solutions technically difficult if not impossible.

In Chapter 2 we will discuss the problem of broken translational invariance in greater detail and investigate a set of models with tuned matter field profiles such that the resulting system is homogeneous but anisotropic which allows one to retain ODEs whilst still having explicit symmetry breaking. We will then calculate the DC conductivity for the

[2]The dual phase is actually a superfluid as the boundary $U(1)$ is a global not gauge symmetry. For the systems of interest this $U(1)$ can be gauged without destroying the physics of interest

resulting models analytically, and the AC conductivity numerically confirming that the DC conductivity is indeed finite. We also see features similar to those of heavy fermion models in the AC conductivity.

1.5.2 Non-relativistic asymptotics

The formulation of the gauge-gravity duality given above describes a relationship between a relativistic boundary field theory and a gravitational theory in one higher spatial dimension. The requirement that the bulk geometry be asymptotically AdS means that the dual theory is relativistic in the sense that time and space scale in the same way under dilatations:

$$t \to \lambda t, \qquad \vec{x} \to \lambda \vec{x}. \tag{1.5.2}$$

The relationship between the bulk and boundary physics in such cases has been well studied in the past, the holographic dictionary for such systems is well established, and the results are applicable to a wide range of problems as we have discussed above.

There are a variety of condensed matter phases that are believed to be described by strongly interacting *non-relativistic* physics, such as fermions at unitarity and potentially an underlying quantum critical point in high T_C superconductors. Non-relativistic systems at criticality are characterised by their different treatment of time and space under dilatations, for example:

$$t \to \lambda^z t, \qquad \vec{x} \to \lambda \vec{x} \tag{1.5.3}$$

where z is called the *dynamical exponent* of the symmetry. It is natural to consider whether such systems can be studied holographically, not only to gain an understanding of the dual condensed matter phases, but also to gain insights into the general principles of holography. The bulk geometries which arise in the study of these non-relativistic symmetries still have a timelike conformal boundary like in standard asymptotically AdS systems, but this boundary is now singular as there is not a single conformal factor that compactifies both the timelike and spacelike metric components simultaneously. The geometries themselves have constant scalar curvature throughout but have infinite tidal forces in the deep interior. Understanding the differences that arise because of the nature of this boundary may perhaps lead to progress in open questions regarding holography for asymptotically flat and asymptotically de Sitter spacetimes

There are two non-relativistic symmetry groups of particular interest to us, namely the Lifshitz group $\mathrm{Lif}_D(z)$ and the Schrödinger group $\mathrm{Sch}_D(z)$ which we now review. To describe the Lifshitz group consider a theory with D spatial dimensions with coordinates x^i and a time coordinate t. The Lifshitz group is the symmetry group of the following

symmetries:

$$\begin{aligned} H: &\quad t \to t + a \\ P^i: &\quad x^i \to x^i + a^i \\ L^{ij}: &\quad x^i \to L^i{}_j x^j \\ \mathcal{D}_z: &\quad t \to \lambda^z t, \quad x^i \to \lambda x^i \end{aligned} \tag{1.5.4}$$

where $L^i{}_j \in SO(D)$, i.e. the group generated by temporal translation invariance, spatial translation invariance, rotations, and the Lifshitz scaling symmetry $\mathcal{D}_z$. The Lifshitz group is neither a subgroup nor a contraction of the conformal group and they do not admit Galilean boosts.

The Schrödinger group is most readily realised in a $D+2$-dimensional theory with D spatial dimensions x^i and two light-cone coordinates $x^\pm$ with the group being generated by the spatial translations P^i and rotations L^{ij} described above as well as the following additional symmetries:

$$\begin{aligned} H: &\quad x^+ \to x^+ + a \\ M: &\quad x^- \to x^- + a \\ C^i: &\quad x^i \to x^i - v^i x^+, \quad x^- \to x^- - v^i x^i \\ \mathcal{D}_z: &\quad x^i \to \lambda x^i, \quad x^+ \to \lambda^z x^+, \quad x^- \to \lambda^{2-z} x^- \end{aligned} \tag{1.5.5}$$

i.e. by light-cone translations H and M, Galilean boosts C^i, and dilatations $\mathcal{D}_z$. The Schrödinger group is a subgroup of the conformal group $SO(D+2,2)$ for any z. In the special case $z=2$ the Schrödinger group can be extended to include one of the special conformal symmetries:

$$K: \qquad x^i \to \frac{x^i}{1+kx^+}, \quad x^+ \to \frac{x^+}{1+kx^+}, \quad x^- \to \frac{x^- + \frac{1}{2}k\, x\cdot x}{1+kx^+} \tag{1.5.6}$$

where $x \cdot x = 2x^+x^- + x^i x^i$. In the more conventional realisation of the Schrödinger group in $D+1$ dimensions it corresponds to a centrally extended Galilean group generated by the symmetries (H, P^i, L^{ij}, C^i, M) where M is represented as the central extension: $[C^i, P^j] = M\delta^{ij}$. When trying to understand the behaviour of the Schrödinger group in the $D+2$ dimensional representation we should therefore consider x^+ as a time coordinate and view the light-cone momentum M of x^- as some mass parameter.

To apply holography to such systems we need a detailed understanding of the holographic dictionary, the generalisation of which to non-relativistic systems is very subtle and is still not completely understood. See [37, 38] for an in depth discussion of this topic for Lifshitz systems.

The most fundamental part of any holographic description of theories with such symmetries is the construction of spacetimes which realise the respective non-relativistic symmetry groups asymptotically. Such geometries exist for both the Schrödinger group and the Lifshitz group:

$$\begin{aligned} \mathrm{Sch}_D(z): &\qquad \mathrm{d}s^2 = -\frac{b^2 \mathrm{d}x^{+2}}{r^{2z}} + \frac{1}{r^2}(\mathrm{d}r^2 + \mathrm{d}x^i \mathrm{d}x_i + 2\mathrm{d}x^+ \mathrm{d}x^-) \\ \mathrm{Lif}_D(z): &\qquad \mathrm{d}s^2 = -\frac{\mathrm{d}t^2}{r^{2z}} + \frac{1}{r^2}(\mathrm{d}r^2 + \mathrm{d}x^i \mathrm{d}x_i), \end{aligned} \tag{1.5.7}$$

where the conformal boundary is located at $r \to 0$ which is now degenerate due to the non-relativistic scaling. Although these geometries may look regular as $r \to \infty$ they are actually singular due to divergent tidal forces which are present whenever $z \neq 1$. These geometries are manifestly invariant under their respective symmetry groups asymptotically and are also invariant globally under an extension of the dilatation symmetry:

$$\begin{aligned} \mathrm{Sch}_D(z): &\quad r \to \lambda r \quad x^i \to \lambda x^i \quad x^+ \to \lambda^z x^+ \quad x^- \to \lambda^{2-z} x^- \\ \mathrm{Lif}_D(z): &\quad r \to \lambda r \quad x^i \to \lambda x^i \quad t \to \lambda^z t. \end{aligned} \tag{1.5.8}$$

Note that when $b = 0$ the Schrödinger geometry becomes that of AdS_{D+3}. This is unsurprising as $\mathrm{Sch}_D(z)$ is a subgroup of $SO(D+2,2)$ and so the dual geometry can be obtained via a deformation of AdS_{D+3}, where b controls the strength of this deformation.

The simplest objects that we might wish to study holographically in such geometries are correlation functions. As in standard quantum field theory, almost all work on holographic correlation functions is done in Euclidean signature using Wick rotations with real time correlators being obtained through analytic continuation. In the geometries presented above the applicability of the Wick rotation is less clear due to the non-relativistic scaling symmetry, indeed a naïve Wick rotation of the Schrödinger geometry will result in a complex geometry due to (x^+, x^-) mixing term.

In Chapter 3 we will review the basics of QFT in real-time and directly calculate propagators for a free scalar with a $z = 2$ Lifshitz symmetry before reviewing the framework of [20] for performing holography in real-time. We will then attempt to extend this framework to calculating propagators in the Schrödinger and Lifshitz geometries introduced above and discuss the various subtleties that arise.

1.5.3 Entanglement entropy

One of the most basic phenomena in quantum physics is that of quantum entanglement, where subsystems of a quantum entangled state cannot be described independently of

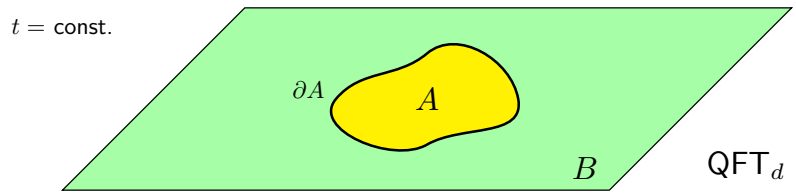

Figure 1.5.2: Entanglement entropy setup in a local field theory.

the other parts even when there is a large separation between such components. We can quantify the amount of entanglement between a subsystem A of a quantum state and the rest of the system $\bar{A}$ via the *entanglement entropy*. To do this we must first partition the Hilbert space $\mathcal{H}$ of the full system into two parts:

$$\mathcal{H} = \mathcal{H}_A \otimes \mathcal{H}_{\bar{A}} \tag{1.5.9}$$

where $\mathcal{H}_A$ is the Hilbert space of the subsystem A. Given such a partitioning of the Hilbert space we can construct the *reduced density matrix* ρ_A for any given state ρ by tracing out the degrees of freedom in $\mathcal{H}_{\bar{A}}$:

$$\rho_A = \mathrm{tr}_{\bar{A}}\rho \tag{1.5.10}$$

from which we define the entanglement entropy S_{EE} to be the von Neumann entropy of this operator:

$$S_{EE} = -\mathrm{tr}_A(\rho_A \log \rho_A). \tag{1.5.11}$$

In a local field theory one can partition the system into two sub-regions by considering a co-dimension 1 spatial region A with boundary ∂A, as shown in Figure 1.5.2. In this case the boundary is often called the *entangling surface*, and S_{EE} is sometimes called the *geometric entropy*.

In non-trivial systems such as in a quantum field theory it is often technically difficult to calculate the entanglement entropy using equation (1.5.11). It is easier to calculate powers of the reduced density matrix $\mathrm{tr}_A{\rho_A}^n$ and calculate the entanglement entropy using the *replica trick*. Such powers can be calculated using the path integral formalism:

$$\mathrm{tr}_A{\rho_A}^n = \frac{Z(n)}{Z(1)^n} \tag{1.5.12}$$

where $Z(n)$ is the partition function on a singular space obtained by gluing n copies of the original space together along ∂A. Assuming that these can be calculated and they are analytic in n we can calculate S_{EE} as

$$S_{EE} = -\lim_{n\to 1} n\, \partial_n[\log Z(n) - n \log Z(1)]. \tag{1.5.13}$$

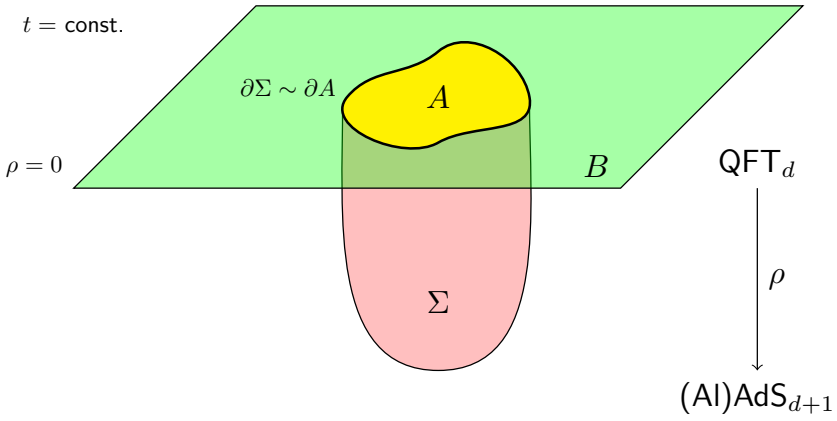

Figure 1.5.3: Holographic entanglement entropy setup.

A more detailed introduction to the replica trick can be found in [39].

The entanglement entropy gives us a direct way to study the entanglement structure of a quantum system and indeed it has some nice properties. Firstly, since it is defined as an entropy one would expect that it is related to the degrees of freedom in the system which can be realised precisely in 2-dimensions where the entanglement entropy is proportional to the central charge. It is also non-zero at zero temperature which means we can use it to probe properties of the ground state. We can also use it as an order parameter for topological phase transitions as it is a non-local quantity.

In a continuum theory, the entanglement entropy is always UV divergent since the entanglement between A and B occurs most strongly at the boundary ∂A from the exchange of short wavelength modes. Indeed, if we introduce a UV cutoff $\epsilon \ll 1$ then the leading divergence for ground states in a local CFT takes the form

$$S_{EE} = \gamma \frac{\text{Area}(\partial A)}{\epsilon^{D-1}} + \dots \tag{1.5.14}$$

where D is the number of spatial dimensions of the theory, and γ is a theory dependent constant. This result is called the *area law* for entanglement and is a universal result in continuum theories where $D > 1$ [40]. The subleading terms are not universal and depend on the different length scales present, such as geometric scales arising from the entangling region ∂A and its singularities, and mass scales present arising from operator sources.

As with any well defined QFT quantity we should be able to extend the holographic dictionary so that we can calculate the entanglement entropy holographically. The original proposal for a holographic formula came in the form of the *Ryu-Takayanagi* (RT) pre-

scription [41, 42]:

$$S_{EE} = \frac{\text{Area}(\Sigma)}{4G_N^{(D+2)}} \tag{1.5.15}$$

where Σ is the D dimensional bulk minimal surface with boundary $\partial\Sigma = \partial A$ as illustrated in Figure 1.5.3, and $G_N^{(d+2)}$ is the bulk Newton constant. The minimal surface Σ must also satisfy a technical constraint [43] of being homologous to A but this constraint will not affect our work and so we will not discuss it further. Although originally presented as a conjecture inspired by the formula for black hole entropy, this proposal has since been made concrete due to the work of Lewkowycz and Maldacena who gave a holographic proof of the RT proposal based on the replica trick [44] which we will review in Section 5.5.

The RT prescription for a smooth and compact ∂A predicts that the divergence structure of the entanglement entropy for a CFT in vacuum is given by

$$S_{EE} = \gamma_1 \left(\frac{l}{\epsilon}\right)^{D-1} + \gamma_3 \left(\frac{l}{\epsilon}\right)^{D-3} + \cdots + \begin{cases} \gamma_{D-1}\left(\frac{l}{\epsilon}\right) + \gamma_D + \cdots & D \text{ even} \\ \gamma_{D-2}\left(\frac{l}{\epsilon}\right)^2 + \tilde{c}\log\left(\frac{l}{\epsilon}\right) + \cdots & D \text{ odd} \end{cases} \tag{1.5.16}$$

where l is some characteristic length scale of ∂A, ϵ is a UV cutoff, the γ_i are theory dependent constants, and $\tilde{c}$ is related to the central charges for odd D.

The presence of the central charges in the logarithmic terms of the entanglement entropy in even D has led to proposals that the $\tilde{c}$ coefficient is a suitable quantity to use in the c- and a-theorems [45] which state that there exists a positive real function in any QFT that is finite at UV and IR fixed points and decreases monotonically along any RG flow from the UV to the IR. Such quantities are useful as they allow us to define a measure of the degrees of freedom present at points along an RG flow and at fixed points. There is no analogue of the c- or a-theorem for D odd however there have been promising results in the literature that the free energy of a theory defined on the 3-sphere is a suitable quantity, and moreover it is equal to the finite part of the entanglement entropy γ_D of a disk region. This conjectured result is called the F-theorem but has escaped a general proof. In Chapter 4 we discuss past works that provide evidence for the F-theorem, and then we construct an explicit holographic counterexample that invalidates the strongest form of the conjecture.

It is clear from equation (1.5.16) that we need a rigorously defined renormalization method to make the entanglement entropy a well defined quantity. In Chapter 5 we discuss previous attempts in the literature to define a renormalized entanglement entropy and their problems, and then extend the framework of holographic renormalization to define a renormalized holographic entanglement entropy and interpret its field theoretic dual using the replica trick. We demonstrate this method in Chapter 6 where we calculate the

renormalized holographic entanglement entropy for slab entangling regions for non-conformal brane backgrounds, and explicit realisations of RG flows via the Coulomb branch of $\mathcal{N} = 4$ SYM and the GPPZ flow.

CHAPTER 2

Inhomogeneity simplified

2.1 Introduction

Holographic modelling of strongly coupled condensed matter systems has generated a great deal of interest over recent years; for reviews see [46, 10]. It is remarkable that many features of strongly coupled matter can be captured by static, isotropic solutions of Einstein-Maxwell-dilaton models. Nonetheless as one tries to develop more realistic models it is clear that such holographic geometries cannot adequately capture many important features of strongly interacting systems.

The focus of this chapter will be on modelling systems with broken spatial translational symmetry. Realistic condensed matter systems never have perfect translational symmetry: the symmetry is explicitly broken both by lattice effects and by the presence of inhomogeneities. This breaking of translational invariance is necessary for particles to dissipate momentum, without which there would be a delta function in the conductivity at zero frequency.

Diffeomorphism invariance of a field theory implies conservation of the stress energy tensor T_{ij} via the diffeomorphism Ward identity which arises from insisting that the variation of the generating functional under the infinitesimal generators of bulk diffeomorphisms vanishes identically. If one considers a field theory which has a conserved current J_i and a scalar operator $\mathcal{O}$ then diffeomorphism invariance is violated when-

ever there is a position dependent source A_i for the current J_i or a similar source ϕ for the scalar operator, and the corresponding operators acquire expectation values. In this case the diffeomorphism Ward identity takes the form

$$\nabla^i \langle T_{ij} \rangle - \langle J^i \rangle F_{ij} + \langle \mathcal{O} \rangle \partial_j \phi = 0, \tag{2.1.1}$$

with $F_{ij} = \partial_i A_j - \partial_j A_i$. The temporal component of this identity gives rise to the energy conservation constraint, whereas the spatial compontents gives the momentum conservation constraints.

From this Ward identity it is evident that one can generically violate momentum conservation, while preserving energy density conservation, by introducing background sources in the field theory which depend on the spatial coordinates. Note that spontaneous breaking of the translational symmetry on its own is not enough to dissipate momentum as both $\langle O \rangle$ and $\partial_j \phi$ need to be non-zero to contribute to the Ward identity. The introduction of such sources is rather natural: a source for A_i with periodicity in the spatial directions represents an ionic lattice while other lattice effects can be captured by a periodic scalar field.

Holographically, spatially dependent sources for the conserved current can be modelled by a dual gauge field which is spatially modulated. The backreaction of this field onto the metric and other fields gives rise to fields which are stationary but inhomogeneous. In $(d+1)$ bulk dimensions one therefore has to solve partial differential equations in the radial coordinate and the spatial coordinates which are only tractable numerically. Numerical analysis has shown that such explicit breaking of translational invariance indeed removes the delta function in the conductivity at zero frequency [47, 48].

The optical conductivity is a transport property that can be defined for any QFT current J_i and is given by

$$\sigma_i(x) = \frac{\langle J_i \rangle}{i\omega A_{i(0)}} \tag{2.1.2}$$

where $A_{x(0)}$ is the homogeneous source $A_{x(0)} \sim e^{-i\omega t} a_{x(0)}$ for the current, and $< J_i >$ is the expectation value of the current in the presence of this source. There is considerable interest in the behaviour of the optical conductivity $\sigma(\omega)$ in holographic models at higher frequencies, in the range $T < \omega < \mu$, where μ is the chemical potential. Over such a range of frequencies certain high temperature superconductors in the normal phase exhibit scaling law behaviour of the form

$$\sigma(\omega) = K \omega^{\gamma - 2} e^{i \frac{\pi}{2}(2-\gamma)} \tag{2.1.3}$$

with $\gamma \approx 1.35 \approx 4/3$ and K a constant. This complex phase to the optical conductivity indicates that the current is out of phase with the source. These systems are considered

to be strongly coupled with the scaling law potentially a signal of underlying quantum criticality. Rather surprisingly, the introduction of a lattice into holographic models not only results in finite DC conductivity but also apparently induces scaling behaviour in the optical conductivity for a range of frequencies [47, 48] (see also [49, 50]):

$$|\sigma| = c + K\omega^{\gamma-2} \tag{2.1.4}$$

with (c, K) constants, $\gamma \approx 1.35$ and the phase of the conductivity approximately constant. Note that σ here refers to the homogeneous part of the conductivity. These results have proven controversial and no further evidence has been found to support them, see for example [51].

Clearly it would be interesting to understand the origin of this scaling behaviour better but the scaling emerges from the numerical analysis and does not make evident which ingredients are crucial to obtain a scaling regime. For example, it is known that one can obtain scaling behaviour for the AC conductivity without explicitly breaking translational invariance; scaling with the correct exponent arises in Einstein-Maxwell-Dilaton models, although solutions with the required value of γ appear to be thermodynamically unstable [52]. While one expects that the scaling is associated with an underlying quantum critical state, the scaling itself emerges at finite temperature and, from the holographic viewpoint, is therefore not associated not only with the spacetime region immediately adjacent to the horizon but also with regions further from the horizon. From this perspective it is not obvious to what extent the scaling should be sensitive to the details of the far IR or the mechanism of translational symmetry breaking.

As explored in [53, 54, 55], simplified models of translational symmetry breaking can be obtained by imposing symmetries on the bulk solutions: one can tune matter field profiles such that the metrics for the equilibrium configurations are homogeneous but anisotropic. The resulting equations of motion therefore simplify, reducing to ordinary differential equations in the radial coordinates, although these equations nonetheless still need to be solved numerically. In such models one does not find scaling behaviour of the AC conductivity, which indicates that this behaviour is non-generic. An interesting feature of these models is that one finds transitions between metallic and insulator behaviour as parameters are adjusted; see also [56, 57, 58] for related discussions on metal-insulator transitions.

In this chapter we will explore the simplest possible models of translational symmetry breaking, namely those for which the inhomogeneous matter field profiles are chosen such that the metrics for the equilibrium configurations remain both homogeneous and isotropic. The equations of motion for the equilibrium black brane solutions can therefore be solved explicitly analytically. The presence of inhomogeneous matter field pro-

files nonetheless guarantees that momentum can be dissipated by fluctuations propagating around these equilibrium solutions, and therefore one obtains finite DC conductivities.

Massive gravity models [59, 60, 61, 62] have been proposed as translational symmetry breaking models of this type. However, massive gravity is a bottom up phenomenological theory and it is not clear that it is well-defined at the quantum level. The holographic dictionary between the background metric used in massive gravity and the dual field theory is obscure. It is therefore preferable to work with models whose top down origin can be made more manifest.

As discussed above, switching on any operator source with spatial dependence triggers momentum dissipation. Moreover, any scalar field action with shift symmetry admits solutions for which the scalar field is linear in the spatial coordinates and thus the scalar contributions to the stress energy tensor are homogeneous. As shown in [63], by choosing an action with a number of massless scalar fields equal to the number of spatial directions one can engineer scalar field profiles such that the bulk stress energy tensor and hence the resulting black brane geometry are both homogeneous and isotropic. See also the earlier work in [64] in which homogeneous and isotropic black branes supported by fluxes were classified; it would be interesting to find AdS/CFT applications for these solutions.

In this chapter we will explore general actions with shift symmetry which admit homogeneous and isotropic black brane solutions and realise momentum relaxation. In particular, we will be led to consider square root terms:

$$\mathcal{L} = -a_{1/2} \sum_I \sqrt{(\partial \phi_I)^2} \tag{2.1.5}$$

where the summation is over spatial directions, labelled by I, and reality of the action requires that $\partial \phi_I$ is not timelike. Such Lagrangians clearly have shift symmetry and, as we explain in Section 2.2, can be used to engineer the required homogeneous and isotropic geometries.

Square root actions are unconventional but have arisen in several related contexts. For example, time dependent profiles of scalar fields associated with the cuscuton square root action have been proposed in the context of dark energy [65, 66]. The same action arose in the context of holography for Ricci flat backgrounds: the holographic fluid on a timelike hypersurface outside a Rindler horizon has properties consistent with a hydrodynamic expansion around a $\phi = t$ background solution of the cuscuton model [67, 68].

We will show in Section 2.2 that the action (2.1.5) is directly related to one of the mass

terms in massive gravity. Four-dimensional massive gravity consists of the usual Einstein-Hilbert term together with mass terms for the graviton $g_{\mu\nu}$ of the following form:

$$\mathcal{L} = m^2 \left(\alpha_1 \sqrt{g^{\mu\nu} h_{\mu\nu}} + \alpha_2 (g^{\mu\nu} h_{\mu\nu} - \sqrt{h^{\mu\nu} h_{\mu\nu}}) + \cdots \right) \tag{2.1.6}$$

where $h_{\mu\nu}$ is a reference metric and $h^{\mu\nu} = g^{\mu\rho} g^{\nu\sigma} h_{\rho\sigma}$. The terms in ellipses are higher order in the reference metric and vanish in four dimensions when the reference metric only has two non-vanishing eigenvalues. The coupling constants α_1 and α_2 are independent.

It was shown in [63] that the α_2 term of massive gravity is related to massless scalar fields: the background brane solutions are completely equivalent and certain transport properties (shear modes) agree. Note that not all transport properties agree, since the linearised equations are only equivalent for a subset of fluctuations, those with constrained momenta in the spatial directions. In Section 2.2 we will show that the α_1 term of massive gravity is related to the square root terms (2.1.5). Again, the background brane solutions are completely equivalent and DC conductivities also agree but as in [63] the models are not completely equivalent; even at the linearised level the equations of motion for fluctuations with generic spatial momenta do not agree. The inequivalence between the models is made manifest when one uses a Stückelburg formalism for massive gravity.

There has been considerable debate about stability and ghosts in massive gravity, as well as the scale at which non-linear effects occur and effective field theory breaks down, see for example [69, 70, 71, 72, 73, 74, 75, 76]. Clearly all such issues are absent in models based on massless scalar fields but related issues occur in the square root models (2.1.5): perturbation theory around the trivial background $\phi_I = 0$ is ill-defined. From the holographic perspective, it is not a priori obvious that the bulk fields ϕ_I are dual to local operators in the conformal field theory whose dimensions are real and above the unitary bound and whose norms are positive.

In Section 2.3 we show that the fields ϕ_I are dual to marginal operators in the conformal field theory. The bulk field equations admit a systematic asymptotic expansion near the conformal boundary for any choice of non-normalizable and normalizable modes of these scalar fields, in which all terms in the asymptotic expansion are determined in terms of this data. The bulk action can be holographically renormalized in the standard way. This analysis provides evidence that the action (2.1.5) is physically reasonable.

We also show in Section 2.3 that correlations functions of the operators dual to the square root scalar fields ϕ_I of (2.1.5) can be computed in any holographic background in which there are non-vanishing profiles for these fields. These operators indeed be-

have as marginal operators and the norms of their two point functions are positive for $a_{1/2} > 0$. However, the expressions we obtain for the two point functions are not analytic as the background profiles for the scalar fields are switched off.

The action (2.1.5) is reminiscent of the volume term in a brane action. In Section 2.3 we show that such actions can indeed arise as tensionless limits of brane actions: the fields ϕ_I then correspond to transverse positions of branes.

In Section 2.4 and Section 2.5 we consider phenomenological models based on massless scalar fields and square root terms:

$$S = \int \mathrm{d}^{d+1}x\sqrt{-g}\left(R + d(d-1) - \frac{1}{4}F^2 - \sum_{I=1}^{d-1}(a_{1/2}\sqrt{(\partial\psi_I)^2} + a_1(\partial\chi_I)^2)\right) \tag{2.1.7}$$

Such actions admit charged homogeneous isotropic brane solutions characterised by their temperature, chemical potential and two additional parameters $(\tilde{\alpha}, \tilde{\beta})$ associated with the two types of scalar fields (ψ_I, χ_I) respectively.

We show that such models have a finite DC conductivity, as expected, and analyse the temperature dependence of the DC conductivity. The parameter $\tilde{\alpha}$, which is non-zero whenever there are background profiles for the square root fields, leads to a linear increase in the resistivity with temperature at low temperature in a field theory in three spacetime dimensions. In dimensions greater than three the DC conductivity increases with temperature for all values of the parameters $(\tilde{\alpha}, \tilde{\beta})$.

We explore the low frequency behaviour of the optical conductivity at low temperature, finding that for all values of our parameters there is a peak at zero frequency, indicating metallic behaviour. However, we show that our models do not fit Drude behaviour even at very low temperature: the effective relaxation constant is complex, indicating that momentum not only dissipates but oscillates.

Perhaps unsurprisingly, we see no signs of scaling behaviour of the optical conductivity at intermediate frequencies but our numerical analysis indicates minima can arise in the conductivity at intermediate frequencies and low temperatures (in three spacetime dimensions). The behaviour of the optical conductivity in our models is similar to that of heavy fermion compounds: these also have a DC conductivity which increases linearly with temperature at low temperature and they exhibit a transition to a decoherent phase at low temperature in which the conductivity has a minimum at finite frequency. In heavy fermions the origin of this minimum is a hybridisation gap, caused by f-electrons hybridising with conduction electrons, while the dip in the conductivity in our model is a strongly coupling phenomenon, associated with the mixing between scalar and gauge field perturbations.

The plan of this chapter is as follows. In Section 2.2 we explore models for translational symmetry breaking based on shift invariant scalar field actions and we show how such models are related to massive gravity and to scaling limits of branes. In Section 2.3 we analyse square root models, demonstrating that a well-defined holographic dictionary can be constructed. In Section 2.4 we build phenomenological models and compute DC and AC conductivity in these models, showing that features reminiscent of heavy fermions are obtained. In Section 2.5 we analyse generalisations of our models. We conclude in Section 2.6.

2.2 The simplest models of explicit translational symmetry breaking

In this section we consider an Einstein-Maxwell model with cosmological constant, coupled to matter, i.e. an action

$$S = \int \mathrm{d}^{d+1}x\sqrt{-g}\left(R + d(d-1) - \frac{1}{4}F^2 + \mathcal{L}_{(M)}\right). \tag{2.2.1}$$

The gravity and gauge field equations of motion can be written as

$$\begin{aligned} R_{\mu\nu} =& -dg_{\mu\nu} + \frac{1}{2}(F_{\mu\rho}F_{\nu}^{\ \rho} - \frac{1}{2(d-1)}F^2 g_{\mu\nu}) + \bar{T}_{\mu\nu}; \\ \nabla_\mu(F^{\mu\nu}) =& 0, \end{aligned} \tag{2.2.2}$$

where $\bar{T}_{\mu\nu}$ is the trace adjusted stress energy tensor for the matter.

Note that in this section we will exclusively use Greek indices $\mu, \nu, \ldots$ to refer to bulk manifold coordinates, and Latin indices $a, b, \ldots$ to refer to boundary spatial directions. Expressions involving both pairs of indices should be interpreted as having an implicit projection matrix to ensure that Latin index terms only contribute to the boundary spatial parts of bulk tensors.

When the matter vanishes, the equations of motion admit the standard electric AdS-RN black brane solution:

$$\mathrm{d}s^2 = \frac{1}{z^2}\left(-f(z)\mathrm{d}t^2 + \frac{\mathrm{d}z^2}{f(z)} + \mathrm{d}x\cdot\mathrm{d}x\right) \tag{2.2.3}$$

$$\begin{aligned} A =& \mu(1-z^{d-2})\mathrm{d}t \\ f =& 1 - m_0 z^d + \frac{\mu^2}{\gamma^2}z^{2(d-1)}, \end{aligned} \tag{2.2.4}$$

where m_0 is the mass parameter and μ is the chemical potential. It is often convenient

to choose m_0 such that

$$m_0 = 1 + \frac{\mu^2}{\gamma^2}, \qquad f(z) = (1 - z^d) + \frac{\mu^2}{\gamma^2} z^d (z^{d-2} - 1) \tag{2.2.5}$$

and the horizon is located at $z = 1$. The constant γ is given by

$$\gamma^2 = \frac{2(d-1)}{(d-2)}. \tag{2.2.6}$$

We will consider matter actions which are scalar functionals of the following form:

$$S_{(M)} = \int \mathrm{d}^{d+1}x \sqrt{-g} \mathcal{L}(X) \tag{2.2.7}$$

where $X = (\partial\phi)^2$, i.e. the Lagrangian has shift invariance by construction. The equation of motion for the scalar in the charged black brane background is then

$$\nabla^\mu \left(\nabla_\mu \phi \frac{\delta \mathcal{L}}{\delta X} \right) = 0, \tag{2.2.8}$$

which, due to the shift symmetry of X, always admits the solution

$$\phi = \mathbf{c} = c_a x^a, \qquad X = z^2 \mathbf{c} \cdot \mathbf{c}, \tag{2.2.9}$$

for any choice of functional of X and any choice of spacelike vector $\mathbf{c}$[1]. The stress energy tensor associated with the scalar matter is given by

$$T_{\mu\nu} = \frac{1}{2} \left(-2(\partial_\mu \phi)(\partial_\nu \phi) \frac{\delta \mathcal{L}}{\delta X} + g_{\mu\nu} \mathcal{L} \right) \tag{2.2.10}$$

Evaluated on the solution above, this stress energy tensor is by construction homogeneous but not spatially isotropic.

Now consider a matter action which is a multi-scalar functional of the following form:

$$S = \int \mathrm{d}^{d+1}x \sqrt{-g} \sum_{I=1}^{d-1} \mathcal{L}(X_I) \tag{2.2.11}$$

where $X_I = (\partial\phi_I)^2$. The equations of motion in the charged black brane background are

$$\nabla^\mu \left(\nabla_\mu \phi_I \frac{\delta \mathcal{L}}{\delta X_I} \right) = 0, \tag{2.2.12}$$

[1] One could also choose ϕ to be linear in time, but such backgrounds would violate energy conservation and will not be considered here.

which admit the solutions

$$\phi_I = \mathbf{c}_I, \qquad X_I = z^2 \mathbf{c}_I \cdot \mathbf{c}_I, \tag{2.2.13}$$

for any choice of functional and any choices of the spatial vectors $\mathbf{c}_I = c_{Ia} x^a$. The stress energy tensor is given by

$$T_{\mu\nu} = \frac{1}{2} \sum_{I=1}^{d-1} \left(-2(\partial_\mu \phi_I)(\partial_\nu \phi_I) \frac{\delta \mathcal{L}(X_I)}{\delta X_I} + g_{\mu\nu} \mathcal{L}(X_I) \right) \tag{2.2.14}$$

A special case in which spatial isotropy is restored is the following: choose all $(d-1)$ scalar Lagrangians to take the same functional form. Then by choosing $\mathbf{c}_I = c x^a$, i.e. $c_{Ia} = c$ we obtain a stress energy tensor which restores rotational symmetry in the spatial directions:

$$T_{\mu\nu} = \frac{1}{2} \left(-\sum_{a=1}^{d-1} 2c^2 \delta_{ab} \frac{\delta \mathcal{L}(X)}{\delta X} + (d-1) g_{\mu\nu} \mathcal{L}(X) \right). \tag{2.2.15}$$

Here we use the fact that X_I evaluated on the solution is $(cz)^2$ for all values of I. Therefore for each I, both $\mathcal{L}(X_I)$ and its derivative take the same values, which we denote without the subscripts.

Another possibility to restore rotational symmetry in the spatial directions is the following:

$$S = \int \mathrm{d}^{d+1} x \sqrt{-g} \mathcal{L}(\sum_{I=1}^{d-1} X_I) \tag{2.2.16}$$

where $X_I = (\partial \phi_I)^2$. The equations of motion in the charged black brane background remain

$$\nabla^\mu \left(\nabla_\mu \phi_I \frac{\delta \mathcal{L}}{\delta X_I} \right) = 0, \tag{2.2.17}$$

which always admit the solutions

$$\phi_I = \mathbf{c}_I, \qquad X_I = z^2 \mathbf{c}_I \cdot \mathbf{c}_I, \tag{2.2.18}$$

for any choice of functional and any choices of the spatial vectors $\mathbf{c}_I = c_{Ia} x^a$. The stress energy tensor is given by

$$T_{\mu\nu} = \frac{1}{2} \left(-2 \sum_I (\partial_\mu \phi_I)(\partial_\nu \phi_I) \frac{\delta \mathcal{L}(X)}{\delta X} + g_{\mu\nu} \mathcal{L}(X) \right), \tag{2.2.19}$$

where we have defined

$$X = \sum_I X_I \tag{2.2.20}$$

The special case in which spatial isotropy is restored is the following: choose $\mathbf{c}_I = c x^a$,

i.e. $c_{Ia} = c$ and $X = (d-1)(cz)^2$. The stress energy tensor is

$$T_{\mu\nu} = \frac{1}{2}\left(-\sum_{a=1}^{d-1} 2c^2\delta_{ab}\frac{\delta\mathcal{L}(X)}{\delta X} + g_{\mu\nu}\mathcal{L}(X)\right), \tag{2.2.21}$$

which is very similar to the previous form (2.2.15).

In summary, given any Lagrangian functional built out of $(d-1)$ scalar fields with shift symmetry, one can construct solutions for which the stress energy tensor preserves spatial isotropy and homogeneity. The backreaction on the black brane metric therefore preserves the usual black brane form for the metric, with a different blackening factor. The breaking of translational invariance by the scalar fields ensures that the momenta of fluctuations can be dissipated. In the remainder of this section we will consider the physical interpretations of various types of functionals.

2.2.1 Polynomial Lagrangians

Consider first the case of (2.2.11). If the Lagrangian is of polynomial form, i.e. $\mathcal{L}(X) = X^m$, then the stress tensor takes the particularly simple form evaluated on the scalar field profiles:

$$T_{\mu\nu} = \frac{1}{2}X^m\left(-2mg_{ab} + (d-1)g_{\mu\nu}\right) \tag{2.2.22}$$

where g_{ab} denotes the metric in the spatial directions. The trace adjusted stress energy tensor $\bar{T}_{\mu\nu}$ is defined as

$$\bar{T}_{\mu\nu} = T_{\mu\nu} - \frac{1}{(d-1)}Tg_{\mu\nu} \tag{2.2.23}$$

and is given by

$$\bar{T}_{\mu\nu} = (cz)^{2m}\left(-mg_{ab} + (m-1)g_{\mu\nu}\right). \tag{2.2.24}$$

If the Lagrangian can be expressed as a sum of such terms, namely $\mathcal{L}(X) = -\sum_m a_m X^m$, the corresponding trace adjusted stress energy tensor is

$$\bar{T}_{\mu\nu} = \sum_m a_m(c_m z)^{2m}\left(mg_{ab} - (m-1)g_{\mu\nu}\right). \tag{2.2.25}$$

Note that this class includes the special case of $m = 1$, i.e. massless scalar fields.

Scalar field profiles for which the stress energy tensor preserves rotational symmetry in the spatial directions by construction give rise to backreacted solutions which much

satisfy a homogeneous black brane metric ansatz

$$\begin{aligned} \mathrm{d}s^2 =& \frac{1}{z^2}\left(-F(z)\mathrm{d}t^2 + \frac{\mathrm{d}z^2}{F(z)} + \mathrm{d}x\cdot\mathrm{d}x_{d-1}\right) \\ A =& \mu(1-z^{d-2})\mathrm{d}t. \end{aligned} \tag{2.2.26}$$

In the limit that the matter fields vanish $F(z)$ coincides with the $f(z)$ given in the previous section, (2.2.3). Using the Ricci tensor for the metric (2.2.26),

$$\begin{aligned} R_{tt} &= \left(-dF + \frac{1}{2}(d+1)zF' - \frac{1}{2}z^2F''\right)g_{tt}; \\ R_{zz} &= \left(-dF + \frac{1}{2}(d+1)zF' - \frac{1}{2}z^2F''\right)g_{zz}; \\ R_{ab} &= \left(-dF + zF'\right)g_{ab}, \end{aligned} \tag{2.2.27}$$

we note that such an ansatz is required given the form of the matter stress energy tensor.

The solution for the blackening function F can be written as

$$F(z) = f(z) + \sum_m \frac{a_m}{2m-d}(c_m z)^{2m}, \tag{2.2.28}$$

with $f(z)$ given previously in (2.2.26). This expression assumes that $d \neq 2m$; in the latter case the solution for F involves logarithms, i.e. we obtain a term

$$a_m(c_m z)^d \log(z), \tag{2.2.29}$$

which gives rise to non-analytic behaviour.

Solutions to (2.2.16) in the case that $\mathcal{L}$ is polynomial, i.e. $\mathcal{L} = -b_m(\sum_\lambda X_\lambda)^m$, are very similar. Evaluated on the scalar field profiles one obtains

$$T_{\mu\nu} = -\frac{b_m}{2}X^m\left(-\frac{2m}{(d-1)}g_{ab} + g_{\mu\nu}\right). \tag{2.2.30}$$

with $X = (d-1)c_m^2 z^2$. Therefore the trace adjusted stress energy tensor is

$$\bar{T}_{\mu\nu} = -b_m\left((d-1)c_m^2z^2\right)^m\frac{1}{(d-1)}\left(-mg_{ab} + (m-1)g_{\mu\nu}\right) \tag{2.2.31}$$

This coincides with the expression above in the case of $m = 1$ (massless scalar fields) as the Lagrangians are the same. The corresponding solutions for the blackening functions are

$$F(z) = f(z) + \frac{b_m}{2m-d}(d-1)^{m-1}(c_m z)^{2m}, \tag{2.2.32}$$

with $f(z)$ given previously in (2.2.26). Again the case $d = 2m$ will involve logarithmic

terms.

2.2.2 Relation to massive gravity

In this section we will discuss the relation between massive gravity and our scalar field models. Let us consider the following Lagrangian

$$\mathcal{L} = -a_{1/2}\sum_I \sqrt{(\partial\phi_I)^2} - a_1\sum_I (\partial\chi_I)^2. \tag{2.2.33}$$

The trace adjusted stress energy tensor is

$$\begin{aligned}\bar{T}_{\mu\nu} =& \frac{1}{2(d-1)}a_{1/2}\sum_I \sqrt{(\partial\phi_I)^2}g_{\mu\nu} + \frac{1}{2}a_{1/2}\sum_I \frac{1}{\sqrt{(\partial\phi_I)^2}}\partial_\mu\phi_I\partial_\nu\phi_I \\ &+ a_1\sum_I \partial_\mu\chi_I\partial_\nu\chi_I\end{aligned} \tag{2.2.34}$$

The scalar field profiles

$$\phi_I = c_{1/2}x^I; \qquad \chi_I = c_1 x^I \tag{2.2.35}$$

give rise to a trace adjusted stress energy tensor which is

$$\bar{T}_{\mu\nu} = \frac{1}{2}a_{1/2}(c_{1/2}z)\left(g_{ab}+g_{\mu\nu}\right) + a_1(c_1 z)^2 g_{ab}. \tag{2.2.36}$$

The backreacted blackening function is

$$F(z) = f(z) - \frac{1}{(d-1)}a_{1/2}c_{1/2}z - \frac{1}{(d-2)}a_1(c_1 z)^2, \tag{2.2.37}$$

which in $d=3$ has precisely the same form as the massive gravity solution found in [59].

One can also consider a slightly different Lagrangian

$$\mathcal{L} = -a_{1/2}\left(\sqrt{\sum_I (\partial\phi_I)^2}\right) - a_1\left(\sum_I (\partial\chi_I)^2\right). \tag{2.2.38}$$

for which the trace adjusted stress energy tensor is

$$\begin{aligned}\bar{T}_{\mu\nu} =& \frac{1}{2(d-1)}a_{1/2}\sqrt{\sum_I (\partial\phi_I)^2}g_{\mu\nu} + \frac{1}{2}a_{1/2}\frac{1}{\sqrt{\sum_I (\partial\phi_I)^2}}\sum_I \partial_\mu\phi_I\partial_\nu\phi_I \\ &+ a_1\sum_I \partial_\mu\chi_I\partial_\nu\chi_I.\end{aligned} \tag{2.2.39}$$

Evaluated on the scalar field profiles

$$\phi_I = c_{1/2} x^I; \qquad \chi_I = c_1 x^I \tag{2.2.40}$$

the trace adjusted stress energy tensor becomes

$$\bar{T}_{\mu\nu} = \frac{1}{2\sqrt{d-1}} a_{1/2}(c_{1/2} z)\,(g_{ab} + g_{\mu\nu}) + a_1 (c_1 z)^2 g_{ab}. \tag{2.2.41}$$

The corresponding backreacted blackening function is

$$F(z) = f(z) - \frac{1}{(d-1)^{\frac{3}{2}}} a_{1/2} c_{1/2} z - \frac{1}{(d-2)} a_1 (c_1 z)^2, \tag{2.2.42}$$

which in $d = 3$ again has precisely the same form as the massive gravity solution found in [59] and further analysed in [60] and [61].

To understand the relation with massive gravity in four bulk dimensions, let us first recall that the action for massive gravity consists of the Einstein-Hilbert terms plus the following mass terms:

$$\mathcal{L} = m^2 \sum_i \alpha_i \mathcal{U}_i(g, h), \tag{2.2.43}$$

where in terms of the matrix $\mathcal{K}^\mu_\nu \equiv \sqrt{g^{\mu\rho} h_{\rho\nu}}$

$$\begin{aligned} \mathcal{U}_1 =& [\mathcal{K}]\,; \\ \mathcal{U}_2 =& [\mathcal{K}]^2 - \left[\mathcal{K}^2\right]\,; \\ \mathcal{U}_3 =& [\mathcal{K}]^3 - 3\,[\mathcal{K}]\left[\mathcal{K}^2\right] + 2\left[\mathcal{K}^3\right]\,; \\ \mathcal{U}_4 =& [\mathcal{K}]^4 - 6\left[\mathcal{K}^2\right][\mathcal{K}]^2 + 8\left[\mathcal{K}^3\right][\mathcal{K}] - 3\left[\mathcal{K}^2\right]^2 - 6\left[\mathcal{K}^4\right]\,; \end{aligned} \tag{2.2.44}$$

The notation $[Y]$ denotes the matrix trace. Here $h_{\mu\nu}$ is a fiducial metric, which can be expressed via a coordinate transformation in terms of scalar (Stückelburg) fields π^a whenever it is flat, i.e.

$$h_{\mu\nu} = \eta_{ab} \partial_\mu \pi^a \partial_\nu \pi^b \tag{2.2.45}$$

Unitary gauge is then defined as $\pi^a = x^\mu \delta^a_\mu$. The restriction to a degenerate fiducial metric in which only the spatial components are non-vanishing was obtained in [59] using only two non-vanishing scalar fields, π^1 and π^2, which take an analogous form to those given above, namely

$$\pi^1 = x^1; \qquad \pi^2 = x^2 \tag{2.2.46}$$

From the first two terms in (2.2.44) one obtains a trace adjusted stress energy tensor

$$\bar{T}_{\mu\nu} = \frac{1}{2} m^2 \alpha_1 (\mathcal{K}_{\mu\nu} + \frac{1}{2}\,[\mathcal{K}]\,g_{\mu\nu}) - m^2 \alpha_2 (\mathcal{K}^2_{\mu\nu} - [\mathcal{K}]\,\mathcal{K}_{\mu\nu}). \tag{2.2.47}$$

The final two terms in (2.2.44) give rise to a vanishing stress energy tensor in four dimensions, as expected, as the spatial gauge only involves two non-vanishing eigenvalues for the matrix. Higher order terms in $[\mathcal{K}]$ would contribute in dimensions greater than four but massive gravity in dimensions higher than four has not been explored in detail in earlier literature.

Evaluated on the particular background given by the two scalar fields

$$\bar{T}_{\mu\nu} = \frac{1}{2}m^2\alpha_1 z(g_{ab} + g_{\mu\nu}) + m^2\alpha_2 z^2 g_{ab}, \tag{2.2.48}$$

where we assume that the metric ansatz $g_{11} = g_{22} = z^{-2}$ remains consistent, which is then justified a posteriori. The expressions (2.2.48) and (2.2.36) clearly match under the identifications

$$m^2\alpha_1 = a_{1/2}c_{1/2}; \qquad m^2\alpha_2 = a_1 c_1^2, \tag{2.2.49}$$

and (2.2.48) and (2.2.36) similarly can be matched.

While the black brane solutions in our models match those of massive gravity, it is clear that fluctuations and hence transport properties of these solutions will differ between massive gravity and the scalar field models. For the terms quadratic in $\mathcal{K}$, corresponding to the massless scalar fields in our models, this issue was discussed in [63]. Focussing on the terms linear in $\mathcal{K}$, note that

$$[\mathcal{K}] = \sqrt{(\partial\pi^1)^2 + (\partial\pi^2)^2}, \tag{2.2.50}$$

and therefore the second term in (2.2.47) seems to resemble the first term in (2.2.39). However, the scalar fields in the massive gravity model are assumed to depend only on the spatial components as given in (2.2.46) whereas the scalar fields in (2.2.39) are completely unrestricted. The first term in (2.2.47) can be written explicitly in terms of

$$\mathcal{K}_{\mu\nu} = g_{\mu\rho}\sqrt{\sum(\partial^\rho\pi)(\partial_\nu\pi)}, \tag{2.2.51}$$

which is not of the same form as the second term in (2.2.39) unless we restrict the scalar fields to the form (2.2.46). In the background brane solutions the scalar fields indeed necessarily take the form (2.2.46) but this property cannot generically hold for fluctuations around the equilibrium solution. We will show in Section 2.4 why the conductivities nonetheless match those of massive gravity.

Another conceptual difference between our model and massive gravity is the following. In our models the scalar fields ϕ_I and χ_I are treated as independent fields but in massive gravity they are identified as the same field. As we discuss in Section 2.5, it is however straightforward to restrict to the case in which these fields are identified.

2.2.3 Relation to branes

From the perspective of top-down models, the appearance of square root terms is unconventional. In this section we will show that similar terms can arise from tensionless limits of branes. Consider the following action:

$$S = -b_{1/2}\int \mathrm{d}^{d+1}x\sqrt{-\det(g_{\mu\nu}+\sum_{I=1}^{d-1}\partial_\mu\phi_I\partial_\nu\phi_I)} \equiv -b_{1/2}\int \mathrm{d}^{d+1}x\sqrt{-\det M}. \quad (2.2.52)$$

This action can be interpreted in terms of a brane with a $(d+1)$ dimensional world volume, which is probing $(d-1)$ flat transverse directions. To show this, recall that the DBI term in the action for a p-brane is

$$S_{DBI} = -T\int \mathrm{d}^{p+1}x\sqrt{-\det(g_{MN}\partial_\mu X^M\partial_\nu X^N + F_{\mu\nu})}, \quad (2.2.53)$$

where T is the brane tension, $F_{\mu\nu}$ is the worldvolume gauge field strength; X^M are the brane positions and g_{MN} is the metric of the spacetime in which the brane propagates. Fixing static gauge for the brane corresponds to choosing $X^\mu \equiv x^\mu$ and the gauge fixed action is

$$S_{DBI} = -T\int \mathrm{d}^{p+1}x\sqrt{-\det(g_{\mu\nu}+g_{m(\mu}\partial_{\nu)}X^m + g_{mn}\partial_\mu X^m\partial_\nu X^n + F_{\mu\nu})}, \quad (2.2.54)$$

where the transverse coordinates are denoted as X^n. Whenever the background metric is diagonal $g_{m\nu} = 0$. If there are no Wess-Zumino terms sourcing the gauge field, then the gauge field strength may also always be set to zero. This results in a brane probing the transverse directions:

$$S_{DBI} = -T\int \mathrm{d}^{p+1}x\sqrt{-\det(g_{\mu\nu}+g_{mn}\partial_\mu X^m\partial_\nu X^n)}, \quad (2.2.55)$$

and clearly when $g_{mn} = \delta_{mn}$ the action reduces to (2.2.52), with $b_{1/2}$ being identified as the brane tension.

The trace adjusted stress energy tensor following from (2.2.52) is

$$\bar{T}_{\mu\nu} = -\frac{b_{1/2}\sqrt{-\det M}}{2\sqrt{-g}}\left(M_{\mu\nu} - \frac{1}{(d-1)}M^{\rho\sigma}M_{\rho\sigma}g_{\mu\nu}\right). \quad (2.2.56)$$

Again the specific solution $\phi_I = cx^I$ preserves spatial homogeneity and isotropy with the trace adjusted stress energy tensor being

$$\bar{T}_{\mu\nu} = -\frac{1}{2}b_{1/2}(1+c^2z^2)^{\frac{d-1}{2}}\left(\frac{2}{(1-d)}g_{\mu\nu} - c^2z^2g_{\mu\nu} + c^2\delta_{ab}\right) \quad (2.2.57)$$

and the blackening factor taking the form

$$F(z) = f(z) + b_{1/2} z^d \int \frac{dz}{(d-1)z^{d+1}} (1 + c^2 z^2)^{\frac{d-1}{2}}. \tag{2.2.58}$$

Expanding the second term for small z near the AdS boundary gives

$$- b_{1/2} \left(\frac{1}{d(d-1)} + \frac{c^2 z^2}{2(d-2)} + \cdots \right), \tag{2.2.59}$$

i.e. there is an effective shift of the AdS radius as well as subleading terms in the expansion. When d is odd the integral gives an analytic expression; for example, for $d = 3$ one obtains

$$F(z) = f(z) - b_{1/2} \left(\frac{1}{6} + \frac{1}{2} c^2 z^2 \right) \tag{2.2.60}$$

but d even generates logarithmic terms and therefore $F(z)$ is not analytic, e.g. for $d = 4$

$$F(z) = f(z) - b_{1/2} \left(\frac{1}{8} + \frac{3}{4} c^2 z^2 - \frac{3}{2} c^4 z^4 \log(z) - \frac{1}{4} c^6 z^6. \right) \tag{2.2.61}$$

Working perturbatively around AdS, this brane type Lagrangian leads to a shift in the cosmological constant along with a spectrum of $(d-1)$ massless scalar fields, dual to $(d-1)$ marginal couplings in the field theory. It therefore reproduces analogous behaviour to the massless scalar fields discussed in the previous sections.

Another brane model can be obtained as follows. Consider $(d-1)$ branes of equal tension, each probing one transverse flat direction only:

$$S = -b_{1/2} \sum_{I=1}^{d-1} \int \mathrm{d}^{d+1} x \sqrt{- \det(g_{\mu\nu} + \partial_\mu \phi_I \partial_\nu \phi_I)}. \tag{2.2.62}$$

Using Sylvester's determinant theorem this action can be rewritten as

$$S = -b_{1/2} \sum_{I=1}^{d-1} \int \mathrm{d}^{d+1} x \sqrt{- \det g} \sqrt{1 + \partial^\mu \phi_I \partial_\mu \phi_I}. \tag{2.2.63}$$

The trace adjusted stress tensor is

$$\bar{T}_{\mu\nu} = - \frac{b_{1/2} \sum_I \sqrt{- \det M_I}}{2\sqrt{-g}} \left(M_{I\mu\nu} - \frac{1}{(d-1)} M_I^{\rho\sigma} M_{I\rho\sigma} g_{\mu\nu} \right) \tag{2.2.64}$$

where now

$$M_{I\mu\nu} = g_{\mu\nu} + \partial_\mu \phi_I \partial_\nu \phi_I. \tag{2.2.65}$$

The solution with $\phi_I = c x^I$ is homogeneous and isotropic with the blackening factor

being

$$F(z) = f(z) + b_{1/2} z^d \int \frac{\mathrm{d}z}{z^{d+1}} (1 + c^2 z^2)^{\frac{1}{2}} \left(1 + \frac{1}{2} c^2 z^2 (d-2)\right), \tag{2.2.66}$$

which coincides with (2.2.58) in $d = 2$.

The action (2.2.63) admits a scaling limit in which the brane tension is taken to zero $b_{1/2} \to 0$ with $\psi_I = b_{1/2}\phi_I$ remaining finite. This limit results in

$$S \approx -\sum_{I=1}^{d-1} \int \mathrm{d}^{d+1}x \sqrt{-g} \sqrt{(\partial \psi_I)^2}, \tag{2.2.67}$$

which is of the square root form.

2.3 Square root models

While one can obtain solutions for any polynomial functional, one would usually restrict to the case of $m = 1$, i.e. massless scalar fields. In AdS/CFT the operators dual to these scalar fields are marginal scalar operators and the bulk scalar profiles are therefore immediately interpretable in the dual theory as linear profiles for the associated couplings.

For integer $m > 1$ the action is higher derivative and for non-integer m the action would be considered non-local. In this section we will argue that both cases may in some limits nonetheless be relevant in bottom up models.

Consider first the case of integer $m > 1$. In the previous section, we assumed that the scalar fields appearing in polynomials of different order were independent. However, in the solutions of interest, the scalar field profiles are the same for each order polynomial. Therefore there is no reason why we should not identify the scalar fields, e.g. we could consider

$$\mathcal{L} = -a_1 \sum_I (\partial \phi_I)^2 - a_2 \sum_I \left((\partial \phi_I)^2\right)^2 \tag{2.3.1}$$

or

$$\mathcal{L} = -a_1 \sum_I (\partial \phi_I)^2 - a_2 \left(\sum_I (\partial \phi_I)^2\right)^2 \tag{2.3.2}$$

The fourth order terms can be viewed as higher derivative corrections to the leading order action; a_2 should therefore be considered as parametrically small compared to a_1 (which can always be rescaled to the canonical value by rescaling the fields). However, it makes sense to consider how a small a_2 would affect transport and thermodynamic properties of charged black branes, although we will not pursue this further here.

Now let us turn to non-integer m, focussing on the case of $m = 1/2$, i.e. a Lagrangian of the form

$$\mathcal{L} = -\sqrt{(\partial\phi)^2} \tag{2.3.3}$$

Note that reality of the Lagrangian requires that $(\partial\phi)$ is not timelike. This is certainly an unconventional Lagrangian in holography, although similar actions have arisen in several contexts. For example, time dependent profiles of scalar fields associated with the cuscuton action

$$\mathcal{L} = \sqrt{-(\partial\phi)^2} \tag{2.3.4}$$

have been proposed in the context of dark energy [65, 66]. The same action arose in the context of holography for Ricci flat backgrounds: the holographic fluid on a timelike hypersurface outside a Rindler horizon has properties consistent with a hydrodynamic expansion around a $\phi = t$ background solution of the cuscuton model [67, 68].

In the remainder of this section we will explore the behaviour of the (2.3.3) model. It is subtle to work at linear order around an AdS background as the corresponding scalar field equations remain non-linear in this limit: we obtain a field equation of the form

$$\bar{\nabla}^\mu \left(\frac{1}{\sqrt{(\partial\phi)^2}} \bar{\nabla}_\mu \phi \right) = 0, \tag{2.3.5}$$

where $\bar{\nabla}_\mu$ is the AdS connection and here ϕ is implicitly treated perturbatively, i.e. the amplitude of the scalar field is small.

When one works perturbatively around the AdS background, we need to take into account the fact that the scalar field perturbation is of the same order as the backreaction of the metric. (Note that in the exact, non-linear, black brane solutions the backreaction on the metric is indeed of the same order as the scalar field itself.) It is convenient to express the coupled metric and scalar field equations using

$$\begin{aligned} \nabla_\mu v^\mu &= 0; \\ \bar{T}_{\mu\nu} &= -\frac{1}{2}\sqrt{X}(g_{\mu\nu} + 2v_\mu v_\nu), \end{aligned} \tag{2.3.6}$$

where $X = \sqrt{(\partial\phi)^2}$ while the velocity field v_μ is conserved and satisfies $v^\mu v_\mu = 1$. In terms of the scalar field one can express the velocity field as the gradient flow

$$v_\mu = \frac{\nabla_\mu \phi}{\sqrt{X}}. \tag{2.3.7}$$

Working perturbatively around the AdS background requires that $\phi \sim \delta$ with $\delta \ll 1$. The metric perturbation is then of the same order as the scalar field and the non-linearity is manifest in the fact that the velocity field is of order one.

We can now proceed to solve these equations as follows. Working perturbatively in the amplitude δ let

$$v^\mu = v_0^\mu + v_1^\mu \delta + \mathcal{O}(\delta^2) \qquad g_{\mu\nu} = \bar{g}_{\mu\nu} + h_{1\mu\nu}\delta + \mathcal{O}(\delta^2), \tag{2.3.8}$$

where $\bar{g}_{\mu\nu}$ is the AdS metric and v_0 is any conserved globally spacelike vector in this metric, which can then be normalised such that $v_0^\mu v_{0\mu} = 1$. Solving the conservation equation up to order δ gives

$$v_{1\mu} = -\frac{1}{2} v_{0\mu} h_1 \tag{2.3.9}$$

with $h_1 = \bar{g}^{\mu\nu} h_{1\mu\nu}$. Substituting into the trace adjusted stress energy tensor we obtain at order δ

$$\bar{T}_{1\mu\nu} = -3h_{1\mu\nu} - \frac{1}{2}\sqrt{X}(\bar{g}_{\mu\nu} + 2v_{0\mu}v_{0\nu}), \tag{2.3.10}$$

with $\sqrt{X}$ a function of the spacetime coordinates. Therefore the metric perturbation $h_{1\mu\nu}$ is determined by the Einstein equation in terms of $\sqrt{X}$ and the conserved vector field $v_{0\mu}$. Using the linearised Ricci tensor in de Donder gauge ($\bar{\nabla}^\mu h_{1\mu\nu} = 0$) gives

$$\frac{1}{2}\bar{\Box} h_{1\mu\nu} + \frac{1}{2}\bar{\nabla}_\mu \bar{\nabla}_\nu h_1 + h_1 \bar{g}_{\mu\nu} = \frac{1}{2}\sqrt{X}(\bar{g}_{\mu\nu} + 2v_{0\mu}v_{0\nu}). \tag{2.3.11}$$

Tracing this equation with $\bar{g}^{\mu\nu}$ results in

$$\bar{\Box} h_1 + (d+1)h_1 = (d+3)\sqrt{X}. \tag{2.3.12}$$

Therefore, the leading order defining data is a scalar field satisfying (2.3.5), which is a non-linear equation; we will discuss its solution in Section 2.3.3. Note that an asymptotic expansion of the field equations near the conformal boundary exists as we will discuss in the next Section 2.3.1.

As in the cuscuton and holographic fluid models, one can find simple solutions of the equations of motion with non-vanishing scalar field profiles, and the equations of motion are linear when expanded around such backgrounds. To understand this, let us consider the action

$$\mathcal{L} = -a_{1/2} \sum_I \sqrt{(\partial \phi_I)^2} \tag{2.3.13}$$

for which the coupled gravity/scalar field system admits the homogeneous and isotropic solution

$$\mathrm{d}s^2 = \frac{1}{z^2}\left(-(1 - \frac{a_{1/2}c_{1/2}}{(d-1)}z)\mathrm{d}t^2 + \frac{\mathrm{d}z^2}{(1 - \frac{a_{1/2}c_{1/2}}{(d-1)}z)} + \mathrm{d}x \cdot \mathrm{d}x_{d-1}\right) \tag{2.3.14}$$

with $\phi_I = c_{1/2}\delta_{Ia}x^a$. This is the $\mu \to 0$, $m_0 \to 0$ limit of the solution given in the previous section. As discussed above, the backreaction on the metric is linear in the scalar field

amplitude and therefore cannot be neglected even for small $c_{1/2}$.

Note that when $a_{1/2} > 0$ the geometry has a horizon, with the entropy and temperature being

$$\mathcal{S} = \frac{1}{4G_{d+1}} V_{d-1} \left(\frac{a_{1/2} c_{1/2}}{(d-1)} \right)^{d-1}; \qquad T = \frac{a_{1/2} c_{1/2}}{4\pi (d-1)}, \tag{2.3.15}$$

where G_{d+1} is the Newton constant. Analogous behaviour was noted in the massless scalar field model of [63]. If $a_{1/2} < 0$ there is a curvature singularity as $z \to \infty$; this can most easily be seen from the expression for the Ricci scalar

$$R = \left(-d(d+1)F - zz^2 F'' + 2dzF' \right) = \left(-d(d+1) + da_{1/2} c_{1/2} z \right). \tag{2.3.16}$$

The singularity is at infinite proper distance and would presumably therefore not affect the computation of correlation functions. It is a good singularity, in the sense of [77], since it is shielded in the black brane solutions of the previous section for which $m_0 > 0$. We will discuss the linearised equations of motion in such backgrounds in section (2.3.3).

2.3.1 Holographic renormalization for square root models

In this section we explore asymptotically locally AdS solutions of the action

$$S = \frac{1}{16\pi G_{d+1}} \int \mathrm{d}^{d+1} x \sqrt{-g} \left(R + d(d-1) - a_{1/2} \sum_I^{d-1} \sqrt{(\partial \phi_I)^2} \right). \tag{2.3.17}$$

Despite the subtleties discussed in the previous section, one can solve the field equations iteratively near the conformal boundary and systematically set up holographic renormalization in the standard way [15, 23, 78].

The on-shell action, including Gibbons-Hawking boundary term, is

$$S_{\text{bare}} = \frac{1}{16\pi G_{d+1}} \int \mathrm{d}^{d+1} x \sqrt{-g} \left(-2d + a_{1/2} \sum_I^{d-1} \sqrt{(\partial \phi_I)^2} \right) - \frac{1}{8\pi G_{d+1}} \int \mathrm{d}^d x \sqrt{-\gamma} K. \tag{2.3.18}$$

One can rewrite the bulk scalar field term as

$$\begin{aligned} &\frac{1}{16\pi G_{d+1}} \int \mathrm{d}^{d+1} x \sqrt{-g} \left(a_{1/2} \sum_I^{d-1} \frac{(\partial \phi_I)^2}{\sqrt{(\partial \phi_I)^2}} \right) \\ &= \frac{1}{16\pi G_{d+1}} \int \mathrm{d}\Sigma_\mu a_{1/2} \sum_I^{d-1} \left(\frac{\phi_I \partial^\mu \phi_I}{\sqrt{(\partial \phi_I)^2}} \right), \end{aligned} \tag{2.3.19}$$

using the scalar field equation.

In the neighbourhood of the conformal boundary the metric can be expanded as

$$\mathrm{d}s^2 = \frac{d\rho^2}{4\rho^2} + \frac{1}{\rho} g_{ij}\mathrm{d}x^i \mathrm{d}x^j \tag{2.3.20}$$

where

$$g_{ij} = g_{(0)ij}(x) + \rho^{1/2} g_{(1)ij}(x) + \rho g_{(2)ij}(x) + \cdots + \rho^{\frac{d}{2}} \left(g_{(d)ij}(x) + \log(\rho) h_{(d)ij} \right) + \cdots \tag{2.3.21}$$

We will show that there exist scalar field solutions such that

$$\phi_I = \phi_{(0)I}(x) + \rho \phi_{(2)I}(x) + \cdots + \rho^{\frac{(d+1)}{2}} (\phi_{(d+1)/2I}(x) + \log(\rho)\tilde{\phi}_{(d+1)/2I}(x)) + \cdots \tag{2.3.22}$$

and the metric expansion takes the above form.

In the Fefferman-Graham coordinate system the Ricci tensor can be expressed as

$$\begin{aligned} R_{\rho\rho} =& \frac{1}{4}\mathrm{Tr}(g^{-1}g')^2 - \frac{1}{2}\mathrm{Tr}(g^{-1}g'') - \frac{d}{4\rho^2}; \\ R_{\rho j} =& \frac{1}{2}\nabla^i g'_{ij} - \frac{1}{2}\nabla_j(\mathrm{Tr}(g^{-1}g')); \\ R_{ij} =& \mathcal{R}_{ij} + (d-2)g'_{ij} + \mathrm{Tr}(g^{-1}g')g_{ij} - \rho(2g'' - 2g'g^{-1}g' + \mathrm{Tr}(g^{-1}g')g')_{ij} - d\frac{g_{ij}}{\rho}, \end{aligned} \tag{2.3.23}$$

where $\mathcal{R}$ is the curvature of g_{ij}, for which the associated connection is ∇_i.

The scalar field equations can be expressed in this coordinate system as

$$\rho^{1+\frac{d}{2}} \frac{1}{\sqrt{-g}} \partial_\rho \left(\frac{4\sqrt{-g}}{\rho^{\frac{d-1}{2}}} \frac{\partial_\rho \phi_I}{Y_I} \right) + \rho^{\frac{1}{2}} \nabla_i \left(\frac{\partial^i \phi_I}{Y_I} \right) = 0, \tag{2.3.24}$$

where implicitly $\partial^i \phi_I = g^{ij}\partial_j \phi_I$ and

$$Y_I = \sqrt{g^{jk}\partial_j\phi_I \partial_k \phi_I + 4\rho(\partial_\rho \phi_I)^2} \tag{2.3.25}$$

The trace adjusted stress energy tensor can be written as

$$\begin{aligned} \bar{T}_{\rho\rho} =& -\frac{d}{4\rho^2} + \frac{a_{1/2}}{2\rho^{3/2}} \sum_I \frac{1}{Y_I} \left(\rho \partial_\rho \phi_I \partial_\rho \phi_I + \frac{1}{4(d-1)} (g^{ij}\partial_i\phi_I \partial_j \phi_I) + \frac{\rho}{(d-1)} (\partial_\rho \phi_I)^2 \right); \\ \bar{T}_{\rho i} =& \frac{a_{1/2}}{2\rho^{1/2}} \sum_I \frac{1}{Y_I} \left(\partial_i \phi_I \partial_\rho \phi_I \right); \\ \bar{T}_{ij} =& -\frac{dg_{ij}}{\rho} + \frac{a_{1/2}}{2\rho^{1/2}} \sum_I \frac{1}{Y_I} \left(\partial_i\phi_I \partial_j \phi_I + \frac{1}{(d-1)} (g^{kl}\partial_k \phi_I \partial_l \phi_I + 4\rho(\partial_\rho \phi_I)^2) g_{ij} \right). \end{aligned} \tag{2.3.26}$$

Tracing the (ij) Einstein equations with g^{ij} gives

$$\mathcal{R} + 2(d-1)\mathrm{Tr}(g^{-1}g') - 2\rho\mathrm{Tr}(g^{-1}g'') + 2\rho\mathrm{Tr}(g^{-1}g')^2 - \rho(\mathrm{Tr}(g^{-1}g'))^2 \qquad (2.3.27)$$
$$= \frac{1}{2\rho^{1/2}} a_{1/2} \sum_I \left(\frac{\partial^i\phi\partial_i\phi}{Y_I} + \frac{d}{(d-1)} Y_I \right).$$

The latter equation is not independent but is useful in the analysis below.

The leading order term in the scalar field equation is at order $\rho^{1/2}$ and enforces

$$\phi_{(2)I} = \frac{\sqrt{g^{kl}_{(0)}\partial_k\phi_{(0)I}\partial_l\phi_{(0)I}}}{2(d-1)} \nabla_{(0)i} \left(\frac{\partial^i\phi_{(0)I}}{\sqrt{g^{kl}_{(0)}\partial_k\phi_{(0)I}\partial_l\phi_{(0)I}}} \right), \qquad (2.3.28)$$

where all indices are raised using $g^{(0)ij}$ and $\nabla_{(0)ij}$ is the connection of $g_{(0)ij}$. This expression may be written more compactly using the shorthand notation of $Y_{(0)I}$ for the square root term as

$$\phi_{(2)I} = \frac{Y_{(0)I}}{2(d-1)} \nabla_{(0)i} \left(\frac{\partial^i\phi_{(0)I}}{Y_{(0)I}} \right). \qquad (2.3.29)$$

Using the radial terms in (2.3.24) one can see that the normalizable mode of the scalar field occurs at order $(d+1)/2$ in the expansion. The coefficient of this term, $\phi_{(d+1)/2I}(x)$, is undetermined by the asymptotic analysis. In general one also needs a logarithmic term at the same order to satisfy the field equation; this term $\tilde{\phi}_{(d+1)/2I}(x)$ is determined in terms of $\phi_{(0)I}(x)$, as we will see below.

From the leading $\rho^{-3/2}$ component of the $(\rho\rho)$ Einstein equation one obtains

$$\mathrm{Tr}(g^{-1}_{(0)}g_{(1)}) = a_{1/2} \sum_I \frac{1}{(d-1)} Y_{(0)I} \qquad (2.3.30)$$

From the leading $\rho^{-1/2}$ component of the (ij) Einstein equations one finds

$$g_{(1)ij} = a_{1/2} \sum_I \frac{1}{(d-1)Y_{(0)I}} \partial_i\phi_{(0)I}\partial_j\phi_{(0)I} \qquad (2.3.31)$$

which is manifestly consistent with the trace. This equation is also consistent with the exact solution (2.3.14) expressed as a Fefferman-Graham expansion.

The expansion up to this order is sufficient to determine the counterterms

$$S_{ct} = -\frac{1}{16\pi G_{d+1}} \int \mathrm{d}^d x\sqrt{-\gamma} \left(2(1-d) + a_{1/2} \frac{1}{(d-1)} \sum_I^{d-1} \sqrt{(\partial\phi_I)^2} + \cdots \right), \qquad (2.3.32)$$

where the first term is the standard volume term derived in [15, 79]. Note that the second

counterterm can also be written as

$$\frac{1}{16\pi G_{d+1}}\int \mathrm{d}^d x\sqrt{-\gamma}\alpha_{1/2}\frac{1}{(d-1)^2}\sum_I^{d-1}\phi_I\nabla_i\left(\frac{\partial^i\phi_I}{\sqrt{(\partial\phi_I)^2}}\right), \tag{2.3.33}$$

using partial integration.

Let us now restrict to $d=2$ and calculate the conformal anomaly and the renormalized mass. We need only consider the following additional terms in the metric

$$g_{ij}=g_{(0)ij}+\rho^{1/2}g_{(1)ij}+\rho(g_{(2)ij}+\log(\rho)h_{(2)ij})+\cdots \tag{2.3.34}$$

The $(\rho\rho)$ Einstein equation at order $1/\rho$ fixes $\mathrm{Tr}(g_{(0)}^{-1}h_{(2)})=0$. From (2.3.27) we obtain

$$\begin{aligned}&\mathcal{R}+2(d-1)\mathrm{Tr}(g_{(0)}^{-1}g_2)-(d-1)\mathrm{Tr}(g_{(0)}^{-1}g_1)^2-\frac{1}{4}(\mathrm{Tr}(g_{(0)}^{-1}g_1))^2 \\ &=-a_{1/2}\sum_I\frac{(2d-1)}{4(d-1)Y_{(0)}}g_{(1)}^{jk}\partial_j\phi_{(0)I}\partial_k\phi_{(0)I},\end{aligned} \tag{2.3.35}$$

where the indices of $g_{(1)}^{ij}$ have been raised with $g_{(0)}^{-1}$. This equation can be solved to give

$$\mathrm{Tr}(g_{(0)}^{-1}g_{(2)})=-\frac{\mathcal{R}}{2(d-1)}+\frac{a_{1/2}^2}{8(d-1)^3}(\sum_I Y_{(0)I})^2+\frac{a_{1/2}^2(2d-3)}{8(d-1)^3}\sum_{I,J}\frac{X_{(0)I}^{ij}X_{(0)Jij}}{Y_{(0)I}Y_{(0)J}} \tag{2.3.36}$$

with

$$X_{(0)Iij}=\partial_i\phi_{(0)I}\partial_j\phi_{(0)I}. \tag{2.3.37}$$

The term involving the Ricci scalar agrees with [78][2]. In $d=2$ there is only one species of scalar field and the expression simplifies to give

$$\mathrm{Tr}(g_{(0)}^{-1}g_{(2)})=-\frac{\mathcal{R}}{2}+\frac{1}{4}a_{1/2}^2\partial^i\phi_{(0)}\partial_i\phi_{(0)}. \tag{2.3.38}$$

The divergence of $g_{(2)}$ is determined using the order one terms in the (ρi) Einstein equations

$$\nabla_{(0)}^i g_{(2)ij}=\frac{3a_{1/2}}{2Y_{(0)}}\partial_j\phi_{(0)}\phi_{(3)}+\cdots \tag{2.3.39}$$

In $d=2$ the rest of $g_{(2)ij}$ is not fixed, being related to the expectation value of the energy momentum tensor. The logarithmic term $h_{(2)ij}$ vanishes; one can show this using the (ij) equations at order one. Solving the scalar field equation at order ρ gives $\tilde{\phi}_{(3)}=0$, i.e. the logarithmic term in the scalar field expansion vanishes.

Using these expressions one can show that there is a logarithmic contribution to the

[2]Note that their curvature conventions differ from ours.

on-shell action in $d = 2$

$$S_{\rm div} = \frac{1}{16\pi G_3}\int \mathrm{d}^2x\sqrt{-g_{(0)}}\log\epsilon\left(\mathcal{R}(g_{(0)})\right) \tag{2.3.40}$$

which can be removed by the logarithmic counterterm

$$S_{\rm ct} = -\frac{1}{16\pi G_3}\int \mathrm{d}^2x\sqrt{-\gamma}\log\epsilon\left(\mathcal{R}(\gamma)\right). \tag{2.3.41}$$

Note that the metric variation of this term is zero, in agreement with the fact that $h_{(2)ij} = 0$.

The total action in $d = 2$ is therefore the sum of (2.3.18), (2.3.32) and (2.3.41)

$$S_{\rm ren} = S_{\rm bare} + S_{\rm ct} + S_{\rm finite}, \tag{2.3.42}$$

where the last term denotes finite counterterms, i.e. scheme dependent terms. The most relevant such term, which we will discuss further below is

$$S_{\rm finite} = \frac{\gamma_s}{16\pi G_3}\int \mathrm{d}^2x\sqrt{-\gamma}(\partial\phi)^2, \tag{2.3.43}$$

where γ_s is an arbitrary c-number.

Varying the renormalized on-shell action with respect to $g_{(0)ij}$ gives the renormalized stress energy tensor, defined as

$$\langle T_{ij}\rangle = \frac{2}{\sqrt{\det(g_{(0)})}}\frac{\delta S_{\rm Eren}}{\delta g^{ij}_{(0)}} = \lim_{\epsilon\to 0}\left(\frac{1}{\epsilon^{d/2-1}}T_{ij}[\gamma]\right). \tag{2.3.44}$$

Here we have analytically continued to Euclidean signature, under which $iS \to -S_E$ with S_E the Euclidean action. From the terms in the action involving only the metric and extrinsic curvature we obtain

$$\langle T_{ij}\rangle = \frac{1}{8\pi G_3}\left(g_{(2)ij} - \mathrm{Tr}(g^{-1}_{(0)}g_{(2)})g_{(0)ij} + \frac{1}{2}\mathrm{Tr}(g^{-1}_{(0)}g_{(1)})^2 g_{(0)ij} - \frac{1}{2}\mathrm{Tr}(g^{-1}_{(0)}g_{(1)})g_{(1)ij}\right), \tag{2.3.45}$$

in agreement with [78] when $g_{(1)ij} = 0$, and the terms involving the scalar field give

$$\langle T_{ij}\rangle = \frac{a^2_{1/2}}{8\pi G_3}\left(\frac{1}{4}\partial_k\phi_{(0)}\partial^k\phi_{(0)}g_{(0)ij} - \frac{1}{4}\partial_i\phi_{(0)}\partial_j\phi_{(0)}\right). \tag{2.3.46}$$

Combining these gives

$$\langle T_{ij}\rangle = \frac{1}{8\pi G_3}\left(g_{(2)ij} + \frac{\mathcal{R}}{2}g_{(0)ij} + a^2_{1/2}\left(-\frac{3}{4}\partial_i\phi_{(0)}\partial_j\phi_{(0)} + \frac{1}{2}(\partial\phi_{(0)})^2 g_{(0)ij}\right)\right). \tag{2.3.47}$$

Note that the additional finite counterterm (2.3.43) contributes an additional traceless scheme dependent term

$$\langle T^s_{ij}\rangle = \frac{\gamma_s}{8\pi G_3}\left(-\partial_i\phi_{(0)}\partial_j\phi_{(0)} + \frac{1}{2}(\partial\phi_{(0)})^2 g_{(0)ij}\right) \tag{2.3.48}$$

The trace gives

$$\langle T^i_i\rangle = \frac{\mathcal{R}}{16\pi G_3}, \tag{2.3.49}$$

i.e. the scalar field drops out of the conformal anomaly, as does the scheme dependent term.

The operators dual to the scalar fields similarly have expectation values defined as

$$\langle \mathcal{O}_I\rangle = \frac{1}{\sqrt{\det g_{(0)}}}\frac{\delta S_{\rm ren}}{\delta\phi_{(0)I}} = \lim_{\epsilon\to 0}\left(\frac{1}{\epsilon\sqrt{\gamma}}\frac{\delta S_{\rm ren}}{\delta\phi_I}\right). \tag{2.3.50}$$

Again this is defined in Euclidean signature. Computing this quantity in $d = 2$ gives

$$\langle\mathcal{O}\rangle = -\frac{3a_{1/2}}{16\pi G_3}\frac{\phi_{(3)}}{Y_{(0)}} + \langle\mathcal{O}^s\rangle. \tag{2.3.51}$$

As anticipated, we note that that the expectation value is the normalizable mode, divided by $Y_{(0)}$. The total scaling weight is therefore two: the dual operator is marginal, despite the fact that the normalizable modes occur at order three in the Fefferman-Graham expansion. The term $\langle\mathcal{O}^s\rangle$ denotes scheme dependent contributions; for the specific counterterm (2.3.43) we obtain

$$\langle\mathcal{O}^s\rangle = \frac{\gamma_s}{8\pi G_3}\Box\phi_{(0)}, \tag{2.3.52}$$

where $\Box$ is the d'Alambertian in the metric $g_{(0)}$.

Using (2.3.39) one can obtain the diffeomorphism Ward identity

$$\nabla^i_{(0)}\langle T_{ij}\rangle = \partial_j\phi_{(0)}\langle\mathcal{O}\rangle. \tag{2.3.53}$$

Switching on a source for $\phi_{(0)}$ which depends on the spatial coordinates, but not the time coordinate, allows momentum to be dissipated while preserving energy conservation.

For $d > 2$ we would need to work out the series expansion to higher order and compute

additional counterterms. However, the general structure will be analogous

$$\begin{aligned}\langle T_{ij}\rangle =&\frac{d}{16\pi G_{d+1}}g_{(d)ij}+\cdots \\ \langle \mathcal{O}_I\rangle =&-\frac{d+1}{16\pi G_{d+1}}\frac{a_{1/2}\phi_{(d+1)I}}{Y_{(0)I}}+\cdots ,\end{aligned} \tag{2.3.54}$$

with the ellipses denoting terms local in $g_{(0)ij}$ and $\phi_{(0)I}$. The leading term in the stress tensor involving the normalizable term in the metric expansion is as in [78].

2.3.2 Thermodynamics of brane solutions

The analysis above allows us to evaluate the on-shell action on black brane solutions (2.3.14) in $d = 2$. In three bulk dimensions the metric (2.3.14) can be rewritten in Fefferman-Graham coordinates as

$$\mathrm{d}s^2=\frac{\mathrm{d}\rho^2}{4\rho^2}+\frac{1}{\rho}\left(1+\frac{\alpha\rho^{1/2}}{4}\right)^4\left(-\mathrm{d}t^2\left(1-\frac{\alpha\rho^{1/2}}{(1+\frac{\alpha\rho^{1/2}}{4})^2}\right)+\mathrm{d}x^2\right). \tag{2.3.55}$$

where we introduce the shorthand notation $\alpha = a_{1/2}c_{1/2}$. The general solution with parameter $m_0 \neq 0$ is

$$\mathrm{d}s^2=\frac{1}{z^2}\left(-(1-\alpha z-m_0z^2)\mathrm{d}t^2+\frac{\mathrm{d}z^2}{(1-\alpha z-m_0z^2)}+\mathrm{d}x^2\right) \tag{2.3.56}$$

and it can be rewritten in Fefferman-Graham coordinates using the transformation

$$\rho^{\frac{1}{2}}=\frac{z}{1-\frac{1}{2}\alpha z+\sqrt{1-\alpha z-m_0z^2}}. \tag{2.3.57}$$

The horizons of the general solution are located at

$$z_\pm=-\frac{\alpha}{2m_0}\pm\frac{1}{2m_0}\sqrt{\alpha^2+4m_0}. \tag{2.3.58}$$

We noted previously that when $m_0 = 0$ a horizon exists only for $\alpha > 0$. When we allow for $m_0 \neq 0$, horizons exist provided that

$$m_0\geq-\frac{\alpha^2}{4};\qquad \alpha\geq 0. \tag{2.3.59}$$

When $m_0 = -\frac{\alpha^2}{4}$ the black brane is extremal. The entropy and temperature of the black brane are given by

$$\mathcal{S}=\frac{V_1}{4G_3z_+}\qquad T=\frac{m_0(z_+-z_-)}{4\pi}. \tag{2.3.60}$$

We can compute the free energy from the renormalized on-shell action. We need to distinguish between the case in which the metric has a horizon and the case in which it has a singularity as $z \to \infty$.

No horizon: In the latter case there are no contributions to the on-shell action from the $z \to \infty$ limit of the volume integral and the renormalized Euclidean on-shell action is

$$S_E^{\text{on-shell}} = -\frac{\beta_T V_1}{16\pi G_3}\left(m_0 + \frac{\alpha^2}{4} + \gamma_s c_1^2\right), \tag{2.3.61}$$

where we have included the finite counterterm (2.3.43). Here β_T is the (arbitrary) period of the imaginary time direction.

Computed on (2.3.14) the expectation value of the scalar operator is zero, which implies that the stress energy tensor is conserved. Using (2.3.55) we can read off

$$g_{(2)tt} = \frac{1}{8}\alpha^2 + \frac{1}{2}m_0; \qquad g_{(2)xx} = \frac{3}{8}\alpha^2 + \frac{1}{2}m_0, \tag{2.3.62}$$

and therefore the conserved mass is

$$\mathcal{M} = \int \mathrm{d}x \langle T_{tt}\rangle = \frac{V_1}{16\pi G_3}\left(-\frac{3}{4}\alpha^2 - \gamma_s c_{1/2}^2 + m_0\right). \tag{2.3.63}$$

The thermodynamic relation

$$-S_E^{\text{onshell}} = \beta_T F = \beta_T \mathcal{M}, \tag{2.3.64}$$

where F is the free energy, is satisfied provided that the coefficient of the scheme dependent term is

$$\gamma_s = -\frac{1}{2}a_{1/2}^2. \tag{2.3.65}$$

Therefore the scheme dependence is fixed by imposing the thermodynamic relation. Note that these solutions are not however physical as the free energy is unbounded from below; they are analogous to negative mass Schwarzschild and indeed when we consider the limit $\alpha = 0$, $m_0 < 0$ we recover negative mass BTZ.

Black brane: In the black brane case the analysis is similar, but there are contributions to the on-shell action from the horizon limit of the volume integral, resting in an on-shell action

$$S_E^{\text{on-shell}} = -\frac{\beta_T V_1}{16\pi G_3}\left(m_0 + \frac{\alpha^2}{4} + \gamma_s c_{1/2}^2 + \left(\frac{\alpha}{z_+} - \frac{2}{z_+^2}\right)\right), \tag{2.3.66}$$

Here V_1 is the regulated length of the spatial direction and β_T is the inverse temperature, which is no longer arbitrary. The conserved mass is as given in (2.3.63). The thermody-

namic relation

$$F = \mathcal{M} - T\mathcal{S} \tag{2.3.67}$$

is again satisfied provided that

$$\gamma_s = -\frac{1}{2}a_{1/2}^2. \tag{2.3.68}$$

These solutions have a mass which is bounded from below

$$\mathcal{M} \geq -\frac{V_1}{32\pi G_3}\alpha^2, \tag{2.3.69}$$

with the bound being saturated by extremal black branes. This is most easily shown by rewriting the mass as

$$\mathcal{M} = \frac{V_1}{16\pi G_3}\left(-\frac{1}{2}\alpha^2 + 4\pi^2 T^2\right), \tag{2.3.70}$$

with the first term being a Casimir term and the second term showing the expected temperature dependence for a dual 2d conformal field theory. To derive the first law, note that one should vary the entropy and mass with respect to the temperature T, keeping the parameter α fixed. Then

$$d\mathcal{M} = \frac{\pi V_1}{2G_3}TdT. \tag{2.3.71}$$

In varying the entropy, it is useful to note that

$$dz_{+|\alpha} = -2\pi z_+^2 dT \tag{2.3.72}$$

and therefore

$$d\mathcal{S} = \frac{V_1}{4G_3}\left(\frac{-dz_+}{z_+^2}\right) = \frac{\pi V_1}{2G_3}dT, \tag{2.3.73}$$

which implies that the first law $d\mathcal{M} = Td\mathcal{S}$ is indeed satisfied.

The black brane solution in $d \geq 2$ with parameter $m_0 \neq 0$ is

$$\mathrm{d}s^2 = \frac{1}{z^2}\left(-(1 - \frac{\alpha}{(d-1)}z - m_0 z^d)\mathrm{d}t^2 + \frac{dz^2}{(1 - \frac{\alpha}{(d-1)}z - m_0 z^d)} + \mathrm{d}x^2\right). \tag{2.3.74}$$

Let us denote the location of the outer horizon as z_0; it is the smallest value of z at which the blackening function has a zero. The black brane has an extremal horizon when the blackening function has a double zero at z_0; this occurs when

$$z_0 = \frac{d}{\alpha}; \qquad m_0 = -\frac{1}{(d-1)d^d}\alpha^d \tag{2.3.75}$$

and (at fixed α) smaller values of m_0 give naked singularities. The entropy and temperature are given by

$$\mathcal{S} = \frac{V_{d-1}}{4G_{d+1}z_0^{d-1}}; \qquad T = \frac{1}{4\pi}\left(\frac{d}{z_0} - \alpha\right). \tag{2.3.76}$$

Using (2.3.54) the mass is given by

$$\mathcal{M} = \frac{V_{d-1}}{16\pi G_{d+1}} \left((d-1)m_0 + \lambda \alpha^d \right), \tag{2.3.77}$$

where λ is a constant which can only be determined by computing the local terms in (2.3.54). The first law is proved as follows: to vary $\mathcal{M}$ at fixed α we use

$$dm_0 = -\frac{dz_0}{z_0^d}\left(\frac{d}{z_0} - \alpha\right) = -4\pi T \frac{dz_0}{z_0^d}. \tag{2.3.78}$$

Therefore

$$d\mathcal{M} = -\frac{V_{d-1}}{4G_{d+1}} \frac{(d-1)T dz_0}{z_0^d} = T d\mathcal{S}. \tag{2.3.79}$$

2.3.3 Two point functions

Solving (2.3.5) and (2.3.1) one can compute the two point function of the scalar operator in the conformal vacuum. The linearised equation

$$\bar{\nabla}^\mu \left(\frac{1}{\sqrt{(\partial \phi_I)^2}} \bar{\nabla}_\mu \phi_I \right) = 0, \tag{2.3.80}$$

admits solutions whose asymptotic expansion around the conformal boundary is given by (2.3.22). The two independent coefficients, $\phi_{(0)I}(x)$ and $\phi_{(d+1)I}(x)$, are related when one solves the equation throughout the bulk, imposing regularity everywhere. Regularity is however made more subtle by the fact that the backreaction on the metric occurs at the same order. The two point function for the dual scalar operator is then given by

$$\langle \mathcal{O}_I(x) \mathcal{O}_I(y) \rangle = \lim_{\phi_{(0)I} \to 0} \left(\frac{(d+1)a_{1/2}}{16\pi G_{d+1}} \frac{\delta \left(\phi_{(d+1)I}(x) / Y_{(0)I}(x) \right)}{\delta \phi_{(0)I}(y)} + \cdots \right) \tag{2.3.81}$$

where the ellipses denote contact terms. We also need to take into account the fact that the backreaction on the metric is at linear order in the amplitude of the scalar field and therefore

$$\langle T_{ij}(x) \mathcal{O}_I(y) \rangle = -\lim_{\phi_{(0)I} \to 0} \left(\frac{d}{16\pi G_{d+1}} \frac{\delta g_{(d)ij}(x)}{\delta \phi_{(0)I}(y)} + \cdots \right) \tag{2.3.82}$$

does not automatically vanish. (Again the ellipses denote contact terms.)

Equation (2.3.80) is hard to solve. Since it is a non-linear equation, one cannot Fourier transform along the x^i directions. One can solve for a single Fourier mode, i.e. letting

$$\phi_I(z, x^i) = \tilde{\phi}_I(z, k_i) e^{i k^i x_i} \tag{2.3.83}$$

the equation becomes

$$z^{d+1}\partial_z\left(\frac{1}{z^d}\frac{\partial_z\tilde{\phi}_I}{\sqrt{\left(\partial_z\tilde{\phi}_I\right)^2+k_ik^i\tilde{\phi}_I^2}}\right)=0, \tag{2.3.84}$$

where we work with the usual Poincaré coordinates for AdS_{d+1}, namely

$$\mathrm{d}s^2=\frac{1}{z^2}\left(dz^2+\mathrm{d}x^i\mathrm{d}x_i\right). \tag{2.3.85}$$

The equation can then immediately be integrated once to give

$$\frac{\partial_z\tilde{\phi}_I}{z^d}=\lambda k^d\sqrt{\left(\partial_z\tilde{\phi}_I\right)^2+k^2\tilde{\phi}_I^2} \tag{2.3.86}$$

where $k^2=k_ik^i$ and λ is a dimensionless constant. This equation can be integrated to give

$$\tilde{\phi}_I(z,k_i)=\tilde{\phi}(k_i)e^{ik^ix_i}\exp\left(\lambda\int\frac{k^{d+1}z^ddz}{\left(1-\lambda^2(kz)^{2d}\right)^{1/2}}\right). \tag{2.3.87}$$

One can fix the constant λ by imposing regularity and thereby relate the non-normalizable and normalizable modes in the asymptotic expansions. However, since one cannot linearly superpose such Fourier modes, one cannot use these solutions to compute the two point function.

Let us now consider perturbations about a background solution with non-vanishing scalar fields. The linearised problem is perfectly well-defined when the square root terms are expanded around any non-vanishing background. However, the metric and scalar field fluctuations are coupled and the equations of motion need to be diagonalised. If the scalar field fluctuations were decoupled from those of the metric, $a_{1/2}$ would need to be positive for the fluctuations to have the correct sign kinetic term (and hence, correspondingly, positive norm correlation functions in the holographically dual theory). Since the metric and scale fluctuations are coupled one cannot immediately conclude that the sign of the coefficient $a_{1/2}$ in (2.3.13) must be positive.

We can compute the linearised equations of motion around (2.3.74) as follows. We perturb the metric as $g_{\mu\nu}\to g_{\mu\nu}+h_{\mu\nu}$ and the scalar fields as $\phi_I\to\phi_I+\delta\phi_I$. Then the linearised scalar field equation is

$$\nabla_\mu\left(\frac{\nabla^\mu\delta\phi_I}{\sqrt{(\partial\phi_I)^2}}\right)-\frac{1}{2}\frac{(\nabla^\mu\phi_I)}{\sqrt{(\partial\phi_I)^2}}\nabla_\mu\left(\frac{\delta(\partial\phi_I)^2}{(\partial\phi_I)^2}\right)=\nabla_\mu\left(\frac{1}{\sqrt{(\partial\phi_I)^2}}(h^{\mu\nu}-\frac{1}{2}hg^{\mu\nu})\nabla_\nu\phi_I\right) \tag{2.3.88}$$

where we define $h=g^{\mu\nu}h_{\mu\nu}$.

The linearised Einstein equations are

$$\delta R_{\mu\nu} = -dh_{\mu\nu} + \delta\bar{T}^{(1/2)}_{\mu\nu} \tag{2.3.89}$$

where

$$\delta R_{\mu\nu} = -\frac{1}{2}\Box h_{\mu\nu} - \frac{1}{2}\nabla_\mu\nabla_\nu h + \frac{1}{2}\nabla^\rho\nabla_\mu h_{\rho\nu} + \frac{1}{2}\nabla^\rho\nabla_\nu h_{\rho\mu} \tag{2.3.90}$$

and

$$\delta\bar{T}^{(1/2)}_{\mu\nu} = \frac{a_{1/2}}{2}\sum_{I=1}^{d-1}\frac{1}{\sqrt{(\partial\phi_I)^2}}\left[\partial_\mu\phi_I\partial_\nu\delta\phi_I + \partial_\mu\delta\phi_I\partial_\nu\phi_I + \frac{1}{d-1}(\delta(\partial\phi_I)^2 g_{\mu\nu} + (\partial\phi_I)^2 h_{\mu\nu})\right.$$
$$\left. -\frac{1}{2}\frac{\delta(\partial\phi_I)^2}{(\partial\phi_I)^2}\left(\partial_\mu\phi_I\partial_\nu\phi_I + \frac{1}{d-1}(\partial\phi_I)^2 g_{\mu\nu}\right)\right] \tag{2.3.91}$$

where $\delta(\partial\phi_I)^2 = 2g^{\mu\nu}\partial_\mu\phi_I\partial_\nu\delta\phi_I - h^{\mu\nu}\partial_\mu\phi_I\partial_\nu\phi_I$. These equations are complicated, since the scalar field profiles break relativistic invariance in the d directions (t, x^I). One can however show that it is consistent to switch on only $h_{tI}(t,z)$, $h_{zI}(t,z)$ and $\delta\phi_I(t,z)$ for a given value of I; such perturbations suffice to compute the autocorrelation function. The three non-trivial equations are then the (tI) Einstein equation, the (zI) Einstein equation and the scalar field equation. Furthermore, one can choose a gauge $h_{zI} = 0$, and show explicitly that the two Einstein equations are compatible with each other. The resulting two equations are then simply

$$\delta\phi_I'' + \left(\frac{F'}{F} - \frac{d}{z}\right)\delta\phi_I' - \frac{1}{F^2}\partial_t^2\delta\phi_I = \frac{c_{1/2}}{F^2}\partial_t H_{tI}; \tag{2.3.92}$$
$$\frac{1}{2F}\partial_t H_{tI}' - \frac{a_{1/2}}{2z}\delta\phi_I' = 0,$$

where we have defined $H_{tI} = h_{tI}z^2$. One can eliminate H_{tI} by taking the z derivative of the first equation and using the second equation. Defining

$$\zeta_I = z^{-d}F\delta\phi_I' \tag{2.3.93}$$

the resulting equation is

$$z^{-d}\left(z^d F\zeta_I'\right)' - \frac{1}{F}\partial_t^2\zeta_I = \frac{1}{z}a_{1/2}c_{1/2}\zeta_I. \tag{2.3.94}$$

Note that the term on the right hand side should not be interpreted as a mass term in the usual sense, as it does not control the powers in the asymptotic expansion of the field ζ_I as $z \to 0$. Indeed ζ_I admits two independent solutions

$$\zeta_I = \zeta_{I(1-d)}(t)z^{1-d} + \cdots + \zeta_{(0)I}(t) + \frac{1}{d}c_{1/2}a_{1/2}\zeta_{(0)I}(t)z + \cdots \tag{2.3.95}$$

which in turn correspond to an expansion

$$\delta\phi_I = \delta\phi_{(0)I}(t) + \cdots + \delta\phi_{(d+1)I}(t) z^{d+1} + \cdots , \tag{2.3.96}$$

in agreement with the full non-linear expression given in (2.3.22). We can give insight into the powers arising in this expansion as follows. For a massive scalar field the on-shell action can be expressed as

$$-\int \mathrm{d}^{d+1}x\sqrt{-g}\left(\nabla^\mu\phi\nabla_\mu\phi + m^2\phi^2\right) = -\int \mathrm{d}\Sigma^\mu\phi\nabla_\mu\phi \approx -\int \mathrm{d}^d x \frac{1}{z^{d-1}}\phi\partial_z\phi \tag{2.3.97}$$

where we use the fact that the metric is asymptotically anti-de Sitter. Scale invariance requires that the non-normalizable mode of ϕ scales as $z^{d-\Delta}$ and acts as the source for an operator of dimension Δ, and the field equation determines that $\Delta(\Delta - d) = m^2$; the normalizable mode of ϕ is related to the expectation value of this operator and scales as z^Δ [19, 13].

Now let us turn to the square root model. Although the scalar field fluctuation is coupled to the metric fluctuation, the latter only affects subleading terms in the scalar field expansion near the conformal boundary: the leading asymptotics are controlled by the first two terms of the first equation in (2.3.92). Therefore we can consider only the scalar field part of the action, i.e.

$$-a_{1/2}\int \mathrm{d}^{d+1}x\sqrt{-g}\sqrt{\left(\partial\phi_I + \partial\delta\phi_I\right)^2} \tag{2.3.98}$$

Since this action is expanded around a solution of the equations of motion, the linear term in $\delta\phi_I$ automatically vanishes on-shell. The on-shell action can be expressed as a boundary term

$$-a_{1/2}\int \mathrm{d}\Sigma^\mu\left(\frac{\delta\phi_I\partial_\mu\delta\phi_1}{2\sqrt{\left(\partial\phi_I\right)^2}}\right) \tag{2.3.99}$$

which gives

$$-a_{1/2}\int \mathrm{d}^d x \frac{1}{c_{1/2}z^d}\delta\phi_I\partial_z\delta\phi_I. \tag{2.3.100}$$

Suppose the non-normalizable mode of $\delta\phi_I$ scales as z^0 and the normalizable mode scales as z^Δ. The boundary term gives a contribution of order z^0 when $\Delta = d + 1$, in agreement with (2.3.96).

The two point autocorrelation function can now be computed by solving (2.3.94) for an arbitrary boundary source $\zeta_{I(1-d)}(t)$ subject to regularity; this will determine the sub-

leading coefficients in (2.3.96) and then

$$\langle \mathcal{O}_I(t)\mathcal{O}_I(t')\rangle = \frac{(d+1)a_{1/2}}{16\pi c_{1/2}G_{d+1}}\frac{\delta\phi_{(d+1)I}(t)}{\delta\phi_{(0)I}(t')}. \tag{2.3.101}$$

It is straightforward to solve (2.3.92) in the limit $m_0 = 0$ with $c_{1/2} \to 0$, as the fields decouple and therefore one can immediately solve for the scalar field. In the frequency domain we obtain

$$\delta\phi_I(\omega) = \delta\phi_{(0)I}(\omega)(\omega z)^{(d+1)/2}K_{(d+1)/2}(\omega z), \tag{2.3.102}$$

where the Bessel function is normalised so that the asymptotic expansion takes the form (2.3.96) and implicitly we are now working in Euclidean signature. Working in $d = 2$, where the complete expression for the one point function was calculated in (2.3.51), we obtain

$$\langle \mathcal{O}_I(\omega,0)\mathcal{O}_I(-\omega,0)\rangle = \frac{a_{1/2}}{16\pi G_3}\frac{\omega^3}{c_{1/2}} + \mathcal{O}(c_{1/2}^0), \tag{2.3.103}$$

where we work in mixed representation, i.e. frequency space and position space for the spatial coordinate. This expression is not analytic as $c_{1/2} \to 0$, i.e. as the background profile for the scalar field is switched off. Recall that the general expression for the Fourier transform of a polynomial in d dimensions is

$$\int \mathrm{d}^d x e^{-i\vec{k}\cdot\vec{x}}(|x|^2)^{-\lambda} = \pi^{d/2}2^{d-2\lambda}\frac{\Gamma(d/2-\lambda)}{\Gamma(\lambda)}(|k|^2)^{\lambda-d/2}, \tag{2.3.104}$$

which is valid when $\lambda \neq (d/2+n)$, where n is zero or a positive integer. Transforming back to the (Euclidean) time domain gives

$$\langle \mathcal{O}_I(t)\mathcal{O}_I(t')\rangle = \frac{3a_{1/2}}{64\pi^2 G_3}\frac{1}{c_{1/2}|t|^4} + \mathcal{O}(c_{1/2}^0). \tag{2.3.105}$$

This condition is consistent with a positive norm provided that $a_{1/2}c_{1/2} > 0$. The off-diagonal correlation function (2.3.82) is of order $c_{1/2}$ or smaller.

2.4 Phenomenological models

In this section we will explore the properties of the following model:

$$S = \frac{1}{16\pi G_{d+1}}\int \mathrm{d}^{d+1}x\sqrt{-g}\left(R + d(d-1) - \frac{1}{4}F^2 - \sum_{I=1}^{d-1}(a_{1/2}\sqrt{(\partial\psi_I)^2} + a_1(\partial\chi_I)^2)\right) \tag{2.4.1}$$

where for clarity we now label the two families of scalar fields as ψ_I and χ_I. The equations of motion for the matter fields are

$$\nabla^\mu \left(\frac{1}{\sqrt{(\partial\psi_I)^2}} \nabla_\mu \psi_I \right) = 0; \qquad \nabla_\mu \nabla^\mu \chi_I = 0; \qquad \nabla_\mu F^{\mu\nu} = 0 \tag{2.4.2}$$

and the Einstein equation is

$$R_{\mu\nu} = -d g_{\mu\nu} + \bar{T}_{\mu\nu} \tag{2.4.3}$$

where $\bar{T}_{\mu\nu}$ is given by

$$\begin{aligned} \bar{T}_{\mu\nu} = \frac{1}{2}\left(F_{\mu\rho}F_\nu{}^\rho - \frac{1}{2(d-1)} F^2 g_{\mu\nu} \right) + \sum_{I=1}^{d-1} a_1 \partial_\mu \chi_I \partial_\nu \chi_I \\ + \sum_{I=1}^{d-1} \frac{a_{1/2}}{2\sqrt{(\partial\psi_I)^2}} \left(\partial_\mu \psi_I \partial_\nu \psi_I + \frac{1}{d-1} (\partial\psi_I)^2 g_{\mu\nu} \right). \end{aligned} \tag{2.4.4}$$

The homogeneous and isotropic black brane solutions are given by

$$\mathrm{d}s^2 = \frac{1}{z^2}\left(-F(z)\mathrm{d}t^2 + \frac{\mathrm{d}z^2}{F(z)} + \mathrm{d}x^2 \right), \tag{2.4.5}$$

with

$$F(z) = 1 - m_0 z^d + \frac{\mu^2}{\gamma^2 z_0^{2(d-2)}} z^{2(d-1)} - \frac{1}{d-1} a_{1/2} c_{1/2} z - \frac{1}{d-2} a_1 (c_1 z)^2 \tag{2.4.6}$$

where $\gamma^2 = 2(d-1)/(d-2)$ and m_0 is fixed by demanding that $F(z_0) = 0$. The Maxwell potential is

$$A = \mu \left(1 - \frac{z^{d-2}}{z_0^{d-2}} \right) \mathrm{d}t \tag{2.4.7}$$

and the scalar fields are given by

$$\chi_I = c_1 x^I; \qquad \psi_I = c_{1/2} x^I. \tag{2.4.8}$$

The temperature is given by

$$T = -\frac{F'(z_0)}{4\pi} = \frac{1}{4\pi}\left(\frac{d}{z_0} - \frac{(d-2)^2 \mu^2 z_0}{2(d-1)} - a_1 c_1^2 z_0 - a_{1/2} c_{1/2} \right). \tag{2.4.9}$$

The entropy is

$$\mathcal{S} = \frac{V_{d-1}}{4 G_{d+1} z_0^{d-1}} \tag{2.4.10}$$

and the potential Φ and charge Q are respectively

$$\Phi = \mu; \qquad Q = \frac{(d-2)V_{d-1}\mu}{16\pi G_{d+1} z_0^{d-2}}. \tag{2.4.11}$$

The charge density q is given by $Q = qV_{d-1}$. The mass is given by

$$\mathcal{M} = \frac{(d-1)}{16\pi G_{d+1}} (m_0 + \cdots) \tag{2.4.12}$$

where the ellipses denote terms involving the non-normalizable modes, i.e $\alpha \equiv a_{1/2}c_{1/2}$ and $\beta \equiv a_1 c_1^2$. This form for the mass is consistent with the mass for the standard Einstein-Maxwell system; one can show that the first law $d\mathcal{M} = Td\mathcal{S} + \Phi dQ$ is satisfied using analogous steps to those in Section 2.3.2.

Systematic holographic renormalization would be required to determine the terms in ellipses in the (2.4.12) and the free energy. The scalar field profiles are non-normalizable modes, associated with deformations of the dual field theory, and therefore the thermodynamically preferred state is that with lowest free energy at fixed $(c_{1/2}, c_1)$. It is possible that the homogeneous black branes (2.4.5) are not the thermodynamically preferred state, particularly at low temperatures, but we will not investigate phase transitions here. Note that the near horizon geometry remains $AdS_2 \times \mathbb{R}^{d-1}$, as in Reissner-Nordström, and the entropy does not vanish at zero temperature.

2.4.1 Linearised perturbations

We now consider linearised perturbations of the fields around the black brane backgrounds, such that:

$$g_{\mu\nu} \to g^{(0)}_{\mu\nu} + h_{\mu\nu}; \qquad A_\mu \to A_\mu + \delta A_\mu; \qquad \psi_I \to \psi_I + \delta\psi_I; \qquad \chi_I \to \chi_I + \delta\chi_I. \tag{2.4.13}$$

In the following, all indices will be raised and lowered using the background metric $g^{(0)}_{\mu\nu}$ and its inverse unless otherwise stated, and all covariant derivatives ∇_μ will be taken with respect to the background metric $g^{(0)}_{\mu\nu}$. Note that $g^{(0)}_{\mu\nu}$ in this section refers to the background black brane metric, and should not be confused with the leading term in the asymptotic Fefferman-Graham metric expansion, $g_{(0)ij}$.

We consider homogeneous fluctuations of the following form

$$\begin{aligned} h_{\mu\nu} &= e^{-i\omega t}\frac{1}{z^2}H_{\mu\nu}(z); & \delta A_\mu &= e^{-i\omega t}a_\mu(z); \\ \delta\psi_I &= e^{-i\omega t}\Psi_I(z); & \delta\chi_I &= e^{-i\omega t}\mathcal{X}_I(z). \end{aligned} \tag{2.4.14}$$

It is straightforward to show that the perturbations $(h_{zI}, h_{tI}, \delta A_I, \delta\chi_I, \delta\psi_I)$ decouple.

One can choose a gauge in which $h_{zI} = 0$, resulting in the following equations of motion. The scalar field equations are

$$\mathcal{X}_I'' + \left[\frac{F'}{F} - \frac{d-1}{z}\right]\mathcal{X}_I' + \frac{\omega^2}{F^2}\mathcal{X}_I - \frac{i\omega c_1}{F^2}H_{tI} = 0 \tag{2.4.15}$$

$$\Psi_I'' + \left[\frac{F'}{F} - \frac{d}{z}\right]\Psi_I' + \frac{\omega^2}{F^2}\Psi_I - \frac{i\omega c_{1/2}}{F^2}H_{tI} = 0 \tag{2.4.16}$$

The I component of the Maxwell equations and the (zI) Einstein equations are

$$a_I'' + \left[\frac{F'}{F} - \frac{d-3}{z}\right]a_I' + \frac{\omega^2}{F^2}a_I - \frac{\mu(d-2)z^{d-3}}{z_0^{d-2}F}H_{tI}' = 0 \tag{2.4.17}$$

$$\frac{i\omega}{2F}H_{tI}' - \frac{a_{1/2}}{2z}\Psi_I' - a_1c_1\mathcal{X}_I' - \frac{i\omega\mu(d-2)z^{d-1}}{2Fz_0^{d-2}}a_I = 0. \tag{2.4.18}$$

For each value of I, i.e. each spatial direction, we have four equations of motion. A homogeneous Maxwell field in the Ith direction is coupled to both the metric perturbation h_{tI} and perturbations of the scalar fields associated with this direction.

It is convenient to eliminate H_{tI} by taking the z-derivative of Equations (2.4.15–2.4.16), and using Equation (2.4.18) to eliminate H_{tI}' from the resulting equations. In the process of doing so it is also useful to introduce the following:

$$\xi_I = \omega^{-1}z^{-(d-1)}F\mathcal{X}_I', \qquad \zeta_I = \omega^{-1}z^{-d}F\Psi_I' \tag{2.4.19}$$

we can rewrite the remaining three field equations as:

$$\begin{aligned} z^{d-3}(z^{-(d-3)}Fa_I')' + \frac{\omega^2}{F}a_I =& (d-2)^2\mu^2\frac{z^{2(d-2)}}{z_0^{2(d-2)}}a_I - i(d-2)\mu a_{1/2}\frac{z^{2(d-2)}}{z_0^{d-2}}\zeta_I \\ &- 2i(d-2)\mu a_1c_1\frac{z^{2(d-2)}}{z_0^{d-2}}\xi_I \end{aligned} \tag{2.4.20}$$

$$z^{-d}(z^dF\zeta_I')' + \frac{\omega^2}{F}\zeta_I = \frac{1}{z}\frac{i(d-2)\mu c_{1/2}}{z_0^{d-2}}a_I + \frac{1}{z}a_{1/2}c_{1/2}\zeta_I + \frac{2}{z}a_1c_1c_{1/2}\xi_I \tag{2.4.21}$$

$$z^{-(d-1)}(z^{d-1}F\xi_I')' + \frac{\omega^2}{F}\xi_I = \frac{i(d-2)\mu c_1}{z_0^{d-2}}a_I + a_{1/2}c_1\zeta_I + 2a_1c_1^2\xi_I \tag{2.4.22}$$

To analyse these equations further it is convenient to rewrite the perturbation field equations in a dimensionless form by making the coordinate change $r = \mu z$, and rescaling the sets of perturbations $\bar{a}_I = \mu^{d-2}a_I$, $\bar{\zeta}_I = \zeta_I/c_{1/2}$, $\bar{\xi}_I = \mu\xi_I/c_1$. After making these

changes the field equations are simply:

$$\begin{aligned}
\ddot{\bar{a}}_I + \left[\frac{\dot{F}}{F} - \frac{d-3}{r}\right]\dot{\bar{a}}_I + \frac{\bar{\omega}^2}{F^2}\bar{a}_I =& \frac{1}{F}\left[(d-2)^2\left(\frac{r}{r_0}\right)^{2(d-2)}\bar{a}_I - i(d-2)\frac{r^{2(d-2)}}{r_0^{d-2}}\tilde{\alpha}\bar{\zeta}_I\right. \\
&\left. -i(d-2)\frac{r^{2(d-2)}}{r_0^{d-2}}\tilde{\beta}\bar{\xi}_I\right] \\
\ddot{\bar{\zeta}}_I + \left[\frac{\dot{F}}{F} + \frac{d}{r}\right]\dot{\bar{\zeta}}_I + \frac{\bar{\omega}^2}{F^2}\bar{\zeta}_I =& \frac{1}{rF}\left[\frac{i(d-2)}{r_0^{d-2}}\bar{a}_I + \tilde{\alpha}\bar{\zeta}_I + \tilde{\beta}\bar{\xi}_I\right] \\
\ddot{\bar{\xi}}_I + \left[\frac{\dot{F}}{F} + \frac{d-1}{r}\right]\dot{\bar{\xi}}_I + \frac{\bar{\omega}^2}{F^2}\bar{\xi}_I =& \frac{1}{F}\left[\frac{i(d-2)}{r_0^{d-2}}\bar{a}_I + \tilde{\alpha}\bar{\zeta}_I + \tilde{\beta}\bar{\xi}_I\right]
\end{aligned} \tag{2.4.23}$$

where $\bar{\omega} = \omega/\mu$ and $r_0 = \mu z_0$. We have also introduced the shorthand $\tilde{\alpha} = a_{1/2}c_{1/2}/\mu$ and $\tilde{\beta} = 2a_1c_1^2/\mu^2$.

It is immediately clear that these equations imply

$$r^{-d}(r^dF\dot{\bar{\zeta}}_I - r^{d-1}F\dot{\bar{\xi}}_I) + \frac{\bar{\omega}^2}{F}\left(\bar{\zeta}_I - \frac{1}{r}\bar{\xi}_I\right) = 0 \tag{2.4.24}$$

and hence there exists a quantity

$$\bar{\kappa}_I = r^dF\left(\bar{\zeta}_I - \frac{1}{r}\bar{\xi}_I\right) \tag{2.4.25}$$

that is radially conserved in the $\bar{\omega} \to 0$ limit. One can easily show that, in the near boundary limit, $\bar{\kappa}_I = O(r^{d+1})$ and hence vanishes on the conformal boundary for all $\bar{\omega}$. We know that $\bar{\kappa}_I$ is also radially conserved in the $\bar{\omega} \to 0$ limit and hence it must vanish everywhere in this limit. Consequentially we find that

$$\dot{\bar{\zeta}}_I = \frac{1}{r}\dot{\bar{\xi}}_I \tag{2.4.26}$$

in the $\bar{\omega} \to 0$ limit.

The equations can be diagonalised to show the existence of two massless modes and hence two conserved quantities in the zero frequency limit. The eigenvectors are

$$\begin{aligned}
\bar{\lambda}_{1I} =& \frac{\tilde{\beta}}{\bar{B}}\left[\bar{a}_I - \frac{i\tilde{\alpha}r_0^{d-2}}{d-2}\left(\bar{\zeta}_I - \frac{1}{r}\bar{\xi}_I\right) - \frac{i(d-2)r^{2(d-2)}}{r_0^{d-2}}\bar{\xi}_I\right]; \\
\bar{\lambda}_{2I} =& \frac{\tilde{\alpha}}{\bar{B}}\left[\frac{1}{r}\bar{a}_I + \frac{i\tilde{\beta}r_0^{d-2}}{d-2}\left(\bar{\zeta}_I - \frac{1}{r}\bar{\xi}_I\right) + \frac{i(d-2)r^{2(d-2)}}{r_0^{d-2}}\bar{\zeta}_I\right] \\
\bar{\lambda}_{3I} =& \frac{1}{\tilde{\alpha}\tilde{\beta}\bar{B}}\left[\frac{(d-2)^2}{r_0^{2(d-2)}}\bar{a}_I - \frac{i(d-2)}{r_0^{d-2}}\left(\tilde{\alpha}\bar{\zeta}_I + \tilde{\beta}\bar{\xi}_I\right)\right].
\end{aligned} \tag{2.4.27}$$

where the quantity $\bar{B}$ is defined as

$$\bar{B}(r) = \frac{\tilde{\alpha}}{r} + \tilde{\beta} + (d-2)^2 \left(\frac{r}{r_0}\right)^{2(d-2)} . \tag{2.4.28}$$

It is clear to see that $\bar{\lambda}_{1I}$ and $\bar{\lambda}_{2I}$ are massless modes as their equations of motion are:

$$\tilde{\beta} r^{d-3} \dot{\bar{\Pi}}_{1I} + \frac{\bar{\omega}^2 \bar{B}}{F} \bar{\lambda}_{1I} = \frac{i\tilde{\alpha}\tilde{\beta} r_0^{d-2}}{d-2} r^{-d} \dot{\bar{\kappa}}_I \tag{2.4.29}$$

$$\tilde{\alpha} r^{d-4} \dot{\bar{\Pi}}_{1/2I} + \frac{\bar{\omega}^2 \bar{B}}{F} \bar{\lambda}_{2I} = -\frac{i\tilde{\alpha}\tilde{\beta} r_0^{d-2}}{d-2} r^{-d} \dot{\bar{\kappa}}_I \tag{2.4.30}$$

where the two momenta are given by

$$\bar{\Pi}_{1I} = r^{-(d-3)} F \left[\dot{\bar{a}}_I + \frac{i(d-2) r^{2(d-2)}}{r_0^{d-2}} \dot{\bar{\xi}}_I \right] \tag{2.4.31}$$

$$\bar{\Pi}_{1/2I} = r^{-(d-3)} F \left[\dot{\bar{a}}_I + \frac{i(d-2) r^{2d-3}}{r_0^{d-2}} \dot{\bar{\zeta}}_I \right] \tag{2.4.32}$$

and are radially conserved in the $\bar{\omega} \to 0$ limit. It is clear that $\bar{\Pi}_{1/2I} - \bar{\Pi}_{1I} = \frac{i(d-2)}{r_0^{d-2}} \bar{\kappa}_I$ and hence not only are they conserved in the $\bar{\omega} \to 0$ limit but they are also equal throughout the bulk in this limit.

To progress further we need to work out the asymptotic expansions near the conformal boundary for the various fluctuations fields under consideration. The three sets of fields a_I, ζ_I, ξ_I have both homogeneous and inhomogeneous contributions. Since the field equations (2.4.20)-(2.4.22) are second order linear ODEs we expect each field to have two homogeneous contributions: one corresponding to a normalizable mode, and one non-normalizable. Since we are primarily interested in computing the conductivity we will turn off the non-normalizable modes for the scalar fields, which correspond to perturbing the sources for the dual operators in the field theory. (Note that the background solution still has sources for these operators.)

We make the following ansatz for the asymptotic expansions of the solutions to the full inhomogeneous equations:

$$a_I = \sum_{k=0}^{\infty} z^k a_{I(k)} + \tilde{a}_{I(d-2)} z^{d-2} \log z + \cdots \tag{2.4.33}$$

$$\zeta_I = \sum_{k=0}^{\infty} z^k \zeta_{I(k)} + \tilde{\zeta}_{I(d-1)} z^{d-1} \log z + \cdots \qquad \xi_I = \sum_{k=0}^{\infty} z^k \xi_{I(k)} + \tilde{\xi}_{I(d-2)} z^{d-2} + \cdots ,$$

where the logarithmic terms are included at the orders at which normalizable modes appear. The ellipses denote further logarithmic terms which we will not need here.

Analysis of the field equations results in the following. From the Maxwell field equation we find that as usual $a_{I(1)} = \cdots = a_{I(d-3)} = 0$ and hence the leading order terms in a_I are

$$a_I = a_{I(0)} + a_{I(d-2)} z^{d-2} + O(z^{d-1}) \tag{2.4.34}$$

where we can identify the coefficients $a_{I(0)}$ as the dual first order perturbation to the gauge potential and $a_{I(d-2)}$ is related to the expectation value of the dual current.

For the scalar fields the leading order terms in the expansions are

$$\begin{aligned} \zeta_I &= \zeta_{I(0)} + \frac{1}{d} c_{1/2} \left(i(d-2)\mu a_{I(0)} + a_{1/2}\zeta_{I(0)} + 2a_1 c_1 \xi_{I(0)} \right) z + \dots \\ \xi_I &= \xi_{I(0)} + \frac{1}{2d} c_1 \left(i(d-2)\mu a_{I(0)} + a_{1/2}\zeta_{I(0)} + 2a_1 c_1 \xi_{I(0)} \right) z^2 + \dots . \end{aligned} \tag{2.4.35}$$

The dimensionless fields therefore have the following asymptotic behaviours:

$$\begin{aligned} \bar{a}_I &= \bar{a}_{I(0)} + \bar{a}_{I(d-2)} r^{d-2} + O(r^{d-1}) & \bar{\zeta}_I &= \bar{\zeta}_{I(0)} + O(r) \\ \bar{\xi}_I &= \bar{\xi}_{I(0)} + O(r^2) & \frac{1}{\bar{B}} &= \frac{r}{\tilde{\alpha}} - \frac{\tilde{\beta} r^2}{\tilde{\alpha}^2} + O(r^3) \\ \bar{\lambda}_{1I} &= \bar{a}_{I(0)} + \cdots & \bar{\Pi}_I &= (d-2)\bar{a}_{I(d-2)} + O(r). \end{aligned} \tag{2.4.36}$$

Note that the near horizon expansions of the fields are

$$\begin{aligned} a_I &= (z - z_0)^{i\omega/F'(z_0)} [a_I^H + O((z - z_0))] \\ \zeta_I &= (z - z_0)^{i\omega/F'(z_0)} [\zeta_I^H + O((z - z_0))] \\ \xi_I &= (z - z_0)^{i\omega/F'(z_0)} [\xi_I^H + O((z - z_0))], \end{aligned} \tag{2.4.37}$$

with $(a_I^H, \zeta_I^H, \xi_I^H)$ constants, or in terms of the dimensionless fields

$$\begin{aligned} \bar{a}_I &= (r - r_0)^{i\omega/\dot{F}(r_0)} \left[\bar{a}_I^H + O((r - r_0)) \right] \\ \bar{\zeta}_I &= (r - r_0)^{i\omega/\dot{F}(r_0)} \left[\bar{\zeta}_I^H + O((r - r_0)) \right] \\ \bar{\xi}_I &= (r - r_0)^{i\omega/\dot{F}(r_0)} \left[\bar{\xi}_I^H + O((r - r_0)) \right]. \end{aligned} \tag{2.4.38}$$

where we have imposed in-falling boundary conditions on the horizon. In the zero frequency limit, $\bar{\kappa}_I$ is zero, as it must vanish at the conformal boundary and is conserved. This in turn implies that $\bar{\zeta}_I^H = \bar{\xi}_I^H / r_0$ in the zero frequency limit.

Putting this information together, one can show that a combination of the two massless modes is asymptotic to the source for the gauge field, i.e.

$$\bar{\lambda}_I = \bar{\lambda}_{1I} + \bar{\lambda}_{2I} = a_{I(0)} + O(z^2) \tag{2.4.39}$$

The equation of motion for this mode is given by

$$r^{-(d-3)}\left[\tilde{\beta}\dot{\bar{\Pi}}_{1I}+\frac{\tilde{\alpha}}{r}\dot{\bar{\Pi}}_{1/2I}\right]+\frac{\bar{\omega}^2\bar{B}}{F}\bar{\lambda}_I=0. \tag{2.4.40}$$

It is also clear that $\bar{\Pi}_{1I}$ and $\bar{\Pi}_{1/2I}$ have equivalent near-boundary behaviour:

$$\bar{\Pi}_{1I}=(d-2)\bar{a}_{I(d-2)}+O(z)=\bar{\Pi}_{1/2I} \tag{2.4.41}$$

which is not surprising as they only differ by a multiple of $\bar{\kappa}_I$ which vanishes in the $z\to 0$ limit.

It is clear from equation (2.4.40) that $\dot{\bar{\Pi}}_{1I}/\bar{\lambda}_I\sim O(\bar{\omega}^2)$ and $\dot{\bar{\Pi}}_{1/2I}/\bar{\lambda}_I\sim O(\bar{\omega}^2)$. Similarly we know that $\bar{\Pi}_{1I}/\bar{\lambda}_I\sim O(\bar{\omega})$ and $\bar{\Pi}_{1/2I}/\bar{\lambda}_I\sim O(\bar{\omega})$: these conditions are satisfied at the horizon due to ingoing boundary conditions and are conserved throughout the bulk by the field equations. We will use these properties in deriving the DC conductivity below.

Finally we note that the $\bar{\lambda}_{3I}$ field equation is given by

$$\begin{aligned}0=\bar{B}\ddot{\bar{\lambda}}_{3I}+r_0^{-2d}r^{-5}&\Big[((d-2)^2(3d-5)r_0^4r^{2d}+r_0^{2d}r^3(\tilde{\alpha}(d-2)+\tilde{\beta}r(d-1)))F\\&\qquad+r_0^{2d}r^5\dot{F}\bar{B}\Big]\dot{\bar{\lambda}}_{3I}+\frac{\bar{\omega}^2\bar{B}}{F}\bar{\lambda}_{3I}-\bar{B}^2\bar{\lambda}_{3I}\\&+r^{-6}(-\tilde{\alpha}r^3+2(d-2)^3r^{2d}r_0^{-2(d-2)})(r\dot{F}+(d-2)F)\bar{\lambda}_{3I}\\&+\frac{r_0^{-2d}r^{-7}Fr^d}{\bar{B}}(r_0^{2d}\tilde{\alpha}\tilde{\beta}r^4+(d-2)^2r^{2d}r_0^4((2d-3)^2\tilde{\alpha}+(2d-4)^2\tilde{\beta}r))\bar{\lambda}_{3I}\\&+\frac{r_0^{-2d}r^{-(d+5)}}{\tilde{\alpha}\tilde{\beta}\bar{B}}\Big(r_0^{2d}r^4\tilde{\alpha}\tilde{\beta}(\bar{\Pi}_{1I}-\bar{\Pi}_{1/2I})-(d-2)^2r^{2d}r_0^4((2d-3)\tilde{\alpha}\bar{\Pi}_{1/2I}\\&\qquad+(2d-4)\tilde{\beta}r\bar{\Pi}_{1I})\Big)\end{aligned} \tag{2.4.42}$$

and, in terms of the eigenmodes, $\bar{\Pi}_{1I}$ and $\bar{\Pi}_{1/2I}$ are given by

$$\bar{\Pi}_{1I}=r^{-(d-3)}F\left[\dot{\bar{\lambda}}_{1I}+\dot{\bar{\lambda}}_{2I}+\tilde{\alpha}\tilde{\beta}(2d-4)r^{2d-5}\bar{\lambda}_{3I}+\frac{(d-2)^2}{\tilde{\beta}}\left(\frac{r}{r_0}\right)^{2(d-2)}\dot{\bar{\lambda}}_{1I}\right] \tag{2.4.43}$$

$$\bar{\Pi}_{1/2I}=r^{-(d-3)}F\left[\dot{\bar{\lambda}}_{1I}+\dot{\bar{\lambda}}_{2I}+\tilde{\alpha}\tilde{\beta}(2d-3)r^{2d-5}\bar{\lambda}_{3I}+\frac{(d-2)^2}{\tilde{\alpha}}\left(\frac{r}{r_0}\right)^{2(d-2)}r\dot{\bar{\lambda}}_{2I}\right]. \tag{2.4.44}$$

We will use the structure of these equations to derive the DC conductivity below.

The equations of motion of the massive modes $\bar{\lambda}_{3I}$ are schematically given by

$$L_3\bar{\lambda}_{3I}+p_3(r)\bar{\lambda}_{3I}+\bar{\omega}^2q_3(r)\bar{\lambda}_{3I}\sim\bar{\Pi}_{1I} \tag{2.4.45}$$

where L_3 is a linear differential operator, and $p_3(r)$, $q_3(r)$ are functions of the radial coor-

dinate r with no frequency dependence. The massless modes only couple to $\bar{\lambda}_{3I}$ via $\bar{\Pi}_{1I}$ and the $\bar{\lambda}_{3I}$ equations of motion hence yield that $\bar{\lambda}_{3I} \sim \bar{\Pi}_I$. The conjugate momentum takes the form

$$\bar{\Pi}_{1I} = P(r)\dot{\bar{\lambda}}_I + Q(r)\bar{\lambda}_{3I} \tag{2.4.46}$$

where again $P(r)$ and $Q(r)$ are functions with no frequency dependence. From this we deduce that $\bar{\Pi}_{1I} \sim \dot{\bar{\lambda}}_I$ and hence, recalling that $\bar{\Pi}_{1I}/\bar{\lambda}_I \sim O(\bar{\omega})$, we know that $\dot{\bar{\lambda}}_I/\bar{\lambda}_I \sim O(\bar{\omega})$ as $\bar{\omega} \to 0$. We will use this property below in deriving the DC conductivity.

2.4.2 DC conductivity

In this section we will compute the DC limit of the optical conductivity. Since the equations in different spatial directions decouple, and are identical, we now restrict to perturbations in one of the boundary spatial directions which we will label by x. The optical conductivity in this direction is defined as

$$\sigma_x(\omega) = \frac{\langle J_x \rangle}{i\omega A_{x(0)}} \tag{2.4.47}$$

where $A_{x(0)}$ is the source for the x component of the boundary current and $\langle J_x \rangle$ is its expectation value. The DC conductivity is defined by

$$\sigma_{DC} = \lim_{\omega \to 0} \sigma_x(\omega), \tag{2.4.48}$$

and due to the symmetry of the background and of the equations of motion takes the same value along all spatial directions. Note that the source is given by

$$A_{x(0)} = a_{x(0)} e^{-i\omega t} \tag{2.4.49}$$

and the expectation value of the current is given by

$$\langle J_x \rangle = (d-2) a_{x(d-2)} e^{-i\omega t} + \cdots \tag{2.4.50}$$

where for notational simplicity we set $16\pi G_{d+1} = 1$ for the remainder of this section.

The holographic optical conductivity can be expressed in terms of the dimensionless fields as

$$\frac{\sigma_x(\bar{\omega})}{\mu^{d-3}} = (d-2)\frac{\bar{a}_{x(d-2)}}{i\bar{\omega}\bar{a}_{x(0)}} \tag{2.4.51}$$

with the DC conductivity being the $\bar{\omega} \to 0$ limit of this expression. Using our knowledge of the asymptotic behaviour of the massless modes and conserved quantities we now

define the auxiliary quantity

$$\sigma_{DC}(r) = \mu^{d-3} \lim_{\bar{\omega}\to 0} \frac{\bar{\Pi}_{1x}}{i\bar{\omega}\bar{\lambda}_x}. \tag{2.4.52}$$

From (2.4.39) and (2.4.41) it is clear that this quantity coincides with the DC conductivity at the conformal boundary. However, we will now show that this function is conserved to leading order in ω and it can thus be evaluated at any value of the radius.

Our equations of motion have a similar structure to those in [63, 61] and therefore the proof that (2.4.52) is a conserved quantity closely follows their proofs. Radial conservation of (2.4.52) at leading order in the frequency requires that

$$\frac{d}{dr}\left(\frac{\bar{\Pi}_{1x}}{\bar{\lambda}_x}\right) = \left(\frac{\dot{\bar{\Pi}}_{1x}}{\bar{\lambda}_x} - \frac{\bar{\Pi}_{1x}}{\bar{\lambda}_x}\frac{\dot{\bar{\lambda}}_x}{\bar{\lambda}_x}\right) = O(\bar{\omega}^2). \tag{2.4.53}$$

This result follows if the following three results hold: $\dot{\bar{\Pi}}_{1x}/\bar{\lambda}_x \sim O(\bar{\omega}^2)$; $\bar{\Pi}_{1x}/\bar{\lambda}_x \sim O(\bar{\omega})$ and $\dot{\bar{\lambda}}_x/\bar{\lambda}_x \sim O(\bar{\omega})$ as $\bar{\omega} \to 0$. However, we already showed that all three conditions hold in the previous section.

Since (2.4.52) is radially conserved we can calculate its value on the horizon giving

$$\frac{\sigma_{DC}}{\mu^{d-3}} = r_0^{-(d-3)}\left(1 + \frac{(d-2)^2}{\tilde{\beta} + \tilde{\alpha} r_0^{-1}}\right). \tag{2.4.54}$$

Reinstating all parameters explicitly we obtain

$$\sigma_{DC} = z_0^{-(d-3)}\left(1 + \frac{(d-2)^2\mu^2}{2a_1c_1^2 + z_0^{-1}a_{1/2}c_{1/2}}\right) \tag{2.4.55}$$

and consistency with [63] can be easily verified. Consistency between this result in $d = 3$ and the massive gravity results of [61] can also be seen simply by identifying $e = L = r_h = 1$, $\kappa^2 = 1/2$, and $\beta = -a_1c_1^2$, $\alpha = -a_{1/2}c_{1/2}$. Note that the DC conductivity is not temperature independent in three dimensions, whenever the square root terms are non-vanishing; we will analyse the temperature dependence below.

The background brane solutions coincide between our model and massive gravity. The DC conductivities agree since the fluctuation equations also coincide for homogeneous fluctuations carrying no spatial momenta. We show in Appednix 2.B that the fluctuation equations in our model and in massive gravity are completely equivalent at zero frequency.

2.4.3 Parameter space restrictions

At this point in our analysis we need to place restrictions on the parameter space to obtain a physical model. Any phase of our system can be fully described by three dimensionless parameters: $\tau = T/\mu$, $\tilde{\beta} = 2a_1c_1^2/\mu^2$, and $\tilde{\alpha} = a_{1/2}c_{1/2}/\mu$ where we have used the chemical potential μ to fix the scaling symmetry. Given these values we may use (2.4.9) to fix the horizon location μz_0:

$$\mu z_0 = \begin{cases} \frac{4\pi\tau+\tilde{\alpha}\pm\sqrt{(4\pi\tau+\tilde{\alpha})^2+2dP^2}}{P^2} & P^2 \neq 0 \\ \frac{d}{4\pi\tau+\tilde{\alpha}} & P^2 = 0 \end{cases} \tag{2.4.56}$$

where $P^2 = \tilde{\beta} + \frac{(d-2)^2}{d-1}$.

Positivity of the norms of the two point functions of the scalar operator dual to the massless scalar field (or, equivalently, absence of ghosts) requires that $a_1 \geq 0$. Since c_1 and μ are real, $\tilde{\beta} \geq 0$ and hence $P^2 \geq 0$. The sign of $\tilde{\alpha}$ is more subtle, as it depends on $a_{1/2}$, $c_{1/2}$ and μ. The non-linearity of the square root terms however prevents us from placing restrictions on the sign of $a_{1/2}$. Previously we showed that $a_{1/2}c_{1/2}$ should be positive when $\mu = 0 = a_1$. This suggests $\tilde{\alpha}$ should be positive, for positive μ, and negative for negative μ.

The $\tilde{\beta} \geq 0$ constraint is the only one that we can apply without direct knowledge of the sign of μ. We now consider the cases of positive and negative μ separately, imposing the following constraints:

- $T \geq 0$: The system has a non-negative temperature.
- $z_0 > 0$: The black brane horizon location is at a real and positive position in the holographic bulk direction.
- $\sigma_{DC} \geq 0$: The system has a non-negative conductivity.
- $f(z) > 0$ for $z \in (0, z_0)$: The point $z = z_0$ is indeed the true horizon location, no other horizons exist between this and the boundary.

We do not consider the $\mu = 0$ case here.

For positive chemical potential, the temperature constraint $T \geq 0$ translates simply into $\tau > 0$. Imposing $z_0 > 0$ requires the root μz_0^+ to be the horizon location. Positive DC conductivity requires

$$\frac{(d-2)^2}{\tilde{\beta} + \tilde{\alpha}(\mu z_0)^{-1}} \geq -1 \tag{2.4.57}$$

$\mu > 0$	$\mu < 0$
$a_1 > 0$	$a_1 > 0$
$a_{1/2}c_{1/2} > 0$	$a_{1/2}c_{1/2} > 0$
$\tilde{\beta} > 0$	$\tilde{\beta} > 0$
$\tilde{\alpha} \geq 0$	$\tilde{\alpha} \leq 0$
$\mu z_0 = \mu z_0^- > 0$	$\mu z_0 = \mu z_0^+ < 0$

Table 2.4.1: A summary of the restrictions on the parameter space.

since we know that $z_0 > 0$ for all μ by construction. The constraint is automatically satisfied for $\tilde{\alpha} > 0$, i.e. $a_{1/2}c_{1/2} > 0$. The constraint can be satisfied for negative $\tilde{\alpha}$, but only for a finite range of temperatures. Since we wish to consider only systems which exist for arbitrary temperatures we must therefore restrict to $\tilde{\alpha} > 0$.

Recall that our blackening function $F(z)$ is given by

$$F(z) = 1 - \frac{m_0}{\mu^d}(\mu z)^d + \frac{(d-2)(\mu z)^{2(d-1)}}{2(d-1)(\mu z_0)^{2(d-2)}} - \frac{\tilde{\alpha}(\mu z)}{d-1} - \frac{\tilde{\beta}(\mu z)^2}{2(d-2)} \tag{2.4.58}$$

where the mass parameter m_0 is given by

$$\frac{m_0}{\mu^d} = \frac{1}{(\mu z_0)^d}\left[1 - \frac{\tilde{\alpha}\mu z_0}{d-1} + (\mu z_0)^2\left(-\frac{\tilde{\beta}}{2(d-2)} + \frac{d-2}{2(d-1)}\right)\right]. \tag{2.4.59}$$

We must place the constraint that $F(z) > 0$ for all $0 \leq z < z_0$ to ensure that z_0 is in fact the true horizon of interest. This condition is equivalent to the statement that $F(z)$ has no real roots in the open interval $z \in (0, z_0)$ which we prove in the appendix.

For negative chemical potential, $\tau < 0$ and the correct choice of the horizon location is μz_0^-. Positive DC conductivity requires that $\tilde{\alpha} < 0$, so $a_{1/2}c_{1/2} > 0$. In Table 2.4.1 we summarise the restrictions necessary for a realistic model. Note that the restrictions discussed in this section do not ensure complete thermodynamic stability as other possible phases have not been investigated here.

2.4.4 DC conductivity temperature dependence

The DC conductivity of our model in terms of the dimensionless parameters is given by

$$\sigma_{DC}/\mu^{d-3} = (\mu z_0)^{-(d-3)}\left(1 + \frac{(d-2)^2}{\tilde{\beta} + (\mu z_0)^{-1}\tilde{\alpha}}\right) \tag{2.4.60}$$

The model presented in [63] found that σ_{DC} was independent of temperature in $d = 3$ at fixed $\tilde{\beta}$. This can indeed be seen from the above. Due to the presence of this additional $\tilde{\alpha}$ term and the accompanying factor of $(\mu z_0)^{-1}$ our model is *not* independent of

temperature even in $d = 3$.

Using (2.4.9) one can show that

$$\frac{d(\mu z_0)}{d\tau} = -\frac{8\pi(\mu z_0)^2(d-1)}{P^2(\mu z_0)^2 + 2d} \tag{2.4.61}$$

and thus μz_0 decreases monotonically with τ. In the bulk this corresponds to the location of the horizon moving towards the boundary as we go to higher temperatures.

One can also show that

$$\frac{d}{d\tau}\left(\frac{\sigma_{DC}}{\mu^{d-3}}\right) = -\frac{d(\mu z_0)}{d\tau}\left[(d-3)\frac{\sigma_{DC}}{\mu^{d-3}}(\mu z_0)^{-1} - \frac{(d-2)^2(\mu z_0)^{-(d-1)}\tilde{\alpha}}{\left(\tilde{\beta} + (\mu z_0)^{-1}\tilde{\alpha}\right)^2}\right] \tag{2.4.62}$$

and hence we can see that, in $d = 3$, σ_{DC} will increase (decrease) with τ if $\tilde{\alpha}$ is negative (positive). For $d > 3$, the DC conductivity always increases with temperature.

Figure 2.4.2 shows a plot of σ_{DC}/μ^{d-3} as a function of τ for various choices of $\tilde{\alpha}$ and $\tilde{\beta}$ in $d = 3$. The DC conductivity decreases linearly with temperature for $T/\mu \lesssim 0.5$ and the slope decreases at higher temperatures.

Recall that for the $\mu < 0$ plots decreasing τ corresponds to increasing T. The symmetry between the $\mu > 0$ and the $\mu < 0$ branches is easily understood because $\tilde{\alpha}(\mu z_0)^{-1}$ is invariant under $\mu \to -\mu$, $\tilde{\alpha} \to -\tilde{\alpha}$, $\tau \to -\tau$.

Shown in Figure 2.4.3 is a plot of σ_{DC}/μ^{d-3} against τ for the same choices of $\tilde{\alpha}$ and $\tilde{\beta}$ in $d = 4$. Note that the reflection symmetry between the $\mu > 0$ and $\mu < 0$ branches is broken due to σ_{DC}/μ^{d-3} gaining a minus sign due to the odd power of μ in the $\mu < 0$ branch. We note that for $d > 3$ σ_{DC} always increases with T, even in the $\tilde{\alpha} = 0$ case, whereas in $d = 3$ it is constant or decreases with T.

2.4.5 Finite frequency behaviour at low temperature

The low frequency behaviour of the AC conductivity at low temperature can be obtained by rewriting the fluctuation equations as Schrödinger equations and matching asymptotics between IR and UV regions. This technique has been applied to a number of AdS/CMT models, see for example [80, 81, 82, 83, 52, 57].

Following this framework we work in the near extremal limit and apply a matching argument to relate the IR Green's functions to the UV current-current Green's function

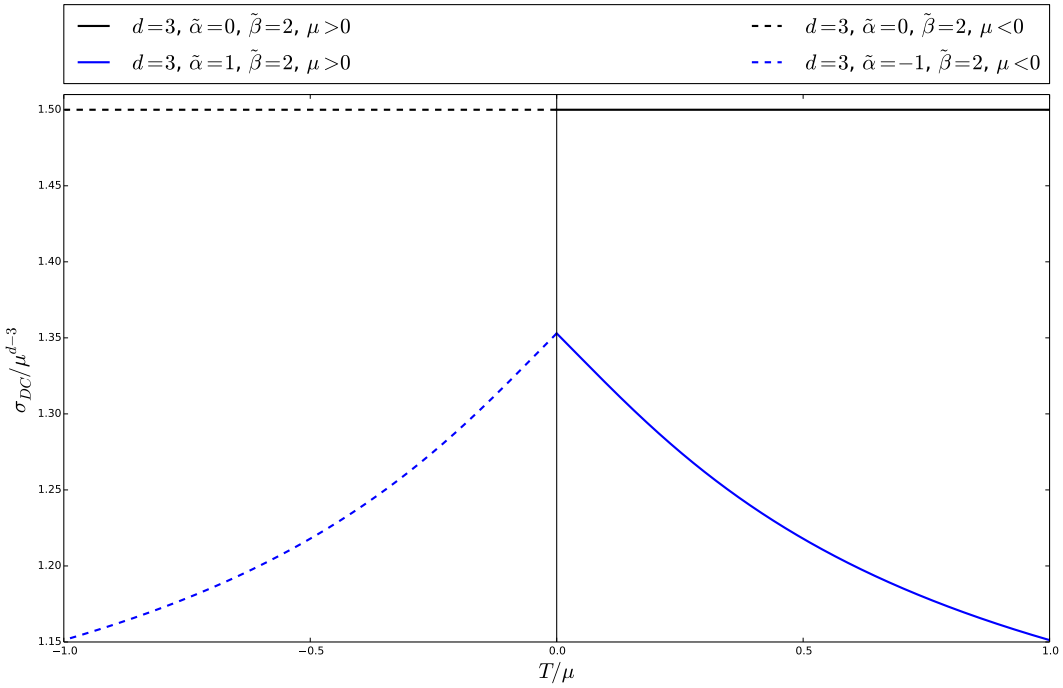

Figure 2.4.2: Plots of σ_{DC}/μ^{d-3} against T/μ in $d = 3$ for the given values of $\tilde{\alpha}$ and $\tilde{\beta}$. Solid lines denote results for the $\mu > 0$ branch, dashed lines denote results for the $\mu < 0$ branch. Note that σ_{DC} decreases with T for $\tilde{\alpha}$ non-zero.

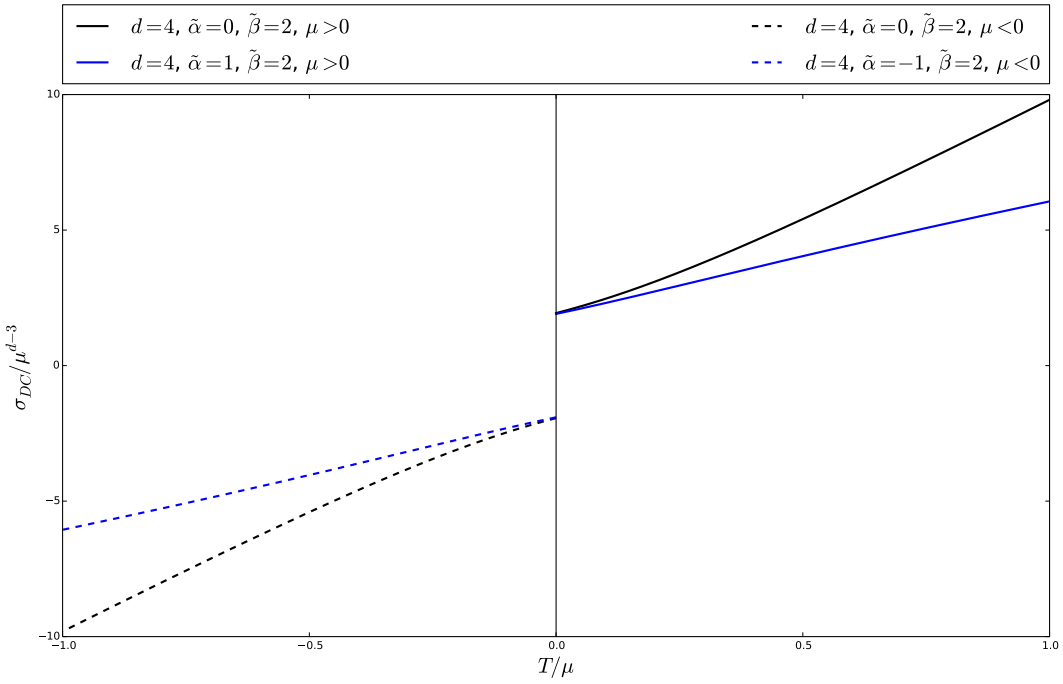

Figure 2.4.3: Plots of σ_{DC}/μ^{d-3} against T/μ in $d = 4$ for the given values of $\tilde{\alpha}$ and $\tilde{\beta}$. Note that σ_{DC} is strictly increasing in T.

via

$$\mathrm{Im}[G^R_{\mathcal{J}^x\mathcal{J}^x}(\omega,T)] = \sum_M d^M \mathrm{Im}[G^R_{\mathcal{O}_M\mathcal{O}_M}(\omega,T)] \tag{2.4.63}$$

where M runs over all the IR irrelevant operators $\mathcal{O}_M$ coupling to the current $\mathcal{J}^x$, and d^M are certain numerical constants whose values are unimportant for our discussion. The operators involved are the current itself and the two scalar operators dual to the scalar fields associated with the x direction, corresponding to the perturbations $a_x, \mathcal{X}_x, \Psi_x$.

The strategy is as follows. The fluctuation equations, after decoupling, can be brought into Schrödinger form:

$$\ddot{\bar{H}} + \omega^2 \bar{H} - V(\rho)\bar{H} = 0, \qquad V(\rho) = \frac{c_H}{\rho^2} + \ldots, \tag{2.4.64}$$

where dots denote derivatives with respect to a suitably defined radial coordinate ρ. Expressed in this form one can immediately extract the scaling behaviour for the imaginary part of the Green's function of the field H_I with dual operator $\mathcal{O}_H$ [83, 57]:

$$\mathrm{Im}[G^R_{\mathcal{O}_H\mathcal{O}_H}(\omega \ll \mu, T=0)] \sim \omega^{\sqrt{4c_H+1}}. \tag{2.4.65}$$

The scaling behaviour of the real part of the optical conductivity is then given by

$$\mathrm{Re}[\sigma(\omega \ll \mu, T=0)] = \frac{1}{\omega}\mathrm{Im}[G^R_{\mathcal{J}^x\mathcal{J}^x}(\omega \ll \mu, T=0)], \tag{2.4.66}$$

where we have used the Kramers-Kronig relation, and is therefore controlled at low frequency by the lowest (IR) dimension operator. From the analysis in the previous sections we know that our system has two massless modes, i.e. two marginal operators, and we will now show that the third mode corresponds to an irrelevant operator in the IR.

All three field equations for the linearised fluctuations involve terms of the form

$$(z^{-\delta}FH')' + \frac{\omega^2}{F}Hz^{-\delta}. \tag{2.4.67}$$

For generic δ and $H(z)$ we can bring (2.4.67) into a form more easily related to the Schrödinger form by making the change of coordinate $z \to \rho$ and change of variables $H(z) = z^{\delta/2}\bar{H}(\rho)$ where we define the radial coordinate as

$$\frac{d\rho}{dz} = F^{-1}. \tag{2.4.68}$$

Carrying out these substitutions yields:

$$(z^{-\delta}FH')' + \frac{\omega^2}{F}z^{-\delta}H = \frac{z^{-\delta/2}}{F}\left[\ddot{\bar{H}} + \omega\bar{H} - V_\delta(\rho)\bar{H}\right] \tag{2.4.69}$$

where the potential term $V_\delta(\rho)$ is given by:

$$V_\delta(\rho) = \frac{\delta}{4z^2}((\delta+2)F^2 - 2z\dot{F}). \tag{2.4.70}$$

The blackening function in near-horizon (IR) limit, in the extremal case, is given by

$$F(z) = \frac{1}{2}(z-z_0)^2 F''(z_0) + O((z-z_0)^3) \tag{2.4.71}$$

Since the extremal limit of the black-brane solution occurs when $F(z_0) = F'(z_0) = 0$ the parameters are related as follows:

$$m_0 = z_0^{-d} + \frac{\mu^2}{\gamma^2 z_0^{d-2}} - \frac{a_{1/2}c_{1/2}}{(d-1)z_0^{d-1}} - \frac{a_1 c_1^2}{(d-2)z_0^{d-2}} \tag{2.4.72}$$

$$\frac{(d-2)\mu^2 z_0^2}{\gamma^2} = d - a_{1/2}c_{1/2}z_0 - a_1 c_1^2 z_0^2. \tag{2.4.73}$$

The near horizon geometry remains $AdS_2 \times R^{d-1}$ in the presence of the scalar field profiles.

Recalling the definition (2.4.68) of ρ, the Schrödinger coordinate, it must have the following relation to z in the extremal IR limit:

$$\rho = -\frac{2}{F''(z_0)(z-z_0)} + O((z-z_0)^{-2}) \tag{2.4.74}$$

so the $z \to z_0$ limit corresponds to the $\rho \to \infty$ limit. In this limit,

$$F(\rho) = \frac{2}{F''(z_0)\rho^2} + O(\rho^{-3}), \qquad \dot{F}(\rho) = -\frac{4}{F''(z_0)\rho^3} + O(\rho^{-4}) \tag{2.4.75}$$

and thus

$$V_\alpha(\rho) = \frac{2\alpha}{F''(z_0)\rho^3 z_0} + O(\rho^4) \tag{2.4.76}$$

where

$$F''(z_0) = \frac{2d(d-1)}{z_0^2} - \frac{2d-3}{z_0}a_{1/2}c_{1/2} - 2(d-2)a_1 c_1^2 \tag{2.4.77}$$

where we have used the conditions $F(z_0) = 0$ and $F'(z_0) = 0$ to eliminate m_0 and μ^2/γ^2 respectively in terms of the other parameters. Clearly $V_\alpha \sim \rho^{-3}$ in the IR limit.

After performing the change of coordinate $z \to \rho$ as discussed above, and introducing the new variables $a_I = az^{(d-3)/2}$, $\zeta_I = \zeta z^{-d/2}$, $\xi_I = \xi z^{-(d-1)/2}$ the three field equations

read, in the IR limit:

$$\begin{aligned}
\ddot{a}+\omega^2 a &= \frac{2}{F''(z_0)\rho^2}\left[(d-2)^2\mu^2 a - i(d-2)\mu a_{1/2} z_0^{-1/2}\zeta - 2i(d-2)\mu a_1 c_1 \xi\right] + O(\rho^{-3}) \\
\ddot{\zeta}+\omega^2\zeta &= \frac{2}{F''(z_0)\rho^2}\left[i(d-2)\mu c_{1/2} z_0^{-1/2} a + a_{1/2}c_{1/2}z_0^{-1}\zeta + 2a_1 c_1 c_{1/2}\xi\right] + O(\rho^{-3}) \\
\ddot{\xi}+\omega^2\xi &= \frac{2}{F''(z_0)\rho^2}\left[i(d-2)\mu c_1 a + a_{1/2}c_1 z_0^{-1/2}\zeta + 2a_1 c_1^2\xi\right] + O(\rho^{-3}).
\end{aligned} \tag{2.4.78}$$

This system can be decoupled with the following linear combinations of fields:

$$\begin{aligned}
\lambda_1 &= a - \frac{ia_{1/2}}{\mu z_0^{1/2}(d-2)}\zeta + i\left(\frac{(d-2)\mu}{c_1} + \frac{a_{1/2}c_{1/2}}{\mu z_0(d-2)}\right)\xi \\
\lambda_2 &= a + iz_0^{1/2}\left(\frac{(d-2)\mu}{c_{1/2}} + \frac{2a_1c_1^2}{\mu c_{1/2}(d-2)}\right)\zeta - \frac{2ia_1c_1}{\mu(d-2)}\xi \\
\lambda_3 &= a - \frac{ia_{1/2}}{\mu z_0^{1/2}(d-2)}\zeta - \frac{2ia_1c_1}{\mu(d-2)}\xi
\end{aligned} \tag{2.4.79}$$

which have field equations:

$$\begin{aligned}
&\ddot{\lambda}_1+\omega^2\lambda_1 = O(\rho^{-3}); \\
&\ddot{\lambda}_2+\omega^2\lambda_2 = O(\rho^{-3}); \\
&\ddot{\lambda}_3+\omega^2\lambda_3 = \frac{2}{F''(z_0)\rho^2}\left((d-2)^2\mu^2 + 2a_1c_1^2 + a_{1/2}c_{1/2}z_0^{-1}\right)\lambda_3 + O(\rho^{-3}).
\end{aligned} \tag{2.4.80}$$

From these we can read off the various coefficients of interest to be:

$$c_{\lambda_1}=0, \quad c_{\lambda_2}=0, \quad c_{\lambda_3}=\frac{2\nu}{F''(z_0)}, \quad \nu=(d-2)^2\mu^2 + a_{1/2}c_{1/2}z_0^{-1} + 2a_1c_1^2 \tag{2.4.81}$$

and so the IR Green's functions have the following scaling behaviour:

$$\begin{aligned}
\mathrm{Im}[G^R_{\lambda_1\lambda_1}(\omega\ll\mu, T=0)]\sim\omega, \quad \mathrm{Im}[G^R_{\lambda_2\lambda_2}(\omega\ll\mu, T=0)]\sim\omega, \\
\mathrm{Im}[G^R_{\lambda_3\lambda_3}(\omega\ll\mu, T=0)]\sim\omega^{\sqrt{8\nu F''(z_0)^{-1}+1}}
\end{aligned} \tag{2.4.82}$$

Hence the dominant behaviour of the optical conductivity is

$$\mathrm{Re}[\sigma(\omega\ll\mu, T=0)]\sim\begin{cases}\omega^{\sqrt{8\nu F''(z_0)^{-1}+1}-1} & -F''(z_0)\leq 8\nu<0 \\ 1 & \nu>0\end{cases} \tag{2.4.83}$$

In the previous section we derived restrictions on our parameter space and with these restrictions $\nu\geq 0$ and thus the third operator (dual to λ_3) is irrelevant. Hence the domi-

nant behaviour of the optical conductivity is controlled by the marginal operators,

$$\mathrm{Re}[\sigma(\omega \ll \mu, T = 0)] \sim 1 \tag{2.4.84}$$

which is consistent with metallic behaviour. In the next sections we will however show that our models do not behave as ordinary metals with sharp Drude peaks but instead display features more reminiscent of heavy fermion systems.

2.4.6 Relation to Drude behaviour

As discussed in [60], in Drude metals momentum is dissipated since

$$\partial_i \langle T^{iI} \rangle = \langle J_i \rangle F^{iI} - (\epsilon + p) {\tau_r}^{-1} u^I. \tag{2.4.85}$$

Here I denotes a spatial direction; i denotes all d space-time directional J^i is the current; F^{iI} is the gauge field strength; τ_r is the relaxation constant; u^I the spatial velocity; ϵ the energy density and p the pressure. This equation reflects a loss of momentum density at a rate proportional to the velocity. Noting that in equilibrium the momentum density P^I is $T^{0I} = (\epsilon + p)u^I$, the quantity τ_r can be interpreted as the momentum relaxation timescale; the equation above is the the covariant generalisation of

$$\frac{dP^I}{dt} = qE^I - \frac{P^I}{\tau_r} \tag{2.4.86}$$

with q the charge density and E^I the electric field. In such a model the optical conductivity takes the Drude form, namely

$$\sigma(\omega) = \frac{\sigma_{DC}}{(1 - i\omega\tau_r)} \tag{2.4.87}$$

where τ_r is the relaxation time given above and the DC conductivity is σ_{DC}.

In the models analysed here, momentum relaxation is governed by the Ward identity

$$\nabla^i \langle T_{ij} \rangle = \langle J^i \rangle F_{ij} + \sum_{I=1}^{d-1} \left(\partial_j \psi_{(0)I} \langle \mathcal{O}_{\psi_I} \rangle + \partial_j \chi_{(0)I} \langle \mathcal{O}_{\chi_I} \rangle \right). \tag{2.4.88}$$

In the equilibrium black brane configurations the gauge field strength of the source F_{ij} is zero and the expectation values of the scalar operators vanish. Working to linearised order in the perturbations

$$\partial^i \langle \delta T_{ij} \rangle = q \delta F_{tj} + \sum_{I=1}^{d-1} \delta_{jI} \left(c_{1/2} \langle \delta \mathcal{O}_{\psi_I} \rangle + c_1 \langle \delta \mathcal{O}_{\chi_I} \rangle \right), \tag{2.4.89}$$

where q is the background charge density, defined below (2.4.11). The time component of this identity reduces to

$$\partial_i \langle \delta T^{i0} \rangle = 0, \tag{2.4.90}$$

so energy is conserved, but momentum is dissipated since

$$\partial^i \langle \delta T_{iI} \rangle = q \delta E_I + \left(c_{1/2} \langle \delta \mathcal{O}_{\psi_I} \rangle + c_1 \langle \delta \mathcal{O}_{\chi_I} \rangle \right). \tag{2.4.91}$$

The operator expectation values can be expressed in terms of terms in the asymptotic expansions near the conformal boundary as follows:

$$\begin{aligned} \langle \delta T_{tI} \rangle &= d(\delta g_{(d)tI}) = d e^{-i\omega t} H_{(d)tI}; \\ \delta E_I &= \partial_t \delta A_{(0)I} = -i\omega e^{-i\omega t} a_{(0)I}; \\ \langle \delta \mathcal{O}_{\psi_I} \rangle &= a_{1/2} \frac{(d+1)}{c_{1/2}} \delta \psi_{(d+1)I} = a_{1/2} \frac{(d+1)}{c_{1/2}} e^{-i\omega t} \Psi_{(d+1)I}; \\ \langle \delta \mathcal{O}_{\chi_I} \rangle &= 2 a_1 d \delta \chi_{(d)I} = 2 a_1 d e^{-i\omega t} \mathcal{X}_{(d)I}. \end{aligned} \tag{2.4.92}$$

The expressions for the stress energy tensor and the operators dual to the square root fields follow from linearising the expressions given in (2.3.54) (with $16\pi G_{d+1} = 1$). The metric and scalar field perturbations are expressed in frequency modes in (2.4.14); $H_{(n)tI}$ refers to the coefficient of the z^n term in the asymptotic expansion as $z \to 0$. The expressions for the expectation values of the operators dual to the massless scalar fields follow from those given in [25], taking into account the non-canonical normalisations of the fields.

The Ward identity (2.4.91) can therefore be expressed in terms of the following algebraic relation between terms in the asymptotic expansions of the fields:

$$i d \omega H_{(d)tI} = i\omega q a_{(0)I} + (d+1) a_{1/2} \Psi_{(d+1)I} + 2 d a_1 c_1 \mathcal{X}_{(d)I}. \tag{2.4.93}$$

This identity is the leading order component of the equation (2.4.18) as $z \to 0$; recall that the diffeomorphism Ward identity follows from the (zI) Einstein equation, which is equivalent to the (tI) Einstein equation (2.4.18). This equation is only of the form (2.4.86) if the last two terms are proportional to the momentum density, i.e. $H_{(d)tI}$, with a real coefficient of proportionality. In the linearised limit, all normalizable modes are proportional to $a_{(0)I}$ but the constants of proportionality depend on the frequency and are complex. There is no guarantee that in the $\omega \to 0$ limit the expression above can be written in the form (2.4.86) with a real relaxation constant. As we discuss in the next section, fitting the conductivity in our model to the Drude form requires a complex relaxation constant, i.e. momentum oscillations as well as dissipation.

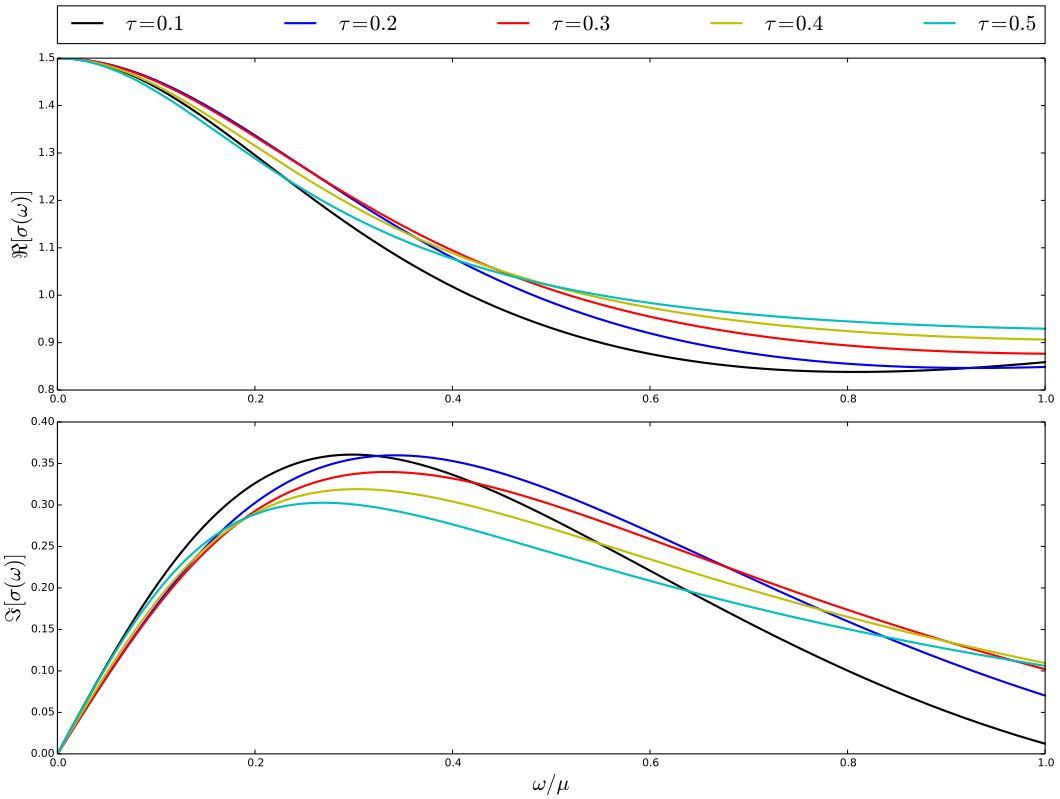

Figure 2.4.4: AC conductivity in $d = 3$ for $\tilde{\alpha} = 0, \tilde{\beta} = 2$.

2.4.7 AC conductivity numerics

In this section we explore the behaviour of the AC conductivity by numerically solving the linearised perturbations equations. To find the values of $\sigma(\omega)/\mu^{d-3}$ numerically we use a Mathematica code to solve the shooting problem of solving these ODEs with the desired near-boundary asymptotics and in-going boundary conditions at the horizon. The code calculates the r series expansions of the dimensionless perturbations near the horizon and the boundary with some randomly chosen initial data. This initial data is then used in Mathematica's `NDSolve` function to integrate the ODEs to some predetermined point in the bulk. At that point the difference between the perturbations and their first derivatives coming from the two ends is computed. The process is then repeated for some initial data that is close to the randomly chosen data to construct an approximation to the Jacobian. We then proceed via the multivariate secant method of root finding to find initial data that is a better approximation to the true data that causes the difference function to vanish. We analysed the case of $d = 3$ but qualitatively similar behaviour is likely to occur in other dimensions.

Included in Figures 2.4.4, 2.4.5, and 2.4.6 are plots of our numerical results for the temperatures $\tau = 0.1,\ 0.2,\ 0.3,\ 0.4$, and $\tau = 0.5$ with various model parameters, in all cases in $d = 3$. The numerical values of $\sigma(0)$ show good agreement with our analytic expression

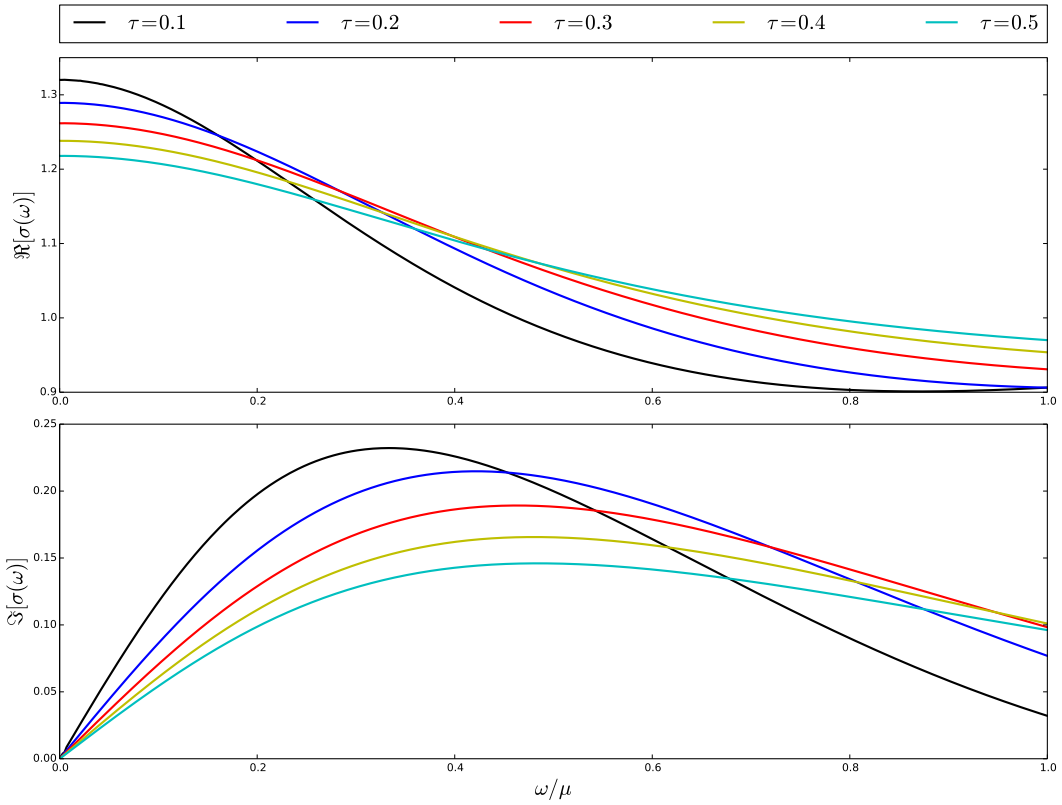

Figure 2.4.5: AC conductivity in $d = 3$ for $\tilde{\alpha} = 1, \tilde{\beta} = 2$.

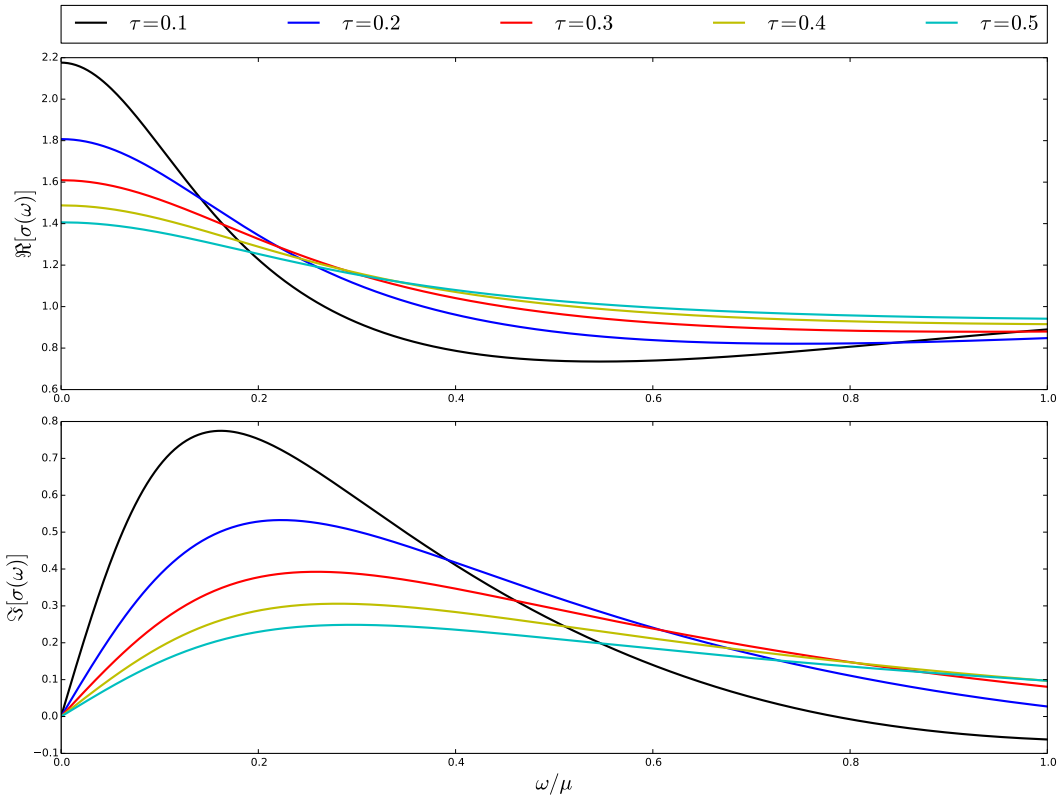

Figure 2.4.6: AC conductivity in $d = 3$ for $\tilde{\alpha} = 1, \tilde{\beta} = 0$.

for σ_{DC}, with no difference above the scale of accuracy set by our integration.

Using the numerical results one can also investigate the fit to a Drude peak at low frequency. The numerics show that one can only fit to a Drude formula using a relaxation time τ_r which is complex; therefore our system does not behave as a Drude metal even at very low temperature.

Unlike [47, 48], we see no clear signs of scaling behaviour of the optical conductivity at intermediate frequencies, $T < \omega < \mu$. The AC conductivity displays several features similar to that of heavy fermion compounds. Heavy fermion materials also have a DC resistivity which increases with temperature, with a transition from normal metal behaviour to hybridised behaviour occurring below the decoherence temperature. In the hybridised phase f-electrons hybridise with conduction electrons, leading to an enhanced effective mass and a hybridisation gap.

Figure 2.4.6 shows that the peak in the conductivity sharpens at low temperatures, and a minimum in the conductivity develops for $\tau \lesssim 0.2$ at intermediate frequencies $\omega/\mu \sim 0.5$. The minimum is enhanced by increasing $\tilde{\alpha}$ and decreasing $\tilde{\beta}$ (i.e. increasing the amplitudes of the square root scalar fields and decreasing the amplitudes of the massless scalar fields). In our models the minima in the conductivity are strong coupling phenomena, with the reduced conductivity being associated with increased amplitudes of the scalar field fluctuations at these frequencies.

There is little work in the literature about the high frequency behaviour of the optical conductivity as these systems are rarely considered at high energies. It would be interesting to see whether this increase at high ω/μ for low T/μ is realised in physical materials or in other models.

2.5 Generalised phenomenological models

In this section we consider other phenomenological models based on actions with combinations of massless scalar fields and square root terms.

2.5.1 Scalar fields identified

As we noted earlier, our results for the DC conductivity replicate the massive gravity results and indeed extend them to $d \geq 3$. To compare further with massive gravity we should identify our two sets of scalar fields: $\psi_I = \chi_I$. At the level of the action this is just

a simple substitution:

$$S = \int_{\mathcal{M}} \mathrm{d}^{d+1}\sqrt{-g}\left(R + d(d-1) - \frac{1}{4}F^2 - \sum_{I=1}^{d-1}(a_{1/2}\sqrt{(\partial\psi_I)^2} + a_1(\partial\psi_I)^2)\right) \tag{2.5.1}$$

and similarly for the Einstein equations:

$$\begin{aligned} R_{\mu\nu} = -dg_{\mu\nu} + \frac{1}{2}\left(F_{\mu\lambda}F_{\nu}{}^{\lambda} - \frac{1}{2(d-1)}F^2 g_{\mu\nu}\right) \\ + \sum_{I=1}^{d-1}\left[\frac{a_{1/2}}{2\sqrt{(\psi_I)^2}}\left(\partial_\mu\psi_I\partial_\nu\psi_I + \frac{1}{d-1}(\psi_I)^2 g_{\mu\nu}\right) + a_1\partial_\mu\psi_I\partial_\nu\psi_I\right] \end{aligned} \tag{2.5.2}$$

with the Maxwell equations being unchanged. The field equations for the scalar fields become:

$$\nabla_\mu\left[\left(2a_1 + \frac{a_{1/2}}{\sqrt{(\partial\psi_I)^2}}\right)\nabla^\mu\psi_I\right] = 0 \tag{2.5.3}$$

which clearly reduce to the field equations for the independent fields case when either one of $a_{1/2}$ or a_1 vanishes. We shall make the same ansatz for the black brane as earlier, with the blackening function being

$$F(z) = 1 - m_0 z^d + \frac{(d-2)}{2(d-1)}(\mu z_0)^2\left(\frac{z}{z_0}\right)^{2(d-1)} - \frac{\tilde{\alpha}(\mu z)}{d-1} - \frac{\tilde{\beta}(\mu z)^2}{2(d-2)} \tag{2.5.4}$$

where now $\tilde{\beta} = 2a_1c^2/\mu^2$ and $\tilde{\alpha} = a_{1/2}c/\mu$, and $\psi_I = cx^I$. This $F(z)$ was to be expected as at the level of the background spacetime imposing $\psi_I = \chi_I$ is equivalent to imposing $c_1 = c_{1/2} = c$.

Now consider homogeneous finite frequency perturbations around this background as before. The perturbation analysis for the metric and Maxwell fields is effectively unchanged whereas the scalar field perturbations $\psi_I = cx^I + e^{-i\omega t}\Psi_I(z)$ now yield:

$$0 = \left(\frac{a_{1/2}}{cz} + 2a_1\right)\left[\Psi_I'' + \left(\frac{F'}{F} - \frac{d-1}{z}\right)\Psi_I' + \frac{\omega^2}{F^2}\Psi_I - \frac{i\omega c}{F^2}H_{tI}\right. \tag{2.5.5}$$

$$\left. -c\left\{H_{zI}' + \left(\frac{F'}{F} - \frac{d-1}{z}\right)H_{zI}\right\}\right] - \frac{a_{1/2}}{cz^2}(\Psi_I' - cH_{zI}) \tag{2.5.6}$$

which reduces to either of the previous two perturbed scalar field equations in the appropriate limits. We shall once again work in the gauge $H_{zI} = 0$. The other two pertur-

bation equations are simply:

$$\frac{i\omega}{F}H_{tI}' - c\left(\frac{a_{1/2}}{cz} + 2a_1\right)\Psi_I' - \frac{i(d-2)\mu\omega z^{d-1}}{Fz_0^{d-2}}a_I = 0; \tag{2.5.7}$$
$$a_I'' + \left[\frac{F'}{F} - \frac{d-3}{z}\right]a_I' + \frac{\omega^2}{F^2}a_I - \frac{(d-2)\mu z^{d-3}}{Fz_0^{d-2}}H_{tI} = 0.$$

We can again eliminate H_{tI} from the scalar perturbation equations by defining a new variable

$$\bar{\xi}_I = \omega^{-1}z^{-(d-1)}\left(\frac{a_{1/2}}{cz} + 2a_1\right)F\Psi_I' \tag{2.5.8}$$

which yields the following pair of field equations:

$$z^{d-3}(z^{-(d-3)}Fa_I')' + \frac{\omega^2}{F}a_I = \frac{(d-2)^2\mu^2}{z_0^{2(d-2)}}z^{2(d-2)}a_I + \frac{i(d-2)\mu c}{z_0^{d-2}}z^{2(d-2)}\bar{\xi}_I; \tag{2.5.9}$$
$$\left(\frac{2a_1cz + a_{1/2}}{cz^d}\right)\left(\frac{cz^d}{2a_1cz + a_{1/2}}F\bar{\xi}_I'\right)' + \frac{\omega^2}{F}\bar{\xi}_I = -\frac{2a_1cz + a_{1/2}}{cz}\left[\frac{i(d-2)\mu c}{z_0^{d-2}}a_I - c^2\bar{\xi}_I\right],$$

which reduce to the equations found earlier and in previous works [63, 57] in the appropriate limits.

The mass matrix has vanishing determinant and as such one massless mode can be found. Consider the following combination of fields:

$$\lambda_{1I} = \frac{1}{B(z)}\left[a_I - \frac{i(d-2)\mu z^{2d-3}}{z_0^{d-2}(2a_1cz + a_{1/2})}\bar{\xi}_I\right]; \tag{2.5.10}$$
$$\lambda_{2I} = \frac{1}{B(z)}\left[\frac{(d-2)^2\mu^2 z^{2d-3}}{z_0^{2(d-2)}(2a_1c^2z + a_{1/2}c)}a_I + \frac{i(d-2)\mu z^{2d-3}}{z_0^{d-2}(2a_1cz + a_{1/2})}\bar{\xi}_I\right],$$

where the coefficient function $B(z)$ is given by

$$B(z) = 1 + \frac{(d-2)^2\mu^2 z^{2d-3}}{z_0^{2(d-2)}(2a_1c^2z + a_{1/2}c)}. \tag{2.5.11}$$

The field equations for λ_{1I} read

$$\left(z^{-(d-3)}Fa_I' - \frac{i(d-2)\mu z^d}{(2a_1cz + a_{1/2})z_0^{d-2}}F\bar{\xi}_I'\right)' + \frac{z^{3-d}\omega^2}{F}\left(a_I - \frac{i(d-2)\mu z^{2d-3}}{z_0^{d-2}(2a_1cz + a_{1/2})}\bar{\xi}_I\right) = 0 \tag{2.5.12}$$

or, equivalently,

$$z^{d-3}\Pi_I' + \frac{\omega^2 B}{F}\lambda_{1I} = 0 \tag{2.5.13}$$

where Π_I is given by

$$\Pi_I = z^{-(d-3)} F a_I' - \frac{i(d-2)\mu z^d}{(2a_1 cz + a_{1/2}) z_0^{d-2}} F \bar{\xi}_I' \tag{2.5.14}$$

and is radially conserved in the limit $\omega \to 0$.

For convenience we can rewrite Π_I in terms of the modes λ_{1I} and λ_{2I} using the following relations:

$$\begin{aligned} a_I &= \lambda_{1I} + \lambda_{2I}; \\ \bar{\xi}_I &= \frac{i(d-2)\mu}{z_0^{d-2} c} \lambda_1 - \frac{i z_0^{d-2}(2a_1 cz + a_{1/2})}{\mu(d-2) z^{2d-3}} . \lambda_2 \end{aligned} \tag{2.5.15}$$

With these relations one can show that Π is given by:

$$\Pi_I = z^{-(d-3)} F B \lambda_{1I} + (2d-3) z^{-(d-2)} \lambda_{2I} + \frac{2a_1 cz}{2a_1 cz + a_{1/2}} z^{-(d-2)} \lambda_{2I}. \tag{2.5.16}$$

Notice that, in the case $a_{1/2} = 0$, this reduces to the previously known conserved quantity of [63].

The asymptotic and near-horizon analysis performed earlier is largely unchanged. We already know the asymptotic behaviour of the Maxwell perturbation a_I:

$$a_I = a_I^{(0)} + \frac{\langle J_I \rangle e^{i\omega t}}{d-2} z^{d-2} + \dots \tag{2.5.17}$$

from our earlier analysis. It is also clear that, as long as $a_{1/2} \neq 0$, $\bar{\xi}_I$ has one normalizable mode z^0, and one non-normalizable mode $z^{-(d-1)}$. In the case $a_{1/2} = 0$ this non-normalizable mode becomes $z^{-(d-2)}$ and the analysis reduces to that in the previous work of [63]. Again we wish to turn off boundary sources for these perturbations, so we turn off non-normalizable modes. The asymptotic behaviour is thus given by

$$\bar{\xi}_I = \bar{\xi}_I^{(0)} + O(z) \tag{2.5.18}$$

The coefficient $1/B(z)$ has asymptotic behaviour given by

$$\frac{1}{B(z)} = 1 - \frac{(d-2)^2 \mu^2}{c a_{1/2} z_0^{2(d-2)}} z^{2d-3} + \dots \tag{2.5.19}$$

and hence the massless mode λ_{1I}, and conserved quantity Π_I have the following asymptotic forms

$$\lambda_{1I} = a_I^{(0)} + \dots \qquad \Pi_I = \langle J_I \rangle e^{i\omega t} + \dots \tag{2.5.20}$$

The near-horizon behaviour of the Maxwell field is unchanged:

$$a_I = (z - z_0)^{i\omega/F'(z_0)}[a_I^H + O((z - z_0))] \tag{2.5.21}$$

Making a similar ansatz as earlier one can deduce that, to leading order, we have

$$\bar{\xi}_I = (z - z_0)^{i\omega/F'(z_0)}[\bar{\xi}_I^H + O((z - z_0))] \tag{2.5.22}$$

Recalling that the optical conductivity is defined by (2.4.47) and that the DC conductivity is the $\omega \to 0$ limit of this we define the following auxiliary quantity:

$$\sigma_{DC}(z) = \lim_{\omega\to 0} \frac{\Pi_I}{i\omega\lambda_{1I}}. \tag{2.5.23}$$

Following the same steps as earlier we can show that this quantity is radially conserved and thus we may evaluate it on the horizon to find its value. Clearly $\sigma_{DC} = \lim_{z\to 0} \sigma_{DC}(z)$ from the above analysis. Hence the DC conductivity for this model is given by

$$\sigma_{DC} = \sigma_{DC}(z_0) = z_0^{-(d-3)} B(z_0) = z_0^{-(d-3)} \left(1 + \frac{(d-2)^2\mu^2}{2a_1c^2 + z_0^{-1}a_{1/2}c}\right) \tag{2.5.24}$$

This is consistent with our earlier result where the two sets of scalars were treated as independent fields and it is also consistent with [63, 61].

To understand the behaviour of the optical conductivity we first consider the low temperature, low frequency behaviour. In the extremal limit one can express the fluctuation equations near the horizon as

$$\begin{aligned} \ddot{a}_I + \omega^2 a_I &= \frac{2}{F''(z_0)\rho^2}\left[(d-2)^2\mu^2 a_I - i(d-2)\mu c z_0^{d-2}\bar{\xi}_I\right] + O(\rho^{-3}) \\ \ddot{\bar{\xi}}_I + \omega^2\bar{\xi}_I &= -\frac{2(2a_1 + \frac{a_{1/2}}{cz_0})}{F''(z_0)\rho^2}\left[i(d-2)\mu c z_0^{2-d} a_I - c^2\bar{\xi}_I\right] + O(\rho^{-3}) \end{aligned} \tag{2.5.25}$$

These equations are diagonalised by the combinations

$$\lambda_{1I} = a_I - \frac{(d-2)\mu z_0^{d-2}}{(2a_1c + a_{1/2}z_0^{-1})}\bar{\xi}_I; \qquad \lambda_{2I} = a_I + \frac{iz_0^{d-2}}{\mu(d-2)}\bar{\xi}_I, \tag{2.5.26}$$

resulting in

$$\begin{aligned} \ddot{\lambda}_{1I} + \omega^2\lambda_{1I} &= O(\rho^{-3}) \\ \ddot{\lambda}_{2I} + \omega^2\lambda_{2I} &= \frac{2}{F''(z_0)\rho^2}\left((d-2)^2\mu^2 + 2a_1c^2 + a_{1/2}cz_0^{-1}\right)\lambda_{2I} + O(\rho^{-3}). \end{aligned} \tag{2.5.27}$$

Therefore one obtains one massless mode and one (IR) irrelevant mode, whose dimension is as before, with the identification $c_1 = c_{1/2} = c$. The massless mode controls the

conductivity, which therefore has a peak at zero frequency. Since the fluctuation equations are similar to those in the previous section, we would expect qualitatively similar behaviour in this model.

2.5.2 Other square root models

The final model we will consider is

$$S = \int_{\mathcal{M}} \mathrm{d}^{d+1}x\sqrt{-g}\left(R + d(d-1) - \frac{1}{4}F^2 - a_1\sum_{I=1}^{d-1}(\partial\chi_I)^2 - a_{1/2}\sqrt{\sum_{I=1}^{d-1}(\partial\psi_I)^2}\right). \quad (2.5.28)$$

In general the scalar fields can no longer be considered independently of each other, unlike the previous case. The blackening function in this model is

$$F(z) = 1 - m_0 z^d + \frac{(d-2)^2\mu^2}{2(d-1)}\frac{z^{2(d-1)}}{z_0^{2(d-2)}} - \frac{a_1 c_1^2 z^2}{d-2} - \frac{a_{1/2}c_{1/2}z}{(d-1)^{3/2}} \quad (2.5.29)$$

which is consistent with that of massive gravity in $d = 3$. Now let us consider perturbing the background solutions:

$$\psi_I \to \psi_I + \delta\psi_I, \quad (2.5.30)$$

with corresponding perturbations of the gauge field and metric. At the level of perturbation analysis, and of the background metric, the change $\sum_I\sqrt{(\partial\psi_I)^2} \to \sqrt{\sum_I(\partial\psi_I)^2}$ is equivalent to the rescaling $a_{1/2} \to a_{1/2}/(d-1)^{1/2}$. We can show this as follows. The two Lagrangians are

$$\mathcal{L}_1 = a_{1/2}\sum_{I=1}^{d-1}\sqrt{(\partial\psi_I)^2}, \qquad \mathcal{L}_2 = a'_{1/2}\sqrt{\sum_{I=1}^{d-1}(\partial\psi_I)^2}. \quad (2.5.31)$$

When one evaluates these Lagrangians on-shell with the values $\psi_I = cx^I + \delta\psi_I(t,z)$ to leading quadratic order in the perturbations $\delta\psi_I$ one finds:

$$\mathcal{L}_1 = a_{1/2}\left((d-1)cz + \frac{1}{2cz}\sum_{I=1}^{d-1}(\partial\delta\psi_I)^2\right) \quad (2.5.32)$$

$$\mathcal{L}_2 = \frac{a'_{1/2}}{(d-1)^{1/2}}\left((d-1)cz + \frac{1}{2cz}\sum_{I=1}^{d-1}(\partial\delta\psi_I)^2\right) \quad (2.5.33)$$

which are clearly equivalent under the identification $a_{1/2} = a'_{1/2}/(d-1)^{1/2}$. Any result we found earlier for the model of Section 2.5 can therefore be applied to this model with a rescaling of $a_{1/2}$.

2.6 Conclusions

In this chapter we have focussed on simple models of explicit translational symmetry breaking. The main advantage of these models is that the brane backgrounds are isotropic and homogenous, and can therefore be constructed analytically. The holographic duals to the bulk symmetry breaking can also be explicitly identified, unlike in massive gravity models, and correspond to switching on spatial profiles for marginal couplings in the field theory.

Couplings growing linearly with spatial directions represent a qualitatively different mechanism for momentum dissipation than lattice and phonon effects in an ordinary metal. It is therefore perhaps unsurprising that our models do not exhibit ordinary metal behaviour. Nonetheless these models do show a peak in the optical conductivity at zero frequency; the DC resistivity increases linearly in temperature at low temperature in three boundary dimensions and by tuning the parameters one obtain minima in the optical conductivity at finite frequency. These features are reminiscent of strange metals and heavy fermion systems and suggest that it may be interesting to explore such models further.

The novel phenomenology is associated with the square root actions (2.1.5): when this term is switched off one does not find linear growth of the DC resistivity with temperature, for example. Despite the apparent non-locality of this action, we showed in Section 2.3 that the holographic dictionary is well-defined and one can work perturbatively about any background solution for this action. Moreover, we can view (2.1.5) as a scaling limit of a brane action (2.2.62). Brane actions exhibit no non-analytic behaviours when the background field profiles vanish and should give qualitatively similar phenomenological behaviour to (2.1.5). It would therefore be interesting to develop top-down phenomenological models based on branes, which capture the desirable features of (2.1.5).

One issue with our black brane backgrounds is that they have finite entropy at zero temperature, indicating that they may not be the preferred phase at very low temperatures. Generic Einstein-Maxwell-dilaton models admit Lifshitz and hyperscaling violating solutions whose entropy scales to zero at zero temperature, see [84, 85, 81, 82, 86, 87, 88, 89, 90, 53, 91, 92], and it would be straightforward to extend our discussion of translational symmetry breaking using massless and square root scalar fields to such models.

2.A Blackening function roots

Theorem. *Let $F(z)$ be the smooth polynomial obeying the Einstein equation and the constraints $F(0) = 1$, $F(z_0) = 0$, $F'(z_0) = -4\pi T \leq 0$, with $\tilde{\beta} > 0$ and $\tilde{\alpha}/(\mu z_0) > 0$. If z_c is*

a root of $F(z)$ in the open interval $(0, z_0)$ then $F'(z_c) < 0$.

Proof. Using the Einstein equation one can prove that at any root z_c of $F(z)$:

$$z_c F'(z_c) = -d + \frac{(d-2)}{2(d-1)}(\mu z_0)^2 \left(\frac{z_c}{z_0}\right)^{2(d-1)} + \frac{\tilde{\alpha}\mu z_c}{d-1} + \frac{\tilde{\beta}(\mu z_c)^2}{2(d-2)} \tag{2.A.1}$$

and hence one can show that

$$\begin{aligned} z_c F'(z_c) - z_0 F'(z_0) =& \frac{(d-2)}{2(d-1)}(\mu z_0)^2 \left[\left(\frac{z_c}{z_0}\right)^{2(d-1)} - 1\right] + \frac{\tilde{\alpha}\mu z_0}{d-1}\left[\frac{z_c}{z_0} - 1\right] \\ &+ \frac{\tilde{\beta}(\mu z_0)^2}{2(d-2)}\left[\left(\frac{z_c}{z_0}\right)^2 - 1\right]. \end{aligned} \tag{2.A.2}$$

Consider a root $F(z_c) = 0$ where $z_c \in (0, z_0)$. Clearly $(z_c/z_0)^n < 1$ for any positive integer $n \geq 1$. We know by assumption that $\tilde{\beta} > 0$, $(\mu z_0)^2$, $\tilde{\alpha}\mu z_0 > 0$, hence $z_c F'(z_c) < z_0 F'(z_0) = -4\pi T \leq 0$. Therefore $F'(z_c) < 0$. □

Lemma. *If $T > 0$ or $F''(z_0) > 0, T = 0$ then $F(z)$ has no roots in the open interval $(0, z_0)$. (Note that $F''(z_0)$ is automatically positive at $T = 0$ given the constraints of the previous theorem.)*

Proof of lemma. We know that, since $F'(z_0) \leq 0$ and $F''(z_0) > 0$, $F(z)$ must be positive before the root. Since we also know that $F(0) = 1$ is positive, there must be an even number of odd multiplicity roots and there can be any number of even multiplicity roots in the open interval $(0, z_0)$ to ensure that we can continue from a positive value at 0 to a positive value just before z_0.

We know that if z_c is a root, then $F'(z_c) < 0$. Thus there can be no even multiplicity roots or odd multiplicity roots of multiplicity larger than 1. This is because of the fact that if $p(x) = 0$ is a polynomial with a root at $x = x_c$ of multiplicity n, then $p'(x)$ has a root at $x = x_c$ of multiplicity $n - 1$.

We also know that if z_c is a simple root of $F(z)$ then it must have $F'(z_c) < 0$. There is no way to reconcile having a non-zero number of such roots with the requirement that $F(z)$ must be positive just before the root $z = z_0$. □

2.B DC conductivity and massive gravity

One can also obtain the DC conductivity by switching on zero frequency perturbations, i.e. working strictly in the $\omega = 0$ limit. In this case the Maxwell equation and the (tI)

components of the Einstein equation immediately decouple. The Maxwell equation is

$$a_I'' + \left[\frac{F'}{F} - \frac{d-3}{z}\right] a_I' - \frac{\mu(d-2)z^{d-3}}{F} H_{tI}' = 0 \tag{2.B.1}$$

which can be rewritten as

$$(F z^{3-d} a_I' - \mu(d-2) H_{tI})' = 0. \tag{2.B.2}$$

The Einstein equation is

$$\begin{aligned} -\frac{1}{2} F H_{tI}'' + \frac{F}{2z}(d-1) H_{tI}' + \left(\frac{F'}{z} - \frac{dF}{z^2}\right) H_{tI} = \frac{1}{2}(d-2)\mu z^{d-1} \left(-F a_I'\right. \\ \left. + \frac{d-2}{d-1} \mu z^{d-1} H_{tI}\right) + \frac{1}{2} a_{1/2} c_{1/2} z H_{tI}. \end{aligned} \tag{2.B.3}$$

In the Einstein equation, the term in the second line is the contribution from the scalar field parts of the action.

Now let us compare these equations to those arising in massive gravity. The Maxwell equation is identical and the first line in the Einstein (tI) equation is the same. The contribution in the second line is replaced by the contribution from (2.2.47). Linearizing the latter around the background solution gives

$$\delta \bar{T}_{tI} = \frac{1}{2} m^2 \alpha_1 z H_{tI}, \tag{2.B.4}$$

which using (2.2.49) implies that these perturbation equations match between massive gravity and the scalar model and therefore the DC conductivities must match.

CHAPTER 3

Real-time physics for non-relativistic holography

3.1 Introduction

The gauge/gravity duality provides a powerful framework for studying strongly coupled systems such as those present in condensed matter systems. The holographic dictionary for theories with relativistic scaling symmetries has been well established in the literature for both Euclidean and Lorentzian signature bulk geometries, or equivalently for Wick rotated and non-Wick rotated boundary theories. There are a variety of physical systems that are thought to be described by strongly coupled field theories with a non-relativistic scaling symmetry:

$$t \to t' = \lambda^z t; \qquad x^i \to x'^i = \lambda x^i \tag{3.1.1}$$

in contrast to the relativistic scaling symmetry ($z = 1$) that is often present in systems with holographic duals. There are two common symmetry groups which possess such a non-relativistic scaling symmetry, namely the Schrödinger group $\mathrm{Sch}_D(z)$ and the Lifshitz group $\mathrm{Lif}_D(z)$. The corresponding holographic dictionary for theories with a dual Lifshitz symmetry has been established [93] and the recent progress on the holographic modelling of such theories was reviewed in [37].

Holographic descriptions of field theories which possess either of these non-relativistic symmetry groups requires a geometry that realises these symmetries asymptotically.

Such geometries have been proposed both for the Schrödinger [94] and Lifshitz [84] groups:

$$\mathrm{Sch}_D(z): \qquad \mathrm{d}s^2 = -\frac{b^2 \mathrm{d}x^{+2}}{r^{2z}} + \frac{1}{r^2}(\mathrm{d}r^2 + \mathrm{d}x^i \mathrm{d}x_i + 2\mathrm{d}x^+ \mathrm{d}x^-) \tag{3.1.2}$$

$$\mathrm{Lif}_D(z): \qquad \mathrm{d}s^2 = -\frac{\mathrm{d}t^2}{r^{2z}} + \frac{1}{r^2}(\mathrm{d}r^2 + \mathrm{d}x^i \mathrm{d}x_i) \tag{3.1.3}$$

where the boundary is located at $r \to 0$ and $b \neq 0$ is a free parameter that can be removed through rescalings of the null coordinates in the Schrödinger geometry. These geometries are manifestly invariant under the respective symmetry groups asymptotically, and are also invariant under the scaling symmetry

$$\begin{aligned} \mathrm{Sch}_D(z): &\quad x^+ \to \lambda^z x^+; \quad x^- \to \lambda^{2-z} x^-; \quad x^i \to \lambda x^i; \quad r \to \lambda r \\ \mathrm{Lif}_D(z): &\quad t \to \lambda^z t; \quad x^i \to \lambda x^i; \quad r \to \lambda r. \end{aligned} \tag{3.1.4}$$

Note that when $b = 0$ the Schrödinger geometry becomes AdS_{D+3} in double null coordinates. This is unsurprising as the Schrödinger group is a subgroup of the $D+2$ conformal group, and so the dual geometry can be obtained via a deformation of AdS_{D+3}. This fact will reappear later in the discussion of scalar correlation functions in the Schrödinger spacetime in Section 3.4.2.

As with their relativistic counterparts, these systems have almost exclusively been studied in their Wick-rotated Euclidean analogue where it is technically easier to obtain correlation functions, with Lorentzian signature correlators being obtained through analytic continuation. This is often the most direct way of obtaining a result, however there are many cases where performing the analytic continuation back is technically difficult even though it is in theory possible. Such cases include the study of time dependent phenomena, systems that involve gauge theories in non-trivial pure or mixed states, systems with non-stationary bulk geometries, or more complicated correlators such as a thermal correlator.

The framework for performing holography in real-time has been previously developed for relativistic systems in [21]. In this chapter we aim to extend this prescription to holographic models of systems with dual Lifshitz or Schrödinger symmetries. In Section 3.2 we will review the formalism for performing real time QFT calculations and the corresponding holographic prescription of [21] with some relativistic examples. In Section 3.3 we apply the standard real time QFT framework to a toy model of a free scalar with a $z = 2$ Lifshitz symmetry. We then progress to the holographic modelling of systems with Schrödinger symmetry in Section 3.4 and attempt to apply the real time holography prescription to a free scalar operator. We then perform a similar analysis for holographic models with Lifshitz symmetry in Section 3.5. We conclude in Section 3.6.

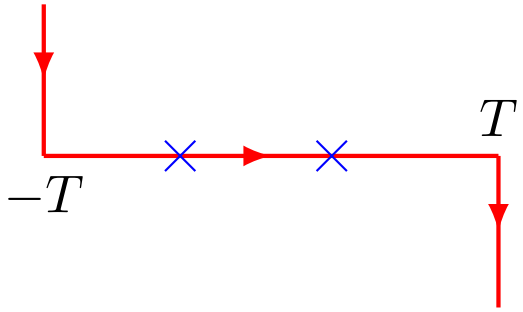

Figure 3.2.1: The contour used for calculating vacuum to vacuum amplitudes.

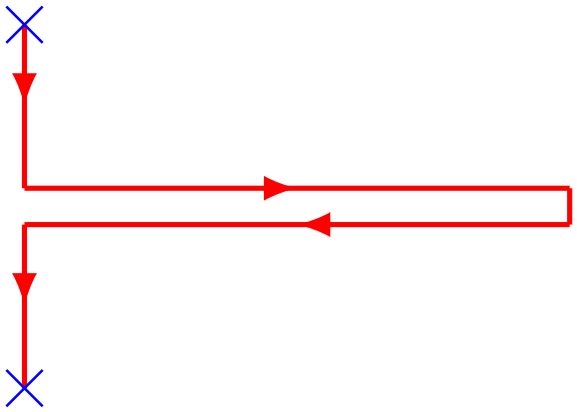

Figure 3.2.2: The contour used for calculating in-in amplitudes.

3.2 Real time QFT and holography

Consider a d-dimensional quantum field theory defined on a Lorentzian space-time with coordinates $(t, \mathbf{x})$, and a set of fundamental fields collectively labelled $\phi(t, \mathbf{x})$ and Lagrangian density $\mathcal{L}[\phi]$. Real-time correlation functions are then computable by specifying a contour in the complex t plane for the path integral. The pure imaginary segments of the contours prepare the initial and final states, and operator insertions lie along the real segments to form n-point contour time ordered correlators.

Commonly used contours include the vacuum-to-vacuum, in-in, and real-time thermal contours. Contour 3.2.1 is used to calculate vacuum to vacuum amplitudes such as $\langle 0, T|\mathcal{O}\cdots|0, -T\rangle$, where the operators are inserted along the Lorentzian part of the contour. Similarly Figure 3.2.2 calculates the in-in contour $\langle\Psi|\mathcal{O}|\Psi\rangle$ where the state $|\Psi\rangle$ is prepared by the initial and final imaginary contour segments via operator insertions and finite integration range.

One can define a generating functional of correlation functions of gauge-invariant operators in non-trivial states which can be constructed from a contour $\mathcal{C}$ via the following

path integral:

$$Z_{QFT}[\phi^I_{(0)};\mathcal{C}] = \int_{\mathcal{C}}[\mathcal{D}\phi]\exp\left(i\int_C \mathrm{d}t\int \mathrm{d}^{d-1}\mathbf{x}\left(\mathcal{L}[\phi]-\phi^I_{(0)}\mathcal{O}_I[\phi]\right)\right). \tag{3.2.1}$$

The desired correlation functions can then be found by specifying the desired contour to prepare the states and the type of correlation function, and then functionally differentiating the sources $\phi^I_{(0)}$ and setting them to zero in the result to choose the operator insertions.

When computing such a generating functional in a relativistic field theory one has to compute the propagator for the corresponding differential operator. In Lorentzian signature there are three distinct propagators that one can compute: the Feynman, the retarded, and the advanced propagators. Each propagator is defined uniquely by an $i\varepsilon$ insertion in the propagator integrand.

3.2.1 Review of scalar field correlation functions in AdS

We now review the holographic approach to real-time correlation functions developed in [21]. This prescription relies on the complex time contour dependence of the correlation functions: one constructs bulk manifolds for each section of the contour, with Euclidean signature manifolds being used for the vertical (imaginary time) segments, and Lorentzian signature manifolds used for the horizontal (real-time) segments. The manifolds are then glued together on hypersurfaces dictated by the contour, with matching conditions are imposed on the fields for consistency. Specifically the two matching conditions are:

1. Continuity of all bulk fields on the matching surfaces.

2. Continuity of all canonical momenta conjugate to bulk fields where these momenta are defined with respect to the complex contour time coordinate.

i.e. fields should be at least C^1 continuous. One can continue to perform holographic renormalization in the Lorentzian manifolds as in the Euclidean ones as the procedure of holographic renormalization is independent of the signature of the spacetime in question. For further details about the holographic renormalization of fields in real-time holography readers should consult [21].

To demonstrate the procedure we will briefly review the example of scalar two point functions analysed in [21]. In this example we are interested in computing the vacuum-to-vacuum time-ordered two point scalar function for a CFT. The relevant bulk manifold is illustrated in Figure 3.2.3.

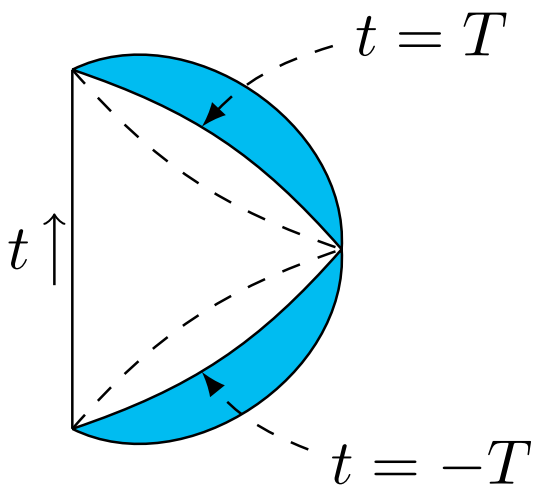

Figure 3.2.3: The bulk manifold used for calculating in-in amplitudes.

Consider a minimally coupled massive scalar field Φ with action:

$$S = -\frac{1}{2}\int \mathrm{d}^{d+1}x\sqrt{-g}(g^{\mu\nu}\partial_\mu\Phi\partial_\nu\Phi + m^2\Phi^2). \tag{3.2.2}$$

To calculate correlation functions we need to find the on-shell action, for solutions that are regular throughout the bulk manifold and which have generic boundary sources in the Lorentzian sections. To this end we need to find the most general solution to the Klein-Gordon equation in the Lorentzian background with non-normalizable asymptotics near the boundary and finiteness in the interior. We do this by constructing the bulk-boundary propagator that reconstructs the full bulk solution given given boundary data.

The solutions on the Euclidean caps can be obtained via the substitution $t \to -i\tau$. There are no sources on these caps so we need only normalizable modes. Furthermore finiteness as $\tau \to \pm\infty$ in general requires that we restrict to negative frequencies on the lower cap and positive ones on the upper cap.

3.2.1.1 Global AdS_3

The Lorentzian metric for global AdS_3 is

$$\mathrm{d}s^2 = -(\rho^2+1)\mathrm{d}t^2 + \frac{\mathrm{d}\rho^2}{(\rho^2+1)} + \rho^2\mathrm{d}\phi^2, \tag{3.2.3}$$

and the Euclidean metric can be obtained by the substitution $t = -i\tau$. In the Lorentzian mode solutions to the scalar field equation behave as

$$e^{i\omega t + ik\phi} f(\omega, |k|, \rho) \tag{3.2.4}$$

where $f(\omega, k, r)$ is expressed in terms of hypergeometric functions as

$$f(\omega, k, \rho) = C_{\omega k l} r^k F((\omega + k + 1 + l)/2, (\omega + k + 1 - l); k + 1; -\rho^2) \tag{3.2.5}$$

with the scalar operator dimension being $\Delta = l + 1$ where l is an integer. Here $C_{\omega k l}$ is a normalisation factor chosen such that the coefficient approaches one as $\rho \to \infty$. The mode solutions are chosen to be regular as $\rho \to 0$. By construction therefore these modes can be used to construct a bulk boundary propagator with a delta function source on the boundary:

$$\begin{aligned} \Phi(t, \phi, \rho) = \frac{1}{4\pi^2} \sum_k \int_C \mathrm{d}\omega \int \mathrm{d}\hat{t}\mathrm{d}\hat{\phi} e^{-i\omega(t-\hat{t}) + ik(\phi - \hat{\phi})} \phi_{(0)}(\hat{t}, \hat{\phi}) f(\omega, |k|, \rho) \\ + \sum_{\pm, k, n} c^{\pm}_{nk} e^{-i\omega^{\pm}_{nk} t + ik\phi} g(\omega_{nk}, |k|, \rho) \end{aligned} \tag{3.2.6}$$

Here $\phi_{(0)}(t, \phi)$ is the boundary source, while the second line gives the normalizable modes. When the frequency equals

$$\omega = \omega^{\pm}_{nk} = \pm(2n + |k| + 1 + l) \tag{3.2.7}$$

with n an integer, terms in the radial expansion of $f(\omega, |k|, \rho)$ being singular. One therefore needs to define a colour around these poles. The difference between any choices of contours is a sum over the residues

$$g(\omega_{nk}, k, \rho) = \oint_{\omega_{nk}} \mathrm{d}\omega f(\omega_{nk}, k, \rho). \tag{3.2.8}$$

These normalizable modes can be added at will to any solution, and therefore they appear in (3.2.6) with arbitrary coefficients $c^{\pm}_{nk}$. The choice of contour C, together with initial and final data, then fixes the $c^{\pm}_{nk}$.

On the Euclidean segments the mode solutions are obtained by replacing $t = -i\tau$. Since there are no sources on the Euclidean boundaries, the solutions consist of only normalizable modes, i.e.

$$\Phi_E(\tau, \phi, \rho) = \sum_{\pm, k, n} d^{\pm}_{nk} e^{-\omega^{\pm}_{nk}\tau + ik\phi} g(\omega_{nk}, |k|, \rho) \tag{3.2.9}$$

with coefficients $d^{\pm}_{nk}$ which are determined by matching conditions. Finiteness as $\tau \to \infty$ implies that $d^{-}_{nk} = 0$, while finiteness as $\tau \to \infty$ implies $d^{+}_{nk} = 0$.

We choose Euclidean time coordinates as $-\infty < \tau < 0$ on the initial cap, with $T < \tau < \infty$ on the final cap. On the Lorentzian segment we let t range from 0 to T. The matching conditions are then given by

$$\begin{aligned} \Phi(t=0,\phi,\rho) &= \Phi_E(\tau=0,\phi,\rho) \qquad & i\partial_t\Phi(t=,\phi,\rho) + \partial_\tau\Phi_E(\tau=0,\phi,\rho) &= 0 \\ \Phi(t=T,\phi,\rho) &= \Phi_E(\tau=T,\phi,\rho) & i\partial_t\Phi(t=T,\phi,\rho) - \partial_\tau\Phi_E(\tau=T,\phi,\rho) &= 0 \end{aligned} \tag{3.2.10}$$

Let us then choose the Feynman contour. The matching conditions determine that $c^-_{nk} = c^+_{nk} = 0$, with $d^\pm_{nk}$ expressible in terms of the source on the Lorentzian boundary.

The one point function for the operator is expressed in terms of the normalizable mode in the asymptotic expansion as

$$\langle \mathcal{O} \rangle = -2l\Phi_{(2l)} + \cdots \tag{3.2.11}$$

where $\Phi_{(2l)}$ is the term of order ρ^{-l-1} in the asymptotic expansion of the solution. Now using $c^\pm_{nk} = 0$ we find that the time ordered two point function is

$$\langle T\mathcal{O}(t,\phi)\mathcal{O}(0,0)\rangle = \frac{l}{4\pi^2}\sum_k \int_C \mathrm{d}\omega e^{-i\omega t + ik\phi} A(\omega,k,l) \tag{3.2.12}$$

where

$$A(\omega,k,l) = -(\psi(\hat{\omega}_{kl}) + \psi(\hat{\omega}_{kl} - \omega - l))\frac{(\hat{\omega}_{kl}-l)_l(\hat{\omega}_{kl}-k-l)_l}{l!(l-1)!} \tag{3.2.13}$$

$$\hat{\omega}_{kl} = \frac{\omega + k + l + 1}{2} \tag{3.2.14}$$

and $\psi(z)$ is the digamma function. The contour C has been completely fixed by the matching conditions and integrating over it C is equivalent to integrating over the real axis with the frequency shifted by $\omega \to \omega(1 + i\varepsilon)$. The Fourier transform can then be inverted to give the position space correlator:

$$\langle T\mathcal{O}(t,\phi)\mathcal{O}(0,0)\rangle = \frac{l^2}{2^{l+1}\pi(\cos(t(1-i\varepsilon)) - \cos(\phi))^{l+1}}. \tag{3.2.15}$$

3.2.1.2 Poincaré AdS

Here the Lorentzian manifold is the Poincaré patch of AdS_{d+1} with the time coordinate t restricted to $-T < t < T$ whereas the Euclidean caps are Euclidean AdS_{d+1} obtained by the replacement $t = -i\tau$. In the lower cap τ is restricted to $\tau < 0$ and in the upper cap it is restricted to $\tau > 0$. The Lorentzian metric is given by

$$\mathrm{d}s^2_{\mathrm{AdS}_{d+1}} = \frac{-\mathrm{d}t^2 + \mathrm{d}z^2 + \mathrm{d}\mathbf{x}^2}{z^2} \tag{3.2.16}$$

and the metrics on the Euclidean caps is obtained via $t = -i\tau$.

The scalar equation in this background is given by

$$z^{d+1}\partial_z(z^{-d+1}\partial_z\Phi) + z^2\Box_0\Phi - m^2\Phi = 0 \tag{3.2.17}$$

where $\Box_0$ is the D'Alembertian operator on the boundary coordinates $(t, \mathbf{x})$. Fourier transforming gives two types of modes labelled by $(\omega, \mathbf{k})$:

$$e^{-i\omega t+i\mathbf{k}\cdot\mathbf{x}}z^{d/2}K_l(qz), \qquad e^{-i\omega t+i\mathbf{k}\cdot\mathbf{x}}z^{d/2}I_l(qz) \tag{3.2.18}$$

where $q^2 = -\omega^2 + \mathbf{k}^2$, $\Delta = l + d/2$, $m^2 = \Delta(\Delta - d)$, and $I_n(z)$ and $K_n(z)$ are the modified Bessel functions. Note that we will need to choose a branch cut for $q = \sqrt{q^2}$ for timelike momenta, we will denote our choice by $q_\varepsilon = \sqrt{-\omega^2 + \mathbf{k}^2 - i\varepsilon}$.

Analysis of the asymptotics of the various modes show that $z^{d/2}K_l(q) \sim z^{d/2-l}$ and $z^{d/2}I_l(qz) \sim z^{d/2+l}$ as $z \to 0$ (i.e. as one approaches the boundary), therefore the $K_l(qz)$ modes are non-normalizable and the $I_l(qz)$ modes are normalizable. Similarly an analysis shows that, for space-like momenta $q^2 > 0$, the only mode that is regular in the bulk is the $K_l(qz)$ mode, whereas for time-like momenta $q^2 < 0$ no linear combination of the two modes is regular. Therefore any solution which remains regular in the bulk should be obtained from an infinite sum over modes.

Now that we have identified the normalizable and non-normalizable modes we can propose that the bulk-boundary propagator $X_1(t, \mathbf{x}, z)$ on the Lorentzian segment is given by:

$$X_1(t, \mathbf{x}, z) = \frac{1}{(2\pi)^d}\int \mathrm{d}\omega\, \mathrm{d}^{d-1}\mathbf{k}\, e^{-i\omega t+i\mathbf{k}\cdot\mathbf{x}}\frac{2^{l+1}q_\varepsilon^l}{\Gamma(l)}z^{d/2}K_l(q_\varepsilon z). \tag{3.2.19}$$

Note that the choice of branch cut earlier is equivalent to a Feynman contour (Figure 3.3.1) in the complex ω plane. This propagator is not unique as we can add any normalizable solution without changing the asymptotics so we are free to add on a normalizable propagator:

$$Y_1(t, \mathbf{x}, z) = \frac{1}{(2\pi)^d}\int \mathrm{d}\omega\, \mathrm{d}^{d-1}\mathbf{k}\, e^{-i\omega t+i\mathbf{k}\cdot\mathbf{x}}\theta(-q^2)c_{[1]}(\omega, \mathbf{k})z^{d/2}J_l(|q|z) \tag{3.2.20}$$

with constraints on the otherwise arbitrary function $c_{[1]}(\omega, \mathbf{k})$ to ensure that it leads to a regular solution in the bulk. Different choices of $c_{[1]}$ correspond to different $i\varepsilon$ insertions.

The bulk-boundary propagator X_1 is not obviously convergent in the deep interior however we can perform in the inverse Fourier transforms and find the position space ex-

pression:

$$X_1(t,\mathbf{x},z) = i\Gamma(l)\Gamma\left(l+\frac{d}{2}\right)\pi^{-d/2}\frac{z^{l+\frac{d}{2}}}{\left(-t^2+\mathbf{x}^2+z^2+i\varepsilon\right)^{l+\frac{d}{2}}} \tag{3.2.21}$$

which is clearly finite in the interior. The bulk-boundary non-normalizable propagators on the two Euclidean caps can be found to be

$$X_0(\tau,\mathbf{x},z) = i\Gamma(l)\Gamma\left(l+\frac{d}{2}\right)\pi^{-d/2}\frac{z^{l+\frac{d}{2}}}{\left(-(-T-i\tau)^2+\mathbf{x}^2+z^2+i\varepsilon\right)^{l+\frac{d}{2}}} \tag{3.2.22}$$

$$X_1(\tau,\mathbf{x},z) = i\Gamma(l)\Gamma\left(l+\frac{d}{2}\right)\pi^{-d/2}\frac{z^{l+\frac{d}{2}}}{\left(-(T-i\tau)^2+\mathbf{x}^2+z^2+i\varepsilon\right)^{l+\frac{d}{2}}}. \tag{3.2.23}$$

It is a simple exercise to show that the matching conditions are given by

$$\Phi(t=T,\mathbf{x},z) = \Phi(\tau=0,\mathbf{x},z) \qquad i\partial_t\Phi(t=T,\mathbf{x},z) + \partial_\tau(\tau=0,\mathbf{x},z) = 0 \tag{3.2.24}$$

$$\Phi(t=-T,\mathbf{x},z) = \Phi(\tau=0,\mathbf{x},z) \qquad i\partial_t\Phi(t=-T,\mathbf{x},z) - \partial_\tau(\tau=0,\mathbf{x},z) = 0 \tag{3.2.25}$$

and that these are satisfied for the X_is. Similarly one can show that the only possible solution for the arbitrary functions appearing in the normalizable contributions that is consistent with the matching conditions is zero.

What we learn from this example is that when we calculate the bulk-boundary propagators in Lorentzian signature we should not expect regularity to be apparent at the level of the Fourier modes, and also that we may have the freedom to specify arbitrary additional normalizable contributions to the propagators. This ambiguity can be resolved by applying the matching conditions and is equivalent to various different $i\varepsilon$ insertions or contour deformations. In turn, these matching conditions are specified by the initial and final conditions of the system, or equivalently the real time QFT contour for the correlation function we are interested in calculating.

3.3 Lifshitz invariant free field theories

Consider the following free scalar field theory in $D+1$ dimensions given by the classical action:

$$S = \frac{1}{2}\int \mathrm{d}t\,\mathrm{d}^D\mathbf{x}\left[(\partial_t\phi)^2 - \kappa^2(\nabla^2\phi)^2\right] \tag{3.3.1}$$

where $\phi = \phi(t,\mathbf{x})$ is a massless scalar field and ∇^2 is the spatial Laplacian, with κ being a real constant. This system explicitly breaks Lorentz symmetry and instead has a $z=2$ Lifshitz scaling symmetry:

$$t \to \lambda^2 t\,; \quad \mathbf{x} \to \lambda\mathbf{x}\,; \quad \phi \to \phi. \tag{3.3.2}$$

In this section we will review the correlation functions for this model, using appendix A of [95].

Following from the above discussion we wish to evaluate the following path integral:

$$\mathcal{Z}[J;\mathcal{C}] = \int [\mathcal{D}\phi] \exp\left(-\frac{i}{2}\int_{\mathcal{C}} \mathrm{d}t \int \mathrm{d}^D\mathbf{x}((\partial_t\phi)^2 - \kappa^2(\nabla^2\phi)^2) + i\int_{\mathcal{C}} \mathrm{d}t \int \mathrm{d}^D\mathbf{x} J(t,\mathbf{x})\phi(t,\mathbf{x})\right), \tag{3.3.3}$$

or more specifically we wish to investigate what the possible propagators are that arise in this generating functional. We will choose the normalisation of the path integral such that $\mathcal{Z}[0;\mathcal{C}] = 1$ for simplicity.

Note that the classical field equation for this theory is given by

$$\partial_t^2\phi + \kappa^2\nabla^4\phi = 0 \tag{3.3.4}$$

where $\nabla^4 = \nabla^2\nabla^2$. Motivated by this, define the linear differential operator $\Delta = \partial_t^2 + \kappa^2\nabla^4$ which reduces the field equation to simply $\Delta\phi = 0$. Using integration by parts we may re-write the action using Δ and simplify $\mathcal{Z}[J;\mathcal{C}]$:

$$\mathcal{Z}[J;\mathcal{C}] = \int [\mathcal{D}\phi] \exp\left(i\int_{\mathcal{C}} \mathrm{d}t \int \mathrm{d}^2\mathbf{x}\left(-\frac{1}{2}\phi\Delta\phi + J\phi\right)\right). \tag{3.3.5}$$

Next we make the change of integration variables to $\phi' = \phi - \Delta^{-1}J$. Under this change the path integral simplifies:

$$\mathcal{Z}[J;\mathcal{C}] = \int [\mathcal{D}\phi'] \exp\left(iS[\phi';\mathcal{C}] + \frac{i}{2}\int_{\mathcal{C}} \mathrm{d}t \int \mathrm{d}^D\mathbf{x} J\Delta^{-1}J\right). \tag{3.3.6}$$

Notice that the second term in the exponential is independent of ϕ' and so can be pulled out of the integral, and that the remaining integral is just $\mathcal{Z}[0;\mathcal{C}]$ which we normalised to unity. Therefore the generating functional is simply:

$$\mathcal{Z}[J;\mathcal{C}] = \exp\left(\frac{i}{2}\int_{\mathcal{C}} \mathrm{d}t \int \mathrm{d}^D\mathbf{x} J\Delta^{-1}J\right) \tag{3.3.7}$$

where the inverse operator Δ^{-1} can be found by solving the equation for the propagator:

$$-\Delta_{t,\mathbf{x}}G(t-t',\mathbf{x}-\mathbf{x}') = \delta(t-t')\delta^{(2)}(\mathbf{x}-\mathbf{x}'). \tag{3.3.8}$$

The problem of finding G simplifies when transforming to $(\omega,\mathbf{k})$ Fourier space. The

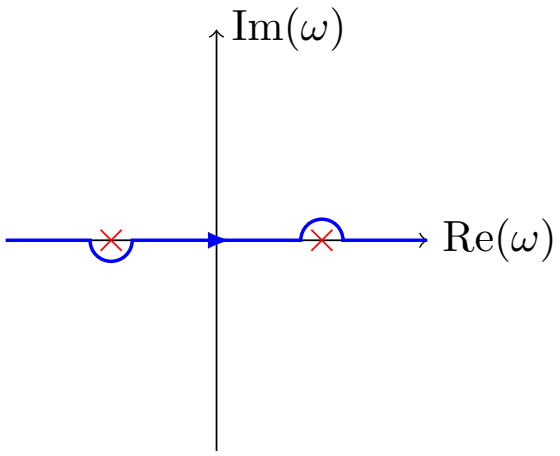

Figure 3.3.1: The Feynman propagator contour; the positive frequency pole contributes for $t > 0$ while the negative frequency pole contributes for $t < 0$.

Fourier transform $\tilde{G}$ of G is given simply by

$$\tilde{G} = -\frac{1}{\omega^2 - \kappa^2 \mathbf{k}^4}. \tag{3.3.9}$$

Carrying out the inverse transform yields:

$$G(t, \mathbf{x}) = -\int \frac{\mathrm{d}\omega \mathrm{d}^D \mathbf{x}}{(2\pi)^{D+1}} \frac{e^{-i\omega t + i\mathbf{k}\cdot\mathbf{x}}}{\omega^2 - \kappa^2 \mathbf{k}^4}. \tag{3.3.10}$$

The integrand has simple poles at $\omega_\pm = \pm\kappa \mathbf{k}^2$, with the dispersion relation reflecting the non-relativistic nature of our system.

There are several possible contour deformations associated with different propagators. The Feynman propagator G_F is given by the insertion $\omega_\pm^F = \pm(\kappa \mathbf{k}^2 - i\varepsilon)$; the retarded propagator G_R has the insertion $\omega_\pm^R = \pm\kappa \mathbf{k}^2 - i\varepsilon$ and the advanced propagator G_A has $\omega_\pm^A = \pm\kappa \mathbf{k}^2 + i\varepsilon$. In all of the above ε is a small positive constant. The three contours that these insertions correspond to are illustrated in Figures 3.3.1 , 3.3.2 and 3.3.3 with the corresponding integral representations with $i\varepsilon$ insertions being:

$$G_F(t, \mathbf{x}) = -\int \frac{\mathrm{d}\omega \mathrm{d}^D \mathbf{k}}{(2\pi)^{D+1}} \frac{e^{-i\omega t + i\mathbf{k}\cdot\mathbf{x}}}{\omega^2 - (\kappa \mathbf{k}^2 - i\varepsilon)^2} \tag{3.3.11}$$

$$G_R(t, \mathbf{x}) = -\int \frac{\mathrm{d}\omega \mathrm{d}^D \mathbf{k}}{(2\pi)^{D+1}} \frac{e^{-i\omega t + i\mathbf{k}\cdot\mathbf{x}}}{(\omega + i\varepsilon)^2 - \kappa^2 \mathbf{k}^4} \tag{3.3.12}$$

$$G_A(t, \mathbf{x}) = -\int \frac{\mathrm{d}\omega \mathrm{d}^D \mathbf{k}}{(2\pi)^{D+1}} \frac{e^{-i\omega t + i\mathbf{k}\cdot\mathbf{x}}}{(\omega - i\varepsilon)^2 - \kappa^2 \mathbf{k}^4}. \tag{3.3.13}$$

For the Feynman contour we may equivalently represent the contour by the shift

$$\omega \to \omega(1 + i\epsilon') \tag{3.3.14}$$

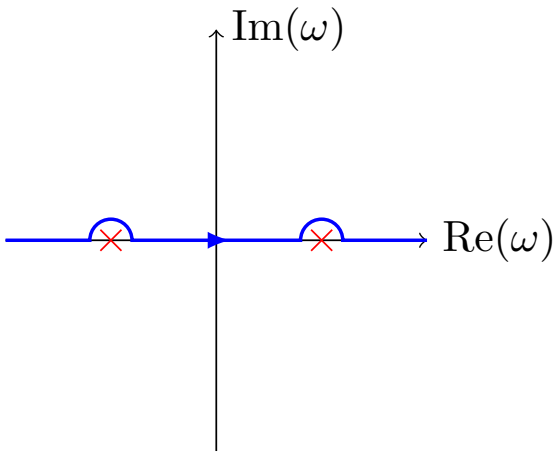

Figure 3.3.2: The retarded propagator contour; the propagator is analytic in the upper half plane.

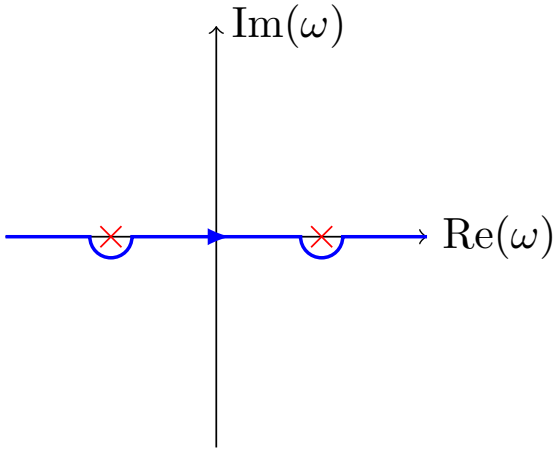

Figure 3.3.3: The advanced propagator contour; the propagator is analytic in the lower half plane.

where ϵ' is positive. Notice that $G_R(t-t', \mathbf{x}-\mathbf{x}') = 0$ if $t < t'$, and similarly $G_A(t-t', \mathbf{x}-\mathbf{x}') = 0$ if $t > t'$. These two results make explicit the notion that one event occurs before (after) another if the difference in one occurs at an earlier (later) time than the other. This is precisely the notion of past/future that occurs in non-relativistic systems.

Now that we have found the propagators we have in theory solved the problem and can now proceed to work out any correlator we want, provided we can perform the remaining integrals. Nothing so far has dictated which of the three possible propagators we should use but this problem is solved by specifying initial conditions for the fields.

Before understanding the Lorentzian physics from a holographic perspective, let us return to the Euclidean correlation functions. In three dimensions ($D = 2$), the integrals above are logarithmically divergent; this divergence is analogous to the divergence of a

relativistic massless boson in two dimensions. In [95] a regularised Euclidean Green's function was used:

$$G_E(\tau,\mathbf{x}) = -\frac{1}{8\pi\kappa}\left[\log\left(\frac{|x|^2}{a^2}\right)+\Gamma\left(0,\frac{|x|^2}{4\kappa\tau}\right)\right], \tag{3.3.15}$$

where τ is the Euclidean time and a is a cutoff, with $\Gamma(0,z)$ being the incomplete Gamma function.

The charge operators in the free theory are given by $\mathcal{O}_n = e^{-in\phi}$ where n is an integer and these operators have correlation functions given by

$$\langle \mathcal{O}_n(\tau,\mathbf{x})\mathcal{O}_n^\dagger(0,0)\rangle = e^{n^2 G_E(\tau,\mathbf{x})} \tag{3.3.16}$$

From the regularised Green function one can then show that for the equal time correlation function

$$\langle \mathcal{O}_n(0,\mathbf{x})\mathcal{O}_n^\dagger(0,0)\rangle = \left(\frac{a}{|\mathbf{x}|}\right)^{\frac{n^2}{4\pi\kappa}} \tag{3.3.17}$$

while for $\tau \gg |\mathbf{x}|$

$$\langle \mathcal{O}_n(\tau,\mathbf{x})\mathcal{O}_n^\dagger(0,0)\rangle \approx \left(\frac{a^2\gamma}{4\kappa|\tau|}\right)^{\frac{n^2}{8\pi\kappa}} \tag{3.3.18}$$

where γ is the Euler constant. This implies that the charge operator has scaling dimension $\Delta = n^2/8\pi\kappa$.

In dimensions four and higher ($D \geq 3$) the scalar field has a non-zero scaling dimension and the integrals have no logarithmic divergences. The Euclidean Green's function is given by

$$G_E(\tau,\mathbf{x}) = \int \frac{\mathrm{d}\omega \mathrm{d}^D\mathbf{k}}{(2\pi)^{D+1}} \frac{e^{-i\omega_E\tau + i\mathbf{k}\cdot\mathbf{x}}}{\omega_E^2+\kappa^2\mathbf{k}^4} \tag{3.3.19}$$

Evaluating this expression in $D=3$ results in

$$G_E(\tau,\mathbf{x}) = \sqrt{\frac{1}{16\pi^3\kappa^3|\tau|}}\exp\left(-\frac{|\mathbf{x}|^2}{4\kappa|\tau|}\right) + \frac{\delta(|\tau|)}{2^{D+1}\pi^D|\kappa|}\int \mathrm{d}^D\mathbf{k}\frac{e^{i\mathbf{k}\cdot\mathbf{x}}}{\mathbf{k}^2}. \tag{3.3.20}$$

For $\tau \neq 0$ this formula describes diffusion in imaginary time, with the effective diffusion constant being κ. This is not surprising, as the equation of motion for the scalar field ϕ is the square of the Schrödinger equation, which is well-known to be a diffusion equation in imaginary time. In general for $D \geq 3$

$$G_E(\tau,\mathbf{x}) \sim \frac{1}{|\tau|^{\frac{D-2}{2}}}\exp\left(-\frac{|\mathbf{x}|^2}{4\kappa|\tau|}\right), \tag{3.3.21}$$

for $\tau \neq 0$ which is consistent with the scaling dimension of the scalar field. In the limit

$|\tau| \gg |\mathbf{x}|$ this reproduces the power law fall-off of correlation functions in $D = 2$.

For $\tau = 0$, this gives precisely the expression for a massless relativistic boson in D spatial dimensions and hence

$$G_E(0, \mathbf{x}) \sim \frac{1}{|\mathbf{x}|^{D-2}}, \tag{3.3.22}$$

which again is in accordance with the scaling dimension of the scalar field. Note that the precise expressions in general require renormalization, to ensure that the correlators are well-defined in a distributional sense.

3.4 Schrödinger invariant theories

3.4.1 Schrödinger invariant field theories

In this section we will review the implications of Schrödinger invariance for correlation functions. Let us begin by considering the action of the Schrödinger group on a theory in D spatial dimensions $\vec{x}$ and a Euclidean time coordinate τ (such that $t = -i\tau$). The Schrödinger group is the maximal group which transforms solutions of the (Euclidean) Schrödinger equation,

$$\left(-\frac{\partial}{\partial\tau} + \frac{1}{2\mathcal{M}}\nabla^2\right)\Psi = 0, \tag{3.4.1}$$

into other solutions. The generators of this group are time translations $H = \partial_\tau$, spatial translations $P_i = \partial_i$, the dilatation generator $D = \tau\partial_\tau + \frac{1}{2}x^i\partial_i$, the Galilean boosts $S_i = \tau\partial_i + Mx^i$ and the special Schrödinger symmetry

$$K = \tau^2\partial_\tau + \tau x^i\partial_i - \frac{1}{2}Mx^i x_i. \tag{3.4.2}$$

Here M is a central term, i.e.

$$[P_i, S_j] = M\delta_{ij}. \tag{3.4.3}$$

The Schrödinger symmetry then fixes uniquely the two-point function of quasi-primary operators $\mathcal{O}(\tau, x^i)$ of scaling dimension Δ to be

$$\langle\mathcal{O}(\tau, x^i)\mathcal{O}(0,0)\rangle \propto \frac{1}{\tau^\Delta}\exp\left(-\frac{M}{2}\frac{|x|^2}{\tau}\right), \tag{3.4.4}$$

where the operators must have the same scaling dimension to have a non-vanishing two point function. Note that this is exactly the same form as in the free Lifshitz theory, but in this case is fixed by symmetry for any Schrödinger invariant theory.

The correlation function is clearly not well-defined as $\tau \to 0$ and $x^i \to 0$; one needs to renormalize appropriately. Note also that, unlike the general Lifshitz case, the correlation function does not have a good limit as $\tau \to 0$ at finite x^i: the special conformal

symmetry equation can only be solved in this limit if $M = 0$, in which case the correlator becomes

$$\langle \mathcal{O}(0, x^i)\mathcal{O}(0,0)\rangle \propto \frac{1}{|x|^{2\Delta}}\delta_M, \tag{3.4.5}$$

which follows from the scaling symmetry.

Now let us consider real time physics. Analytically continuing $\tau = it$, the retarded correlation function is given by

$$\langle \mathcal{O}(t, x^i)\mathcal{O}(0,0)\rangle = \theta(t)\frac{C}{t^\Delta}\exp\left(i\frac{M}{2}\frac{|x|^2}{t}\right), \tag{3.4.6}$$

where C is the overall normalisation. As a particular case, one can consider a non-relativistic spinless particle of mass $\mathcal{M}$ (3.4.1) for which the propagator is

$$G(t, x^i) = -\frac{i}{\hbar}\theta(t)\left(\frac{\mathcal{M}\hbar}{2\pi t}\right)^{\frac{D}{2}}\exp\left(i\frac{\mathcal{M}}{2\hbar}\frac{|x|^2}{t}\right), \tag{3.4.7}$$

i.e. the central term is precisely the mass in units of $\hbar$ and the scaling dimension is $D/2$.

The latter can be expressed in momentum space as

$$G(\omega, k^i) = \frac{1}{\omega - \frac{|k|^2}{2\mathcal{M}}}, \tag{3.4.8}$$

where we have again set $\hbar = 1$. Hence the propagator has a pole at $\omega = |k|^2/2\mathcal{M}$. This is the non-relativistic dispersion relation; note that unlike the free Lifshitz model, the propagator is not symmetric under $\omega \to -\omega$ as the original system does not have time-reversal symmetry.

More generally, we can Fourier transform the retarded correlation function along the x^i directions to obtain

$$\langle \mathcal{O}(t, \vec{k})\mathcal{O}(0, -\vec{k})\rangle = \theta(t)\frac{C'}{t^\Delta}\left(\frac{t}{\mathcal{M}}\right)^{\frac{D}{2}}\exp\left(i\frac{1}{2\mathcal{M}}|k|^2 t\right), \tag{3.4.9}$$

where C' is a rescaled normalisation constant. Recall that the general expression for the Fourier transform of a power in d dimensions is

$$\int \mathrm{d}^d x e^{-i\vec{k}\cdot\vec{x}}|x|^{-2\lambda} = \pi^{d/2}2^{d-2\lambda}\frac{\Gamma(d/2-\lambda)}{\Gamma(\lambda)}|k|^{2\lambda-d}, \tag{3.4.10}$$

where implicitly we assume that λ is not zero or a negative integer and that $d/2 - \lambda$ is not a negative integer. (In such cases we will need to use an appropriate method such as differential regularisation to define the integrals.) From this expression we can infer

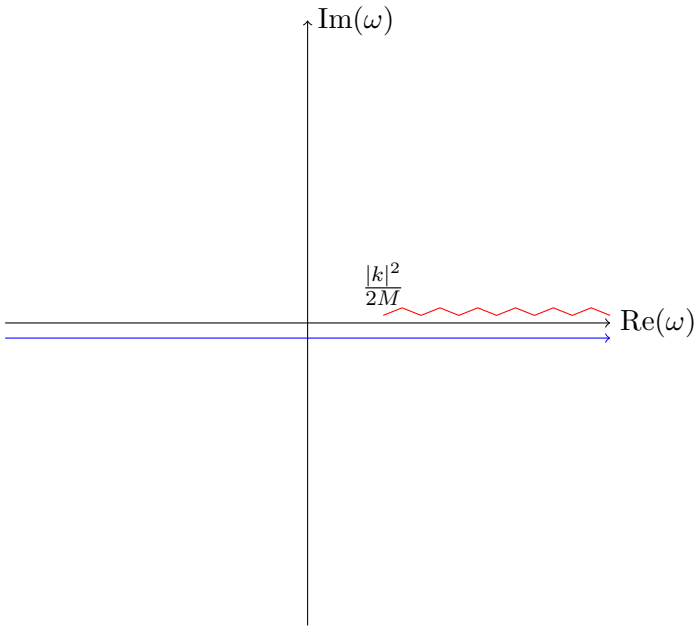

Figure 3.4.1: The complex frequency plane for Schrödinger, with the retarded/Feynman correlation function integration contour shown in blue.

that

$$\langle \mathcal{O}(\omega,\vec{k})\mathcal{O}(-\omega,-\vec{k})\rangle \sim \left(\omega - \frac{|k|^2}{2M}\right)^{(\Delta-\frac{D}{2}-1)} \tag{3.4.11}$$

i.e. for generic dimension operators the correlation function has a branch point at $\omega = |k|^2/2M$. This analytic structure is illustrated in Figure 3.4.1. Note that in this case the Feynman and retarded integration contours are indistinguishable, as the correlation function is analytic in the left half of the complex frequency plane.

3.4.2 Holographic Schrödinger theories

The following $(D+3)$-dimensional metric exhibits Schrödinger symmetry with scaling exponent z:

$$\mathrm{d}s^2 = -\frac{b^2}{r^{2z}}\mathrm{d}t^2 + \frac{1}{r^2}\left(2\mathrm{d}t\mathrm{d}v + \mathrm{d}\vec{x}^2 + \mathrm{d}r^2\right). \tag{3.4.12}$$

The parameter b could be removed by rescaling the (t,v) coordinates, but we include it here to make manifest the AdS limit as $b \to 0$. This metric exhibits a scaling symmetry

$$t \to \lambda^z t \qquad v \to \lambda^{2-z} v \qquad \vec{x} \to \lambda\vec{x} \qquad r \to \lambda r \tag{3.4.13}$$

for any value of z. The geometry only admits the additional special Schrödinger symmetry for $z = 2$ and we will concentrate on this case in what follows. Note that the hypersurfaces of constant t are null, while hypersurfaces of constant v are timelike for $b \neq 0$ and null for $b = 0$.

The geometry can be supported by massive vectors and arises as a solution of higher derivative gravity theories. As in earlier sections, we will concentrate on minimally coupled scalar fields, which are not affected by the choice of matter supporting the geometry. The equation of motion for such a minimally coupled scalar field of mass m^2 is thus

$$B^2 r^{4-2z}\partial_v^2\psi + 2r^2\partial_t\partial_v\psi + r^2\partial_i^2\psi + r^2\partial_r^2\psi - (D+1)r\partial_r\psi = m^2\psi. \tag{3.4.14}$$

Now consider modes of particular frequency

$$\psi = e^{-ilv}\psi_l(t, x^i, r). \tag{3.4.15}$$

For $z = 2$ such modes satisfy

$$r^2\left(-2il\partial_t + \partial_i^2 + \partial_r^2 - \frac{D+1}{r}\partial_r\right)\psi_l = (m^2 + b^2l^2)\psi_l \equiv m_l^2\psi_l. \tag{3.4.16}$$

This is exactly the same differential equation as in AdS_{D+3}, but with the mass shifted by a term depending on b and l. Thus the scaling dimension of the dual operator is

$$\Delta_l(D+2-\Delta_l) = m_l^2, \tag{3.4.17}$$

i.e. the modes ψ_l of different $|l|$ correspond to operators $\mathcal{O}_l(t, x^i)$ of distinct scaling dimension Δ_l. Given this fact, we work entirely in momentum space l rather than in coordinate space v.

Using the asymptotic expansion of the scalar field ψ_l

$$\psi_l = r^{D+2-\Delta_l}\left(\psi_{l(0)} + \cdots\right) + r^{\Delta_l}\left(\psi_{l(\Delta_l)} + \cdots\right) \tag{3.4.18}$$

we can calculate the one-point function to be

$$\langle\mathcal{O}_l(t, x^i)\rangle = (D+2-2\Delta_l)\psi_{l(\Delta_l)}(t, x^i) + \cdots \tag{3.4.19}$$

and hence

$$\langle\mathcal{O}_l(t, x^i)\mathcal{O}_{-l}(0, 0)\rangle = -(D+2-2\Delta_l)\frac{\delta\psi_{l(\Delta_l)}(t, x^i)}{\delta\psi_{l(0)}(0, 0)} + \cdots \tag{3.4.20}$$

where the ellipses denote contact terms which we will not compute explicitly. Note that the symmetry of (3.4.16) under $l \to -l$ and $t \to -t$ implies that

$$\langle\mathcal{O}_l(t, x^i)\mathcal{O}_{-l}(0, 0)\rangle = \langle\mathcal{O}_{-l}(-t, x^i)\mathcal{O}_l(0, 0)\rangle \tag{3.4.21}$$

and hence one can straightforwardly construct the time ordered two point function

which is defined as

$$\langle \mathcal{T}\mathcal{O}_l(t,x^i)\mathcal{O}_{-l}(0,0)\rangle = \theta(t)\langle \mathcal{O}_l(t,x^i)\mathcal{O}_{-l}(0,0)\rangle + \theta(-t)\langle \mathcal{O}_l(0,0)\mathcal{O}_{-l}(t,x^i)\rangle. \tag{3.4.22}$$

Now let us consider solutions of (3.4.16). Fourier transforming the t and x^i coordinates results in

$$r^2\left(2l\omega - k^2 + \partial_r^2 - \frac{D+1}{r}\partial_r\right)\tilde{\psi}_l = m_l^2\tilde{\psi}_l. \tag{3.4.23}$$

The general solutions are then of the same form as for Poincaré AdS:

$$\begin{aligned} &\tilde{\psi}_l = Ar^{\frac{1+D}{2}}K_\nu(qr) + Br^{\frac{1+D}{2}}I_\nu(qr) \qquad q^2 = k^2 - 2l\omega > 0 \\ &\tilde{\psi}_l = Cr^{\frac{1+D}{2}}K_\nu(q_\epsilon r) + Dr^{\frac{1+D}{2}}J_\nu(|q|r) \qquad q_\epsilon = \sqrt{k^2 - 2l\omega + i\epsilon} \qquad q^2 < 0, \end{aligned} \tag{3.4.24}$$

where in the latter we have chosen a branch cut, with ϵ being positive,

$$\nu = \sqrt{m_l^2 + \frac{1}{4}(D+2)^2} \tag{3.4.25}$$

and we define $q_\epsilon = -i|q|$.

When $q^2 > 0$, regularity as $r \to \infty$ sets $B = 0$. For $q^2 < 0$, the modes involving $K_\nu(q_\epsilon r)$ correspond to sources while the other modes $J_\nu(|q|r)$ correspond to normalizable modes. Neither mode solution is finite as $r \to \infty$. By constriction the solution $K_\nu(q_\epsilon r)$ is applicable for both $q^2 > 0$ and $q^2 < 0$ and, for fixed positive l, there is a branch cut from $\omega = k^2/2l$ to infinity. The $i\epsilon$ insertion fixes this branch cut to be just above the real axis.

Guided by the Euclidean AdS propagator, let us consider for $l > 0$

$$G(l;t,x^i,r) = \frac{1}{(2\pi)^{D+1}}\int_C \mathrm{d}\omega \int \mathrm{d}\vec{k} e^{i\omega t - i\vec{k}\cdot\vec{x}}\frac{2^{\nu+1}q_\epsilon^\nu}{\Gamma(\nu)}r^{\frac{1+D}{2}}K_\nu(q_\epsilon r), \tag{3.4.26}$$

where the $i\epsilon$-prescription is equivalent to the contour in the frequency plane shown in Figure 3.4.1. Calculating the Fourier transform gives

$$G(l;t,x^i,r) = C\theta(t)\frac{l^{\Delta_l - 1}r^{\Delta_l}}{t^{\Delta_l}}\exp\left(-\frac{il}{2t}(\vec{x}^2 + r^2)(1 - i\epsilon)\right). \tag{3.4.27}$$

with

$$C = -\frac{i^{\Delta_l+1}}{2^{\Delta_l}\pi^{\frac{D+2}{2}}\Gamma(\nu)} \tag{3.4.28}$$

The choice of contour therefore guarantees that the propagator is regular as $r \to \infty$ for

$l > 0$. One can then read off the retarded two point function as

$$\langle \mathcal{O}_l(t, x^i)\mathcal{O}_{-l}(0,0)\rangle = C(2\Delta_l - D - 2)\theta(t)\frac{l^{\Delta_l - 1}}{t^{\Delta_l}} \exp\left(-\frac{il}{2t}\vec{x}^2(1 - i\epsilon)\right). \tag{3.4.29}$$

The addition of other normalizable modes would be associated with a different choice of integration contour, and correspondingly different initial conditions, as we will discuss further below.

We can similarly calculate the time ordered two point function as

$$\begin{aligned}\langle \mathcal{T}\mathcal{O}_l(t, x^i)\mathcal{O}_{-l}(0,0)\rangle = {} & C(2\Delta_l - D - 2)\theta(t)\frac{l^{\Delta_l - 1}}{t^{\Delta_l}} \exp\left(-\frac{il}{2t}\vec{x}^2(1 - i\epsilon)\right) \\ & + C(2\Delta_l - D - 2)\theta(-t)\frac{l^{\Delta_l - 1}}{t^{\Delta_l}} \exp\left(\frac{il}{2t}\vec{x}^2(1 - i\epsilon)\right).\end{aligned} \tag{3.4.30}$$

Note that this two point function decays as a power law as $t \to \pm\infty$ at fixed $\vec{x}^2$. Let us now consider the matching between the Lorentzian segment and Euclidean segments. A priori it is not obvious how to analytically continue the Schrödinger geometry to the Euclidean. However, from the above discussions, it is clear that t plays the role of time and that the matching with Euclidean segments should be on hypersurfaces of $t = \pm T$. We therefore consider the Euclidean segments obtained by the replacement $t = -i\tau$. The resulting metric is

$$\mathrm{d}s^2 = \frac{b^2}{r^{2z}}\mathrm{d}\tau^2 + \frac{1}{r^2}\left(-2i\mathrm{d}\tau\mathrm{d}v + \mathrm{d}\vec{x}^2 + \mathrm{d}r^2\right). \tag{3.4.31}$$

Note that this metric is complex and surfaces of constant τ are null.

If however we consider the scalar field equation in this background we obtain for $z = 2$

$$r^2\left(2l\partial_\tau + \partial_i^2 + \partial_r^2 - \frac{D+1}{r}\partial_r\right)\psi_l = (m^2 + b^2l^2)\psi_l \equiv m_l^2\psi_l \tag{3.4.32}$$

where we focus on modes of specific positive frequency l with respect to the v coordinate as in (3.4.15). This equation of motion is both real and elliptic and the resulting bulk boundary propagator is

$$G(l; \tau, x^i, r) = C'\frac{l^{\Delta_l - 1}r^{\Delta_l}}{\tau^{\Delta_l}} \exp\left(\frac{l}{2\tau}(\vec{x}^2 + r^2)\right). \tag{3.4.33}$$

with

$$C' = -\frac{ie^{i\pi x}}{2^{\Delta_l}\pi^{\frac{D+2}{2}}\Gamma(\nu)}. \tag{3.4.34}$$

The propagator is manifestly regular as $r \to \infty$ and as $\tau \to \infty$ and the normalisation follows from matching with the Lorentzian propagator on the surface $t = T$.

3.4.3 Extended Schrödinger spacetimes

Recently some authors [96, 97] have been interested in extensions to the Schrod·inger spacetime (3.4.12) through the apparent singularity at $r = \infty$. A smooth extension exists for $z \geq 2$ and is given by the coordinate transformation

$$t = \frac{1}{\omega}\tan\omega T, \quad r = R\sec\omega T, \quad \vec{x} = \vec{X}\sec\omega T, \quad v = -V - \frac{\omega}{2}(R^2 + \vec{X}^2)\tan\omega T \quad (3.4.35)$$

where ω is some arbitrary real parameter. In these new coordinates the metric reads

$$\mathrm{d}s^2 = -(\cos\omega T)^{2z-4}\frac{b^2\mathrm{d}T^2}{R^4} + \frac{1}{R^2}(-2\mathrm{d}T\mathrm{d}V - \omega^2(R^2 + X^2)\mathrm{d}T^2 + \mathrm{d}R^2 + \mathrm{d}\vec{X}^2) \quad (3.4.36)$$

where the T-translational symmetry is restored only for $z = 2$. The free parameter ω was not considered in the previous discussions of [96] however it is necessary to realise the original scaling symmetry explicitly. This new metric is invariant under the scaling symmetry

$$T \to \lambda^z T, \quad V \to \lambda^{2-z}V, \quad \vec{X} \to \lambda\vec{X}, \quad R \to \lambda R, \quad \omega \to \lambda^{-z}\omega. \quad (3.4.37)$$

A free scalar field ψ of mass μ propagating on this background without backreaction obeys the Klein-Gordon equation:

$$-2R^2\psi_{,VT} + (b^2 + \omega^2 R^2(R^2 + X^2))\psi_{,VV} + R^2\psi_{,RR} - (D+1)R\psi_{,R} + R^2\nabla_X^2\psi = \mu^2\psi \quad (3.4.38)$$

where ∇_X^2 denotes the flat space Laplacian on the $\mathbb{R}^D$ for the $\vec{X}$ boundary spatial directions. We can decompose solutions of this equation into spherical harmonic modes:

$$\psi = e^{-iET}e^{-imV}\Psi(R)\phi_{n,l}(\rho)Y_l(\theta_i) \quad (3.4.39)$$

where (ρ, θ_i) are spherical coordinates for the $\vec{X}$, and $Y_l(\theta_i)$ are the spherical harmonics of weight $-l(l + D - 2)$ on S^{D-1}.

The mode functions $\Psi(R)$ and $\phi_{n,l}(\rho)$ satisfy the following equation:

$$\nu = \frac{1}{\Psi}\left[\Psi'' - \frac{D+1}{R}\Psi' + \left(2mE - m^2R^2 - \frac{\mu^2 + m^2b^2}{R^2}\right)\Psi\right] \quad (3.4.40)$$

$$= -\frac{1}{\phi}\left[\phi'' + \frac{D-1}{\rho}\phi' - \left(\frac{l(l+D-2)}{\rho} + m^2\rho^2\right)\phi\right] \quad (3.4.41)$$

where ν is some constant. Both of these equations can be solved exactly in terms of the confluent hypergeometric functions $U(a, b, z)$ and $\mathbf{M}(a, b, z)$, as in the Lifshitz case.

Imposing that the ρ mode function to convergent at $\rho = 0$ and that it be well behaved at

infinity yields

$$\phi_{n,l}(\rho) = e^{-\frac{1}{2}m\omega\rho^2}\rho^l L_n^{\left(l+\frac{d}{2}-1\right)}(m\omega\rho^2) \tag{3.4.42}$$

where $n \in \mathbb{N}$, and $L_n^{(\alpha)}(z)$ are the generalised Laguerre polynomials.

The most general solution for the R mode function is given by

$$\begin{aligned}\Psi(R) = e^{-\frac{1}{2}m\omega\rho^2}\Big[&\Psi_{(0)}R^{\Delta_-}\frac{\Gamma(a_+)}{\Gamma(N_2)}U(a_-, 1-N_2, m\omega R^2) \\ &+\Psi_{(M)}R^{\Delta_+}\mathbf{M}(a_+, 1+N_2, m\omega R^2)\Big]\end{aligned} \tag{3.4.43}$$

where the constants are $\Delta_\pm = \frac{1}{2}(D+2) \pm N_2$, $N_2 = \frac{1}{2}\sqrt{(D+2)^2 + 4(\mu^2 + b^2m^2)}$, and $a_\pm = \frac{1}{2}\left(l + 2n + \Delta_\pm - \frac{E}{\omega}\right)$ and the normalisation of the U mode has been chosen such that $\Psi(R) = R^{\Delta_-}\Psi_{(0)} + \ldots$ for small R.

The U modes are non-normalizable except in the degenerate case of $a_+ = -p \in -\mathbb{N}$ in which $R^{\Delta_-}U(a_-, 1-N_2, z) \propto R^{\Delta_+}\mathbf{M}(a_+, 1+N_2, z)$, i.e. they degenerate into $\mathbf{M}$ modes. These modes are exponentially suppressed in the $R \to \infty$ limit assuming $m\omega > 0$.

The $\mathbf{M}$ modes are always normalizable as $\mathbf{M}(a, b, z)$ is always a constant to leading order in z. In the special case where $a_+ = -p \in -\mathbb{N}$ these modes are exponentially suppressed as $\mathbf{M}(a_+, 1+N_2, m\omega R^2)$ is a polynomial in R^2 of degree at most p, otherwise they are exponentially divergent.

Restricting to modes where $a_+ = -p$ is the ideal choice for the normalizable modes, however there does not appear to be any reason *a priori* to restrict to the similar case of $a_- = -p$ for the non-normalizable modes. Moreover, if one restricts to this case then the U modes degenerate into normalizable modes whenever $N_2 \in \mathbb{N}$ which is a case that arises often in supergravity models.

This leads us to the somewhat unsatisfactory conclusion that the energy E is a continuous parameter for the non-normalizable modes, and a discrete parameter for the normalizable modes with $E = E_p^+ = \omega(l + 2(n+p) + \Delta_+)$. The most general solution to the Klein-Gordon equation (3.4.38) for a mode of fixed V momentum m is:

$$\begin{aligned}\psi_m(T, R, \vec{X}) = \sum_{l,n} e^{-\frac{1}{2}m\omega R^2}\phi_{n,l}(\rho)Y_l(\theta_i) \\ \times\left(\int dE\, e^{-iET}R^{\Delta_-}\psi_{(0)}(l,n,E)\frac{\Gamma(a_+)}{\Gamma(N_2)}U(a_-, 1-N_2, m\omega R^2)\right. \\ \left. + \sum_p e^{-iE_p^+T}R^{\Delta_+}d_{l,n,p}L_p^{(N_2)}(m\omega R^2)\right)\end{aligned} \tag{3.4.44}$$

where the $d_{l,n,p}$ are unknown constants that should be fixed with the appropriate match-

ing conditions.

It is not obvious how to invert this expression into a position space propagator, even though we accomplished this quite easily in the original coordinate system. Moreover the propagator (3.4.27) found in the original coordinate chart can be easily rewritten in terms of the extended coordinates as

$$G(l;t,x^i,r) = C\theta\left(\frac{1}{\omega}\tan(\omega T)\right) l^{\Delta_l-1}\left(\frac{R\omega}{\sin(\omega T)}\right)^{\Delta_l} e^{ilV} \times \exp\left(-\frac{il\omega}{2\sin(2\omega T)}(R^2+X^2)(1+\cos(2\omega T)-2i\epsilon)\right) \tag{3.4.45}$$

which manifestly solves the Klein-Gordon equation (3.4.38). It is clear that these extended coordinates provide no advantage in finding the propagator for holographic Schrödinger spacetimes.

3.5 Lifshitz holography

The following bulk metric is dual to the vacuum state of a quantum field theory with Lifshitz symmetry:

$$\mathrm{d}s^2_{d+2} = L^2\left(-\frac{\mathrm{d}t^2}{r^{2z}} + \frac{\mathrm{d}\mathbf{x}^2}{r^2} + \frac{\mathrm{d}r^2}{r^2}\right) \tag{3.5.1}$$

where r is the holographic direction with $r \to 0$ corresponding to the boundary, L is the curvature radius, z is the dynamic Lifshitz exponent, and $(t, \mathbf{x})$ are the coordinates on the $D+1$ dimensional boundary. Here D represents the number of spatial dimensions. The Lifshitz scaling isometry is $t \to \lambda^z t, \mathbf{x} \to \lambda\mathbf{x}, r \to \lambda r$ where λ is a positive real constant. Note that in the case $z = 1$ this spacetime reduces to the Poincaré patch of AdS_{D+2}. This spacetime is not a solution of the Einstein equations with negative cosmological constant but can be supported by appropriate matter fields such as a massive vector field.

We will consider a minimally coupled massive scalar field ψ propagating without back-reaction in this spacetime. The action for the scalar field is given by:

$$S = -\frac{1}{2}\int \mathrm{d}t\,\mathrm{d}^D\mathbf{x}\,\mathrm{d}r\,\sqrt{-g}\left(g^{\mu\nu}\partial_\mu\psi\partial_\nu\psi + m^2\psi^2\right) \tag{3.5.2}$$

and the equation of motion is thus:

$$r^2\partial_r^2\psi - r(d+z-1)\partial_r\psi - r^{2z}\partial_t^2\psi + r^2\partial_{\mathbf{x}}^2\psi - (mL)^2\psi = 0. \tag{3.5.3}$$

For simplicity we will consider the case of vacuum-to-vacuum correlators, similar to

the above relativistic case and illustrated in Figure 3.2.3. Note that now the bulk manifold segments will be of the form given by equation (3.5.1) and not Poincaré patch AdS. As in the relativistic case our aim will be to compute the bulk-boundary propagator for the various segments of the bulk manifold and then apply the matching conditions to attempt to resolve any ambiguities and determined the correct $i\varepsilon$ insertions. Since the equation of motion is a second order differential equation in r we would expect that there will be two families of linearly independent solutions with different near boundary behaviour. We begin by reviewing the correspondence between asymptotics and normalizable and non-normalizable solutions.

A standard analysis of the equation motion shows that the scalar field solutions asymptotically behave as

$$\psi \sim r^{\Delta_+}\psi_+ + r^{\Delta_-}\psi_- \tag{3.5.4}$$

where $\Delta_\pm$ are roots of $\Delta(\Delta-(D+z)) = m^2L^2$ or explicitly:

$$\Delta_\pm = \frac{1}{2}(D+z) \pm N_z; \qquad N_z = \frac{1}{2}\sqrt{(D+z)^2 + 4(mL)^2} \tag{3.5.5}$$

We require that $\Delta_\pm \in \mathbb{R}$ is real, which in turn leads to the generalisation of the Breitenlohner-Freedman bound to Lifshitz spacetime:

$$(mL)^2 \geq -\frac{(D+z)^2}{4}. \tag{3.5.6}$$

This assumption is equivalent to requiring that $N_z \geq 0$.

Modes with the asymptotic behaviour r^{Δ_-} are non-normalizable as can be demonstrated by considering the following

$$\int \mathrm{d}r\, \sqrt{-g}\psi^2 \sim \int \mathrm{d}r\, r^{-1-2N_z} \tag{3.5.7}$$

which is always divergent as $r \to 0$. Similarly we have that modes with r^{Δ_+} asymptotics are normalizable:

$$\int \mathrm{d}r\, \sqrt{-g}\psi^2 \sim \int \mathrm{d}r\, r^{-1+2N_z}. \tag{3.5.8}$$

As in AdS, where Δ_+ and Δ_- differ by an integer, the second solution with develop logarithmic contributions. For example, at $N_z = 0$ the two independent modes behave as

$$\psi \sim r^{\frac{1}{2}(D+z)}\psi_+ + r^{\frac{1}{2}(D+z)}\log r\psi_- \tag{3.5.9}$$

with ψ_- corresponding to the non-normalizable (source) mode. In what follows we will for simplicity mostly work with the generic case in which logarithmic terms do not arise in the asymptotic expansions.

As in the relativistic case, we will calculate the bulk-boundary propagator $G(r,t,\mathbf{x})$ which constructs a full bulk solution $\psi(r,t,\mathbf{x})$ of the equation of motion from some boundary data $\psi_{(0)}(t,\mathbf{x})$ via

$$\psi(r,t,\mathbf{x}) = \int \mathrm{d}t'\,\mathrm{d}^d\mathbf{x}' G(r,t-t',\mathbf{x}-\mathbf{x}')\psi_{(0)}(t',\mathbf{x}') \tag{3.5.10}$$

subject to the boundary conditions that $\psi(r,t,\mathbf{x})$ is regular as $r\to\infty$, and that $\psi_{(0)}$ corresponds to a non-normalizable source, i.e.:

$$\lim_{r\to 0} r^{-\Delta_-}\psi(r,t,\mathbf{x}) = \psi_{(0)}(t,\mathbf{x}). \tag{3.5.11}$$

This problem can be simplified by performing the Fourier transform in the $(t,\mathbf{x})$ boundary space so that (3.5.10) becomes simply

$$\tilde{\psi}(r,\omega,\mathbf{k}) = \tilde{G}(r,\omega,\mathbf{k})\tilde{\psi}_{(0)}(\omega,\mathbf{k}) \tag{3.5.12}$$

which simplifies the equation of motion to

$$r^2\partial_r^2\tilde{G} - r(D+z-1)\partial_r\tilde{G} - (-\omega^2 r^{2z} + \mathbf{k}^2 r^2 + m^2L^2)\tilde{G} = 0. \tag{3.5.13}$$

We can also simplify the asymptotic behaviour constraint (3.5.11) to simply

$$\lim_{r\to 0} r^{-\Delta_-}\tilde{G}(r,\omega,\mathbf{k}) = 1. \tag{3.5.14}$$

Note that as in relativistic examples [21] we should not expect to be able to apply the bulk regularity constraint at the level of the Fourier transform, rather we must insist it after taking the inverse transform back to position space.

It is technically difficult to find analytic solutions to equation (3.5.13) for arbitrary z and ω though various limits exist which make the system more tractable. In the $z=1$ limit this reduces to the relativistic case with solutions given in terms of (modified) Bessel functions

$$\tilde{G} = c_1 r^{(D+1)/2}K_{N_1}(qr) + c_2 r^{(D+1)/2}I_{N_1}(qr) \tag{3.5.15}$$

which is exactly the relativistic case discussed above. Note that here the quantity labelled l earlier is now N_1. Another directly tractable limit is the $\omega\to 0$ limit where once again the solutions are given by modified Bessel functions:

$$\tilde{G} = c_1 r^{(D+z)/2}K_{N_z}(|\mathbf{k}|r) + c_2 r^{(D+z)/2}I_{N_z}(|\mathbf{k}|r). \tag{3.5.16}$$

This is not entirely surprising as at zero frequency the system does not feel the non-relativistic scaling directly; it is only felt through a modified effective dimension which sends $D+1\to D+z$. Although this limit is not directly useful in the calculation of the

bulk-boundary propagator for generic z it does highlight the universal zero-frequency limiting behaviour of the solutions for generic z.

3.5.1 Specialisation to $z = 2$

We will now specialise to the case of $z = 2$ where the scalar field equation is tractable analytically. Consider a function $y(r)$ which obeys the general confluent hypergeometric differential equation given by:

$$y'' + \left(\frac{2A}{r} + 2f' + \frac{bh'}{h} - h' - \frac{h''}{h'}\right) y' \tag{3.5.17}$$

$$+ \left[\left(\frac{bh'}{h} - h' - \frac{h''}{h'}\right)\left(\frac{A}{r} + f'\right) + \frac{A(A-1)}{r^2} + \frac{2Af'}{r} + f'' + f'^2 - \frac{ah'^2}{h}\right] y = 0, \tag{3.5.18}$$

where A, a, and b are constants, and $f(r)$ and $h(r)$ are differentiable functions. This equation has two linearly independent solutions given by [98]:

$$\begin{aligned} y_M(r) &= r^{-A} e^{-f(u)} M(a, b, h(r)) \\ y_U(r) &= r^{-A} e^{-f(u)} U(a, b, h(r)) \end{aligned} \tag{3.5.19}$$

where $M(a, b, w)$ and $U(a, b, w)$ are the confluent hypergeometric functions of the first and second kind respectively. $M(a, b, w)$ is often referred to as the Kummer function while $U(a, b, w)$ is the Tricomi function.

To demonstrate the claim that equation (3.5.13) is indeed a confluent hypergeometric differential equation we will make the following ansatze $f(r) = \mu r^2$ and $h(r) = \lambda r^2$ which yield the following five constraints

$$\lambda = 2\mu, \quad 2b + 2A = -D, \quad A(2b + A - 2) = -(mL)^2, \quad 4\mu(b - 2a) = -\mathbf{k}^2, \quad -4\mu^2 = \omega^2. \tag{3.5.20}$$

In total these five constraints can be solved to yield

$$\begin{aligned} \mu^2 &= -\frac{1}{4}\omega^2, \qquad \lambda = 2\mu \\ A_\pm &= -\frac{1}{2}(D+2) \mp \frac{1}{2}\sqrt{(D+2)^2 + 4(mL)^2} = -\Delta_\pm \\ a_\pm &= \frac{\mathbf{k}^2}{8\mu} + \frac{1}{2}b_\pm \\ b_\pm &= 1 \pm \frac{1}{2}\sqrt{(D+2)^2 + 4(mL)^2} = 1 \pm N_2. \end{aligned} \tag{3.5.21}$$

$M(a, b, z)$ is undefined when b is a non-positive integer, which will generically occur whenever N_2 is an integer, e.g. when $m = 0$. This problem can be avoided by consid-

ering the regularised confluent hypergeometric function $\mathbf{M}(a,b,z)$ which is related to $M(a,b,z)$ whenever b is not a non-positive integer via $M(a,b,z) = \Gamma(b)\mathbf{M}(a,b,z)$. The regularised confluent hypergeometric function is defined for all values of b so we will work with this version of the function to avoid having to restrict N_2.

Therefore, the most general solutions to equation (3.5.13) for $z = 2$ are given by

$$\begin{aligned}\tilde{G}^{\pm}_{\mathbf{M}} &= r^{\Delta_\pm} e^{-\mu r^2} \mathbf{M}\left(\frac{\mathbf{k}^2}{8\mu} + \frac{1}{2}(1 \pm N_2), 1 \pm N_2, 2\mu r^2\right) \\ \tilde{G}^{\pm}_{U} &= r^{\Delta_\pm} e^{-\mu r^2} U\left(\frac{\mathbf{k}^2}{8\mu} + \frac{1}{2}(1 \pm N_2), 1 \pm N_2, 2\mu r^2\right).\end{aligned} \tag{3.5.22}$$

We now need to choose two linearly independent solutions; these solutions are not all linearly independent. First note that the choice of sign for any of A, a, or b fixes the signs of the other two quantities. The confluent hypergeometric functions are also related to each other through various identities known as Kummer's relations and these relations allow us to choose one set of signs without loss of generality. Firstly we can use the relation

$$U(a,b,w) = z^{1-b} U(a-b+1, 2-b, w) \tag{3.5.23}$$

while a second identity, valid whenever N_2 is not an integer, is:

$$U(a_+,b_+,w) = \frac{\pi}{\sin \pi b_+}\left(\frac{\mathbf{M}(a_+,b_+,w)}{\Gamma(a_-)} - w^{-N_2}\frac{\mathbf{M}(a_-,b_-,w)}{\Gamma(a_+)}\right). \tag{3.5.24}$$

Similarly when N_2 is an integer one can show the following

$$w^{-N_2}\Gamma(a_-)\mathbf{M}(a_-,b_-,w) = \Gamma(a_+)\mathbf{M}(a_+,b_+,w) \tag{3.5.25}$$

Therefore we have the following three relations linear relations between the solutions:

$$\begin{aligned}\tilde{G}^{\pm}_{U} &= (2\mu)^{\mp N_2}\tilde{G}^{\mp}_{U} \qquad (3.5.26)\\ \tilde{G}^{\pm}_{U} &= \Gamma(\mp N_2)\Gamma(1 \pm N_2)\left(\frac{\tilde{G}^{\pm}_{\mathbf{M}}}{\Gamma(a_\mp)} - \frac{\tilde{G}^{\mp}_{\mathbf{M}}}{\Gamma(a_\pm)}\right) \qquad (N_2 \notin \mathbb{N}) \\ \Gamma(a_\pm)\tilde{G}^{\pm}_{\mathbf{M}} &= \Gamma(a_\mp)\tilde{G}^{\mp}_{\mathbf{M}} \qquad (N_2 \in \mathbb{N}).\end{aligned}$$

Let us choose $\tilde{G}^{-}_{\mathbf{M}}$ and $\tilde{G}^{-}_{U}$ as the independent solutions. Our solution is therefore:

$$\tilde{G} = e^{-\mu r^2} r^{\Delta_-}\left[\alpha U(a_-,b_-,2\mu r^2) + \beta \mathbf{M}(a_-,b_-,2\mu r^2)\right] \tag{3.5.27}$$

where α and β are integration constants which remain to be determined. Note that the parameter μ appears in a_-.

It is convenient to first analyse the solution in Euclidean signature, i.e. letting $\omega^2 = -\omega_E^2$,

so that $\mu = \pm\frac{1}{2}\omega_E$. Again one can fix a choice of sign without loss of generality, as Kummer's relations relate $U(a,b,\pm w)$ and $\mathbf{M}(a,b,\pm w)$. Choosing the positive sign we obtain

$$\tilde{G} = e^{-\frac{1}{2}\omega_E r^2} r^{\Delta_-} \left[\alpha U(a_-,b_-,\omega_E r^2) + \beta \mathbf{M}(a_-,b_-,\omega_E r^2)\right]. \tag{3.5.28}$$

Note that the parameter μ appears in a_- and thus we have fixed

$$a_- = \frac{\mathbf{k}^2}{4\omega_E} + \frac{1}{2}b_-. \tag{3.5.29}$$

We now need to apply the boundary conditions to fix the integration constants. In [84], it was argued that the condition that $\tilde{G}$ is regular as $r \to \infty$ fixes $\beta = 0$. This argument follows from the asymptotic behaviours of the confluent hypergeometric functions at large argument:

$$U(a,b,w) \sim w^{-a} \qquad \mathbf{M}(a,b,w) \sim \frac{1}{\Gamma(a)} e^w w^{a-b} \tag{3.5.30}$$

where the latter expression holds for $|\mathrm{Arg}(w)| \leq \pi/2$ i.e. in the right hand complex plane of z.

However, implicitly [84] was assuming that ω_E is real and positive: clearly for $\mathcal{R}e(\omega_E) < 0$ the exponential prefactor in the above solution diverges as $r \to \infty$. Moreover, the Tricomi function $U(a,b,z)$ has a branch cut along the negative real axis.

Extending to the complex frequency plane, and imposing the normalisation condition (3.5.14), we find that

$$\tilde{G} = \frac{\Gamma(1+a_--b_-)}{\Gamma(a_-)} e^{-\frac{1}{2}\omega_E r^2} r^{\Delta_-} U(a_-,b_-,\omega_E r^2) \tag{3.5.31}$$

for $\mathcal{R}e(\omega_E) > 0$. This function is analytic over the domain $\mathcal{R}e(\omega_E) > 0$. To see this, note that

$$\Gamma(1+a_--b_-) = \Gamma\left(\frac{1}{2} + \frac{1}{2}N_2 + \frac{\mathbf{k}^2}{4\omega_E}\right). \tag{3.5.32}$$

The Gamma function has poles at negative integers, but for $\mathcal{R}e(\omega_E) > 0$ the argument $(1+a_--b_-)$ never takes negative integer values. Since the Gamma function has no zeros and $U(a,b,z)$ is analytic for $\mathcal{R}e(z) > 0$, the solution is indeed analytic over the domain.

However, for $\mathcal{R}e(\omega_E) < 0$ we should instead choose

$$\tilde{G} = \frac{\Gamma(1+\tilde{a}_--b_-)}{\Gamma(\tilde{a}_-)} e^{\frac{1}{2}\omega_E r^2} r^{\Delta_-} U(\tilde{a}_-,b_-,-\omega_E r^2), \tag{3.5.33}$$

to ensure that the function is bounded as $r \to \infty$ for ω_E real and negative. Here we denote

$$\tilde{a}_- = -\frac{\mathbf{k}^2}{4\omega_E} + \frac{1}{2}b_-, \tag{3.5.34}$$

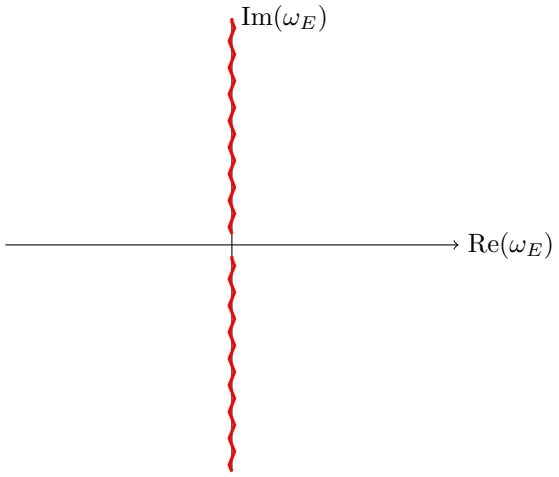

Figure 3.5.1: The complex Euclidean frequency plane.

i.e. we take into account the switch in sign of μ in this parameter. By the same arguments as before, this function is analytic over this domain.

Both functions (3.5.31) and (3.5.33) reduce to the same limit as $\omega_E \to 0$ along the real axis. However, the two solutions are clearly discontinuous as one crosses the imaginary axis, i.e. we need to introduce branch cuts, as shown in Figure 3.5.1.

We can now extract the Euclidean two point functions in the standard way. First of all, we need to calculate the renormalized one point function. To do this, we note that the counter terms for the scalar field action are

$$S^E_{\rm ct} = -\frac{1}{2}\Delta_- \int d^d x \sqrt{g}\psi^2 + \cdots \tag{3.5.35}$$

where the superscript E denotes that we work in Euclidean signature and the ellipses denote additional counter terms, depending on derivatives of the scalar field. The latter contribute to contact terms in the correlation functions, which we will suppress in what follows. Let us now write the near boundary expansion of the scalar field as

$$\psi = r^{\Delta_-}\left(\psi_{(0)} + r^2\psi_{(2)} + \cdots\right) + r^{\Delta_+}\left(\psi_{(\Delta_+)} + r^2\psi_{(\Delta_++2)} + \cdots\right) \tag{3.5.36}$$

where, as discussed earlier, the asymptotic expansion contains logarithmic terms when $(\Delta_+ - \Delta_-)$ is an integer. Defining the renormalized action as

$$S^E_{\rm ren} = S^E + S^E_{\rm ct} \tag{3.5.37}$$

then the one point function for the scalar operator is given by

$$\langle \mathcal{O}_\psi(\tau, x)\rangle = -\frac{\delta S^E}{\delta \psi_{(0)}} = -N_z \psi_{(\Delta_+)}(\tau, x) + \ldots \tag{3.5.38}$$

where the ellipses denote contact terms. (This expression is not applicable to integral N_z for which logarithmic terms arise in the asymptotic expansion.) Differentiating a second time gives

$$\langle \mathcal{O}_\psi(\tau,x)\mathcal{O}_\psi(\tau',x')\rangle = N_z \frac{\delta\psi_{(\Delta_+)}(\tau,x)}{\delta\psi_{(0)}(\tau',x')}. \tag{3.5.39}$$

Thus we find for $z=2$ that

$$\langle \mathcal{O}_\psi(\omega_E,k)\mathcal{O}_\psi(-\omega_E,-k)\rangle = N_2 \frac{\Gamma(-N_2)}{\Gamma(N_2)}\frac{\Gamma(a_+)}{\Gamma(a_-)}\omega_E^{N_2}, \tag{3.5.40}$$

for $\mathcal{R}e(\omega_E)>0$ while

$$\langle \mathcal{O}_\psi(\omega_E,k)\mathcal{O}_\psi(-\omega_E,-k)\rangle = N_2 \frac{\Gamma(-N_2)}{\Gamma(N_2)}\frac{\Gamma(\tilde{a}_+)}{\Gamma(\tilde{a}_-)}(-\omega_E)^{N_2}, \tag{3.5.41}$$

for $\mathcal{R}e(\omega_E)<0$.

For integral values of N_2 for $\mathcal{R}e(\omega_E)>0$ and one finds that

$$\langle \mathcal{O}_\psi(\omega_E,k)\mathcal{O}_\psi(-\omega_E,-k)\rangle \sim (a_-)_{N_2}\Psi(a_+)\omega_E^{N_2} \tag{3.5.42}$$

where $a_n=\Gamma(a+n)/\Gamma(a)$ is the Pochhammer symbol and $\Psi(x)$ is the digamma function. For $\mathcal{R}e(\omega_E)<0$, the corresponding expression is obtained by replacing $\omega_E\to-\omega_E$.

The analytic structure of this correlation function is the same as that of the bulk propagator, shown in 3.5.1. The position space correlation function is obtained by the inverse Fourier transform

$$\begin{aligned}\langle \mathcal{O}_\psi(\tau,x)\mathcal{O}_\psi(0,0)\rangle \sim &\int_0^\infty \mathrm{d}\omega_E \int \mathrm{d}\mathbf{k} e^{-i\omega_E\tau+i\mathbf{k}\cdot\mathbf{x}}\frac{\Gamma(a_+)}{\Gamma(a_-)}\omega_E^{N_2} \\ &+\int_{-\infty}^0 \mathrm{d}\omega_E \int \mathrm{d}\mathbf{k} e^{-i\omega_E\tau+i\mathbf{k}\cdot\mathbf{x}}\frac{\Gamma(\tilde{a}_+)}{\Gamma(\tilde{a}_-)}(-\omega_E)^{N_2}\end{aligned} \tag{3.5.43}$$

where we have suppressed numerical prefactors. This expression can be equivalently written in terms of a cosine transform

$$\langle \mathcal{O}_\psi(\tau,x)\mathcal{O}_\psi(0,0)\rangle \sim \int_{-\infty}^\infty \mathrm{d}\omega_E \cos(\omega_E\tau)\int \mathrm{d}\mathbf{k} e^{i\mathbf{k}\cdot\mathbf{x}}\frac{\Gamma(a_+)}{\Gamma(a_-)}\omega_E^{N_2}. \tag{3.5.44}$$

For integral values of N_2 the expressions reduce to integrals over digamma functions; for example, for $N_2=1$ we obtain

$$\langle \mathcal{O}_\psi(\tau,x)\mathcal{O}_\psi(0,0)\rangle \sim \int_0^\infty \mathrm{d}\omega_E \int \mathrm{d}\mathbf{k} e^{-i\omega_E\tau+i\mathbf{k}\cdot\mathbf{x}}|\mathbf{k}|^2\Psi\left(1+\frac{|\mathbf{k}|^2}{4|\omega_E|}\right). \tag{3.5.45}$$

3.5.2 Lorentzian solutions

Now let us turn to Lorentzian solutions, in which $\mu = \pm\frac{1}{2}i\omega$. Applying the near boundary limit $\lim_{r\to 0} r^{-\Delta_-}\tilde{G} = 1$, we can again write

$$\tilde{G} = e^{-\mu r^2} r^{\Delta_-} \frac{\Gamma(a_+)}{\Gamma(N_2)} \left[U(a_-, b_-, 2\mu r^2) + \beta_{\omega k} r^{2N_2} \mathbf{M}(a_+, b_+, 2\mu r^2)\right]. \tag{3.5.46}$$

Let us consider first the case of $\mu = \frac{1}{2}i\omega$:

$$\tilde{G} = e^{-\frac{i}{2}\omega r^2} r^{\Delta_-} \frac{\Gamma(a_+)}{\Gamma(N_2)} \left[U(a_-, b_-, i\omega r^2) + \beta r^{2N_2} \mathbf{M}(a_+, b_+, i\omega r^2)\right] \tag{3.5.47}$$

where

$$a_\pm = -i\frac{\mathbf{k}^2}{4\omega} + \frac{1}{2}(1 \pm N_2) \tag{3.5.48}$$

The U function has a branch cut on the negative real frequency axis while the $\mathbf{M}$ function is entire. Neither the U nor the $\mathbf{M}$ function is bounded on the real frequency axis as $r \to \infty$, but the U function is bounded in the complex frequency lower half plane while the $\mathbf{M}$ function is bounded in the upper half plane. The normalisation factor $\Gamma(a_+)$ has poles when a_+ is a negative integer, i.e. along the positive imaginary axis in the complex frequency plane.

For the other choice $\mu = -\frac{1}{2}i\omega$:

$$\tilde{G} = e^{\frac{i}{2}\omega r^2} r^{\Delta_-} \frac{\Gamma(\tilde{a}_+)}{\Gamma(N_2)} \left[U(\tilde{a}_-, b_-, -i\omega r^2) + \beta r^{2N_2} \mathbf{M}(\tilde{a}_+, b_+, -i\omega r^2)\right] \tag{3.5.49}$$

where

$$\tilde{a}_\pm = i\frac{\mathbf{k}^2}{4\omega} + \frac{1}{2}(1 \pm N_2) \tag{3.5.50}$$

Here, the U function has a branch cut on the positive real frequency axis while the $\mathbf{M}$ function is entire. Neither the U nor the $\mathbf{M}$ function is bounded on the real frequency axis as $r \to \infty$, but the U function is bounded in the complex frequency upper half plane and the $\mathbf{M}$ function is bounded in the lower half plane. The normalisation factor $\Gamma(a_+)$ has poles when $\tilde{a}_+$ is a negative integer, i.e. along the negative imaginary axis in the complex frequency plane. We can therefore see that neither choice of Green's function is by itself satisfactory: note that both choices break the $\omega \to -\omega$ symmetry of the field equation.

Putting these facts together, we can see that we should choose the following combination in the complex frequency upper half plane:

$$\tilde{G}^{ru}(\omega, k, r) = e^{\frac{i}{2}\omega r^2} r^{\Delta_-} \frac{\Gamma(\tilde{a}_+)}{\Gamma(N_2)} U(\tilde{a}_-, b_-, -i\omega r^2) + \beta^u_{\omega k} r^{\Delta_+} e^{-\frac{i}{2}\omega r^2} \mathbf{M}(a_+, b_+, i\omega r^2). \tag{3.5.51}$$

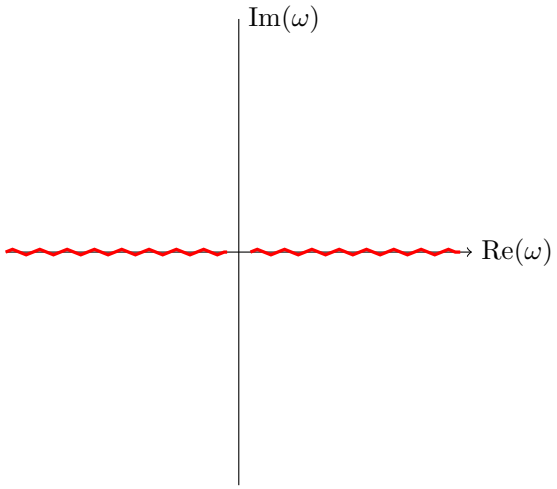

Figure 3.5.2: The complex frequency plane for Lifshitz.

This function is bounded as $r \to \infty$ in the upper half plane and also has no poles in the upper half plane. Similarly in the lower half plane we choose

$$\tilde{G}^d(\omega,k,r) = e^{-\frac{i}{2}\omega r^2} r^{\Delta_-} \frac{\Gamma(a_+)}{\Gamma(N_2)} U(a_-,b_-,i\omega r^2) + \beta^d_{\omega k} r^{\Delta_+} e^{\frac{i}{2}\omega r^2} \mathbf{M}(\tilde{a}_+,b_+,-i\omega r^2). \quad (3.5.52)$$

Note that invariance under $\omega \to -\omega$ requires $\beta^d_{\omega k} = \beta^u_{-\omega k}$. There are two branch cuts in the complex frequency plane, one along the negative real axis and one along the positive real axis (excluding the origin). The analytic structure is shown in Figure 3.5.2.

Thus for general boundary data

$$\begin{aligned}\Phi(t,x,r) &= \frac{1}{(2\pi)^d}\int_C \mathrm{d}\omega \int \mathrm{d}\mathbf{k} \int \mathrm{d}\hat{t}\mathrm{d}\hat{\mathbf{x}} e^{-i\omega(t-\hat{t})+i\mathbf{k}\cdot(\mathbf{x}-\hat{\mathbf{x}})}\phi_{(0)}(\hat{t},\hat{x})\tilde{G}(\omega,k,r), \quad (3.5.53)\\ &= \frac{1}{(2\pi)^d}\int_C \mathrm{d}\omega \int \mathrm{d}\mathbf{k} e^{-i\omega t+i\mathbf{k}\cdot\mathbf{x}}\phi_{(0)}(\omega,k)\tilde{G}(\omega,k,r),\end{aligned}$$

where implicitly we use the appropriate form for $\tilde{G}(\omega,k,r)$. The contour C must be specified; we will consider here the case of the Feynman contour.

To the far past of the sources one can deform the part of the Feynman contour lying in the upper half plane back along the branch cut along the negative real axis. In this regime, assuming that $N_2 = 1+l$ where $l \in \mathbb{N}$, one can show that

$$\begin{aligned}\Phi(t,x,r) = \frac{1}{(2\pi)^d}\int \mathrm{d}^d\mathbf{k} \int_{-\infty}^0 \mathrm{d}\omega\, e^{-i\omega t+i\mathbf{k}\cdot\mathbf{x}} e^{\frac{1}{2}i\omega r^2} r^{\Delta_+} \mathbf{M}(\tilde{a}_+,b_+,-i\omega r^2) \quad (3.5.54)\\ \times \left[\beta^d_{\omega k} - \beta^u_{\omega k} - \phi_{(0)}(\omega,k)\frac{(i\omega)^{l+1}\Gamma(\tilde{a}_+)\Gamma(a_+)e^{-i\pi\tilde{a}_-}}{l!}\right].\end{aligned}$$

Similarly to the far future of the sources the same can be done but in the lower half-

plane:

$$\Phi(t,x,r) = \frac{1}{(2\pi)^d}\int \mathrm{d}^d\mathbf{k}\int_0^\infty \mathrm{d}\omega\, e^{-i\omega t+i\mathbf{k}\cdot\mathbf{x}}e^{-\frac{1}{2}i\omega r^2}r^{\Delta_+}\mathbf{M}(a_+,b_+,i\omega r^2) \times\left[\beta^u_{\omega k}-\beta^d_{\omega k}-\phi_{(0)}(\omega,k)\frac{(-i\omega)^{l+1}\Gamma(\tilde{a}_+)\Gamma(a_+)e^{-i\pi a_-}}{l!}\right] \tag{3.5.55}$$

Now let us turn to the matching with Euclidean caps. On the Euclidean segments the mode solutions are obtained by replacing $t=-i\tau$. Since there are no sources on the Euclidean boundaries, the solutions consist of only normalizable modes. Therefore

$$\Phi_E(\tau,x,r) = \frac{1}{(2\pi)^d}\int \mathrm{d}\omega\mathrm{d}\mathbf{k}\; d^{\pm}_{\omega k}e^{\mp\omega\tau+i\mathbf{k}\cdot\mathbf{x}}r^{\Delta_+}e^{\frac{i}{2}\omega r^2}\mathbf{M}(\tilde{a}_+,b_+,-i\omega r^2) \tag{3.5.56}$$

with coefficients $d^{\pm}_{\omega k}$ which are determined by matching conditions. Finiteness as $\tau\to\infty$ implies that $d^-_{\omega k}=0$ (for $\omega>0$), while finiteness as $\tau\to-\infty$ implies $d^+_{\omega k}=0$ (for $\omega>0$).

Consider for instance the in-out correlator shown in Figure 3.2.1. The matching conditions are given by

$$\begin{aligned}\Phi_0(\tau_0=0,x,r)&=\Phi_1(t=-T,x,r) & \Phi_1(t=T,x,r)&=\Phi_2(\tau_2=0,x,r)\\ i\partial_\tau\Phi_0(\tau_0=0,x,r)&=\partial_t\Phi_1(t=-T,x,r) & \partial_t\Phi_1(t=T,x,r)&=i\partial_\tau\Phi_2(\tau_2=0,x,r)\end{aligned}$$

where the Euclidean propagators are

$$\Phi_0(\tau,x,r) = \frac{1}{(2\pi)^d}\int \mathrm{d}\mathbf{k}\int_{-\infty}^0 \mathrm{d}\omega\; d^-_{\omega k}e^{\omega\tau+i\mathbf{k}\cdot\mathbf{x}}r^{\Delta_+}\; e^{\frac{1}{2}i\omega r^2}\mathbf{M}(\tilde{a}_+,b_+,-i\omega r^2) \tag{3.5.57}$$

$$\Phi_2(\tau,x,r) = \frac{1}{(2\pi)^d}\int \mathrm{d}\mathbf{k}\int_0^\infty \mathrm{d}\omega\; d^+_{\omega k}e^{-\omega\tau+i\mathbf{k}\cdot\mathbf{x}}r^{\Delta_+}\; e^{\frac{1}{2}i\omega r^2}\mathbf{M}(\tilde{a}_+,b_+,-i\omega r^2). \tag{3.5.58}$$

The matching conditions, combined with with the symmetry constraint $\beta^d_{\omega k}=\beta^u_{-\omega k}$ give the following constraints:

$$\beta^d_{\omega k}-\beta^u_{\omega k} = \phi_{(0)}(\omega,k)(i\omega)^{l+1}\frac{\Gamma(\tilde{a}_+)\Gamma(a_+)}{l!}e^{i\pi a_-} \qquad (\mathrm{Re}(\omega)<0) \tag{3.5.59}$$

$$d^+_{\omega k} = e^{-i\omega T}(-i\omega)\frac{\Gamma(\tilde{a}_+)\Gamma(a_+)}{l!}\left(\phi_{(0)}(-\omega,k)e^{-i\pi a_-}-\phi_{(0)}(\omega,k)e^{-i\pi\tilde{a}_-}\right) \tag{3.5.60}$$

$$d^-_{\omega k}=0 \tag{3.5.61}$$

which is insufficient to fix the ambiguity in the normalizable modes. Note that this is only three constraints from four equations as one of the future matching conditions is degenerate. This is not surprising since any further constraints on $d^+_{\omega k}$ would constrain the form of the source term $\phi_{(0)}(\omega,k)$.

3.6 Conclusions

In this chapter we have studied real-time correlators for holographic models of theories which possess either Lifshitz or Schrödinger symmetries. We started by reviewing a toy free scalar model with a $z = 2$ Lifshitz symmetry and demonstrated that the usual propagators and consequentially correlation functions were calculable in the framework of real time QFT.

We then investigated the related case of a probe scalar operator in a holographic model with dual $z = 2$ Lifshitz symmetry where we were unable to fully fix the ambiguity in the normalizable modes by applying the standard matching conditions from the real time holography prescription of [20]. Due to the presence of a branch cut in the propagator we were only able to use the matching conditions to fix the discontinuity of the normalizable modes across the branch cut. It is unclear what additional constraints are required to fully fix this ambiguity, or what the dual interpretation of this residual ambiguity is in the field theory.

In the Schrödinger case we specialised to operators with a fixed x^- momentum and found that their functional form is fully fixed by the K^- special conformal symmetry. This could be seen in the holographic case where the field equation dual to a probe scalar operator of fixed x^- momentum was exactly the same equation arising in AdS_{D+3} with a mass shifted by the x^- momentum and the deformation parameter b. The position space propagator, and consequentially the correlation functions, were simple to calculate via the standard prescription and gave the usual $i\varepsilon$ insertions used when analytically continuing from the Euclidean propagators.

We then attempted to repeat the holographic calculation but using the extended Schrödinger spacetime coordinates of [96] which aim to resolve the coordinate singularity present in the Schrödinger metric. The resulting propagator did not have the desirable features of the propagator found in the AdS_{D+3} case, and was not readily invertible back to position space. It was also unclear what regularity conditions should be applied to limit the available selection of modes, since we were able to reduce to a countable number of normalizable contributions but an uncountable number of non-normalizable modes. From this we must conclude that these extended coordinates are unsuitable for the purposes of real time holography.

It is surprising that the propagator has a form similar to that found in the Lifshitz case considering that the functional form should be fixed by the special conformal symmetry. This is likely due to the fact that the Schrödinger symmetry group, including the special conformal transformation, is realised non-trivially in these coordinates, though we have not confirmed this here. It would be interesting to confirm whether this is the case, and

what implications this may have on the Lifshitz propagator.

CHAPTER 4

The holographic F-theorem

In a three-dimensional quantum field theory, the F quantity is defined in terms of the renormalized partition function of the theory on a three-sphere Z_{S^3} as

$$F = -\log Z_{S^3}; \tag{4.0.1}$$

F gives the free energy on the three-sphere. The conjectured F-theorem [99, 100] states that F is positive in a unitary quantum field theory; F is stationary at a fixed point; $F_{UV} \geq F_{IR}$ for UV and IR fixed points and F decreases monotonically along an RG flow. Evidence in favour of the F theorem has been presented in a number of works. In [99] it was shown in a number of $\mathcal{N} = 2$ theories that $F_{IR} < F_{UV}$; examples included holographic theories described by $AdS_4 \times Y_7$ M theory solutions in which the partition function is [101]

$$F = N^{\frac{3}{2}} \sqrt{\frac{2\pi^6}{27\mathrm{Vol}(Y_7)}} \tag{4.0.2}$$

where $\mathrm{Vol}(Y_7)$ is the volume of the Sasaki-Einstein manifold Y_7 and N is the number of colours in the dual theory.

Many subsequent papers have provided additional evidence that $F_{IR} < F_{UV}$ in holographic and field theory models. For example, [100] considered relevant double trace deformations: given a single trace operator Φ in a CFT of dimension Δ_- such that $1/2 \leq \Delta_- \leq 3/2$, deforming the CFT by Φ^2 causes an RG flow to an IR fixed point where Φ has

dimension $\Delta_+ = 3 - \Delta_-$.

The evidence for stationarity and monotonic decrease of the F quantity along an RG flow is somewhat weaker. Arguments for stationarity are based on the fact that F is extremised with respect to the R charges of an IR CFT [102] and (holographically) with respect to the parameters of the Sasaki-Einstein manifold Y_7 [103, 99]. For monotonic decrease, it was shown in [100] that the free energy decreases monotonically along weakly relevant flows, while [104] argued that the volume of the compact manifold should increase monotonically along an RG flow in holographic examples, implying monotonic decrease of F. In [105] it was shown that F decreases along certain supersymmetric RG flows of deformations of the ABJM theory.

In a conformal field theory, the partition function on the three sphere is related to the (finite terms) in the entanglement entropy for a disk region in flat space by the Casini-Huerta-Myers map [106]. If the finite contribution to the entanglement entropy of a disk region in the ground state of the CFT is

$$S = -2\pi\mathcal{F}, \tag{4.0.3}$$

then $\mathcal{F}$ corresponds precisely to the F quantity, i.e. $\mathcal{F}$ is conjectured to be positive and to decrease monotonically along an RG flow. The F theorem has hence also been explored using entanglement entropy, see for example [107, 45, 108]. Ambiguities in defining the finite contributions can be dealt with by working with the UV finite mutual information [109] or by using renormalized entanglement entropy [110, 111]. There is however evidence that the renormalized entanglement entropy thus defined is not stationary at a fixed point [112].

In this chapter we show that the F quantity does not decrease for holographic RG flows associated with deformations by single trace operators of dimension $d/2 < \Delta_+ < d$. Therefore the strong version of the F theorem, decrease of F under all relevant deformations, is false.

4.1 Holographic RG flows

We begin by discussing holographic realisations of RG flows on curved manifolds. We work in Euclidean signature with a bulk action

$$I_E = -\frac{1}{16\pi G_4}\int \mathrm{d}^4x\sqrt{g}\left(R - \frac{1}{2}(\partial\phi)^2 + V(\phi)\right), \tag{4.1.1}$$

where G_4 is the Newton constant, which in a top-down holographic model is related to the number of colours as $1/G_4 \sim N^{3/2}$, as in (4.0.2). We consider solutions of the

equations of motion such that

$$\mathrm{d}s^2 = \mathrm{d}w^2 + e^{2\mathcal{A}(w)}\mathrm{d}s^2_{\Omega_3} \tag{4.1.2}$$

where Ω_3 is a homogeneous space with Ricci scalar $\mathcal{R}$ and the scalar field ϕ depends only on the radial coordinate w. We will be interested in the case of a unit radius three sphere for which $\mathcal{R} = 6$. The equations of motion are then given by:

$$\begin{aligned} \ddot{\phi} + 3\dot{\mathcal{A}}\dot{\phi} &= -V'(\phi); \\ -\frac{\mathcal{R}}{6}e^{-2\mathcal{A}} - \frac{1}{4}(\dot{\phi})^2 &= \ddot{\mathcal{A}}. \end{aligned} \tag{4.1.3}$$

These equations reduce to the case of flat domain walls when $\mathcal{R} = 0$.

4.1.1 Renormalization of action

We work perturbatively in the scalar field and assume that the potential has the following analytic expansion in ϕ around an AdS background:

$$V(\phi) = 6 - \frac{1}{2}M^2\phi^2 + \cdots \tag{4.1.4}$$

In what follows we solve the field equations to quadratic order in ϕ, taking into account the backreaction onto the metric to this order. In anti-de Sitter the warp factor is:

$$\mathcal{A}(w) \equiv \mathcal{A}_0(w) = \log(\sinh(w)). \tag{4.1.5}$$

Working to quadratic order in the scalar field, the change in the warp factor is quadratic in the scalar field, and therefore to the order required the scalar field equation is that in AdS, i.e.

$$\ddot{\phi} + 3\coth w\dot{\phi} = M^2\phi. \tag{4.1.6}$$

This equation can be solved exactly (see below) and asymptotically near the conformal boundary. The latter can be expressed as

$$\phi = e^{(\Delta_+-3)w}\phi_{(0)} + e^{(\Delta_+-5)w}\phi_{(2)} + \cdots + e^{-\Delta_+ w}\tilde{\phi}_{(0)} + e^{(-\Delta_+-2)w}\tilde{\phi}_{(2)} + \cdots \tag{4.1.7}$$

where

$$\phi_{(2)} = \frac{3(3-\Delta_+)}{(5-2\Delta_+)}\phi_{(0)} \qquad \tilde{\phi}_{(2)} = \frac{3\Delta_+\phi_{(0)}}{(2\Delta_+ - 1)}. \tag{4.1.8}$$

Here we implicitly assume that Δ_+ is neither $3/2$ nor $5/2$, since in these cases terms proportional to w arise in the expansion. (These cases can be straightforwardly analysed but we do not include details in what follows.)

One can then use the other equation of motion to solve for the warp factor up to quad-

ratic order in the scalar field. Letting

$$\mathcal{A} = \mathcal{A}_0 + a \tag{4.1.9}$$

then

$$\ddot{a} - \frac{2}{\sinh^2 w} a = -\frac{1}{4}\dot{\phi}^2. \tag{4.1.10}$$

The on-shell action is divergent for asymptotically locally AdS solutions, but the divergences may be removed by using the asymptotic solutions of the field equations to regulate the bulk action and adding appropriate covariant counterterms i.e. the renormalized action [78].

$$I_{\rm ren} = I_E + I_{\rm ct} \tag{4.1.11}$$

is finite. The AdS/CFT dictionary implies that the F quantity is calculated from the renormalized action in the limit in which the dual theory is well-described by supergravity.

Working to quadratic order in the scalar field ϕ the required counterterms to render the action finite are [78]

$$I_{\rm ct} = \frac{1}{8\pi G_4}\int {\rm d}^3x\sqrt{h}\left(-K + 2 + \frac{1}{2}\mathcal{R}_h + \frac{1}{4}(3-\Delta_+)\phi^2 + \frac{(\Delta_+ - 3)}{16(2\Delta_+ - 5)}\mathcal{R}_h\phi^2\right) \tag{4.1.12}$$

where $\mathcal{R}_h$ is the Ricci scalar for the boundary metric h. We define Δ_+ in terms of the mass as

$$\Delta_+ = \frac{3}{2} + \frac{1}{2}\sqrt{9 + 4M^2} \tag{4.1.13}$$

and we assume that $\frac{3}{2} \leq \Delta_+ \leq 3$. For $\Delta_+ \geq 5/2$, Δ_+ is the dimension of the operator dual to the scalar field of mass M^2. In the mass range

$$-\frac{9}{4} \leq M^2 \leq -\frac{5}{4} \tag{4.1.14}$$

two quantizations are possible [16]; we will discuss this situation below. In (4.1.12) we do not include counterterms which depend on derivatives of the scalar field (see [78]), since the scalar fields under consideration are homogeneous.

Note that the last counterterm in (4.1.12) is only required for $\Delta_+ > 5/2$. The corresponding divergence becomes logarithmic at $\Delta_+ = 5/2$ and in this case the value of the renormalized action can be adjusted by finite counterterms, so the F quantity is inherently scheme dependent. Correspondingly F is also scheme dependent for the Δ_- quantization of the same mass, i.e. $\Delta_- = 1/2$. No finite counterterms arise for other values of Δ_+ in the range of interest, although working to cubic order in the scalar field finite counterterms would arise at integral values of Δ_+; these can be fixed by requiring supersymmetry [105].

In the mass range $-9/4 \leq M^2 \leq -5/4$, two quantizations are possible:

$$\Delta_\pm = \frac{3}{2} \pm \sqrt{9 + 4M^2} \tag{4.1.15}$$

with $1/2 \leq \Delta_- \leq 3/2$ and $3/2 \leq \Delta_+ \leq 5/2$. As discussed in [18], the evaluation of the renormalized action by adding covariant counterterms is not affected by whether the dual operator has dimension Δ_+ or Δ_-. The difference arises in the identification of the functional that generates correlation functions for the dual operator. For the Δ_+ quantization, the coefficient $\phi_{(0)}$ in (4.1.7) acts as the source for the dual operator. The renormalized action (4.1.11) is a functional of this coefficient and acts as the generating functional for the dual operator.

For the Δ_- quantization, the renormalized action (4.1.11) is still a functional of the coefficient $\phi_{(0)}$ in (4.1.7) but this coefficient is not the operator source. As discussed in [18], following [16, 17], the correct generating functional is obtained by a Legendre transformation. Let us define the Legendre transformation as

$$\tilde{I}[\phi_{(0)}, \psi_{(0)}] = I_{\rm ren}[\phi_{(0)}] + \int d^3x \sqrt{g_{(0)}} \phi_{(0)} \psi_{(0)} \tag{4.1.16}$$

where $g_{(0)}$ is the boundary metric. Then extremising gives

$$\tilde{I}_{\rm ren}[\psi_{(0)}] = \tilde{I}[\phi^*_{(0)}(\psi_{(0)}), \psi_{(0)}] \tag{4.1.17}$$

where

$$\left. \frac{\delta I_{\rm ren}[\phi_{(0)}]}{\delta \phi_{(0)}} \right|_{\phi^*_{(0)}} + \psi_{(0)} = 0 \tag{4.1.18}$$

defines $\phi^*_{(0)}(\psi_{(0)})$. Here $\tilde{I}_{\rm ren}[\psi_{(0)}]$ is identified as the renormalized generating functional of correlation functions of the operator of dimension Δ_-.

In the case at hand, we work perturbatively in the scalar field and thus the on-shell renormalized action necessarily has the form

$$I_{\rm ren}[\phi_{(0)}] = (I_0 + I_2 \phi^2_{(0)} + \cdots), \tag{4.1.19}$$

where I_0 and I_2 are numerical coefficients. (Recall that $\phi_{(0)}$ is homogeneous and therefore does not depend on the sphere coordinates.) The Legendre transformed action is then given by

$$\tilde{I}[\phi_{(0)}, \Psi_{(0)}] = (I_0 + I_2 \phi^2_{(0)} + \cdots) + \phi_{(0)} \Psi_{(0)}, \tag{4.1.20}$$

where we denote

$$\Psi_{(0)} \equiv \int \mathrm{d}^3x \sqrt{g_{(0)}} \psi_{(0)}. \tag{4.1.21}$$

Extremising, we obtain

$$2I_2\phi_{(0)} + \Psi_{(0)} = 0 \tag{4.1.22}$$

and hence

$$\tilde{I}_{\rm ren}[\Psi_{(0)}] = I_0 - I_2\phi_{(0)}^2 + \cdots = I_0 - \frac{1}{4I_2}\Psi_{(0)}^2 + \cdots \tag{4.1.23}$$

In the Δ_+ quantization, $\phi_{(0)}$ acts as the source for the dual operator and therefore (4.1.19) gives the free energy to quadratic order in the source. In the Δ_- quantization, $\Psi_{(0)}$ acts as the source for the dual operator and (4.1.23) gives the free energy to quadratic order in the source. The quadratic terms have different signs in the two quantizations: if $I_2 > 0$ the free energy on the S^3 increases for deformations by the Δ_+ quantization operator and decreases for deformations by the Δ_- quantization operator, and vice versa. For $M^2 = -9/4$, the two quantizations coincide; note however that one needs to treat this case separately, as the above formulae degenerate.

4.2 Evaluation of free energy

Having determined the renormalized free energy functional we now consider exact regular solutions of the field equations, to quadratic order in the scalar field. To the required order we can solve the scalar field equation in the anti-de Sitter background. The scalar field solution may be found analytically:

$$\begin{aligned}\phi = {} & \frac{\phi_{(0)}\Gamma\left(\frac{5}{2}-\Delta_+\right)}{2\sqrt{2}\Gamma(3-\Delta_+)}(U-1)^{(3-\Delta_+)/2}(U+1)^{\Delta_+/2} \\ & \left[\Gamma(3-\Delta_+){}_2\tilde{F}_1\left(-\frac{1}{2},\frac{3}{2};\frac{5}{2}-\Delta_+;\frac{1}{2}(1-U)\right)\right. \\ & \left. -\left(\frac{U-1}{U+1}\right)^{\Delta_+-\frac{3}{2}}\Gamma(\Delta_+){}_2\tilde{F}_1\left(-\frac{1}{2},\frac{3}{2};\Delta_+-\frac{1}{2};\frac{1}{2}(1-U)\right)\right] \\ U = {} & \frac{1}{u} = \coth w\end{aligned} \tag{4.2.1}$$

where ${}_1\tilde{F}_2(a,b;c;z)$ is the regularised hypergeometric function, and we have imposed regularity throughout the bulk and have chosen the overall normalisation of the solution to agree with the definition of $\phi_{(0)}$ given in (4.1.7).

To calculate the free energy for the RG flow, we need to solve numerically for the warp factor and thus for the renormalized on-shell action. To carry out the numerics we work with a compactified radial coordinate $u = \tanh w$ for all the calculations. Plotted in Figures 4.2.1–4.2.2 is the change in the free energy normalised by the scalar source and the Newton constant: we define δF as

$$\delta F = F(\phi_{(0)}) - F(0) \equiv F(\phi_{(0)}) - \frac{\pi}{2G_4}, \tag{4.2.2}$$

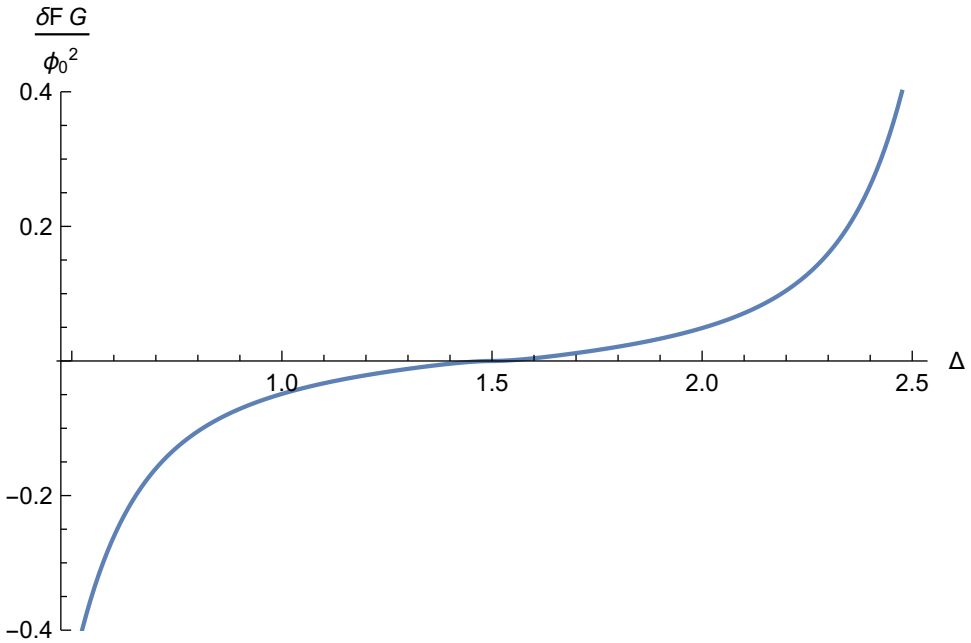

Figure 4.2.1: The change in the renormalized free energy for $\frac{1}{2} < \Delta < \frac{5}{2}$.

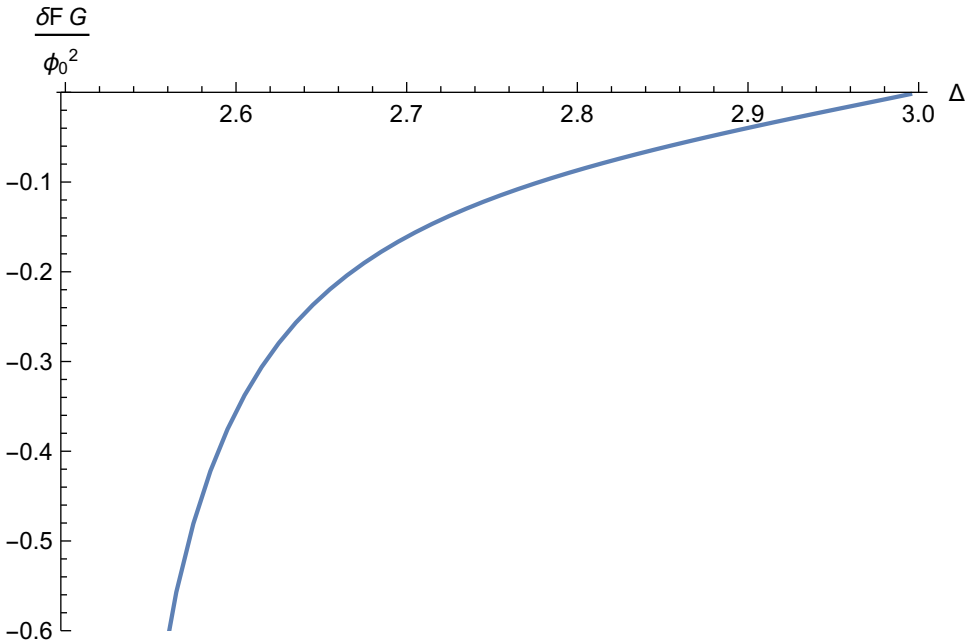

Figure 4.2.2: The change in the renormalized free energy for $\frac{5}{2} < \Delta < 3$.

where implicitly we use the appropriate source for $\Delta < 3/2$.

The change in the free energy vanishes to quadratic order in the source for $\Delta = 3/2$ and for exactly marginal operators. The change in the free energy is however positive for $3/2 < \Delta < 5/2$, with the corresponding change in the free energy for $1/2 < \Delta < 3/2$ therefore being negative, in agreement with the arguments above.

We should note that a related sign change at $\Delta = 3/2$ was found in [113]. This paper calculated one point functions of the deformation operator under relevant deformations, both holographically and using conformal perturbation theory. The sign of this one point function, which is related to the sign of δF found above, indeed changes at $\Delta = d/2$.

Thus, to summarise, working quadratically in the operator source, deformations by operators of dimensions $3/2 < \Delta < 5/2$ lead to increases in the F quantity. Note that we have worked only to quadratic order and changes in the F quantity to higher order in the source would depend on the interactions in the theory.

The F theorem would be satisfied in a holographic theory which contains no operators of dimensions $3/2 < \Delta < 5/2$, but generically such operators do exist. In particular, it is well-known that in four-dimensional $\mathcal{N} = 8$ gauged supergravity there are 35 $\Delta_- = 1$ scalar operators and 35 $\Delta_+ = 2$ pseudoscalars corresponding to the seventy scalars with $M^2 = -2$, i.e. both quantizations arise [114]. (The pseudoscalar nature of the Δ_+ quantization does not affect the arguments given here.) However, for the supersymmetric RG flows in consistent truncations of $\mathcal{N} = 8$ analysed in [105] the F quantity does decrease: in this setup supersymmetry does not allow a single real scalar (in the Euclidean) corresponding to a $\Delta_+ = 2$ operator to be switched on. A complete proof of the F theorem would effectively restrict the allowed holographic theories, i.e. it would throw theories such as those considered here into the swampland.

Now let us return to the relationship between the F quantity and the entanglement entropy of a disk entangling region. One can use holographic renormalization techniques to define renormalized entanglement entropy [2]. The renormalized entanglement entropy of disk regions in theories deformed by relevant operators agrees with the behaviour of the F quantity found above: F increases for RG flows by operators of dimension $3/2 < \Delta < 5/2$ (see also [115]).

Our results do not contradict [103, 99]: these works showed that F is extremal within the parameter spaces of putative conformal field theories. In the holographic setups, an AdS_4 factor is assumed and the volume of the compactifying Sasaki-Einstein is extremised. This analysis does not imply that F is decreased under relevant deformations

which change the geometry away from AdS_4. The scalar field ϕ and the change in the warp factor a do not decrease monotonically along the flow but this does not in itself contradict the arguments of [104]. From a top-down perspective scalar fields in four-dimensional gauged supergravity theories arise not just from breathing modes of the compact manifold, but also from the four-form flux in eleven dimensions.

In two dimensions one defines the Zamolodchikov c-function $c(g_i, \mu)$ in terms of the coupling constants g_i and the energy scale μ. Here implicitly we have defined F as a renormalized quantity, dependent on UV data for coupling constants of the relevant operators. It would be interesting to explore whether one could sharply define an F function with explicit dependence on the energy (i.e. radial) scale holographically. One natural way to do this would be to rewrite the source $\phi_{(0)}$ in terms of the bulk scalar field $\phi(w)$, and interpret w as the energy scale.

Finally, there has been considerable recent interest in how much supersymmetry is required to determine uniquely partition functions on even-dimensional spheres [116].

CHAPTER 5

Renormalized holographic entanglement entropy

5.1 Introduction

In recent years there has been considerable interest in entanglement entropy and its holographic implementation, following the proposal of [41] that entanglement entropy can be computed from the area of a bulk minimal surface homologous to a boundary entangling region. This proposal was proved for spherical entangling regions in conformal field theories in [106] and arguments supporting the Ryu-Takayanagi prescription based on generalised entropy were given in [44]. Entanglement entropy has by now been computed in a wide range of holographic systems, see the review [117]. General properties of holographic entanglement entropy are reviewed in [118].

Entanglement entropy is a UV divergent quantity, with the leading UV divergences scaling with the area of the boundary of the entangling region. For a quantum field theory in D spatial dimensions, the boundary of the entangling region is $(D-1)$-dimensional and thus $S \approx \Lambda^{D-1}\mathcal{A}_{D-1}$ where Λ is the UV cutoff and $\mathcal{A}_{D-1}$ is the area of the boundary of the entangling region.

If one is interested in the entanglement entropy of a discrete system, in which there is a natural UV cutoff set by, for example, the lattice scale, then it may be natural to work with this "bare" entanglement entropy. If however one is interested in entanglement entropy in a quantum field theory context, then it natural to explore whether and how

entanglement entropy can be renormalized.

Finite terms in the entanglement entropy are used in a number of contexts. Firstly, they arise as order parameters for phase transitions, see the pioneering works [119, 86]. Finite terms in the entanglement entropy for disk regions in three dimensional conformal field theories are also related by conformal transformations [106] to the free energy on a three sphere, which is the quantity appearing in the proposed F theorem [99].

As we will review in Section 5.2, in previous works the finite terms in the entanglement entropy have been isolated using differentiation of the entanglement entropy with respect to geometric parameters characterising the entangling region. Such procedures can be implemented in a simple way, both holographically and in field theory calculations, but they have several disadvantages. The differentiation prescriptions depend on the specific geometry of the entangling region, and thus it is hard to implement such renormalization in situations where the shape of the entangling region is itself being varied. Renormalization by differentiation is furthermore not directly related to the renormalization procedures used for other quantum field theory quantities. Thus, in particular, it is hard to understand issues such as the scheme dependence of the finite answer.

In this chapter we will develop a systematic renormalization procedure for entanglement entropy. We begin by setting up holographic renormalization for the Ryu-Takayanagi entanglement entropy functional. Since the entanglement entropy is described by the area of a minimal surface homologous to the boundary entangling region, the UV divergences of the entanglement entropy are in direct correspondence with the area divergences of this minimal surface. Following the holographic renormalization methods of [15, 120, 78] one can identify covariant counterterms on the conformal boundary of the minimal surface which renormalize the area of the minimal surface.

In Section 5.3 we derive the renormalized Ryu-Takayanagi functional for static entangling surfaces in AdS spacetimes. Assuming flat spatial slices of the background for the dual quantum field theory (i.e. a Poincaré representation of AdS_{D+2}) the renormalized functional takes the form

$$\begin{aligned} S_{\text{ren}} =& \frac{1}{4G_{D+2}} \int_{\Sigma} \mathrm{d}^{D}\sigma^{\alpha} \sqrt{\gamma} \\ & - \frac{1}{4G_{D+2}} \int_{\partial\Sigma} \mathrm{d}^{D-1}x \sqrt{\tilde{\gamma}} \left(\frac{1}{D-1} + \frac{1}{2(D-1)^{2}(D-3)} \mathcal{K}^{2} \cdots \right), \end{aligned} \tag{5.1.1}$$

Here Σ is the entangling surface,with induced metric γ, and $\partial\Sigma$ is its boundary, with induced metric $\tilde{\gamma}$. The extrinsic curvature $\mathcal{K}$ refers to the extrinsic curvature of $\partial\Sigma$ embedded into a spatial slice of the boundary of the bulk manifold. The first counterterm

becomes logarithmic for $D = 1$. Only the first counterterm given above is needed for gravity in four bulk dimensions ($D = 2$). The second counterterm becomes logarithmic at $D = 3$ and is needed in the form given above for $D > 3$. Additional counterterms involving higher order curvature invariants are needed for $D \geq 5$. The counterterms for entangling surfaces in general asymptotically locally AdS spacetimes can be found in Section 5.5.

We then show that the renormalized entanglement entropy for a disk region in a three dimensional conformal field theory dual to AdS_4 is in precise agreement with the holographically renormalized Euclidean action for AdS_4 with spherical slicing, i.e. the CHM map [106] holds at the level of renormalized quantities.

In Section 5.4 we consider holographic RG flows in four bulk dimensions which respect Poincaré invariance of the dual theory. For flows driven by a single scalar we compute the renormalized Ryu-Takayanagi functional, expressing the counterterms in terms of the superpotential associated with the flow.

We then use the renormalized entanglement entropy to explore the change in the F quantity along RG flows. In particular, we consider a disk entangling region and calculate the change the renormalized entanglement entropy (and hence F quantity) perturbatively in the source of the relevant deformation, $\phi_{(0)}$. For operators of dimension $3/2 < \Delta_+ < 3$ we find that

$$\delta S_{\rm ren} = \frac{\pi}{16(2\Delta_+ - 5)G_4}\phi_{(0)}^2 R^{2(3-\Delta_+)} + \mathcal{O}\left(\phi_{(0)}^3\right), \tag{5.1.2}$$

where R is the radius of the disk entangling region while $\delta S_{\rm ren} = 0$ for exactly marginal operators. This quantity is clearly negative for $\Delta_+ < 5/2$ which, since $\delta S_{\rm ren} = -\delta F$, corresponds to an increase in the F quantity. We should note however that the corresponding deformations on the three sphere are inhomogeneous and do not therefore correspond to RG flows which respect the $SO(4)$ invariance. Direct calculation of the F quantity for $SO(4)$ invariant RG flows on S^3 driven by such operators also gives an increase in the F quantity to quadratic order in the source, see Chapter 4. It would be interesting to understand whether such flows are unphysical or if the strong version of the proposed F theorem is indeed violated.

In Section 5.5 we show that the holographically renormalized entanglement entropy can be obtained from the holographically renormalized action. Using the replica trick, the entropy associated with a density matrix ρ is expressed as

$$S = -n\partial_n[\log Z(n) - n\log Z(1)]_{n=1} \tag{5.1.3}$$

where $Z(n) = \mathrm{Tr}(\rho^n)$ and $Z(1) = \mathrm{Tr}(\rho)$ is the usual partition function. If we are inter-

ested in the entropy of a thermal state, then $Z(n)$ is constructed by extending the period of the thermal circle by a factor of n. In the case of entanglement entropy, $Z(n)$ is constructed by extending the period of the circle around the boundary of the entangling region by a factor of n, where implicitly n is an integer. Assuming that the resulting expression is analytic in n, one can obtain the entropy by analytically continuing to $n = 1$.

Holographically $Z(n)$ can be computed in terms of the on-shell Euclidean action [44] as

$$S = n\partial_n[I(n) - nI(1)]_{n=1}. \tag{5.1.4}$$

Here $I(1)$ represents the on-shell Euclidean action for the bulk geometry while $I(n)$ represents the on-shell Euclidean action for the replica bulk geometry. For a thermal state, the bulk geometry associated with $Z(1)$ is a black hole and the replica is constructed by extending the period of the thermal circle by a factor of n. For the entanglement entropy, the bulk geometry associated with $Z(1)$ corresponds to the usual bulk dual of the given state in the field theory and the replica is constructed by extending the period of the circle around the entangling region boundary by a factor of n. Following the same logic as in Lewkowycz-Maldacena [44], the expression (5.1.4) localises on the minimal surface corresponding to the extension of the boundary of the entangling region into the bulk. However, the entangling surface itself has area divergences, unlike the black hole setup analysed in detail in [44].

In Section 5.5 we show that the renormalized entanglement entropy can be expressed in terms of the renormalized on-shell action i.e.

$$S_{\rm ren} = n\partial_n[I_{\rm ren}(n) - nI_{\rm ren}(1)]_{n=1}. \tag{5.1.5}$$

In particular, using the standard counterterms for asymptotically locally AdS spacetimes [78], together with results on the curvature invariants of the replica space [121, 122], one obtains exactly the same $S_{\rm ren}$ as computed directly via area renormalization. Thus, the renormalization scheme for the entanglement entropy is inherited directly from the renormalization scheme used for the partition function.

This result provides evidence for the applicability of the replica trick in the holographic context. Note that the derivation of the entanglement entropy functional from the Euclidean action functional requires only the local geometry of the replica; any potential anomalies in the replica symmetry do not affect the derivation. The holographic renormalization counterterms for higher derivative gravity theories such as Gauss-Bonnet also imply counterterms for the entanglement entropy, as we discuss at the end of Section 5.5.

The plan of this chapter is as follows. In Section 5.2 we review the renormalization of

entanglement entropy by differentiation. In Section 5.3 we setup area renormalization for entangling surfaces in AdS spacetimes, and show that the renormalized entanglement entropy for disk regions in AdS_4 indeed agrees with the F quantity. In Section 5.4 we consider entanglement entropy for RG flows while in Section 5.5 we show how the renormalized entanglement entropy can be obtained from the renormalized action via the replica trick. We conclude in Section 5.6.

5.2 Renormalization by differentiation

In previous works, the finite terms in the entanglement entropy have been isolated by differentiation of the entanglement entropy. In the case of a strip of width R, UV divergent contributions to the entanglement entropy in a local quantum field theory are necessarily independent of R and therefore

$$S_R = R\frac{\partial S}{\partial R} \tag{5.2.1}$$

is finite. This expression has been used in a number of earlier works, including [123, 124, 125].

For a spherical entangling region, the radius of the sphere controls the local curvature of the boundary of the entangling region and therefore it is no longer true that UV divergences are independent of the scale of the entangling region. In [110] it was noted that the following quantity

$$F(R) = -S(R) + R\frac{\partial S}{\partial R} \tag{5.2.2}$$

is manifestly finite in any 3d field theory which has a UV fixed point. (Analogous expressions for general dimensions were given in [110].) In particular, for a three-dimensional CFT the regulated entanglement entropy for a disc entangling region is

$$S_{\rm reg} = \frac{a_{-1}R}{\delta} + a_0 \tag{5.2.3}$$

where $\delta \ll 1$ is the UV cutoff and (a_0, a_{-1}) are constants. Then by construction

$$F(R) = -a_0. \tag{5.2.4}$$

For theories with a holographic dual one can show (see Section 5.3) that

$$S_{\rm reg} = \frac{\pi}{2G_4}\left(\frac{R}{\delta} - 1\right) \tag{5.2.5}$$

and therefore

$$F(R) = \frac{\pi}{2G_4}. \tag{5.2.6}$$

The normalisation of (5.2.2) is chosen so that the latter indeed agrees with the F quantity.

The renormalized entanglement entropy defined by (5.2.2) has both positive and negative features. On the positive side, there is evidence that $F(R)$ behaves monotonically as a function of R in free field theory and holographic examples [108, 111]. Also by construction

$$\frac{\partial F}{\partial R} = R\frac{\partial^2 S}{\partial R^2} \tag{5.2.7}$$

and strong subadditivity of the entanglement entropy implies that in any Poincaré invariant field theory $\partial^2 S/\partial R^2 \leq 0$ [45], so $F(R)$ is a non-increasing function of the radius R.

Let us suppose we deform a conformal field theory by an operator $\mathcal{O}_\Delta$ of dimension $\Delta < 3$:

$$I_{CFT} \to I_{CFT} + \int \mathrm{d}^3x\sqrt{h}\lambda\mathcal{O}_\Delta. \tag{5.2.8}$$

The dimension of λ is then $(3-\Delta)$; the coupling provides another dimensionful scale and it is no longer the case that (5.2.3) are the only divergences. There are in general additional divergences which are analytic in the deformation parameter λ and hence for a disk region the change in the entanglement entropy under the relevant deformation is

$$\delta S_{\mathrm{reg}} = a_{5-2\Delta}\frac{\lambda^2 R}{\delta^{\Delta-5/2}} + a_{8-3\Delta}\frac{\lambda^3 R}{\delta^{\Delta-8/3}} + \cdots \tag{5.2.9}$$

where the coefficients a_m are dimensionless. Hence for $\Delta > 5/2$ the relevant deformation generates additional UV divergences in the entanglement entropy; additional divergences arise for $\Delta > 3 - 1/n$ where $n \in \mathbb{N}$. The form of this expression follows from conformal perturbation theory; in particular the term linear in λ vanishes, while all divergences scale extensively with the length of the boundary of the entangling region. By construction $F(R)$ is finite for all such deformations although it is not a priori clear that $F(R)$ agrees with the F quantity.

On the negative side, there is evidence that $F(R)$ is not stationary at a UV fixed point [112]. Consider perturbations of a two-dimensional CFT by a slightly relevant operator of dimension $2 - \delta_\Delta$. Then Zamoldchikov's c-function behaves as

$$c(g) = c_{UV} - g^2\delta_\Delta + \mathcal{O}(g^3) \tag{5.2.10}$$

where g is the renormalized coupling. For a theory with several coupling constants

$$\frac{\partial c}{\partial g^i} = G_{ij}\beta^j \tag{5.2.11}$$

where G_{ij} is the Zamolodchikov metric and $\beta^j = \mu\frac{\partial g^j}{\partial \mu}$ are the beta functions. Then non-

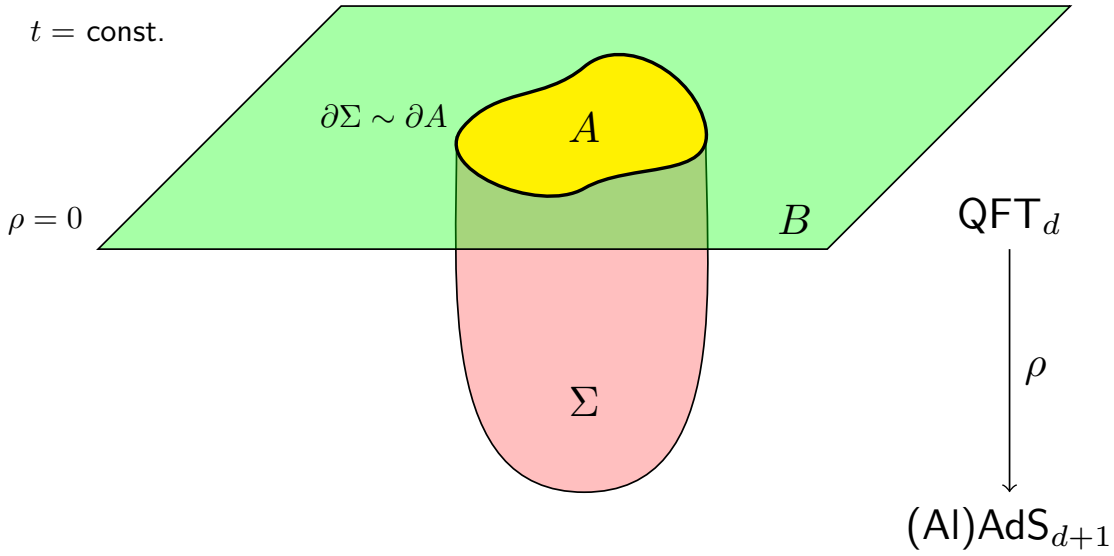

Figure 5.3.1: The entangling surface embedded into the bulk manifold.

singularity of the Zamolodchikov metric guarantees the stationarity of the c function in two dimensions. In [112] it was shown that the proposed $F(R)$ is not stationary in this sense at the UV fixed point in free massive scalar field theory examples.

Another drawback of the definition of the renormalized entanglement entropy (5.2.2) is that the definition is only applicable to disk entangling regions, or to regions which are characterised by one overall scale. This drawback is not an issue for applications to the F theorem, for which only disk regions are needed, but prevents using (5.2.2) to explore the general shape dependence of entanglement entropy.

The renormalization that we propose in this chapter by contrast is inherited directly from the renormalization of the partition function, making scheme dependence and the relation to the F quantity manifest, and is applicable to any shape entangling region. Moreover, our renormalization is applicable in theories which are not conformal in the UV.

5.3 Renormalized entanglement entropy in anti-de Sitter

In this section we will define the renormalized area of (static) entangling surfaces in anti-de Sitter. We parameterise the AdS_{d+1} metric as

$$\mathrm{d}s^2 = \frac{\mathrm{d}\rho^2}{4\rho^2} + \frac{1}{\rho}\eta_{\mu\nu}\mathrm{d}x^\mu \mathrm{d}x^\nu \tag{5.3.1}$$

where $\rho \to 0$ corresponds to the conformal boundary and $\eta_{\mu\nu}$ is the Minkowski metric.

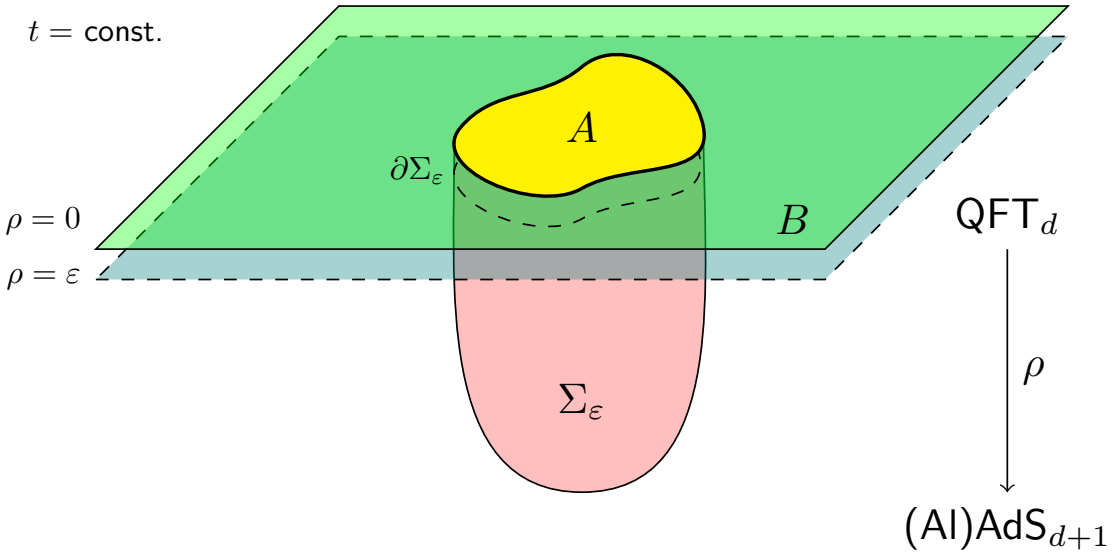

Figure 5.3.2: The cutoff entangling surface.

The Ryu-Takayanagi function for the entanglement entropy is the area functional for a codimension two surface:

$$S = \frac{1}{4G_{d+1}} \int_\Sigma \mathrm{d}^D\sigma^\alpha \sqrt{\gamma} \tag{5.3.2}$$

where G_{d+1} denotes the Newton constant (with the number of spatial dimensions in the field theory being $D = (d-1)$) and γ is the determinant of the induced metric on the surface. Throughout this section we work in a static setup, in which the entangling surface is independent of time. To find the bulk minimal surface Σ, we solve the equations of motion following from (5.3.2), subject to boundary conditions which define the entangling region in the dual field theory. In particular, as shown in Figure 5.3.1, the minimal surface Σ has a conformal boundary $\partial\Sigma$ as $\rho \to 0$ which is conformal to the boundary ∂A of the entangling region A in the dual field theory.

When one evaluates the on-shell value of the functional (5.3.2), it has area divergences which may conveniently be regulated by setting $\rho = \epsilon$, see Figure 5.3.2. Let us denote the bulk manifold as $\mathcal{M}$ and the regulated conformal boundary at $\rho = \epsilon$ as $\partial\mathcal{M}_\epsilon$. Since the entangling surface itself is asymptotically locally hyperbolic, the regulated functional (5.3.2) diverges as

$$S_{\mathrm{reg}} \sim \frac{\mathcal{A}_{\partial A}}{\epsilon^{\frac{d}{2}-1}} + \cdots \tag{5.3.3}$$

where $\mathcal{A}_{\partial A}$ is the area of the $(d-2)$-dimensional boundary of the entangling region ∂A.

Following the principles of [15, 120, 78] we can now define a renormalized functional S_{ren} as

$$S_{\mathrm{ren}} = \lim_{\epsilon\to 0} (S_{\mathrm{reg}} + S_{ct}) \tag{5.3.4}$$

where the counterterm action S_{ct} is defined in terms of covariant properties of the boundary of the minimal surface and of the cutoff surface. Let the induced metric on the cutoff surface be $h_{\mu\nu}$ and the metric on the boundary of the minimal surface be $\tilde{\gamma}_{ab}$. Let us further denote the Ricci scalar of the boundary of the minimal surface as $\mathcal{R}$, with the corresponding Ricci tensor being $\mathcal{R}_{ab}$. Similarly we denote the extrinsic curvature of the minimal surface embedded into the cutoff surface as $\mathcal{K}_{ab}$ with trace $\mathcal{K}$. Then counterterms must be expressible as

$$S_{\rm ct} = \int_{\partial\Sigma} \mathrm{d}^{D-1}x\sqrt{\tilde{\gamma}}\mathcal{L}\left(\mathcal{K}, \mathcal{R}, \mathcal{R}_{ab}\mathcal{R}^{ab}, \mathcal{K}_{ab}\mathcal{K}^{ab}, \cdots\right), \tag{5.3.5}$$

i.e. as a functional of extrinsic and intrinsic curvature invariants. In our setup there are three extrinsic curvatures arising from the following three different embeddings: the embedding of Σ_ε in $\mathcal{M}_\varepsilon$, the embedding of $\partial\Sigma_\varepsilon$ in Σ_ε, and the embedding of $\partial\Sigma_\varepsilon$ in $\partial\mathcal{M}_\varepsilon$. We should emphasise that it is the final one which is relevant for the counterterms, as the first two are not intrinsic to the regulated boundary.

There is a further restriction on the allowed counterterms. The entanglement entropy of region A is the same as the entanglement entropy of the complementary region B. If we require that the renormalized entanglement entropy satisfies the same property, then the counterterms should only depend on even powers of the extrinsic curvature $\mathcal{K}$, since the extrinsic curvature of A is minus the extrinsic curvature of the complementary region B.

Finally, we should note that the intrinsic and extrinsic curvature are related by Gauss-Codazzi relations. Throughout this section we will be interested in the case in which the background for the dual field theory is flat, in which case

$$\mathcal{R} = \mathcal{K}^2 - \mathcal{K}_{ab}\mathcal{K}^{ab}, \tag{5.3.6}$$

with analogous Gauss-Codazzi relations holding between higher order scalar invariants of the intrinsic and extrinsic curvature.

5.3.1 Explicit computation of counterterms

Let us now express the area functional as

$$S = \frac{1}{4G_{d+1}}\int \mathrm{d}\rho \int \mathrm{d}^{D-1}\sigma^a \sqrt{\gamma} \tag{5.3.7}$$

where $\gamma_{\alpha\beta} = g_{mn}\partial_\alpha x^m \partial_\beta x^n$, g_{mn} is the metric on the AdS target space and $x^m(x^\alpha)$ defines the embedding in terms of the worldvolume coordinates σ^α. We have implicitly fixed a static gauge, in which the time coordinate t is constant and ρ is one of the world-

volume coordinates, i.e. $\sigma^\alpha = \{\rho, \sigma^a\}$. The spatial coordinates x^i are then functions of ρ and σ^a and D represents the number of spatial directions in the boundary theory.

In such a gauge the induced metric on the minimal surface is

$$\begin{aligned} \gamma_{\rho\rho} &= \frac{1}{4\rho^2} + \frac{1}{\rho} x^i_{,\rho} x^i_{,\rho} \\ \gamma_{\rho a} &= \frac{1}{\rho} x^i_{,\rho} x^i_{,a} \qquad \gamma_{ab} = \frac{1}{\rho} x^i_{,a} x^i_{,b} \end{aligned} \tag{5.3.8}$$

where we denote $x^i_{,\rho} = \partial_\rho x^i$ and $x^i_{,a} = \partial_{\sigma^a} x^i$. One can often (but not always) further gauge fix, setting $x^a = \sigma^a$ and $x^D \equiv y(\rho, x^a)$, so that

$$\begin{aligned} \gamma_{\rho\rho} &= \frac{1}{4\rho^2} + \frac{1}{\rho} y_{,\rho} y_{,\rho} \\ \gamma_{\rho a} &= \frac{1}{\rho} y_{,\rho} y_{,a} \qquad \gamma_{ab} = \frac{1}{\rho}(\delta_{ab} + y_{,a} y_{,b}), \end{aligned} \tag{5.3.9}$$

reflecting the fact that a codimension one spatial minimal surface has only one transverse direction. Note however that such gauge fixing cannot be used to describe minimal surfaces with cusps which are known to introduce additional logarithmic divergences proportional to some convex function of the cusp angle [126, 127]. In this chapter we will restrict to the case of surfaces without cusps.

The gauge fixed minimal surface action is given by

$$\begin{aligned} S &= \frac{1}{4G_{d+1}} \int \mathrm{d}\rho \int \mathrm{d}^{D-1}x \left(\frac{1}{4\rho^{D+1}} (1 + y_{,a} y_{,a} + 4\rho y^2_{,\rho}) \right)^{1/2} \\ &= \frac{1}{4G_{d+1}} \int \mathrm{d}\rho \int \mathrm{d}^{D-1}x \, \frac{1}{2\rho^{(D+1)/2}} m(\rho, x^a) \end{aligned} \tag{5.3.10}$$

where we have introduced the shorthand $m(\rho, x^a) = \sqrt{1 + y_{,a} y_{,a} + 4\rho y^2_{,\rho}}$.

The regulated action is then of the form

$$\begin{aligned} S_{\mathrm{reg}} &= \frac{1}{4G_{d+1}} \int_\epsilon \mathrm{d}\rho \int \mathrm{d}^{D-1}x \left(\frac{1}{4\rho^{D+1}} (1 + y_{,a} y_{,a} + 4\rho y^2_{,\rho}) \right)^{1/2} \\ &= \frac{1}{4G_{d+1}} \int_{\partial\Sigma} \mathrm{d}^{D-1}x \sum \epsilon^{-k} (a_k(x) + \log \epsilon b_k(x)) + \cdots \end{aligned} \tag{5.3.11}$$

where the explicit powers arising in the divergences and their coefficients $(a_k(x), b_k(x))$ are determined by analysing solutions to the minimal surface equations with the required boundary conditions asymptotically near the conformal boundary.

Note that the action does not depend explicitly on y and the minimal surface equation

is:

$$0 = \partial_a \left(\frac{y_{,a}}{m\, \rho^{3/2}} \right) + \partial_\rho \left(\frac{y_{,\rho}}{m\, \rho^{1/2}} \right), \tag{5.3.12}$$

which should be solved near $\rho = 0$ subject to the boundary condition

$$\lim_{\rho \to 0} y(\rho, x^a) = y_{(0)}(x^a), \tag{5.3.13}$$

where $y_{(0)}(x^a)$ specifies the entangling region in the dual geometry.

We wish to solve this equation iteratively for $y(\rho, x^a)$ as a series expansion in ρ. We consider the following Taylor series expansions for $y(\rho, x^a)$:

$$y(\rho, x^a) = y_{(0)}(x) + y_{(\beta_1)}(x)\rho^{\beta_1} + y_{(\beta_2)}(x)\rho^{\beta_2} + \dots \tag{5.3.14}$$

where we assume that $0 < \beta_1 < \beta_2 < \dots$. To solve the PDE we insert these expansions into the minimal surface equation and set $\rho = 0$. We then fix β_1 and $y_{(\beta_1)}$ to solve the resulting equation such that $y_{(0)}$ remains unconstrained. We then differentiate the minimal surface equation with respect to ρ and repeat to find β_2.

After substituting the expansions into the minimal surface equation, one finds that the leading order terms are ρ^0 and $\rho^{\beta_1 - 1}$. To leave $y_{(0)}$ unconstrained we must therefore set $\beta_1 = 1$ and deduce that:

$$y_{(1)}(x) = 2\sqrt{1 + y_{(0),a} y_{(0),a}}\, \partial_a \left(\frac{\partial_a y_{(0)}}{\sqrt{1 + y_{(0),a} y_{(0),a}}} \right). \tag{5.3.15}$$

To find higher terms in the asymptotic expansion we can use radial derivatives of the minimal surface equations. Before carrying out this procedure, let us consider the regulated on-shell action (5.3.11) and determine the leading divergences, which are

$$S_{\text{reg}} = \frac{1}{4(D-1) G_{d+1} \epsilon^{\frac{1}{2}(D-1)}} \int_{\partial\Sigma} \mathrm{d}^{D-1} x \sqrt{1 + y_{(0),a} y_{(0),a}} + \mathcal{O}\left(\epsilon^{\frac{3-D}{2}} \right) \tag{5.3.16}$$

for $D > 1$. As anticipated above, this divergence scales with the area $\mathcal{A}_{\partial A}$ of the boundary of the entangling region

$$\mathcal{A}_{\partial A} = \int_{\partial\Sigma} \mathrm{d}^{D-1} x \sqrt{1 + y_{(0),a} y_{(0),a}}. \tag{5.3.17}$$

The case of $D = 1$, corresponding to a dual two-dimensional conformal field theory, is degenerate. The divergence is logarithmic:

$$S_{\text{reg}} = \frac{1}{8 G_3} \Sigma_k y_k \log \epsilon \tag{5.3.18}$$

with y_k being the endpoints of the intervals defining the entangling region. The required counterterm action is therefore

$$S_{\rm ct} = -\frac{1}{8G_3}\Sigma_k y_k \log\left(\frac{\epsilon}{\mu}\right), \tag{5.3.19}$$

where μ is an arbitrary renormalization scale.

5.3.2 Entangling surfaces in AdS_4

For minimal surfaces in AdS_4 the only divergence in the on-shell functional is

$$S_{\rm reg} = \frac{1}{4G_4}\int_{\partial\Sigma} {\rm d}x \left(\frac{1}{\epsilon^{\frac{1}{2}}}\sqrt{1+y_{(0),x}y_{(0),x}}\right), \tag{5.3.20}$$

where the entangling region in the boundary is defined by a curve $y_{(0)}(x)$ in two dimensional space. Noting that the induced line element on the boundary of the entangling surface is

$$\gamma^h_{xx} = \frac{1}{\epsilon}(1+y_{,x}y_{,x}) \tag{5.3.21}$$

the divergence is manifestly removed by the covariant counterterm

$$S_{\rm ct} = -\frac{1}{4G_4}\int_{\partial\Sigma} {\rm d}x\sqrt{\tilde{\gamma}}, \tag{5.3.22}$$

where $\tilde{\gamma}$ is the determinant of the induced metric on $\partial\Sigma$. This is the only possible divergent counterterm but the following counterterm is finite:

$$S_{\rm ct} = \frac{a_s}{4}\int_{\partial\Sigma} {\rm d}x\sqrt{\tilde{\gamma}}\mathcal{K} \tag{5.3.23}$$

where $\mathcal{K}$ denotes the trace of the extrinsic curvature of the boundary of the minimal surface embedded into the regulated cutoff surface. For a curve $y(x,\epsilon)$ embedded into the cutoff surface

$${\rm d}s^2 = \frac{1}{\epsilon}\left(-{\rm d}t^2+{\rm d}x^2+{\rm d}y^2\right) \tag{5.3.24}$$

the trace of the extrinsic curvature is

$$\mathcal{K} = \epsilon^{\frac{1}{2}}\frac{y_{,xx}}{(1+y_{,x}^2)^{\frac{3}{2}}} \tag{5.3.25}$$

and thus

$$\sqrt{\gamma^h}\mathcal{K} = \frac{y_{,xx}}{(1+y_{,x}^2)} = \frac{y_{(0),xx}}{(1+y_{(0),x}^2)} + \mathcal{O}(\epsilon), \tag{5.3.26}$$

which is indeed finite.

Thus the complete renormalized action for the minimal surface is

$$S_{\rm ren} = \frac{1}{4G_4}\int_\Sigma \mathrm{d}^2\sigma\sqrt{\gamma} + \frac{1}{4G_4}\int_{\partial\Sigma}\mathrm{d}x\sqrt{\tilde{\gamma}}\,(a_s\mathcal{K}-1)\,. \tag{5.3.27}$$

Note that terms depending on higher powers of the extrinsic curvature cannot contribute in the limit $\epsilon \to 0$. The finite counterterm is however not consistent with the requirement that the renormalized entropy for any region is equal to that of its complement, and we must therefore set $a_s = 0$.

As an example, let us evaluate the renormalized action for a disk entangling region, of radius R. The exact solution for the minimal surface is conveniently expressed in terms of the following coordinates

$$\mathrm{d}s^2 = \frac{\mathrm{d}\rho^2}{4\rho^2} + \frac{1}{\rho}\left(-\mathrm{d}t^2 + \mathrm{d}r^2 + r^2\mathrm{d}\phi^2\right) \tag{5.3.28}$$

as the circularly symmetric surface at constant time:

$$r^2 + \rho = R^2. \tag{5.3.29}$$

The renormalized action for this surface is then

$$S_{\rm ren} = -\frac{\pi}{2G_4}. \tag{5.3.30}$$

Note that this is independent of the choice of the radius R. Implicitly our Newton constant has been fixed to be dimensionless, as we chose the anti-de Sitter metric to have unit radius, absorbing the curvature radius into the overall prefactor of the bulk action. To reinsert the AdS radius we need only rescale the bulk metric by ℓ and the covariant counterterm by a further ℓ. The result of these insertions is to simply rescale the results for the entanglement entropy by ℓ^2:

$$S_{\rm ren} = -\frac{\pi\ell^2}{2G_N}, \tag{5.3.31}$$

where the Newton constant G_N now has the standard dimensions. Since the dual field theory is conformal there is no other scale apart from R and therefore $S_{\rm ren}$, which is dimensionless, cannot depend explicitly on R.

Next we consider an entangling surface of two infinitely long parallel lines with separation R. We will regulate the lines to have length L and by symmetry we may choose these lines to lie in the x direction and to be located at $y = \pm\frac{R}{2}$. The minimal surface can be characterised by worldsheet coordinates (ρ, x) and by symmetry the transverse

coordinate y depends only on ρ. The surface equations can be solved to obtain

$$y(\rho) = \pm\left(-\frac{R}{2} + \frac{\rho^{3/2}}{3\rho_0}{}_2F_1\left(\frac{1}{2}, \frac{3}{4}; \frac{7}{4}, \frac{\rho^2}{\rho_0^2}\right)\right). \tag{5.3.32}$$

We can also rewrite this hypergeometric function in terms of the incomplete beta function $B_z(a, b)$ using the identity

$${}_2F_1(a, b; 1 + b; z) = bz^{-b}B_z(b, 1 - a). \tag{5.3.33}$$

The surface has a turning point at ρ_0, where by symmetry $y(\rho_0) = 0$, and hence

$$y(\rho_0) = 0 \implies \rho_0 = \frac{9\Gamma(5/4)^2}{4\pi\Gamma(7/4)^2}R^2. \tag{5.3.34}$$

The regularised holographic entanglement entropy is then given by

$$S_{\text{reg}} = \frac{L}{8G_4}\int_\varepsilon^{\rho_0} \mathrm{d}\rho \frac{\rho_0}{\sqrt{\rho^3(\rho_0^2 - \rho^2)}}, \tag{5.3.35}$$

This integral is elliptic and can be calculated analytically using

$$\begin{aligned}\int \frac{1}{\sqrt{w^3(a^2 - w^2)}}\mathrm{d}w =& 2\frac{2}{a^2\sqrt{w}}\sqrt{a^2 - w^2} \\ &+ \frac{2}{\sqrt{a^3}}\left(F\left(\sin^{-1}\left(\sqrt{\frac{w}{a}}\right)\middle| -1\right) - E\left(\sin^{-1}\left(\sqrt{\frac{w}{a}}\right)\middle| -1\right)\right)\end{aligned} \tag{5.3.36}$$

where $F(\phi|k^2)$ and $E(\phi|k^2)$ are the incomplete elliptic integrals of the first and second kind respectively.

The renormalized holographic entanglement entropy is:

$$S_{\text{ren}} = -\frac{\sqrt{2}\pi^2\Gamma(7/4)}{3G_4\Gamma(1/4)^2\Gamma(5/4)}\frac{L}{R} \tag{5.3.37}$$

Note that in the above calculation we have implicitly assumed that $L \gg R$ and that there are no contributions from the lines $x = \pm L/2$, $-R/2 \leq y \leq R/2$. To take the limit of $L \to \infty$ we can calculate the renormalized entropy density

$$s_{\text{ren}} = \lim_{L\to\infty}\left(\frac{S_{\text{ren}}}{L}\right) = -\frac{\sqrt{2}\pi^2\Gamma(7/4)}{3RG_4\Gamma(1/4)^2\Gamma(5/4)}. \tag{5.3.38}$$

Finally let us consider the half plane entangling region with a boundary at $y = 0$; again we regulate the x direction to have length L. The bulk minimal surface has worldsheet coordinates (ρ, x) and by symmetry $y = 0$ over the surface. The regularised holographic

entanglement entropy is

$$S_{\rm reg} = \frac{L}{8G_4}\int_\epsilon^\infty \frac{{\rm d}\rho}{\rho^{\frac{3}{2}}} = \frac{L}{4G_4\epsilon^{\frac{1}{2}}} \tag{5.3.39}$$

and this term exactly cancels the counterterm giving

$$S_{\rm ren} = 0 \tag{5.3.40}$$

which was to be expected since there is no other scale in the problem but L and the dual theory is conformal.

The calculation of the renormalized area of a two-dimensional minimal surface in four bulk dimensions has arisen in other contexts, including Wilson loops. In particular, anomalies were discussed in [120] while the counterterm involving the regulated length of the boundary of the surface was discussed in the context of Wilson loops in [126]; the counterterm was derived by requiring a well-defined variational principle. The relation of holographic renormalization to variational principles for minimal surfaces was discussed in detail in [128].

Minimal surfaces in hyperbolic spaces were also analysed in [129]: generalising [120], it was noted that submanifold observables have conformal anomalies for specific codimensions. In particular, the results of [129] imply that codimension two minimal surfaces in odd bulk dimensions have logarithmic divergences in their regulated volumes. This is consistent with our $D = 1$ result above, and the $D = 3$ result we will give below.

According to the results of [129] the renormalized area of a codimension two minimal surface in an even dimensional hyperbolic space should be a conformal invariant. This is not however apparent from the above results: the renormalized entropy of the half plane was found to be zero (5.3.40), while the renormalized entropy of the disk is finite and negative. Yet, as is well known, one can find a conformal bijective map between the disk and the half plane and therefore these entangling regions are conformally equivalent. We will explore this issue further in the next section.

The renormalized entropy for the strip entangling region is negative. This is unsurprising: in [123, 124] the entanglement entropy for free scalars and fermions was calculated for strip entangling regions and it was found that the entanglement entropy contains finite terms of the form

$$S_{\rm finite} = -k\frac{L}{R} \tag{5.3.41}$$

where again L is the regulated length of the strip, R is its width (with $L/R \gg 1$) and k is a *positive* constant, which takes the value of $k = 0.039$ for a real scalar and $k = 0.072$ for a Dirac fermion.

5.3.2.1 Relation to F theorem

More generally, we should be unsurprised about finding negative values for the renormalized entanglement entropy. The conjectured F-theorem in three dimensions is the following. For a three-dimensional CFT we define the F quantity in terms of the (renormalized) partition function of the theory on a three sphere [99], i.e.

$$F = -\log Z_{S^3} \tag{5.3.42}$$

and then the F theorem states that $F_{UV} \geq F_{IR}$. More precisely, in [99] it was conjectured that F is positive in a unitary CFT, that it decreases along any RG flow and that it is stationary at fixed points. Support for the conjecture can be found in [99, 100, 107] and many subsequent works.

In odd spacetime dimensions the finite terms in the entanglement entropy of a spherical region

$$S_{\text{finite}} = (-1)^{\frac{1}{2}(d-1)} 2\pi a_d \tag{5.3.43}$$

are conjectured to satisfy the relation $(a_d)_{UV} \geq (a_d)_{IR}$ for any RG flows between fixed points [130]. Indeed it has been shown that the sphere partition function and the sphere entanglement entropy are proportional using the CHM map [106], thus establishing a connection between the F theorem and monotonous running of the finite part of the disk entanglement entropy. In three dimensions

$$F = 2\pi a_3 \tag{5.3.44}$$

and hence positivity of F is equivalent to negativity of the finite parts of the entanglement entropy.

To understand the relation between (5.3.42) and (5.3.43) it is useful to recall the arguments of CHM [106] in more detail. Let us parameterise the flat three-dimensional metric in as

$$\mathrm{d}s^2 = -\mathrm{d}t^2 + \mathrm{d}r^2 + r^2 \mathrm{d}\phi^2 \tag{5.3.45}$$

Now consider the following change of coordinates

$$\begin{aligned} t =& R \frac{\cos\theta \sinh \tau/R}{(1 + \cos\theta \cosh \tau/R)}; \\ r =& R \frac{\sin\theta}{(1 + \cos\theta \cosh \tau/R)}; \end{aligned} \tag{5.3.46}$$

so that the metric becomes

$$\mathrm{d}s^2 = \Omega^2 \left(-\cos^2\theta \mathrm{d}\tau^2 + R^2 (\mathrm{d}\theta^2 + \sin^2\theta \mathrm{d}\phi^2) \right) \tag{5.3.47}$$

with conformal factor

$$\Omega = (1 + \cos\theta \cosh \tau/R)^{-1}. \tag{5.3.48}$$

One can clearly absorb the R dependence as an overall factor by introducing $\tilde{\tau} = \tau/R$, so that the metric is conformal to the static patch of de Sitter space. Since $0 \leq \theta < \pi/2$ the new coordinates cover $0 < r < R$, i.e. the disk of radius R in the original flat coordinates, with $\theta \to \pi/2$ (the cosmological horizon) corresponding to $r = R$. The limits $\tau \to \pm\infty$ correspond to $t \to \pm R$ and therefore the new coordinates cover the causal development of the disk $r \leq R$ from $t = 0$.

Modular transformations inside the causal development act as time translations in de Sitter space, and therefore the state in the de Sitter geometry is thermal with $\beta = 2\pi R$. One can then identify the entanglement entropy for the disc of radius R in flat space with the thermodynamic entropy of the thermal state in de Sitter space, which in turn is given by

$$S_{\text{deSitter}} = -W \tag{5.3.49}$$

where $W = -\log Z$ is the free energy of the partition function Z. This relation is the origin of the above statement that the disc entanglement entropy is related to the partition function on the sphere, since the analytic continuation of de Sitter is the three-dimensional sphere.

The corresponding Euclidean transformations begin from the metric

$$\mathrm{d}s^2 = \mathrm{d}t_E^2 + \mathrm{d}r^2 + r^2\mathrm{d}\phi^2 \tag{5.3.50}$$

with the transformations being

$$\begin{aligned} t_E =& R\frac{\cos\theta \sin \tau_E/R}{(1 + \cos\theta\cos\tau_E/R)}; \\ r =& R\frac{\sin\theta}{(1 + \cos\theta\cos\tau_E/R)}; \end{aligned} \tag{5.3.51}$$

so that the metric becomes

$$\mathrm{d}s^2 = \Omega^2 \left(\cos^2\theta \mathrm{d}\tau_E^2 + R^2(\mathrm{d}\theta^2 + \sin^2\theta \mathrm{d}\phi^2)\right) \tag{5.3.52}$$

with conformal factor

$$\Omega = (1 + \cos\theta\cos\tau_E/R)^{-1}. \tag{5.3.53}$$

In the transformed coordinates the Euclidean time τ_E is periodic with period $2\pi R$ for the sphere to be regular and $0 \leq \theta < \pi/2$.

Implicitly the finite parts of the partition function on the S^3 are computed by renormalization; the CHM map thus relates the (renormalized) F quantity to the the corresponding

renormalized entanglement entropy i.e.

$$F = -S_{\text{ren}} \tag{5.3.54}$$

with F being positive and decreasing along an RG flow. For the disk entangling region we thus find holographically that

$$F = \frac{\pi}{2G_4} \tag{5.3.55}$$

which is indeed positive.

Let us now review the evaluation of the partition function on S^3 for a conformal field theory with a holographic dual described by Einstein gravity. The renormalized partition function is then calculated by evaluating the renormalized Euclidean action [78]:

$$I = -\frac{1}{16\pi G_4}\int \mathrm{d}^4x\sqrt{g}(R_g + 6) + \frac{1}{8\pi G_4}\int \mathrm{d}^3x\sqrt{h}(1 - \frac{R}{4}), \tag{5.3.56}$$

where R_g is the bulk Ricci scalar and R is the Ricci scalar for the boundary metric h. For the AdS_4 geometry with spherical slicing

$$\mathrm{d}s^2 = \mathrm{d}\rho^2 + \sinh^2\rho\,\mathrm{d}\Omega_3^2 \tag{5.3.57}$$

the renormalized on-shell action is then

$$I = \frac{\pi}{2G_4}. \tag{5.3.58}$$

Comparing (5.3.58) with (5.3.55), the values indeed agree. Note that there is no ambiguity in the holographically renormalized action (5.3.56): there are no candidate covariant finite counterterms. We will explain further in Section 5.5 how the renormalization schemes for the bulk action and for the entanglement entropy are related.

5.3.3 Renormalization for AdS in general dimensions

In this section we describe the holographic renormalization of the entanglement entropy for AdS in general dimensions, noting the generic forms of possible counterterms, anomalies, and finding the first two counterterms.

We begin by establishing the notational conventions we will use in this section. We will take our bulk manifold $\mathcal{M}$ to be AdS_{D+2} and will work exclusively in coordinates in which the metric takes the form

$$\mathrm{d}s^2_{\mathcal{M}} = g_{mn}\mathrm{d}x^m\mathrm{d}x^n = \frac{\mathrm{d}\rho^2}{4\rho^2} - \frac{1}{\rho}\mathrm{d}t^2 + \frac{1}{\rho}\delta_{ij}\mathrm{d}x^i\mathrm{d}x^j \tag{5.3.59}$$

where $i, j = 1, \ldots, D$ are the boundary spatial directions. The entangling surface Σ is a codimension 2 surface of $\mathcal{M}$ satisfying the appropriate boundary conditions. We choose the coordinates on Σ to be (ρ, x^a) where $a = 1, \ldots, D-1$. The embedding of Σ in $\mathcal{M}$ is then given by:

$$X^m = (\rho, t, x^1, \ldots, x^{D-1}, y(\rho, x^a)) \tag{5.3.60}$$

where t is a constant. This is an appropriate gauge whenever the boundary entangling region specified by $y(0, x^a)$ is smooth.

We regulate the bulk as $\mathcal{M}_\varepsilon$ by restricting $\rho \geq \varepsilon > 0$, and similarly define the regulated entangling surface Σ_ε by the same restriction. The surface Σ_ε is a constant time hypersurface of $\mathcal{M}_\varepsilon$. The metric $\gamma_{\alpha\beta}$ on Σ_ε is given by

$$\mathrm{d}s^2_{\Sigma_\varepsilon} = \left(\frac{1}{4\rho^2} + \frac{1}{\rho} y_{,\rho}^2\right) \mathrm{d}\rho^2 + \frac{2}{\rho} y_{,\rho} y_{,a} \mathrm{d}x^a + \frac{1}{\rho}(\delta_{ab} + y_{,a} y_{,b}) \mathrm{d}x^a \mathrm{d}x^b. \tag{5.3.61}$$

In this gauge the regulated bare entanglement entropy is given by

$$S_{\mathrm{reg}} = \frac{1}{4G_{D+2}} \int_{\partial\Sigma_\varepsilon} \mathrm{d}^{D-1} \int_\varepsilon^{\rho_0} \mathrm{d}\rho \frac{1}{2\rho^{(D+1)/2}} \sqrt{1 + 4\rho y_{,\rho}^2 + y_{,a}^2} \tag{5.3.62}$$

where summation is implicit for the $a, b, \ldots$ indices.

From the action one can find the equation of motion for $y(\rho, x^a)$, as in the previous section. Expanding the solution near the conformal boundary one finds:

$$y(\rho, x^a) = y^{(0)} + y^{(1)}\rho + O(\rho^2); \qquad y^{(1)} = \frac{1}{2(D-1)} \left(y^{(0)}_{,aa} - \frac{y^{(0)}_{,a} y^{(0)}_{,ab} y^{(0)}_{,b}}{1 + {y^{(0)}_{,c}}^2} \right). \tag{5.3.63}$$

Note that this result agrees with the $D = 2$ case we considered above.

Inserting the asymptotic expansion into the regulated functional yields for AdS_5 ($D = 3$)

$$S_{\mathrm{reg}} = \frac{1}{4G_5} \int_{\partial\Sigma_\varepsilon} \mathrm{d}^2 x (1 + {y^{(0)}_{,c}}^2)^{1/2} \left(\frac{1}{2\varepsilon} - \frac{y^{(0)}_{,a} y^{(1)}_{,a} + 2{y^{(1)}}^2}{2(1 + {y^{(0)}_{,b}}^2)} \log \varepsilon + \ldots \right) \tag{5.3.64}$$

where the ellipses denote finite terms. Similarly for $D > 3$

$$S_{\mathrm{reg}} = \frac{1}{4G_{D+2}} \int_{\partial\Sigma_\varepsilon} \mathrm{d}^{D-1} x (1 + {y^{(0)}_{,c}}^2)^{1/2} \left(\frac{\varepsilon^{-\frac{(D-1)}{2}}}{D-1} + \frac{\varepsilon^{-\frac{(D-3)}{2}}}{D-3} \frac{y^{(0)}_{,a} y^{(1)}_{,a} + 2{y^{(1)}}^2}{1 + {y^{(0)}_{,b}}^2} + \ldots \right) \tag{5.3.65}$$

where the ellipses denote subleading divergences and terms that are finite as $\varepsilon \to 0$.

Our task is now to find counterterms which are integrals of covariant quantities defined

on $\partial\Sigma_\varepsilon$, i.e. scalars constructed from the intrinsic and extrinsic curvature tensors. The induced metric on $\partial\Sigma_\varepsilon$, $\tilde{\gamma}_{ab}$ is given by

$$\mathrm{d}s^2_{\tilde{\gamma}} = \frac{1}{\varepsilon}(\delta_{ab} + y_{,a}y_{,b})\mathrm{d}x^a\mathrm{d}x^b \tag{5.3.66}$$

which has determinant

$$\tilde{\gamma} = \det(\tilde{\gamma}_{ab}) = \varepsilon^{-\frac{D-1}{2}}(1 + y^2_{,a}) \tag{5.3.67}$$

by Sylvester's determinant theorem.

Using the asymptotic expansion we can expand the volume form to first subleading order in ε as:

$$\sqrt{\tilde{\gamma}} = \varepsilon^{-\frac{D-1}{2}}\left(1 + {y^{(0)}_{,c}}^2\right)^{1/2}\left(1 + \varepsilon\frac{y^{(0)}_{,b}y^{(0)}_{,b}}{1 + {y^{(0)}_{,c}}^2} + \dots\right). \tag{5.3.68}$$

On dimensional grounds we can show that all curvature scalars will be at least $O(\varepsilon^{1/2})$ and so we can uniquely identify the leading divergence in S_{ren} as coming from the area divergence, as expected. Our first counterterm is therefore

$$S_{ct,1} = -\frac{1}{4G_{D+2}}\frac{1}{D-1}\int_{\partial\Sigma_\varepsilon}\mathrm{d}^{D-1}x\sqrt{\tilde{\gamma}} \tag{5.3.69}$$

which is again consistent with our previously found AdS_4 ($D = 2$) result.

We now need to find the counterterms for the subleading divergences. Let us consider first the case of $D = 3$. Using integration by parts we can rewrite:

$$\int_{\partial\Sigma_\varepsilon}\mathrm{d}^{D-1}x\frac{y^{(0)}_{,A}y^{(1)}_{,A}}{\left(1 + {y^{(0)}_{,C}}^2\right)^{1/2}} = -\int_{\partial\Sigma_\varepsilon}\mathrm{d}^{D-1}x\frac{{y^{(1)}}^2}{\left(1 + {y^{(0)}_{,C}}^2\right)^{1/2}} \tag{5.3.70}$$

and hence for $D = 3$

$$S_{\mathrm{reg}} + S_{ct,1} = -\frac{1}{8G_5}\int_{\partial\Sigma_\varepsilon}\mathrm{d}^2x\sqrt{\tilde{\gamma}}\frac{{y^{(1)}}^2}{1 + {y^{(0)}_{,C}}^2}\ln\varepsilon + \dots \tag{5.3.71}$$

To rewrite this term covariantly we note that the metric on a constant time hypersurface of the regulated boundary is given by

$$\mathrm{d}s^2_D = \tilde{g}_{ij}\mathrm{d}x^i\mathrm{d}x^j = \frac{1}{\varepsilon}\delta_{ij}\mathrm{d}x^i\mathrm{d}x^j \tag{5.3.72}$$

and the embedding of $\partial\Sigma_\varepsilon$ is given by $x^D \equiv y(\varepsilon, x^a)$. The unit normal covector is then given by

$$n_\flat = \varepsilon^{-\frac{1}{2}}(1 + y^2_{,c})^{-\frac{1}{2}}(y_{,a}\mathrm{d}x^a - \mathrm{d}x^D) \tag{5.3.73}$$

From this we define the induced metric $\tilde{\gamma}_{ij}$, and the extrinsic curvature $\mathcal{K}_{ij}$ by

$$\tilde{\gamma}_{ij} = \tilde{g}_{ij} - n_i n_j \qquad \mathcal{K}_{ij} = \tilde{\gamma}_i^k \nabla_k n_j \tag{5.3.74}$$

where ∇_k is the covariant derivative with respect to $\tilde{g}_{ij}$. The trace of the extrinsic curvature is then given by

$$\mathcal{K} = \frac{\varepsilon^{\frac{1}{2}}}{(1+y_{,c}^2)^{\frac{1}{2}}}\left(y_{,aa} - \frac{y_{,a}y_{,ab}y_{,b}}{1+y_{,e}^2}\right) = 2(D-1)\frac{\varepsilon^{\frac{1}{2}}y^{(1)}}{(1+y_{,c}^{(0)2})^{\frac{1}{2}}} + \ldots \tag{5.3.75}$$

By contrast, the Ricci scalar has a qualitatively different structure:

$$\mathcal{R} = \frac{2\varepsilon}{(1+y_{,e}^2)}\left(y_{,aa}^2 - y_{,ab}y_{,ab} - y_{,a}y_{,b}\frac{y_{,ab}y_{,cc} - y_{,ac}y_{,bc}}{1+y_{,d}^2}\right) \tag{5.3.76}$$

Comparing with (5.3.71) we can see that the required logarithmic counterterm is hence written in terms of the extrinsic curvature as

$$S_{ct,2} = \frac{1}{64G_5}\int_{\partial\Sigma_\varepsilon} \mathrm{d}^2x\sqrt{\tilde{\gamma}}\mathcal{K}^2 \ln\frac{\varepsilon}{\mu}, \tag{5.3.77}$$

with μ a cutoff scale.

Similarly for $D > 3$ we can show that

$$S_{EE} + S_{ct,1} = \frac{1}{4G_{D+2}}\frac{2}{(D-3)}\int_{\partial\Sigma_\varepsilon} \mathrm{d}^{D-1}x\sqrt{\tilde{\gamma}}\frac{\varepsilon {y^{(1)}}^2}{1+y_{,C}^{(0)2}} + \ldots \tag{5.3.78}$$

At this order the only possible intrinsic curvature term would be $\mathcal{R}$, the Ricci scalar on $\partial\Sigma_\varepsilon$ but from (5.3.76) this does not have the right structure to be the correct counterterm. Using (5.3.75) we can show that the required counterterm is

$$S_{ct,2} = -\frac{1}{8G_{D+2}}\frac{1}{(D-1)^2(D-3)}\int_{\partial\Sigma_\varepsilon} \mathrm{d}^{D-1}x\sqrt{\tilde{\gamma}}\mathcal{K}^2. \tag{5.3.79}$$

Note that other extrinsic curvature invariants again either do not have the correct ε structure or the correct ${y^{(1)}}^2$ behaviour to arise as possible counterterms.

In the $D = 2$ analysis we found that $\mathcal{K}$ would be a finite counterterm, but it is excluded by the requirement that the renormalized entanglement entropy of the complementary region is equal to that of the original region. For $D > 2$ we can further note that

$$\int_{\partial\Sigma_\varepsilon} \mathrm{d}^{D-1}x\sqrt{\tilde{\gamma}}\mathcal{K}^{D-1} \tag{5.3.80}$$

are finite counterterms. The complementarity requirement rules out such counterterms for even D (corresponding to field theories in odd spacetime dimensions). For odd D (corresponding to field theories in even spacetime dimensions), these counterterms are consistent with the requirement that the entropy of the complement is the same as that of the original region. Indeed we already saw that such a term arises in $D = 3$: it is automatically included in (5.3.77) in the μ dependent part.

In addition, higher dimensions allows the possibility of other finite counterterms constructed from curvature invariants such as

$$\int_{\partial\Sigma_\varepsilon} \mathrm{d}^{D-1}x\sqrt{\tilde{\gamma}}(\mathcal{K}_{ab}\mathcal{K}^{ab})^{(D-1)/2}; \quad \int_{\partial\Sigma_\varepsilon} \mathrm{d}^{D-1}x\sqrt{\tilde{\gamma}}\tilde{R}^{(D-1)/2} \tag{5.3.81}$$

which are both valid for odd D, so that they are analytic. These counterterms are however not linearly independent of each other, due to the Gauss-Codazzi relations. In general there will always be finite counterterms possible in even spacetime dimensions and the number of such terms will increase with D implying there are an increasing number of scheme dependent terms. We will understand in Section 5.5 how these finite counterterms relate to the scheme dependence of the partition function.

Thus, to summarise the results in this section, the renormalized entanglement entropy for static surfaces in AdS_{D+2} is

$$\begin{aligned} S_{\mathrm{ren}} =& \frac{1}{4G_{D+2}}\int_\Sigma \mathrm{d}^D\sigma^\alpha\sqrt{\gamma} \\ &- \frac{1}{4G_{D+2}}\int_{\partial\Sigma}\mathrm{d}^{D-1}x\sqrt{\tilde{\gamma}}\left(\frac{1}{D-1}+\frac{1}{2(D-1)^2(D-3)}\mathcal{K}^2\cdots\right), \end{aligned} \tag{5.3.82}$$

where D represents the number of spatial dimensions in the dual field theory. The first counterterm is logarithmic for $D = 1$. Only the first counterterm given above is needed for gravity in four bulk dimensions ($D = 2$). The second counterterm is logarithmic at $D = 3$ and is needed in the form given above for $D > 3$. Additional counterterms involving higher order curvature invariants are needed for $D \geq 5$; the additional counterterms are associated with logarithmic divergences (i.e. conformal anomalies) in odd dimensions.

The analysis in this section assumed a Poincaré parameterisation of AdS_{D+2}, i.e. we assumed a flat background metric for the dual field theory. We will generalise these results in Section 5.5. Note that although the renormalized entanglement entropy can be covariantized as shown in Section 5.5 the complete holographic dictionary would also need to take into account real time issues [21] for non-static setups.

5.4 Entanglement entropy for holographic RG flows

A holographic RG flow (for a field theory in a flat background) can be described by a domain wall geometry

$$\mathrm{d}s^2 = \mathrm{d}w^2 + e^{2\mathcal{A}(w)}\mathrm{d}x^\mu \mathrm{d}x_\mu \tag{5.4.1}$$

where the warp factor $\mathcal{A}(w)$ is linear in w at a fixed point. The geometry satisfies the equations of motion derived from Einstein gravity coupled to scalar fields ϕ^A, and the scalar fields have corresponding radial profiles $\phi^A(w)$. In what follows we will consider the case of a single scalar field with the bulk action being

$$I = \frac{1}{16\pi G_4}\int \mathrm{d}^4x\,\sqrt{-g}\left(R_g - \frac{1}{2}(\partial\phi)^2 + V(\phi)\right), \tag{5.4.2}$$

with $V(\phi)$ being the scalar potential. The generalisation to multiple scalar fields would be straightforward.

We restrict to UV conformal theories, so that the scalar potential $V(\phi)$ can be expanded as a power series in ϕ near the boundary:

$$V(\phi) = 6 - \sum_{n=1}^{\infty}\frac{\lambda_{(2n)}}{(2n)!}\phi^{2n}. \tag{5.4.3}$$

The mass M of the scalar is then given by $M^2 = \lambda_{(2)}$, so the scalar field is dual to a dimension Δ operator in the boundary CFT where $M^2 = \Delta(\Delta - 3)$. In what follows we will denote

$$\Delta_+ = \frac{3}{2} + \frac{1}{2}\sqrt{9 + 4M^2}. \tag{5.4.4}$$

For $-9/4 < M^2 < -5/4$, two quantizations are possible with the operator dimension corresponding to the second quantization being

$$\Delta_- = \frac{3}{2} - \frac{1}{2}\sqrt{9 + 4M^2}. \tag{5.4.5}$$

The equations of motion are

$$\begin{aligned}\ddot{\mathcal{A}} &= -\frac{1}{4}(\dot{\phi})^2 \\ \ddot{\phi} + 3\dot{\mathcal{A}}\dot{\phi} &= -\frac{dV}{d\phi}\end{aligned} \tag{5.4.6}$$

where a dot denotes a derivative with respect to w. It is well-known, see [131], that these equations are always equivalent to first order equations

$$\dot{\mathcal{A}} = W \qquad \dot{\phi} = -4\frac{dW}{d\phi} \tag{5.4.7}$$

where the superpotential $W(\phi)$ is given by

$$V = -2\left(4\left(\frac{dW}{d\phi}\right)^2 - 3W^2\right), \tag{5.4.8}$$

with

$$W = 1 + \frac{1}{8}(3 - \Delta_+)\phi^2 + \cdots \tag{5.4.9}$$

Note that the superpotential is not unique at higher orders in the scalar field: different choices are associated with different RG flows and in a supersymmetric theory only one choice will be supersymmetric. For flat sliced domain walls corresponding to holographic RG flows, the appropriate counterterm for the bulk action can be expressed in terms of the superpotential as

$$I_{\rm ct} = -\frac{1}{4\pi G_4}\int_{\mathcal{M}_\epsilon} \mathrm{d}^3x\sqrt{-h}W. \tag{5.4.10}$$

To match with conventions in earlier sections, it is convenient to express the asymptotically AdS_4 domain wall spacetime in the coordinates

$$\mathrm{d}s^2 = \frac{\mathrm{d}\rho^2}{4\rho^2} + \frac{1}{\rho}e^{A(\rho)}\eta_{\mu\nu}\mathrm{d}x^\mu\mathrm{d}x^\nu \tag{5.4.11}$$

where $\rho \to 0$ corresponds to the conformal boundary, $\eta_{\mu\nu}$ is the flat metric, with coordinates (t, x, y). Near the conformal boundary

$$e^{A(\rho)} = 1 + \ldots, \tag{5.4.12}$$

where the subleading terms depend on the form of the scalar potential. In these coordinates the Einstein and scalar equations become

$$A'' + \frac{1}{\rho}A' = -\frac{1}{4}(\phi')^2; \qquad 4\rho^2\phi'' + 2(3\rho A' - 1)\rho\phi' = -\frac{dV}{d\phi}. \tag{5.4.13}$$

These equations can also be rewritten in terms of the superpotential as

$$-\rho A' = \tilde{W} \qquad \rho\phi' = 2\frac{d\tilde{W}}{d\phi} \tag{5.4.14}$$

where $\tilde{W} = W - 1$.

5.4.1 Renormalization of entanglement entropy

Consider a codimension two minimal spacelike surface probing the domain wall spacetime. The entanglement entropy functional is

$$S = \frac{1}{4G_4}\int \mathrm{d}\rho\,\mathrm{d}x\,\sqrt{\gamma} \tag{5.4.15}$$

where $\gamma_{\mu\nu} = g_{mn}\partial_\mu X^m(\rho,x)\partial_\nu X^n(\rho,x)$, g_{mn} is the metric on the full target space, and $X^m(\rho,x)$ is the embedding. We will again work in static gauge where the embedding is given by $X^m(\rho,x) = (\rho,t,x,y(\rho,x))$ and t is a constant. Therefore

$$\begin{aligned}\gamma_{\rho\rho} &= \frac{1}{4\rho^2} + \frac{e^{A(\rho)}}{\rho}y_\rho^2 \\ \gamma_{\rho x} &= y_\rho y_x \frac{e^{A(\rho)}}{\rho} \\ \gamma_{xx} &= \frac{1}{\rho}e^{A(\rho)} + \frac{e^{A(\rho)}}{\rho}y_x^2\end{aligned} \tag{5.4.16}$$

where we denote $y_\rho = \partial_\rho y$ and $y_x = \partial_x y$. The entanglement entropy is thus given by

$$\begin{aligned}S &= \frac{1}{4G_4}\int \mathrm{d}\rho\,\mathrm{d}x\,\frac{e^{A(\rho)/2}}{2\rho^{3/2}}\sqrt{1+y_x^2+4\rho e^A y_\rho^2} \\ &= \frac{1}{4G_4}\int \mathrm{d}\rho\,\mathrm{d}x\,\frac{e^{A/2}}{2\rho^{3/2}}m(\rho,x)\end{aligned} \tag{5.4.17}$$

where we have introduced the shorthand $m(\rho,x) = \sqrt{1+y_x^2+4\rho e^A y_\rho^2}$.

The minimal surface equation is:

$$\begin{aligned}0 = {} & (1+4\rho e^A y_\rho^2)y_{xx} + \rho e^A(1+y_x^2)y_{\rho\rho} - 5\rho e^A y_\rho y_x y_{\rho x} \\ & + \frac{1}{2}e^A y_\rho(\rho A'(3+3y_x^2+8\rho e^A y_\rho^2) - 1 - y_x^2 - 8\rho e^A y_\rho^2).\end{aligned} \tag{5.4.18}$$

We now solve this equation iteratively for $y(\rho,x)$ as a series expansion in ρ. We assume the following Taylor series expansions for $A(\rho)$ and $y(\rho,x)$:

$$\begin{aligned}e^{A(\rho)} &= 1 + A_{(\alpha)}\rho^\alpha + \ldots \\ y(\rho,x) &= y_{(0)}(x) + y_{(\beta_1)}(x)\rho^{\beta_1} + y_{(\beta_2)}(x)\rho^{\beta_2} + \ldots\end{aligned} \tag{5.4.19}$$

where we assume that $\alpha > 0$ and $0 < \beta_1 < \beta_2 < \ldots$. To solve the PDE we insert these expansions into equation (5.4.19) and set $\rho = 0$. We then fix β_1 and $y_{(\beta_1)}$ to solve the resulting equation to leave $y_{(0)}$ unconstrained and differentiate equation (5.4.19) with respect to ρ and repeat to find β_2.

After substituting the expansions into the minimal surface equation, one finds that the leading order behaviour is a term constant in ρ and a term scaling as ρ^{β_1-1}. To leave $y_{(0)}$ unconstrained we must set $\beta_1 = 1$ (as before) and deduce that:

$$y_{(1)}(x) = \frac{2y_{(0)xx}}{1+(y_{(0)x})^2}. \tag{5.4.20}$$

Next we substitute the expansions into the ρ derivative of equation (5.4.19). In all cases the lowest power involving β_2 is ρ^{β_2-2} and we choose β_2 so as to cancel the leading order divergence involving α.

In the case that $\alpha < 1$ the leading order divergence involving α goes as $\rho^{\alpha-1}$ which requires $\beta_2 = 1+\alpha$ and the following value of $y_{(1+\alpha)}$ to cancel the divergence:

$$y_{(1+\alpha)} = -\frac{A_{(\alpha)}(3\alpha-1)y_{(1)}}{2\alpha^2+\alpha-1} \tag{5.4.21}$$

Note that the denominator here vanishes when $\alpha = \frac{1}{2}$ (and when $\alpha = -1$ which is excluded by the boundary conditions) and this case needs to be treated separately.

In the case $\alpha > 1$ the leading order term involving α is not divergent and we can set $\beta_2 = 2$ with

$$y_{(2)} = \frac{4y_{(1)}^3 + 6y_{(1)}y_{(0)x}y_{(1)x} - 4y_{(1)}^2 y_{(0)xx} - y_{(1)xx}}{1+(y_{(0)x})^2} \tag{5.4.22}$$

In the case where $\alpha = 1$ these two results overlap to give $\beta_2 = 2$ and

$$y_{(2)} = \frac{4y_{(1)}^3 + 6y_{(1)}y_{(0)x} - 4y_{(1)}^2 y_{(0)xx} - y_{(1)xx}}{1+(y_{(0)x})^2} - A_{(1)}y_{(1)}. \tag{5.4.23}$$

One can similarly analyse the asymptotic expansions to higher order but this will not be needed in calculating the regularised entanglement entropy.

Let us now turn to the regularisation of the entanglement entropy functional. Using the series expansion for $y(\rho,x)$ the small ρ behaviour of the action is

$$S = \frac{1}{4G_4}\int \mathrm{d}x\,\mathrm{d}\rho \frac{e^{A/2}}{2\rho^{3/2}}\sqrt{1+(y_{(0)x})^2}\left(1+\frac{1}{2}\rho B(\rho,x)+\ldots\right). \tag{5.4.24}$$

where $B(\rho,x)$ is a function which is constant in ρ to leading order. The full expression for $B(\rho,x)$ is given by

$$\rho B(\rho,x) = \frac{y_x^2 + 4\rho e^A y_\rho^2 - (y_{(0)x})^2}{1+(y_{(0)x})^2} \tag{5.4.25}$$

where it is understood that the series expansions for e^A and y are inserted above. It is

clear that

$$\int \mathrm{d}x \int_{\varepsilon} \mathrm{d}\rho \frac{e^{A/2}}{4} \sqrt{1+(y_{(0)x})^2}\rho^{-1/2} B \sim \varepsilon^{1/2} + \dots \tag{5.4.26}$$

which vanishes as the cutoff is removed.

Hence to find the regularised action we only need to expand the function $e^{A(\rho)/2}$ and keep terms which are powers of $\rho^{1/2}$ or lower:

$$S_{\mathrm{reg}} = \frac{1}{4G_4} \int \mathrm{d}x \sqrt{1+(y_{(0)x})^2} \int \mathrm{d}\rho \frac{e^{A/2}}{2\rho^{3/2}} \tag{5.4.27}$$

The latter radial integral depends only on the background and not on the specific embedding.

The first counterterm we require is needed in all cases independently of α: this is the volume divergence associated with the asymptotically AdS background. The necessary counterterm here is as before

$$S_{\mathrm{ct}} = -\frac{1}{4G_4} \int_{\partial\Sigma} \mathrm{d}x \sqrt{\tilde{\gamma}}. \tag{5.4.28}$$

The remaining divergent terms depend explicitly on $A_{(\alpha)}$ and α. These terms can only be non-trivial if there is a non-trivial matter content in the bulk and consequentially the counterterms must be functions of the scalar fields on the $\rho = \varepsilon$ slice pulled back on to the minimal surface.

Solving the field equations (5.4.13) to leading orders in ρ implies that

$$\phi = \phi_{(0)} \rho^{\frac{1}{2}(3-\Delta_+)} + \cdots \tag{5.4.29}$$

and for the warp factor:

$$\alpha = 3 - \Delta_+; \qquad A_{(\alpha)} = -\frac{1}{8}\phi_{(0)}^2. \tag{5.4.30}$$

Subleading divergences in the entanglement entropy are only present when $\Delta_+ > 5/2$. The regulated on-shell action up to the first subleading divergence is:

$$S_{\mathrm{reg}} = \frac{1}{4G_4} \int_{\partial\Sigma_\epsilon} \mathrm{d}x \sqrt{\tilde{\gamma}} \left(1 + \frac{3-\Delta_+}{8(5-2\Delta_+)} \phi_{(0)}^2 \varepsilon^{3-\Delta_+} + \dots\right) \tag{5.4.31}$$

and to leading order we also know that on the $\rho = \varepsilon$ hypersurface $\phi = \phi_{(0)}\varepsilon^{(3-\Delta_+)/2}$ so it is simple to write the $n = 1$ divergence in a covariant form so that the corresponding counterterm can then be read off:

$$S_{\mathrm{ct}} = -\frac{1}{4G_4} \int_{\partial\Sigma} \mathrm{d}x \sqrt{\tilde{\gamma}} \frac{3-\Delta_+}{8(5-2\Delta_+)} \phi^2. \tag{5.4.32}$$

At $\Delta_+ = 5/2$ the divergence becomes logarithmic and is associated with a conformal anomaly; we will discuss such anomalies further below.

Given a superpotential for the RG flow one can find an exact expression for the counterterms to all orders as follows. We have argued that the counterterms can be written covariantly as

$$S_{\rm ct} = -\frac{1}{4G_4}\int_{\partial\Sigma} \mathrm{d}x\,\sqrt{\tilde{\gamma}}Y(\phi) \tag{5.4.33}$$

where $Y(\phi)$ is analytic in the scalar field. (Here we exclude conformal anomalies, which we will discuss below.) By construction the counterterm is chosen to cancel divergences and hence

$$\int_\epsilon \mathrm{d}\rho \frac{e^{\frac{A}{2}}}{2\rho^{\frac{3}{2}}} = \frac{e^{\frac{A}{2}}}{\epsilon^{\frac{1}{2}}}Y(\phi), \tag{5.4.34}$$

where implicitly the latter is evaluated at $\rho = \epsilon$. Differentiating this expression with respect to the radius we then obtain

$$A'Y + 2\frac{dY}{d\phi}\phi' - \frac{Y}{\rho} = -\frac{1}{\rho}. \tag{5.4.35}$$

One can then substitute in the superpotential to get

$$(1+\tilde{W})Y - 4\frac{dY}{d\phi}\frac{d\tilde{W}}{d\phi} = 1, \tag{5.4.36}$$

i.e. an expression for $Y(\phi)$ in terms of the superpotential $\tilde{W}(\phi)$ with no explicit radial dependence. The superpotential $\tilde{W}(\phi)$ can be expressed as

$$\tilde{W}(\phi) = \sum_{n\geq 2} w_n \phi^n \qquad w_2 = \frac{1}{8}(3-\Delta_+) \tag{5.4.37}$$

and correspondingly

$$Y(\phi) = 1 + \sum_{n\geq 2} y_n \phi^n \tag{5.4.38}$$

with

$$y_2 = \frac{(3-\Delta_+)}{8(5-2\Delta_+)}; \qquad y_3 = \frac{1+24y_2}{(8-3\Delta_+)}w_3, \tag{5.4.39}$$

and so on. Here the cubic counterterm is required for $\Delta_+ > 8/3$, and there is a corresponding logarithmic divergence at $\Delta_+ = 8/3$ which is cubic in the scalar field.

For a free scalar in the bulk $w_n = 0$ for $n > 2$, but the expansion of $Y(\phi)$ does not terminate at $n = 2$:

$$Y(\phi) = e^{\frac{1}{4}\phi^2}\sum_{m\geq 0}\frac{(-1)^m}{4^m m!}\frac{\phi^{2m}}{(2m\Delta_+ - 2m + 1)}. \tag{5.4.40}$$

However, one should implicitly only retain terms from this series which contribute to divergences. The order m term is required for

$$\Delta_+ > 3 - \frac{1}{2m}. \tag{5.4.41}$$

The associated divergence becomes logarithmic at $\Delta_+ = 3 - 1/2m$: the coefficient at order m in (5.4.40) becomes ill-defined, corresponding to the breakdown of the assumed form of the counterterms. Note that logarithmic terms appear in the asymptotic expansion of the scalar field ϕ for half integer conformal dimensions but these are not related to conformal anomalies in the entanglement entropy.

In the $m = 1$ case the regulated on-shell action has a logarithmic divergence when $\Delta_+ = 5/2$

$$S_{\rm reg} = \frac{1}{4G_4}\int \mathrm{d}x\,\sqrt{\tilde{\gamma}}\left(1 - \frac{1}{4}A_{3-\Delta_+}\varepsilon^{1/2}\log\varepsilon\right) + \dots \tag{5.4.42}$$

Here $A_{1/2} = -\frac{1}{8}\phi_{(0)}^2$ and $\phi = \phi_{(0)}\varepsilon^{1/4} + \dots$, so we can write this divergence as

$$S_{\rm reg} = \frac{1}{4G_4}\int \mathrm{d}x\,\sqrt{\tilde{\gamma}}\left(1 + \frac{1}{32}\phi^2\log\varepsilon\right) + \dots . \tag{5.4.43}$$

The corresponding logarithmic counterterm is then simply

$$S_{ct} = -\frac{1}{4G_4}\int \mathrm{d}x\,\sqrt{\tilde{\gamma}}\frac{1}{32}\phi^2\log\varepsilon. \tag{5.4.44}$$

This result is consistent with that of [132] who found a logarithmic divergence, in their notation, given by

$$\delta S = \frac{\mathcal{A}}{8G_N}(d-2)\lambda^2 h_0 \log(\varepsilon/\varepsilon_{IR}) \tag{5.4.45}$$

which matches our expression under the substitutions $4G_N = 1$, $\mathcal{A} = \int \mathrm{d}x\,\sqrt{\tilde{\gamma}}$, $d = 3$, $h_0 = \frac{1}{8}$, $\lambda = \phi$ and the relabelling of the cut-off $\varepsilon \to \varepsilon^{1/2}$. This relabelling of the cut off is necessary as theirs is imposed on a $z = \varepsilon$ surface where $\rho = z^2$.

Thus, to summarise the results of this section, the required counterterms are

$$S = -\frac{1}{4G_4}\int_{\partial\Sigma}\mathrm{d}x\sqrt{\tilde{\gamma}}\left(1 + \frac{3-\Delta_+}{8(5-2\Delta_+)}\phi^2 + \cdots\right), \tag{5.4.46}$$

where the ellipses denote terms involving higher powers of the scalar field. The counterterm quadratic in scalar fields is necessary for $\Delta_+ > 5/2$ and is logarithmic at $\Delta_+ = 5/2$. More generally, new logarithmic divergences involving n powers of the scalar field arise at

$$\Delta_+ = 3 - \frac{1}{n} \tag{5.4.47}$$

and an additional counterterm involving n powers of the scalar field is switched on for

$\Delta_+ > 3 - 1/n$. The counterterms can be expressed compactly in terms of an analytic function of the scalar field $Y(\phi)$

$$S = -\frac{1}{4G_4}\int_{\partial\Sigma} \mathrm{d}x\sqrt{\tilde{\gamma}}Y(\phi), \tag{5.4.48}$$

where $Y(\phi)$ is defined in terms of the superpotential for the flow by (5.4.36). We should emphasise that both expressions (5.4.46) and (5.4.48) are applicable to entangling surfaces in holographic RG flows with flat slicings. For entangling surfaces in generic Einstein-scalar backgrounds there could be additional counterterms dependent on gradients of the scalar field.

5.4.2 Entanglement entropy change under relevant perturbation

In this section we will calculate the change in the renormalized entanglement entropy of a disk entangling region under a small relevant perturbation of the CFT, i.e. we work perturbatively in $\phi_{(0)}$, the source of the relevant operator. As in [133, 134] it is convenient to express the change in the bare entanglement entropy as

$$\delta S = \frac{1}{8G_4}\int \mathrm{d}^2x\sqrt{\gamma}T^{mn}_{\min}\delta g_{mn} \tag{5.4.49}$$

where γ is the metric on the unperturbed minimal surface, $T^{mn}_{\min}$ is the energy momentum tensor for the minimal surface

$$T^{mn}_{\min} = \gamma^{\alpha\beta}\partial_\alpha X^m \partial_\beta X^n \tag{5.4.50}$$

and δg_{mn} is the change in the (Einstein) metric induced by the relevant deformation. The latter can always be parameterised as

$$\mathrm{d}s^2 = \frac{\mathrm{d}\rho^2}{4\rho^2}(1+\delta f(\rho)) + \frac{1}{\rho}(1+\delta h(\rho))\mathrm{d}x^\mu \mathrm{d}x^\mu, \tag{5.4.51}$$

and we can furthermore use the gauge freedom to fix $\delta f(\rho) = 0$. The latter gauge choice was implicit in our earlier parameterisation of domain wall geometries.

One can then show that the change in the regulated (bare) entanglement entropy for a disk is

$$\delta S_{\mathrm{reg}} = \frac{\pi R}{4G_4}\int_\epsilon^{R^2} \frac{\mathrm{d}\rho}{\rho^{\frac{3}{2}}}(1+\frac{\rho}{R^2})\delta h(\rho). \tag{5.4.52}$$

Note that this expression holds for any small perturbation of the metric which preserves Poincaré invariance of the dual field theory.

Working perturbatively in the scalar field amplitude, and taking into account Poincaré

invariance, the most general solution possible for the scalar field is

$$\phi = \phi_{(0)}\rho^{\frac{1}{2}(3-\Delta_+)} + \phi_{(\Delta_+)}\rho^{\frac{1}{2}\Delta_+} \tag{5.4.53}$$

(where we assume that $\Delta_+ \neq 3/2$) and $\phi_{(\Delta_+)}$ is the normalizable mode of the scalar field. Correspondingly the warp factor is given by

$$\delta h = -\frac{1}{8}\left(\phi_{(0)}^2\rho^{(3-\Delta_+)} + \frac{8\Delta_+}{9}(3-\Delta_+)\phi_{(0)}\phi_{(\Delta_+)}\rho^{\frac{3}{2}} + \phi_{(\Delta_+)}^2\rho^{\Delta_+}\right) \tag{5.4.54}$$

Since we are working perturbatively in the scalar field, we need only retain counterterms which are quadratic in the scalars. In the case of a single scalar field this implies that the only contributing counterterms are those given in (5.4.46). At $\Delta_+ = 5/2$, the change in the entanglement entropy involves a logarithmic divergence, and thus the renormalized entanglement entropy will be renormalization scheme dependent.

The change in the renormalized entanglement entropy is hence (for $\Delta_+ \neq 5/2$)

$$\begin{aligned}\delta S_{\rm ren} =& \frac{\pi}{16(2\Delta_+ - 5)G_4}\phi_{(0)}^2 R^{2(3-\Delta_+)} \\ &+ \frac{\pi}{36G_4}\Delta_+(\Delta_+ - 3)\phi_{(0)}\phi_{(\Delta_+)}R^3 + \frac{\pi}{16(2\Delta_+ - 1)G_4}\phi_{(\Delta_+)}^2 R^{2\Delta_+}.\end{aligned} \tag{5.4.55}$$

Working to quadratic order in the scalar field one cannot impose regularity in the bulk as $\rho \to \infty$ as both modes are unbounded. On dimensional grounds, however,

$$\phi_{(\Delta)} \propto \phi_{(0)}^{\frac{\Delta_+}{(3-\Delta_+)}} \tag{5.4.56}$$

for $\frac{3}{2} < \Delta_+ < 3$. Hence $\phi_{(\Delta_+)} \sim \phi_{(0)}^{\delta}$ with $\delta > 1$, and the normalizable mode is subleading in powers of the non-normalizable mode, as we will see in the full solution given in the next section.

Therefore

$$\delta S_{\rm ren} = \frac{\pi}{16(2\Delta_+ - 5)G_4}\phi_{(0)}^2 R^{2(3-\Delta_+)} + \cdots \tag{5.4.57}$$

where ellipses denote terms which are of higher order in the source. This quantity is positive for $\Delta_+ > 5/2$ but negative for relevant deformations with $3/2 < \Delta_+ < 5/2$. Recalling that the F quantity is proportional to minus the renormalized entanglement entropy the change in the F quantity is *positive* for relevant deformations with $3/2 < \Delta_+ < 5/2$. A related result was obtained in [115], although the sign of the quantity was not explicitly identified in that work.

For operators of dimension $\Delta_- < 3/2$, the non-normalizable mode $\phi_{(0)}$ is not the operator source: the correct source is obtained from a Legendre transformation of the on-

shell action [16]. Such a Legendre transformation cannot be carried out without working to higher orders in the non-normalizable mode $\phi_{(0)}$ and thus we cannot obtain the entanglement entropy for this case without knowledge of the higher order solution.

Now let us consider the special case of $\Delta = 3$, i.e. marginal operators. In this case the warp factor is unchanged by the non-normalizable mode of the scalar field $\phi_{(0)}$, i.e. integrating the equations of motion we obtain

$$\delta h = -\frac{1}{8}\phi_{(3)}^3 \rho^3. \tag{5.4.58}$$

Since the non-normalizable mode does not affect the metric, there are no new divergences and no counterterms depending on the scalar field to leading order in the perturbation. This suggests that the F quantity should be stationary to leading order under a marginal deformation, which is consistent with the numerical results seen earlier in Figure 4.2.2. At $\Delta = 3$ there are also no possible finite counterterms since the finite counterterm

$$S_{\text{ct}} = -\frac{1}{4G_4}\int \mathrm{d}x \sqrt{\gamma^h}\left(\mathcal{K}\phi^2\right) \tag{5.4.59}$$

does not respect the complementarity requirement. The renormalized entanglement entropy for a marginal deformation is thus

$$\delta S_{\text{ren}} = \frac{\pi}{80G_4}\phi_{(3)}^2 R^6.$$

In the vacuum of the marginally deformed conformal field theory $\phi_{(3)} = 0$ and the change in the renormalized entanglement entropy is therefore zero for the vacuum of the deformed conformal field theory. Note that the change in the renormalized entanglement entropy is hence implicitly not analytic in the operator dimension as $\Delta \to 3$; this is however permissible, since the spectrum of operators is discrete.

We can also compute the change in the quantity $F(R)$ defined in Section 5.2:

$$\delta F(R) = -\delta S_{\text{reg}}(R) + R\frac{\partial S_{\text{reg}}(R)}{\partial R} \tag{5.4.60}$$

For $\Delta < 3$

$$\delta F(R) = -\frac{\pi\phi_{(0)}^2}{16G_4}R^{6-2\Delta} \tag{5.4.61}$$

which is negative for all relevant deformations. This does not agree numerically with δS_{ren}, but it is the latter which is by construction related to the renormalized F quantity by the CHM map.

For $\Delta = 3$, the change in the regulated entanglement entropy is zero, as the metric is

unchanged, and therefore

$$\delta F(R) = 0. \tag{5.4.62}$$

Note that implicitly the change in $\delta F(R)$ is therefore also non-analytic at $\Delta \to 3$.

It may seem surprising that the F quantity increases along RG flows generated by operators of dimensions $3/2 < \Delta_+ < 5/2$. The results discussed above actually follow directly from the subadditivity property of the (regularised) entanglement entropy: recall that the latter implies that $\partial^2 S_{\rm reg}/\partial R^2 \leq 0$. Our analysis implies that the counterterms scale with the size of the entangling region, i.e. $S_{\rm ct} \propto R$. Therefore subadditivity implies

$$\frac{\partial^2 S_{\rm ren}}{\partial R^2} = \frac{\partial^2 S_{\rm reg}}{\partial R^2} \leq 0. \tag{5.4.63}$$

However, on dimensional grounds, when we work to quadratic order in the source $S_{\rm ren}$ must take the form

$$S_{\rm ren} = -\frac{\pi}{2G_4} + a_{2(3-\Delta_+)}\phi_{(0)}^2 R^{2(3-\Delta_+)} + \cdots \tag{5.4.64}$$

for $\Delta_+ > 3/2$ where $a_{2(3-\Delta_+)}$ is a dimensionless constant. Here we use the explicit form for the leading term, which is independent of R. Differentiating twice with respect to R then gives

$$\frac{\partial^2 S_{\rm ren}}{\partial R^2} = 2(3-\Delta_+)(5-2\Delta_+)a_{2(3-\Delta_+)}\phi_{(0)}^2 R^{2(2-\Delta_+)} + \cdots \tag{5.4.65}$$

This is negative semi-definite (as required by strong subadditivity) provided that

$$(3-\Delta_+)(5-2\Delta_+)a_{2(3-\Delta_+)} \leq 0, \tag{5.4.66}$$

i.e. provided that $a_{2(3-\Delta_+)} \geq 0$ for $\Delta_+ \geq 5/2$ and $a_{2(3-\Delta_+)} \leq 0$ for $\Delta_+ \leq 5/2$, as we found above.

A related result is found by directly computing the change in the free energy to quadratic order in the source for holographic RG flows on a sphere driven by the same operators. Deformations of the theory on the sphere

$$I_{\rm CFT} \to I_{\rm CFT} + \int_{S^3} {\rm d}^3\Omega\ \psi_{(0)}\mathcal{O}_{\Delta_+}, \tag{5.4.67}$$

where the source $\psi_{(0)}$ is independent of the spherical coordinates and $d\Omega$ is the measure on the S^3, may be described holographically by spherical sliced domain walls. Again working to quadratic order in the source, the change in the free energy is positive for operators of dimensions $3/2 < \Delta_+ < 5/2$ [2].

Note that such deformations are not equivalent to conformal transformations of the holographic RG flows considered here, which are dual to deformations of the theory on

flat space:

$$I_{\mathrm{CFT}} \to I_{\mathrm{CFT}} + \int_{R^3} \mathrm{d}^3 x \phi_{(0)} \mathcal{O}_{\Delta_+}. \tag{5.4.68}$$

To understand this point further, it is useful to recall the relationship between spherical and Poincaré coordinates for anti-de Sitter. The former can be described in terms of the following embedding into $R^{1,4}$:

$$X^0 = \cosh w \qquad X^1 + iX^2 = \sinh w \cos\theta e^{i\tau_E} \qquad X^3 + iX^4 = \sinh w \sin\theta e^{i\phi} \tag{5.4.69}$$

so that

$$\mathrm{d}s^2 = \mathrm{d}w^2 + \sinh^2 w \left(\mathrm{d}\theta^2 + \cos^2\theta \mathrm{d}\tau_E^2 + \sin^2\theta \mathrm{d}\phi^2\right). \tag{5.4.70}$$

Poincaré coordinates can be obtained by setting

$$\begin{aligned} X^0 + X^1 =& \frac{1}{\rho^{1/2}} \qquad X^0 - X^1 = \left(\rho^{1/2} + \frac{1}{\rho^{1/2}}(t_E^2 + x^2 + y^2)\right) \\ X^2 =& \frac{t}{\rho^{1/2}} \qquad X^3 = \frac{x}{\rho^{1/2}} \qquad X^4 = \frac{y}{\rho^{1/2}}, \end{aligned} \tag{5.4.71}$$

resulting in

$$\mathrm{d}s^2 = \frac{\mathrm{d}\rho^2}{4\rho^2} + \frac{1}{\rho}\left(\mathrm{d}t_E^2 + \mathrm{d}x^2 + \mathrm{d}y^2\right). \tag{5.4.72}$$

From these relations it is clear that the radial coordinate in spherical slicings, w, depends on both ρ and $|x| \equiv (t_E^2 + x^2 + y^2)^{\frac{1}{2}}$. Conversely the Poincaré radial coordinate ρ depends on (w, θ, τ_E). Therefore flows which depend only on w or ρ, respectively, are not equivalent to each other: a flow which depends only on w will depend on the Poincaré norm $|x|$ as well as ρ.

From the field theory perspective, the theories on the S^3 and on R^3 are related by the conformal transformation described earlier, with the relevant conformal factor being given by (5.3.53). While the original conformal field theory is of course unaffected by this conformal factor, mapping (5.4.68) to the sphere results in

$$\phi_{(0)} \to \Omega^{\Delta_+ - 3}(\theta, \tau_E)\phi_{(0)}, \tag{5.4.73}$$

i.e. the transformed source is not homogeneous over the S^3, and therefore the deformations on S^3 and R^3 by homogeneous sources are not conformally equivalent. Thus, while the change in the renormalized entanglement entropy is related to a change in the free energy on the S^3, the latter is the change under a deformation which breaks the $SO(4)$ invariance.

5.4.3 Top down RG flow

Let us now consider entanglement entropy in holographic RG flows which have top down embeddings. We will discuss the following single scalar example, taken from [18]. Let the potential be

$$V(\phi) = 6\cosh\left(\frac{\phi}{\sqrt{3}}\right) \tag{5.4.74}$$

which arises in a consistent truncation of $\mathcal{N} = 8$ gauged supergravity, which in turn is a consistent truncation of M theory compactified on S^7. The RG flow equations can be used to construct analytic domain wall solutions in which the metric is conveniently expressed as

$$\mathrm{d}s^2 = \frac{(1+\nu r+\sqrt{1+2\nu r+r^2})}{2r^2\sqrt{1-r^2}(1+2\nu r+r^2)}\mathrm{d}r^2 + \frac{\sqrt{1-r^2}}{2r^2}(1+\nu r+\sqrt{1+2\nu r+r^2})\mathrm{d}x^\mu \mathrm{d}x_\mu \tag{5.4.75}$$

and the scalar field profile is

$$\phi = \sqrt{3}\tanh^{-1}(r). \tag{5.4.76}$$

The parameter $\nu \geq -1$ is arbitrary with $\nu = -1$ corresponding to a supersymmetric domain wall of the supergravity theory. Here $r \to 0$ corresponds to the conformal boundary. Note that in all cases the metric has a singularity at $r = 1$; this singularity is null in the supersymmetric case and timelike in all other cases but the singularity is good according to the standard criteria. The scalar mass associated with the potential is $M^2 = -2$, which corresponds to the cases of $\Delta_- = 1$ and $\Delta_+ = 2$, i.e. the mass is such that both quantisations are possible and mixed boundary conditions can be considered.

We can reintroduce the scalar field amplitude as a parameter by letting

$$r = c\tilde{r}; \qquad x^\mu = c\tilde{x}^\mu \tag{5.4.77}$$

so that

$$\begin{aligned}\mathrm{d}s^2 =& \frac{(1+\nu c\tilde{r}+\sqrt{1+2\nu c\tilde{r}+c^2\tilde{r}^2})}{2\tilde{r}^2\sqrt{1-c^2\tilde{r}^2}(1+2\nu c\tilde{r}+c^2\tilde{r}^2)}\mathrm{d}\tilde{r}^2 \\ &+ \frac{\sqrt{1-c^2\tilde{r}^2}}{2\tilde{r}^2}(1+\nu c\tilde{r}+\sqrt{1+2\nu c\tilde{r}+c^2\tilde{r}^2})\mathrm{d}\tilde{x}^\mu \mathrm{d}\tilde{x}_\mu \\ \phi =& \sqrt{3}\tanh^{-1}(c\tilde{r}).\end{aligned} \tag{5.4.78}$$

We can then change coordinates for $c\tilde{r} \ll 1$ as

$$\tilde{r}^2 = \rho + \nu c\rho^{\frac{3}{2}} + \cdots \tag{5.4.79}$$

to obtain

$$\begin{aligned} \mathrm{d}s^2 =& \frac{d\rho^2}{4\rho^2} + \frac{1}{\rho}(1 - \frac{3}{8}c^2\rho + \cdots)\mathrm{d}\tilde{x}^\mu \mathrm{d}\tilde{x}_\mu; \\ \phi =& \sqrt{3}c\left(\rho^{\frac{1}{2}} + \frac{1}{2}\nu c\rho + \cdots\right) \end{aligned} \tag{5.4.80}$$

from which we can read off that

$$\phi_{(0)} = \sqrt{3}c; \qquad \phi_{(\Delta_+)} \equiv \phi_{(1)} = \frac{1}{2}\sqrt{3}\nu c^2, \tag{5.4.81}$$

i.e. the normalizable mode is of order the non-normalizable mode squared. (This had to be true on dimensional grounds in a solution which depends on only one dimensionful parameter, c.) Thus substituting into (5.4.55) we obtain

$$\delta S_{\mathrm{ren}} = -\frac{\pi}{48G_4}\phi_{(0)}^2 R^4 + \mathcal{O}\left(\phi_{(0)}^3\right), \tag{5.4.82}$$

in agreement with (5.4.57) in the case of $\Delta_+ = 2$.

The result (5.4.82) can be interpreted as follows. There are only two physical scales in the field theory: the source for the operator deformation c and the size of the entangling region R. When $cR \ll 1$, the entangling surface is small and does not penetrate far into the bulk. The region probed by the entangling surface is well-described by the asymptotic Fefferman-Graham expansion (5.4.80), and therefore one can use the results of the previous section to compute the entanglement entropy. Note that the result does not depend on the parameter ν, i.e. it is same for supersymmetric and non-supersymmetric RG flows.

Now consider increasing the radius of the entangling surface at fixed source. On dimensional grounds δS_{ren} is a function of $\phi_{(0)}R$. Since $\partial^2 S_{\mathrm{ren}}/\partial R^2 \leq 0$, $\partial \delta S_{\mathrm{ren}}/\partial R$ must decrease monotonically with the radius R and δS_{ren} must be negative for all R.

5.5 Renormalization via the replica trick

In the previous sections we have described a renormalization procedure for entanglement entropy which is based on the holographic realisation of entanglement entropy in terms of minimal surfaces. It is difficult to translate this procedure directly into a field theoretic definition of renormalization, since the Ryu-Takayanagi functional itself does not follow directly from field theory.

A conceptual derivation of the Ryu-Takayanagi functional has been obtained by Lewkowycz-Maldacena [44] via the replica trick. The entropy associated with a density ma-

trix ρ is expressed as

$$S = -n\partial_n[\log Z(n) - n \log Z(1)]_{n=1} \tag{5.5.1}$$

where $Z(n) = \mathrm{Tr}(\rho^n)$ and $Z(1) = \mathrm{Tr}(\rho)$ is the usual partition function. If we are interested in the entropy of a thermal state, then $Z(n)$ is constructed by extending the period of the thermal circle by a factor of n. In the case of entanglement entropy, $Z(n)$ is constructed by extending the period of the circle around the boundary of the entangling region by a factor of n, where implicitly n is an integer. Assuming that the resulting expression is analytic in n, one can obtain the entropy by analytically continuing to $n = 1$.

Holographically $Z(n)$ can be computed in terms of the Euclidean actions:

$$S = n\partial_n[I(n) - nI(1)]_{n=1}. \tag{5.5.2}$$

Here $I(1)$ represents the on-shell Euclidean action for the bulk geometry while $I(n)$ represents the on-shell Euclidean action for the replica bulk geometry. For a thermal state, the bulk geometry associated with $Z(1)$ is a black hole and the replica is constructed by extending the period of the thermal circle by a factor of n. It was shown by Lewkowycz-Maldacena [44] that for a bulk theory described by Einstein gravity (5.5.1) then localises on the horizon of the black hole, i.e.

$$S = \frac{A}{4G_{d+1}}. \tag{5.5.3}$$

In particular, the volume divergences of the on-shell actions (associated with UV divergences in the field theory) by construction cancel, since the replica geometry asymptotically matches n copies of the original geometry.

For the entanglement entropy, the bulk geometry associated with $Z(1)$ corresponds to the usual bulk dual of the given state in the field theory. The replica is constructed by extending the period of the circle around the entangling region boundary by a factor of n. Following the same logic as in Lewkowycz-Maldacena, the expression (5.5.2) localises on the minimal surface corresponding to the extension of the boundary of the entangling region into the bulk (see the discussions in [135]). However, unlike the black hole case, the volume divergences of the bulk actions in (5.5.2) do not cancel, as the entangling surface itself has area divergences.

We can formally write down a renormalized entanglement entropy as

$$S_{\mathrm{ren}} = n\partial_n[I_{\mathrm{ren}}(n) - nI_{\mathrm{ren}}(1)]_{n=1} \tag{5.5.4}$$

where the quantities appearing on the right hand side are the renormalized bulk actions.

Equivalently,

$$S_{\rm ct} = n\partial_n[I_{\rm ct}(n) - nI_{\rm ct}(1)]_{n=1} \tag{5.5.5}$$

Let us first focus on the specific case of entangling surfaces in AdS_4, for which the usual counterterms for the on-shell action are [78]

$$I_{\rm ct}(1) = \frac{1}{4\pi G_4}\int_{\partial\mathcal{M}} \mathrm{d}^3x\sqrt{h}\left(-\frac{1}{2}K + 1 + \frac{1}{4}R\right). \tag{5.5.6}$$

Here we define the bulk geometry to be $\mathcal{M}$ and its boundary to be $\partial\mathcal{M}$, and K denotes the trace of the extrinsic curvature of $\partial\mathcal{M}$ embedded into $\mathcal{M}$. (The first term is the usual Gibbons-Hawking term.)

Since the replica geometry is also asymptotically locally AdS_4, the counterterms are

$$I_{\rm ct}(n) = \frac{1}{4\pi G_4}\int_{\partial\mathcal{M}_n} \mathrm{d}^3x\sqrt{h_n}\left(-\frac{1}{2}K_n + 1 + \frac{1}{4}R_n\right). \tag{5.5.7}$$

where h_n is the boundary metric for the replica geometry and K_n and R_n are the associated extrinsic curvature and Ricci scalar, respectively. Now the replica geometry by construction matches the original geometry except at the fixed point set of ∂_τ, where τ is the circle around the boundary of the entangling region and its extension into the bulk. At this fixed point set the metric and the extrinsic curvature of the replica match the original metric, but the intrinsic curvature invariants of the replica receive contributions from the conical singularity. In the case of interest $R = 0$ but in the replica geometry due to the conical singularity

$$\int \mathrm{d}^3x\sqrt{h_n}R_n = 4\pi(1-n)\int_{\partial\Sigma}\mathrm{d}x\sqrt{\tilde{\gamma}} \tag{5.5.8}$$

and hence we find that

$$S_{\rm ct} = -\frac{1}{4G_4}\int_{\partial\Sigma}\mathrm{d}x\sqrt{\tilde{\gamma}}, \tag{5.5.9}$$

which matches the counterterm obtained by our explicit calculations in Section 5.3.

For the case of entangling surfaces in holographic RG flows the counterterms to quadratic order in the scalar field are [78]

$$I_{\rm ct}(1) = \frac{1}{4\pi G_4}\int_{\partial\mathcal{M}} \mathrm{d}^3x\sqrt{h}\left(1 + \frac{1}{16}(3-\Delta_+)\phi^2 + \frac{1}{4}R + \frac{\Delta_+ - 3}{32(2\Delta_+ - 5)}R\phi^2\right), \tag{5.5.10}$$

where we drop the Gibbons-Hawking term as it does not contribute to the entanglement entropy counterterms, and we also neglect terms involving derivatives of the scalar field, i.e. we restrict to homogeneous scalar field configurations. Following the same steps as

above, we can then show that

$$S_{\rm ct} = -\frac{1}{4G_4}\int_{\partial\Sigma} \mathrm{d}x\sqrt{\tilde{\gamma}}\left(1+\frac{\Delta_+-3}{8(2\Delta_+-5)}\phi^2\right) \tag{5.5.11}$$

which is again in agreement with our explicit results of Section 5.4.

Let us now move to general dimensions. For an asymptotically locally AdS_{D+2} spacetime the counterterms are [78]

$$\begin{aligned} I_{\rm ct}(1) =& \frac{1}{16\pi G_{D+2}}\int_{\partial\mathcal{M}} \mathrm{d}^{D+1}x\sqrt{h}\left(2D+\frac{1}{(D-1)}R\right. \\ &\left.+\frac{1}{(D-3)(D-1)^2}\left(R_{ab}R^{ab}-\frac{D+1}{4D}R^2\right)+\cdots\right). \end{aligned} \tag{5.5.12}$$

This expression should be understood as containing only the appropriate divergent terms in any given dimension; moreover, for odd D there are logarithmic counterterms. In particular, for $D=3$ the third counterterm is replaced by the logarithmic counterterm

$$\frac{1}{16\pi G_5}\int_{\partial\mathcal{M}_\varepsilon} \mathrm{d}^4x\sqrt{h}\frac{1}{8}\left(R_{ab}R^{ab}-\frac{1}{3}R^2\right)\log\varepsilon. \tag{5.5.13}$$

In the replica geometry, the contributions to the curvature from the conical singularity are given by [121]

$$\begin{aligned} R_n =& R+4\pi(1-n)\delta_{\partial\Sigma}+\mathcal{O}(1-n)^2; \\ R_{nab} =& R_{ab}+2\pi(1-n)n_an_b\delta_{\partial\Sigma}+\mathcal{O}(1-n)^2, \end{aligned} \tag{5.5.14}$$

where $\delta_{\partial\Sigma}$ is a delta function localised on the entangling surface. Here n_a^k with $k=1,2$ represent orthonormal vectors to the entangling surface and

$$n_an_b = \sum_k n_a^k n_b^k. \tag{5.5.15}$$

Following the same steps as above, we can immediately read off the leading counterterm for the entanglement entropy as

$$S_{\rm ct,1} = -\frac{1}{4(D-1)G_{D+2}}\int_{\partial\Sigma}\mathrm{d}^{D-1}x\sqrt{\tilde{\gamma}}, \tag{5.5.16}$$

in agreement with our earlier result.

For the higher order counterterms, one can use the following expressions [122]

$$\int_{\partial\mathcal{M}_n} \mathrm{d}^{D+1}x\sqrt{h_n}R_n^2 = n\int_{\partial\mathcal{M}} \mathrm{d}^{D+1}x\sqrt{h}R^2 + 8\pi(1-n)\int_{\partial\Sigma} \mathrm{d}^{D-1}x\sqrt{\tilde{\gamma}}R \tag{5.5.17}$$
$$\int_{\partial\mathcal{M}_n} \mathrm{d}^{D+1}x\sqrt{h_n}R_{nab}R_n^{ab} = n\int_{\partial\mathcal{M}} \mathrm{d}^{D+1}x\sqrt{h}R_{ab}R^{ab} + 4\pi(1-n)\int_{\partial\Sigma} \mathrm{d}^{D-1}x\sqrt{\tilde{\gamma}}(R_{ii} - \frac{1}{2}k^2),$$

where implicitly we work to leading order in $(1-n)$ and we define

$$k^2 = \sum_k \left(\mathcal{K}^k\right)^2 \tag{5.5.18}$$

with R_{ii} corresponding to invariant projections of the Ricci tensor onto the subspace orthogonal to $\partial\Sigma$, see [121].

In Section 5.3, we analysed the entanglement entropy counterterms assuming that the entangling surface is static and that the curvature of the boundary metric is zero. In such a case $R_{ii} = R = 0$ and the extrinsic curvature in the time direction is zero. Thus the second counterterm becomes

$$S_{\mathrm{ct},2} = -\frac{1}{8(D-1)^2(D-3)G_{D+2}}\int_{\partial\Sigma} \mathrm{d}^{D-1}x\sqrt{\tilde{\gamma}}\mathcal{K}^2, \tag{5.5.19}$$

where $\mathcal{K}$ refers to the trace of the extrinsic curvature of the surface embedded into a constant time hypersurface. Similarly in $D=3$ the logarithmic counterterm is

$$S_{\mathrm{ct},2} = \frac{1}{64G_5}\int_{\partial\Sigma} \mathrm{d}^3x\sqrt{\tilde{\gamma}}\mathcal{K}^2\ln\varepsilon, \tag{5.5.20}$$

which is in agreement with the expression obtained in [121] for the anomaly in the entanglement entropy for 4d CFTs with a holographic dual. (See [121] for the conformal anomaly in a general 4d conformal field theory in which $a \neq c$.)

One can now immediately generalise the entanglement entropy counterterms to the case of a general embedding into a curved boundary metric obtaining

$$\begin{aligned} S_{\mathrm{ct}} = &-\frac{1}{4(D-1)G_{D+2}}\int_{\partial\Sigma} \mathrm{d}^{D-1}x\sqrt{\tilde{\gamma}} \\ &-\frac{1}{4(D-1)^2(D-3)G_{D+2}}\int_{\partial\Sigma} \mathrm{d}^{D-1}x\sqrt{\tilde{\gamma}}\left(R_{ii} - \frac{1}{2}k^2 - \frac{D+1}{2D}R\right), \end{aligned} \tag{5.5.21}$$

where one can use the Gauss-Codazzi relations to write R_{ii} and R in terms of intrinsic and extrinsic curvatures of $\partial\Sigma$.

5.5.1 Higher derivative generalisations

Using the replica trick, we can derive the renormalized entanglement entropy functional from any higher derivative gravity for which the renormalized bulk action is known. Let us consider the particular example of Gauss-Bonnet gravity, with bulk action

$$I = -\frac{1}{16\pi G_{D+2}} \int_{\mathcal{M}} \mathrm{d}^{D+2}x\sqrt{g}\left[R_g + D(D+1) + \lambda\left(R_{mnpq}R^{mnpq} - 4R_{mn}R^{mn} + R_g^2\right)\right] \tag{5.5.22}$$

where λ is the Gauss-Bonnet coupling.

One can derive the entanglement entropy functional by the replica trick used above, see [122, 136], using the bulk versions of (5.5.17) together with the additional relation

$$\begin{aligned}\int_{\mathcal{M}_n} \mathrm{d}^{D+2}x\sqrt{g}R_{mnpq}R^{mnpq} =& n\int_{\mathcal{M}_n} \mathrm{d}^{D+2}x\sqrt{g}R_{mnpq}R^{mnpq} \\ &+ 8\pi(1-n)\int_{\Sigma} \mathrm{d}^{D}y\sqrt{\gamma}\left(R_{ijij} - \mathrm{Tr}(k^2)\right),\end{aligned} \tag{5.5.23}$$

where we neglect terms of higher order in $(n-1)$ and R_{ijij} denotes the projection of the Riemann tensor in the directions orthogonal to the entangling surface. Also

$$\mathrm{Tr}(k^2) = \sum_{k=1}^{2} \mathcal{K}^k_{ab}\mathcal{K}^{kab}. \tag{5.5.24}$$

Thus the entanglement entropy functional consists of the usual Ryu-Takayanagi term plus additional terms

$$S = \frac{1}{4G_{D+2}}\int_{\Sigma} \mathrm{d}^{D}y\sqrt{\gamma} + \frac{\lambda}{G_{D+2}}\int_{\Sigma} \mathrm{d}^{D}y\sqrt{\gamma}\left(R_{ijij} - \mathrm{Tr}(k^2) - 2R_{ii} + k^2 + R\right), \tag{5.5.25}$$

where implicitly all terms can be written in terms of extrinsic and intrinsic curvatures on the entangling surface. As shown in [122], in five bulk dimensions the latter term can be simplified using the Gauss-Codazzi relations to give

$$S = \frac{1}{4G_5}\int_{\Sigma} \mathrm{d}^{3}y\sqrt{\gamma}\left(1 + 2\lambda\hat{R}\right), \tag{5.5.26}$$

with $\hat{R}$ the intrinsic curvature of the entangling surface.

Now the bulk equations of motion admit as AdS_5 as a solution, but the radius of the AdS_5 depends on the Gauss-Bonnet coupling, i.e. the AdS_5 metric is

$$\mathrm{d}s^2 = l^2(\lambda)\left(\frac{\mathrm{d}\rho^2}{4\rho^2} + \frac{1}{\rho}\mathrm{d}x\cdot\mathrm{d}x\right) \tag{5.5.27}$$

where the radius is given by

$$l^4(\lambda) - l^2(\lambda) + 2\lambda = 0. \tag{5.5.28}$$

One can then straightforwardly show that the leading order counterterm for the entanglement entropy is given by

$$S_{\rm ct} = -\frac{1}{8G_5}\int_{\partial\Sigma} \mathrm{d}^2x\sqrt{\tilde{\gamma}}\left(l(\lambda) - 12\frac{\lambda}{l(\lambda)}\right), \tag{5.5.29}$$

where we use the fact that the entangling surface is asymptotically locally hyperbolic and thus $\hat{R} = -6/l(\lambda)^2 + \cdots$. There is also a subleading logarithmic divergence associated with the conformal anomaly; this is known from the work of [121].

Now the leading order counterterm for the entanglement entropy is inherited from the subleading counterterm for the bulk action, i.e. the counterterm

$$I_{ct} = a_2\int \mathrm{d}^4x\sqrt{h}R. \tag{5.5.30}$$

This counterterm is not known to all orders in λ, although it was derived perturbatively in λ in [137, 138, 139]. The relation with entanglement entropy immediately gives the coefficient of this counterterm to be

$$a_2 = \frac{1}{32G_5}\left(l(\lambda) - 12\frac{\lambda}{l(\lambda)}\right), \tag{5.5.31}$$

i.e. the entanglement entropy counterterms provide a quick method of deriving or verifying counterterms in the bulk action involving the curvature.

5.5.2 Domain walls

In this section we show how the counterterms for asymptotically locally AdS solutions of a theory with a single scalar imply the entanglement entropy counterterms discussed in Section 5.4. The bulk Euclidean action is

$$I = -\frac{1}{16\pi G_4}\int_{\mathcal{M}} \mathrm{d}^4x\sqrt{g}\left(R_g - \frac{1}{2}(\partial\phi)^2 + V(\phi)\right). \tag{5.5.32}$$

In general the counterterms for asymptotically locally AdS solutions of this action can be expressed in the form

$$I_{ct} = \frac{1}{16\pi G_4}\int_{\partial\mathcal{M}} \mathrm{d}^3x\sqrt{h}\left(\mathcal{W}(\phi) + \mathcal{Y}(\phi)R + \cdots\right), \tag{5.5.33}$$

where $\mathcal{W}(\phi)$ and $\mathcal{Y}(\phi)$ are analytic functions of the scalar field ϕ. Here the ellipses denote terms which depend on gradients of the scalar field; as in the discussions above,

such terms are not relevant when using the replica trick to derive the entanglement entropy counterterms. In the above expression we assume generic values of the dual operator dimension such that there are no conformal anomalies; for specific values of the operator dimension there will however be conformal anomalies.

For a flat domain wall solution, characterised by a given superpotential $W(\phi)$, the only contributing counterterm is $\mathcal{W}(\phi) = 4W(\phi)$, since in this case $R = 0$. To use the replica trick we need to know how the counterterms for the bulk action depend on the curvature of the boundary metric i.e. we cannot restrict to flat sliced domain walls: the counterterm for the entanglement entropy follows from the term involving the Ricci scalar above, i.e.

$$S_{\rm ct} = -\frac{1}{4G_4}\int_{\partial\Sigma} \mathrm{d}x\sqrt{\tilde{\gamma}}\mathcal{Y}(\phi). \tag{5.5.34}$$

We can understand the specific form of $\mathcal{Y}(\phi)$ for entanglement entropy in a flat sliced domain wall as follows. We begin with solutions of the equation of motion corresponding to domain walls with homogeneous slicing, i.e. the metric is

$$\mathrm{d}s^2 = \mathrm{d}w^2 + e^{2\mathcal{A}(w)}\mathrm{d}\Omega_3^2 \tag{5.5.35}$$

and the scalar field profile is $\phi(w)$. We let the Ricci scalar of the slicing be $\hat{r}$ where, for example, $\hat{r} = 6$ for unit radius spherical slices. The equations of motion are then

$$\ddot{\phi} + 3\dot{\phi}\dot{\mathcal{A}} = -V'(\phi); \qquad -\frac{\hat{r}}{6}e^{-2\mathcal{A}} - \frac{1}{4}\dot{\phi}^2 = \ddot{\mathcal{A}}. \tag{5.5.36}$$

These equations are identical to those discussed in Section 5.4, apart from the curvature contribution to the second equation.

Now let us work in the limit that $\hat{r} \ll 1$. For $\hat{r} = 0$, the equations admit the first order form discussed in Section 5.4, in terms of the superpotential $W(\phi)$. For $\hat{r} \ll 1$, the equations of motion are solved to order $\hat{r}^2$ by

$$\dot{\mathcal{A}} = W \qquad \dot{\phi} = -4\frac{dW}{d\phi} + \hat{r}f(\phi) \tag{5.5.37}$$

provided that

$$\begin{aligned} 3Wf(\phi) - 4\frac{d}{d\phi}\left(f(\phi)\frac{dW}{d\phi}\right) = 0; \\ f(\phi)\frac{dW}{d\phi} = \frac{1}{6}e^{-2\mathcal{A}}. \end{aligned} \tag{5.5.38}$$

The regulated on-shell action (including the Gibbons-Hawking term) thus becomes

$$\begin{aligned} I_{\text{reg}} &= -\int^R \mathrm{d}w \int \mathrm{d}\Omega_3 \left(e^{\mathcal{A}}\hat{r} + \mathcal{O}(\hat{r}^2)\right) - \frac{1}{4\pi G_4}\int \mathrm{d}\Omega_3 \left[e^{3\mathcal{A}}W\right]_R, \\ &= -\frac{1}{16\pi G_4}\int^R \mathrm{d}w \int \mathrm{d}\Omega_3 \left(e^{\mathcal{A}}\hat{r} + \mathcal{O}(\hat{r}^2)\right) - \frac{1}{4\pi G_4}\int_{\partial M} \mathrm{d}^3x\sqrt{h}W, \end{aligned} \tag{5.5.39}$$

where we have used the field equations to linear order in $\hat{r}$ and in the second line we write the boundary term in covariant form. The bulk term can be expressed as a covariant boundary term

$$-\frac{1}{16\pi G_4}\int_{\partial M} \mathrm{d}^3x\sqrt{h}RY(\phi) \tag{5.5.40}$$

provided that

$$\frac{d}{dw}\left(\sqrt{h}RY(\phi)\right) = e^{\mathcal{A}}\hat{r}. \tag{5.5.41}$$

However,

$$\frac{d}{dw}\left(\sqrt{h}RY\right) = \hat{r}\frac{d}{dw}\left(e^{\mathcal{A}}Y\right) = e^{\mathcal{A}}\hat{r}\left(WY - 4\frac{dW}{d\phi}\frac{dY}{d\phi}\right), \tag{5.5.42}$$

where we drop terms of higher order in $\hat{r}$ and use the field equations. Therefore the required counterterms are

$$I_{\text{ct}} = \frac{1}{16\pi G_4}\int_{\partial M} \mathrm{d}^3x\sqrt{h}\left(4W + RY\right), \tag{5.5.43}$$

with

$$\left(WY - 4\frac{dW}{d\phi}\frac{dY}{d\phi}\right) = 1, \tag{5.5.44}$$

as we found in Section 5.4. Note that terms of higher order in $\hat{r}$ would not contribute to the counterterms, as they do not give rise to divergent terms.

We calculated the curvature term in (5.5.43) by working with a homogeneous domain wall. To use the replica trick, we need to consider a replica space in which the curvature of the boundary is given by (5.5.14), in the limit that $n \to 1$, i.e. it is not homogeneous, but (5.5.43) is covariant and still applies. Note that the slices of the domain wall are flat, up to conical singularity terms which are proportional to $(n-1)$, and hence R is small as $n \to 1$. It is therefore indeed true to leading order in $(n-1)$ that the replica geometry is still governed by the superpotential W. Following the same steps as earlier in this section, we can then immediately read off the counterterm action for the entanglement entropy as

$$S_{\text{ct}} = -\frac{1}{4G_4}\int_{\partial\Sigma} \mathrm{d}x\sqrt{\tilde{\gamma}}Y(\phi), \tag{5.5.45}$$

as we found in Section 5.4.

It is important to note that this expression holds specifically for flat domain wall geome-

tries associated with a superpotential W. A generic curved domain wall geometry is not governed by a single real superpotential (see [140, 141]) and the analysis above would need to be generalised for such cases.

5.6 Conclusions

In this chapter we have shown how the holographic entanglement entropy may be renormalized using appropriately covariant boundary counterterms. This renormalization procedure is inherited directly from the renormalization of the partition function, using the replica trick.

We analysed renormalization for entangling surfaces in asymptotically locally AdS spacetimes in any dimension and in flat sliced holographic RG flows in four bulk dimensions. We also showed that the renormalization procedure can be extended to higher derivative theories such as Gauss-Bonnet. It would be straightforward to generalise our results to include entangling surfaces with cusps and to non-conformal holographic setups using [142]. It would be interesting to explore real-time holography in the context of entanglement entropy, using the techniques of [21] for the HRT functional [143].

While it is difficult to relate the area renormalization of the holographic entanglement entropy functional directly to field theory renormalization, the replica trick expresses our renormalized entanglement entropy in terms of renormalized partition functions, i.e.

$$S_{\rm ren} = -n\partial_n[\log Z_{\rm ren}(n) - n\log Z_{\rm ren}(1)]_{n=1}. \tag{5.6.1}$$

This expression can be directly implemented in a field theoretical calculation: having fixed a renormalization scheme for the partition function, the partition function on the replica space (which has the same UV divergence structure) will inherit a renormalization scheme and thus $S_{\rm ren}$ will be determined. This assumes that the replica trick is applicable but in practice most explicit calculations of entanglement entropy in field theory do in any case make use of the replica trick. Computations of the renormalized entanglement entropy in free field theory examples will be presented elsewhere.

There has been considerable interest recently in supersymmetric renormalization schemes for field theories on curved spaces and, in particular, in analysing how much supersymmetry is required for the partition function to be uniquely defined [116]. It would be interesting to understand the role of supersymmetry in our analysis.

In Section 5.4 we showed that the renormalized entanglement entropy of a disk decreases under deformations of a conformal field theory by operators of dimension $3/2 < \Delta < 5/2$. Under the CHM map, this corresponds to an increase in the F quantity when

one makes corresponding deformations of the theory on a three sphere; note however that these deformations do not preserve the symmetry of the S^3. In Chapter 4 we found analogous results for flows which are homogeneous on the three sphere. It would be interesting to understand whether these examples indeed disprove the strong version of the F theorem, or whether the flows under consideration are unphysical.

CHAPTER 6

Examples of renormalized holographic entanglement entropy

6.1 Introduction

Entanglement entropy is widely used in condensed matter physics, quantum information theory and, more recently, in high energy physics and black holes. Consider a reduced density matrix ρ_A, obtained from tracing out certain degrees of freedom from a quantum system. The associated entanglement entropy is then the von Neumann entropy:

$$S = -\mathrm{tr}_A \left(\rho_A \log \rho_A\right). \tag{6.1.1}$$

Throughout this chapter we will be interested in the case for which a quantum system is subdivided into two, via partitioning space. In such a case A is a spatial region, with boundary ∂A.

The entanglement entropy characterises the nature of the quantum state of a system. For example, in the ground state of a quantum critical system in D spatial dimensions:

$$S = c_{1-D}\frac{\mathrm{Area}(\partial A)}{\epsilon^{D-1}} + \cdots + c_0 \log\left(\frac{R}{\epsilon}\right) + \tilde{c}_0 + \cdots, \tag{6.1.2}$$

where c_{1-D}, c_0 and $\tilde{c}_0$ are dimensionless; R is a characteristic scale of the region A, and ϵ is a UV cutoff. Logarithmic terms arise when D is odd, and their coefficients are related to the a anomalies of the stress energy tensor. More generally, the famous area

law leading term characterises the ground state of a system and can be used to test trial ground state wavefunctions. Entanglement entropy can also be used to distinguish between different phases of a system, such as the confining/deconfining phase transition [119, 144, 145].

Continuum quantum field theory (with a cutoff) is often used as a tool to describe discrete condensed matter systems. In this context, the cutoff appearing in (6.1.2) is related to the underlying physical lattice scale in the discrete system and the coefficients of power law terms such as c_{1-D} capture the leading physical contributions to the entanglement entropy. From the quantum field theory perspective, the expansion in (6.1.2) implicitly assumes the use of a direct energy cutoff as a regulator. Different methods of regularisation result in different regulated divergences and thus the power law divergences are often called non-universal. By contrast logarithmic divergences are often denoted as universal as their coefficients are related to the anomalies of the theory.

In even spatial dimensions, the logarithmic term in (6.1.2) is absent but the constant term $\tilde{c}_0$ is believed to be related to the number of degrees of freedom of the system. However, $\tilde{c}_0$ is manifestly dependent on the choice of the cutoff. In two spatial dimensions, if

$$S = c_{-1}\frac{R}{\epsilon} + \tilde{c}_0 + \cdots \tag{6.1.3}$$

for a spatial region with boundary of length R, then changing the cutoff as

$$\epsilon \to \epsilon' \left(1 + \alpha\frac{\epsilon'}{R} + \cdots\right) \tag{6.1.4}$$

for any choice of the dimensionless constant α gives

$$S = c_{-1}\frac{R}{\epsilon'} + (\tilde{c}_0 - \alpha c_{-1})\,, \tag{6.1.5}$$

so the constant term in the entanglement entropy clearly depends on the choice of regulator.

If one is interested in isolating finite contributions to the entanglement entropy, one can evade the issue of regulator dependence. For example, if the entangling region is a strip of width L and regulated length $R \gg L$, then the divergent contributions in (6.1.3) cannot, by locality of the quantum field theory, depend on the width of slab, so

$$c(L) = \frac{\partial S}{\partial L} = \frac{\partial \tilde{c}_0}{\partial L} \tag{6.1.6}$$

is finite as $\epsilon \to 0$ [124, 125, 111]. However, such an approach has several drawbacks. The regularisation is specific to the shape of the geometry (a slab) and a modified prescription is needed for curved entangling region boundaries such as spheres, for which the

scale of the entangling region is related to the local curvature of the entangling region boundary (see proposals in [110]). Any such prescription depends explicitly on the UV behaviour of the theory. More generally, extraction of finite terms by differentiation obscures scheme dependence: there is no connection with the renormalization scheme used for other QFT quantities such as the partition function and correlation functions.

From a quantum field theory perspective, as opposed to a condensed matter perspective, it is very unnatural to work with a regulated rather than a renormalized quantity. In the previous Chapter 5, we introduced a systematic renormalization procedure for entanglement entropy, in which the counterterms are inherited directly from the partition function counterterms. As we review in Section 6.2, such renormalization guarantees that the counterterms depend only on the quantum field theory sources (non-normalizable modes in holographic gravity realisations) and not on the state of the quantum field theory (normalizable modes in holographic gravity realisations).

The renormalized entanglement entropy $S^{\rm ren}$ expressed as a function of a characteristic scale of the entangling region L implicitly captures the behaviour of the theory under an RG flow: small entangling regions probe the UV of the theory, while larger regions probe the IR. In this chapter we will establish how these finite contributions to entanglement entropy behave in a variety of theories using holographic models.

The outline of this chapter is as follows. In Section 6.2 we review the definition of renormalized entanglement entropy introduced in Chapter 5. In Section 6.3 we calculate the entaglement entropy for a slab region in anti-de Sitter (in general dimensions). The latter is relevant for the non-conformal branes discussed in Section 6.4 as they can be viewed as dimension reduction of anti-de Sitter theories in general dimensions. In Section 6.4 we also compute the renormalized entanglement entropy for a slab region in the Witten holographic model for QCD. Section 6.5 explores renormalized entanglement entropy for operator driven holographic RG flows, which are UV conformal.

6.2 Renormalized entanglement entropy

Entanglement entropy is usually calculated using the replica trick. The Rényi entropies are defined as

$$S_n = \frac{1}{(1-n)} \left(\log Z(n) - n \log Z(1) \right) \tag{6.2.1}$$

where $Z(1)$ is the partition function and $Z(n)$ is the partition function on the replica space obtained by gluing n copies of the geometry together along the boundary of the entangling region. The entanglement entropy is obtained as the limit

$$S = \lim_{n \to 1} S_n. \tag{6.2.2}$$

Note that this limit implicitly assumes that the Rényi entropies are analytic in n.

Both sides of (6.2.1) are UV divergent. In a local quantum field theory, the UV divergences of $\log Z(n)$ cancel with those of $n \log Z(1)$ except at the boundary of the entangling region; therefore the UV divergences of $S(n)$ scale with the area of this boundary.

We can formally define the renormalized entanglement entropy as

$$S_n^{\rm ren} = \frac{1}{(1-n)} \left(\log Z^{\rm ren}(n) - n \log Z^{\rm ren}(1) \right) \tag{6.2.3}$$

with $S^{\rm ren} = S_1^{\rm ren}$. Here the renormalized partition functions are defined with any suitable choice of renormalization scheme.

The replica space matches the original space, except at the boundary of the entangling region where there is a conical singularity. To define the renormalization on the replica space it is therefore natural to work within a renormalization method that works for generic curvature backgrounds for the quantum field theory.

6.2.1 Direct cutoff: field theory

Consider for example a Euclidean free massive scalar field theory on a background geometry $\mathcal{M}$ of dimension d and let $Z(1)$ be the partition function in the ground state. Using locality of the quantum field theory and dimensional analysis, the UV divergences in the partition function behave as

$$\log Z(1) = a_d V_d \Lambda^d + a_{d-2} m^2 V_d \Lambda^{d-2} + b_{d-2} \Lambda^{d-2} \int_{\mathcal{M}} {\rm d}^d x \sqrt{h} \mathcal{R} + \cdots \tag{6.2.4}$$

where Λ is the UV cutoff, V_d is the volume of the background (Euclidean) geometry, m^2 is the mass and $\mathcal{R}$ is the Ricci scalar. The coefficients $a_d, a_{d-2}, b_{d-2}, \ldots$ are dimensionless and in the above expressions we ignore boundaries of $\mathcal{M}$.

The divergences of the partition function on the replica space $Z(n)$ have exactly the same structure and coefficients. However, the curvature of the replica space has an additional term from the conical singularity [121]

$$\mathcal{R}_n = \mathcal{R} + 4\pi(n-1)\delta(\partial\Sigma) + \mathcal{O}(n-1)^2, \tag{6.2.5}$$

where $\delta(\partial\Sigma)$ is localised on a constant time hypersurface, on the boundary of the entangling region. (Here and in what follows we consider only static situations.) Therefore, when we use the replica formula (6.2.2) the leading divergences of the partition func-

tions cancel so that the leading divergence in the entanglement entropy behaves as

$$S_{\rm reg} = 4\pi b_{d-2}\Lambda^{d-2}\int_{\partial\Sigma} {\rm d}^{d-2}x\sqrt{\gamma} + \cdots \tag{6.2.6}$$

Such a divergence can clearly be cancelled by the counterterm

$$S_{\rm ct} = -4\pi b_{d-2}\Lambda^{d-2}\int_{\partial\Sigma} {\rm d}^{d-2}x\sqrt{\gamma}, \tag{6.2.7}$$

which is covariantly expressed in terms of the geometry of the entangling region.

6.2.2 Holographic renormalization

In gauge-gravity duality, the defining relation is [19, 13]

$$I_E = -\log Z, \tag{6.2.8}$$

where I_E is the on-shell action for the bulk theory dual to the field theory. In the supergravity limit this is given by the on-shell Euclidean Einstein-Hilbert action together with appropriate matter terms i.e.

$$I_E = -\frac{1}{16\pi G_{d+1}}\int_{\mathcal{Y}_n} {\rm d}^{d+1}x\sqrt{g}\,(R+\cdots) - \frac{1}{8\pi G_{d+1}}\int_{\partial\mathcal{Y}_n} {\rm d}^{d}x\sqrt{h}\,(K+\cdots)\,, \tag{6.2.9}$$

where the latter is the usual Gibbons-Hawking-York boundary term. The volume divergences of the bulk gravity action correspond to UV divergences of the dual quantum field theory; these divergences can be removed by appropriately covariant counterterms at the conformal boundary. For example, in the case of asymptotically locally anti-de Sitter solutions of Einstein gravity the action counterterms are

$$I_{\rm ct} = \frac{1}{8\pi G_{d+1}}\int_{\partial\mathcal{Y}_n} {\rm d}^{d}x\sqrt{h}\left((d-1) + \frac{\mathcal{R}}{2(d-2)} + \cdots\right) \tag{6.2.10}$$

where the ellipses denote terms of higher order in the curvature and logarithmic counterterms arise for d even.

Applying the replica formula to the bulk terms in the action, and using the analogue of (6.2.5) for the bulk curvature, namely,

$$R_n = R + 4\pi(n-1)\delta(\Sigma) \tag{6.2.11}$$

gives the Ryu-Takayanagi functional for the entanglement functional:

$$S = \frac{1}{4G_{d+1}}\int_{\Sigma}\sqrt{h}. \tag{6.2.12}$$

Applying the replica formula to the counterterms gives

$$S_{\rm ct} = -\frac{1}{4(d-2)G_{d+1}} \int_{\partial\Sigma} \sqrt{\gamma}\,(1+\cdots)\,, \tag{6.2.13}$$

with the leading counterterm being proportional to the regulated area of the entangling surface boundary. Analogous expressions for higher derivative gravity and gravity coupled to scalars can be found in Chapter 5.

Using a radial cutoff to regulate is perhaps the most geometrically natural way to renormalize the area of the minimal surface but it is not the only holographic renormalization scheme. Dimensional renormalization for holography was developed in [146] and this method could be used to renormalize the holographic entanglement entropy.

6.3 AdS entanglement entropy in general dimensions

In this section we derive the renormalized entanglement entropy for a slab domain in general dimensions. Let us parameterise AdS_{D+2} as

$$\mathrm{d}s^2 = \frac{1}{\rho^2}\left(\mathrm{d}\rho^2 - \mathrm{d}t^2 + \mathrm{d}x\cdot\mathrm{d}x_D\right). \tag{6.3.1}$$

The entangling functional is

$$S = \frac{1}{4G_{D+2}} \int_\Sigma \mathrm{d}^D x\sqrt{h} \tag{6.3.2}$$

We now consider an entangling region in the boundary of width L in the x direction, on a constant time hypersurface, longitudinal to the other $(D-1)$ coordinates y^α. The bulk entangling surface is then specified by the hypersurface $x(\rho)$ minimising

$$S = \frac{1}{4G_{D+2}} \int \mathrm{d}^{D-1}y^\alpha \int \frac{\mathrm{d}\rho}{\rho^D}\sqrt{1+(x')^2} \tag{6.3.3}$$

where $x' = \partial_\rho x$. The equation of motion admits the first integral

$$(x')^2 = \frac{\rho^{2D}}{(\rho_0^{2D}-\rho^{2D})}, \tag{6.3.4}$$

where ρ_0 is the turning point of the surface, related to L via

$$L = 2\int_0^{\rho_0} \frac{\rho^D \mathrm{d}\rho}{\sqrt{\rho_0^{2D}-\rho^{2D}}}, \tag{6.3.5}$$

or equivalently

$$L = 2\rho_0 \int_0^1 \frac{x^D \mathrm{d}x}{\sqrt{1-x^{2D}}} = \rho_0 \left(\frac{2\sqrt{\pi}\,\Gamma\left(\frac{1+D}{2D}\right)}{\Gamma\left(\frac{1}{2D}\right)}\right). \tag{6.3.6}$$

The regulated on-shell value of the entangling functional is then

$$S_{\rm reg} = \frac{V_y}{2G_{D+2}} \int_\epsilon^{\rho_0} \frac{{\rm d}\rho}{\rho^D \sqrt{1-\frac{\rho^{2D}}{\rho_0^{2D}}}} \tag{6.3.7}$$

where V_y is the regulated volume of the y^α directions. For $D > 0$ the only contributing counterterm is the regulated area of the boundary i.e.

$$S_{\rm ct} = -\frac{1}{4(D-1)G_{D+2}} \int_{\partial\Sigma} {\rm d}^{D-1}\sqrt{\tilde{h}} \tag{6.3.8}$$

(where we assume that $D \neq 1$) and therefore

$$S_{\rm ren} = \frac{V_y}{2G_{D+2}} \left[\int_\epsilon^{\rho_0} \frac{{\rm d}\rho}{\rho^D \sqrt{1-\frac{\rho^{2D}}{\rho_0^{2D}}}} - \frac{1}{(D-1)\epsilon^{D-1}} \right], \tag{6.3.9}$$

which can be rewritten in terms of dimensionless quantities as

$$S_{\rm ren} = \frac{V_y}{2G_{D+2}\rho_0^{D-1}} \left[\int_{\tilde{\epsilon}}^1 \frac{{\rm d}x}{x^D \sqrt{1-x^{2D}}} - \frac{1}{(D-1)\tilde{\epsilon}^{D-1}} \right]. \tag{6.3.10}$$

This can be evaluated to give

$$S_{\rm ren} = \frac{\sqrt{\pi} V_y}{4DG_{D+2}\rho_0^{D-1}} \frac{\Gamma\left(\frac{1}{2D} - \frac{1}{2}\right)}{\Gamma\left(\frac{1}{2D}\right)} \tag{6.3.11}$$

and hence

$$S_{\rm ren} = -\frac{V_y}{4(D-1)GL^{D-1}} \left(\frac{2\sqrt{\pi}\Gamma\left(\frac{1}{2D} + \frac{1}{2}\right)}{\Gamma\left(\frac{1}{2D}\right)} \right)^D \tag{6.3.12}$$

In the case of $D = 1$ (AdS_3) the entangling functional is logarithmically divergent, and the renormalized entanglement entropy depends explicitly on the renormalization scale: for a single interval

$$S_{\rm ren} = \frac{1}{2G_3} \log\left(\frac{2}{\mu}\right), \tag{6.3.13}$$

where μ is the (dimensionless) renormalization scale.

6.4 Non-conformal branes

In this section we will consider entangling surfaces in Dp-brane and fundamental string backgrounds. It is convenient to express these backgrounds in the so-called dual frame in ten dimensions as [147]

$$I_{10} = -\frac{N^2}{(2\pi)^7 \alpha'^4} \int {\rm d}^{10}x \sqrt{G} N^\gamma e^{\gamma\phi} \left(R(G) + \beta(\partial\phi)^2 - \frac{1}{2(8-p)!N^2} |F_{8-p}|^2 \right) \tag{6.4.1}$$

where the constants (β, γ) are given below for Dp-branes and fundamental strings respectively. (Note that it is convenient to express the field strength magnetically, so for $p < 3$ we use $F_{p+2} = *F_{8-p}$.)

The field equations admit $AdS_{p+2} \times S^{8-p}$ solutions with a linear dilaton. The field equations following from the action above can be reduced over a sphere, truncating to a $(p+2)$-dimensional metric and scalar. The resulting action is then

$$I_{d+1} = -\mathcal{N} \int \mathrm{d}^{d+1}x \sqrt{g} e^{\gamma\phi} \left(R + \beta(\partial\phi)^2 + C \right) \tag{6.4.2}$$

where $d = p + 1$ and the constants $(\mathcal{N}, \beta, \gamma, C)$ depend on the type of brane under consideration.

For Dp-branes

$$\begin{aligned} \gamma &= \frac{2(p-3)}{(7-p)} & \beta &= \frac{4(p-1)(p-4)}{(7-p)^2} \\ C &= \frac{2(9-p)(7-p)}{(5-p)^2} & \mathcal{N} &= \delta_p N^{\frac{7-p}{5-p}} g_d^{2(p-3)/(5-p)} \end{aligned} \tag{6.4.3}$$

where

$$\delta_p = \frac{2^{\frac{2(p-4)}{p-5}} (5-p)^{\frac{9-p}{p-5}} \pi^{\frac{p+1}{p-5}} \Gamma\left(\frac{7-p}{2}\right)^{\frac{p-7}{p-5}}}{\Gamma\left(\frac{9-p}{2}\right)} \tag{6.4.4}$$

and g_d^2 is the dimensionful coupling of the dual field theory, which is related to the string coupling by

$$g_d^2 = g_s (2\pi)^{p-2} (\alpha')^{\frac{p-3}{2}}. \tag{6.4.5}$$

At any length scale l there is an effective dimensionless coupling constant

$$g_{\text{eff}}^2(l) = g_d^2 N l^{3-p} \tag{6.4.6}$$

For the fundamental string

$$\gamma = \frac{2}{3}, \qquad \beta = C = 0, \qquad \mathcal{N} = \frac{g_s N^{\frac{3}{2}} (\alpha')^{1/2}}{6\sqrt{2}} \tag{6.4.7}$$

and the dimensionful coupling is

$$g_f^2 = \frac{1}{2\pi g_s^2 \alpha'}, \tag{6.4.8}$$

so

$$\mathcal{N} = \frac{N^{\frac{3}{2}}}{12\sqrt{\pi} g_f}. \tag{6.4.9}$$

In all cases, the dual frame is chosen such that the equations of motion admit an AdS_{d+1} solution:

$$\mathrm{d}s^2 = \frac{1}{\rho^2}\left(\mathrm{d}\rho^2 + \mathrm{d}x\cdot\mathrm{d}x_d\right), \qquad e^{\phi} = \rho^{2\alpha} \tag{6.4.10}$$

where the constant α again depends on the case of interest: for Dp-branes

$$\alpha = -\frac{(p-7)(p-3)}{4(p-5)} \tag{6.4.11}$$

while $\alpha = -3/4$ for fundamental strings. In general the equations admit an AdS solution with linear dilaton provided that the parameters are related as

$$\alpha = -\frac{\gamma}{2(\gamma^2-\beta)}, \qquad C = \frac{(d(\gamma^2-\beta)+\gamma^2)(d(\gamma^2-\beta)+\beta)}{(\gamma^2-\beta)^2}. \tag{6.4.12}$$

For further discussion of this point, see [142].

The non-conformal branes are formally related to AdS gravity in the following way. Let us define a parameter σ as

$$\sigma = \frac{d}{2} - \alpha\gamma. \tag{6.4.13}$$

Now we consider $(2\sigma+1)$-dimensional gravity with cosmological constant $\Lambda = -\sigma(2\sigma-1)$, so that the action is

$$I_{(2\sigma+1)} = -\mathcal{N}_{\mathrm{AdS}}\int \mathrm{d}^{2\sigma+1}x\sqrt{g_{2\sigma+1}}\left(R_{2\sigma+1} + 2\sigma(2\sigma-1)\right). \tag{6.4.14}$$

Reducing on a $(2\sigma-d)$-dimensional torus with coordinates z^a via a diagonal reduction ansatz

$$\mathrm{d}s^2 = \mathrm{d}s^2_{d+1}(x) + \exp\left(\frac{2\gamma\phi}{(2\sigma-d)}\right)\mathrm{d}z^a\mathrm{d}z_a \tag{6.4.15}$$

results in the action (6.4.2) where

$$\mathcal{N} = \mathcal{N}_{\mathrm{AdS}}V_{(2\sigma-d)}, \tag{6.4.16}$$

with $V_{(2\sigma-d)}$ the volume of the compactification torus.

6.4.1 Entanglement functional and surfaces

The entanglement functional follows from the replica trick: in the dual frame

$$S = 4\pi\mathcal{N}\int_{\Sigma}\mathrm{d}^{d-1}x\sqrt{h}e^{\gamma\phi} \tag{6.4.17}$$

The equations for the entangling surface can be expressed geometrically as

$$K_m = \gamma \left(\partial_m \phi - h^{ij} \partial_i X^p \partial_j X^n g_{mn} \partial_p \phi \right) = 0 \tag{6.4.18}$$

where g_{mn} is the background metric, h_{ij} is the induced metric on the entangling surface, $X^m(x^i)$ specifies the embedding of the entangling surface into the background and K_m are the associated traces of the extrinsic curvatures.

The dual frame entanglement functional follows directly from the reduction of the pure gravity entanglement functional

$$S = 4\pi \mathcal{N}_{\text{AdS}} \int_{\Sigma_{2\sigma-1}} \mathrm{d}^{2\sigma-1} x \sqrt{H}, \tag{6.4.19}$$

when one again uses the diagonal reduction ansatz (6.4.15), and assumes that the entangling surface wraps the torus and that the shape of the surface does not vary along the torus directions. In the upstairs picture the entangling surface satisfies

$$\mathcal{K}_M = 0, \tag{6.4.20}$$

where the background metric is now denoted $g_{(2\sigma+1)MN}$ and $\mathcal{K}_M$ denotes the traces of the extrinsic curvatures. Thus, any AdS entangling surface which factorises as $\Sigma_{2\sigma-1} = T^{(2\sigma-d)} \times \Sigma$ will give an entangling surface for non-conformal branes; moreover, the non-conformal brane surface will inherit its renormalized entanglement entropy from the upstairs entangling surface.

As an example, let us consider slab entangling regions, characterised by a width $\Delta x = L$. The bulk entangling surface is specified as $x(\rho)$ and in the background (6.4.10) the entangling functional is

$$S = 4\pi \mathcal{N} V_y \int \frac{\mathrm{d}\rho}{\rho^{2\sigma-1}} \sqrt{1 + (x')^2}, \tag{6.4.21}$$

which is indeed precisely the functional obtained in (6.3.3), identifying $D = (2\sigma - 1)$. The renormalized entanglement entropy can then be expressed as

$$S_{\text{ren}} = -\frac{2\pi \mathcal{N} V_y}{(\sigma-1) L^{2(\sigma-1)}} \left(\frac{2\sqrt{\pi}\Gamma(\frac{1}{2(2\sigma-1)} + \frac{1}{2})}{\Gamma(\frac{1}{2(2\sigma-1)})} \right)^{2\sigma-1} \tag{6.4.22}$$

The renormalized entanglement entropy for a strip in the F1 background can be expressed as

$$S_{\text{ren}} = -\frac{4\pi^{\frac{3}{2}} \left(\Gamma(\frac{3}{4})\right)^2}{3\left(\Gamma(\frac{1}{4})\right)^2} \frac{N^2}{g_{\text{eff}}(L)} \tag{6.4.23}$$

where the effective coupling is expressed as $g^2_{\text{eff}}(L) = g_f^2 N L^2$. The expression for the renormalized entanglement entropy of a strip in the D1 background is analogous:

$$S_{\text{ren}} = -\frac{4\pi^{\frac{3}{2}}(\Gamma(\frac{3}{4}))^2}{3\sqrt{2}(\Gamma(\frac{1}{4}))^2}\frac{N^2}{g_{\text{eff}}(L)} \tag{6.4.24}$$

6.4.2 Witten model

The Witten [148] model for 4-dimensional Yang-Mills can be expressed in terms of the following six-dimensional background:

$$\mathrm{d}s^2 = \frac{\mathrm{d}\rho^2}{\rho^2 f(\rho)} + \frac{1}{\rho^2}\left(-\mathrm{d}t^2 + \mathrm{d}x\cdot\mathrm{d}x_3 + f(\rho)\mathrm{d}\tau^2\right), \qquad e^{\phi} = \frac{1}{\rho^{\frac{3}{2}}}, \tag{6.4.25}$$

where

$$f(\rho) = \left(1 - \frac{\rho^6}{\rho^6_{KK}}\right). \tag{6.4.26}$$

Regularity of the geometry requires that the circle direction τ must have periodicity

$$L_\tau = \frac{2\pi}{3}\rho_{KK}. \tag{6.4.27}$$

This model originates from D4-branes wrapping the circle τ with anti-periodic boundary conditions for the fermions which breaks the supersymmetry. At low energies the model resembles a four-dimensional gauge theory, with the gauge coupling being $g^2 = g_5^2/L_\tau$. The gravity solution captures the behaviour of this theory in the limit of large 't Hooft coupling $\lambda^2 = g^2 N \gg 1$.

One of the main applications of this model is in the context of flavour physics: Sakai and Sugimoto [149, 150] introduced D8-branes wrapped around the S^4 on which the theory is reduced from ten to six dimensions. These D8-branes model chiral flavours in the dual gauge theory and the resulting Witten-Sakai-Sugimoto model has been used extensively as a simple holographic model of a non-supersymmetric gauge theory with flavours.

The operator content of the dual theory captured by the metric and scalar field is the four-dimensional stress energy tensor T_{ab}, a scalar operator $\mathcal{O}_\tau$ corresponding to the component of the five-dimensional stress energy tensor $T_{\tau\tau}$ and the gluon operator $\mathcal{O}$ corresponding to the bulk scalar field. These operators satisfy a Ward identity

$$\langle T^a_a\rangle + \langle\mathcal{O}_\tau\rangle + \frac{1}{g^2}\langle\mathcal{O}\rangle = 0 \tag{6.4.28}$$

and their expectation values can be extracted from the above geometry. For example,

the condensate of the gluon operator

$$\langle \mathcal{O} \rangle = \frac{2^5 \pi^2}{3^7} \frac{\lambda^2 N}{L_\tau^4} \tag{6.4.29}$$

and therefore L_τ controls the QCD scale of the theory.

Next we can consider a slab entangling region, wrapping the circle direction τ, characterised by a width $\Delta x = L$. Entanglement entropy in this theory was previously discussed in [119], with the confinement transition being associated with a discontinuity in the derivative of the entanglement entropy with respect to L. The bare entanglement functional is

$$S = 4\pi \mathcal{N} V_2 L_\tau \int \frac{\mathrm{d}\rho}{\rho^5} \sqrt{1 + f(\rho)(x')^2} \tag{6.4.30}$$

where V_2 is the volume of the two-dimensional cross-section of the slab. The entanglement entropy can then be written as

$$S_{\mathrm{reg}} = 8\pi \mathcal{N} V_2 L_\tau \int_\epsilon^{\rho_*} \frac{\mathrm{d}\rho}{\rho^5} \sqrt{1 + f(\rho)(x')^2} \tag{6.4.31}$$

where ρ_* is the turning point of the surface, related to the width of the entangling region as

$$L = 2\rho_{KK} \int_0^{v_*} \mathrm{d}v \sqrt{\frac{1}{f(v)\left(\frac{v_*^{10} f(v)}{v^{10} f(v_*)} - 1\right)}} \tag{6.4.32}$$

where $\rho = \rho_{KK} v$. This can be renormalized as before, with the counterterm contributions being

$$S_{\mathrm{ct}} = -2\pi \mathcal{N} V_2 \frac{L_\tau}{\epsilon^4}. \tag{6.4.33}$$

For large entangling regions, the only possible entangling surface is the disconnected configuration, for which the renormalized entanglement entropy is

$$\begin{aligned} S_{\mathrm{ren}} &= 8\pi \mathcal{N} V_2 L_\tau \left(\int_\epsilon^{\rho_{KK}} \frac{\mathrm{d}\rho}{\rho^5} - \frac{1}{4\epsilon^4} \right) \\ &= -\frac{4\pi^2 \mathcal{N}}{3} \frac{V_2}{\rho_{KK}^3} \end{aligned} \tag{6.4.34}$$

For small entangling regions the condensate is negligible and the renormalized entanglement entropy is controlled by the conformal structure

$$S_{\mathrm{ren}} \approx -\pi \mathcal{N} \left(\frac{2\sqrt{\pi}\Gamma(3/5)}{\Gamma(1/10)} \right)^5 \frac{V_2 L_\tau}{L^4} \tag{6.4.35}$$

The renormalized entaglement entropy is plotted in Figure 6.4.1. As discussed in [119] there is a discontinuity in the derivative of the entanglement entropy for slab widths

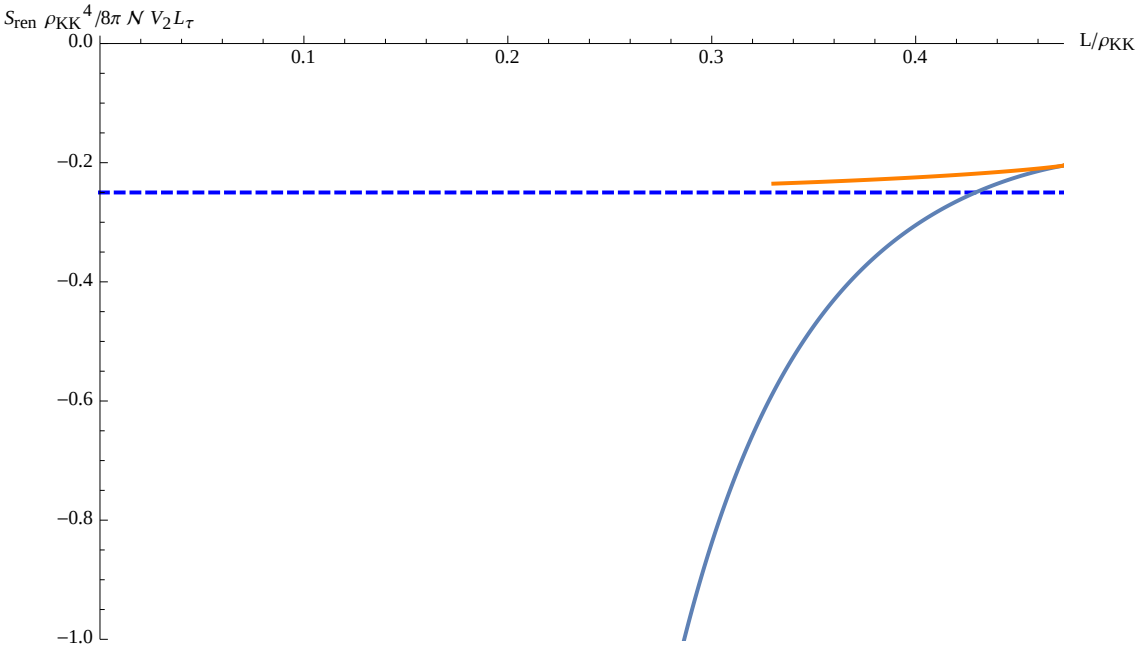

Figure 6.4.1: The renormalized entanglement entropy for the Witten model. The solid blue and orange lines indicate the renormalized entropy for the two possible connected minimal surfaces. The dotted line denotes the disconnected solution.

around $L \sim 0.4\rho_{KK}$. For larger values of L the entanglement entropy saturates at a constant value.

6.5 Renormalized entanglement entropy along RG flows

In this section we will consider holographic entanglement entropy in geometries dual to RG flows. We work in Euclidean signature with a bulk action

$$I = -\frac{1}{16\pi G}\int \mathrm{d}^{d+1}x\sqrt{g}\left(R - \frac{1}{2}(\partial\phi)^2 + V(\phi)\right). \tag{6.5.1}$$

Holographic RG flows with flat radial slices can be expressed as

$$\mathrm{d}s^2 = \mathrm{d}r^2 + \exp(2A(r))\mathrm{d}x^i\mathrm{d}x_i, \tag{6.5.2}$$

where the warp factor $A(r)$ is related to a radial scalar field profile $\phi(r)$ via the equations of motion

$$\frac{d^2\phi}{dr^2} + d\left(\frac{dA}{dr}\right)\left(\frac{d\phi}{dr}\right) = -\frac{dV}{d\phi} \qquad \frac{d^2A}{dr^2} = -\frac{1}{2(d-1)}\left(\frac{d\phi}{dr}\right)^2. \tag{6.5.3}$$

These equations can always be expressed as first order equations

$$\frac{dA}{dr} = W \qquad \frac{d\phi}{dr} = -2(d-1)\frac{dW}{d\phi} \tag{6.5.4}$$

where the superpotential $W(\phi)$ is related to the potential as

$$V = -(d-1)^2\left(2\left(\frac{dW}{d\phi}\right)^2 - \frac{d}{d-1}W^2\right). \tag{6.5.5}$$

Near the conformal boundary the potential can be expanded in powers of the scalar field as

$$V = d(d-1) - \frac{1}{2}m^2\phi^2 + \cdots \tag{6.5.6}$$

and hence the superpotential can be written as

$$W = 1 + \frac{(d-\Delta)}{4(d-1)}\phi^2 + \cdots \tag{6.5.7}$$

where $\Delta = d/2 + \sqrt{d^2+4m^2}/2$. The higher order terms in the superpotential are not unique, as different choices are associated with different RG flows.

Note that for flat domain walls, a single counterterm (in addition to the usual Gibbons-Hawking term) is sufficient

$$I_{\rm ct} = -\frac{(d-1)}{8\pi G_4}\int \mathrm{d}^d x\sqrt{\gamma}W, \tag{6.5.8}$$

although the derivation of the entanglement entropy counterterms requires knowledge of the counterterms for a curved background (since the replica space is curved).

The entanglement entropy for a slab region $\Delta x = L$ in the RG flow geometry is

$$S = \frac{V_y}{4G}\int \mathrm{d}r e^{(D-1)A(r)}\sqrt{1+e^{2A(r)}(x')^2}, \tag{6.5.9}$$

where D is the number of spatial directions in the dual theory, V_y is the regulated volume of the longitudinal directions and $x(r)$ defines the entangling surface. Then

$$L = 2\int_{r_0}^{\infty}\frac{e^{DA_0}\mathrm{d}r}{e^{A(r)}\sqrt{e^{2DA(r)}-e^{2DA_0}}}, \tag{6.5.10}$$

where at the turning point r_0 of the surface $A(r) = A_0$. The regulated on-shell action is

$$S_{\rm reg} = \frac{V_y}{2G}\int_{r_0}^{\Lambda}\mathrm{d}r\frac{e^{(2D-1)A(r)}}{\sqrt{e^{2DA(r)}-e^{2DA_0}}}, \tag{6.5.11}$$

with the cutoff being $r = \Lambda$.

The entanglement entropy counterterms for RG flows driven by relevant deformations were discussed in Chapter 5, working perturbatively in the deformation. Here we will analyse both spontaneous and explicit symmetry breaking, using exact supergravity solutions.

6.5.1 Spontaneous symmetry breaking: Coulomb branch of $\mathcal{N} = 4$ SYM

In this section we consider the case of VEV driven flow, i.e. spontaneous symmetry breaking. In such a situation, the scalar field has only normalizable modes and thus asymptotically the scalar field behaves as

$$\phi \to \phi_{(0)} e^{-\Delta r} + \cdots \tag{6.5.12}$$

where $\phi_{(0)}$ is related to the operator expectation value as

$$\langle \mathcal{O} \rangle = -(2\Delta - d)\phi_{(0)}. \tag{6.5.13}$$

From (6.5.4) and (6.5.7), one can immediately read off the asymptotic form of the warp factor:

$$A(r) = r - \frac{(d-\Delta)}{4\Delta(d-1)} \phi_{(0)}^2 e^{-2\Delta r} + \cdots \tag{6.5.14}$$

Substituting into the regulated action, we then obtain

$$S_{\rm reg} = \frac{V_y}{2G} \left(\frac{e^{(d-2)\Lambda}}{(d-2)} - \frac{(d-\Delta)}{4\Delta(d-1)(d-2-2\Delta)} e^{(d-2-2\Delta)\Lambda} + \cdots \right) \tag{6.5.15}$$

The second term vanishes as $\Lambda \to \infty$ for $\Delta > (d-2)/2$, and is logarithmically divergent for $\Delta = (d-2)/2$. (The latter case does not however arise holographically, as when the lower bound on the conformal dimension is saturated the operator automatically obeys free field equations.) Therefore, for VEV driven flows the only counterterm required is the regulated area of the boundary of the entangling surface:

$$S_{\rm ct} = -\frac{1}{4(d-2)G} \int_{\partial\Sigma} \mathrm{d}^{d-2}x \sqrt{h}. \tag{6.5.16}$$

Note that one can derive the same result from the bulk action counterterms, using the replica trick; see below for the case of the Coulomb branch of $\mathcal{N} = 4$ SYM. Thus the renormalized entanglement entropy for slabs in VEV driven flows is

$$S_{\rm ren} = \frac{V_y}{2G} \left(\int_{r_0}^{\Lambda} \mathrm{d}r \frac{e^{(2D-1)A(r)}}{\sqrt{e^{2DA(r)} - e^{2DA_0}}} - \frac{e^{(d-2)\Lambda}}{(d-2)} \right). \tag{6.5.17}$$

Now let us consider the general structure of the renormalized entropy. In the vacuum of the conformal field theory, the renormalized entropy must behave as

$$S_{\rm ren} = c_0 \frac{V_y}{GL^{D-1}} \tag{6.5.18}$$

with c_0 a dimensionless constant on dimensional grounds: the entropy scales with the longitudinal volume V_y and the width of the entangling region L is the only other dimensionful scale in the problem. The value of c_0 in holographic theories is given in (6.3.12).

Now working perturbatively in the operator expectation value $\langle \mathcal{O} \rangle$ the renormalized entropy must behave as

$$S_{\rm ren} = \frac{V_y}{GL^{D-1}} \left(c_0 + c_1 \langle \mathcal{O} \rangle^2 L^{2\Delta} + \cdots \right) \tag{6.5.19}$$

where c_1 is dimensionless and we work in a limit in which

$$\langle \mathcal{O} \rangle \ll \frac{1}{L^{\Delta}} \tag{6.5.20}$$

i.e. the width of the entangling region is much smaller than the length scale set by the condensate.

6.5.1.1 Coulomb branch disk distribution

We now analyse a specific example: the renormalized entanglement entropy of slab domains on the Coulomb branch of $\mathcal{N} = 4$ SYM. We consider the case of a disk distribution of branes preserving $SO(4) \times SO(2)$ symmetry, for which the equations of motion follow from (6.5.1), with the superpotential being [151]

$$W(\phi) = \frac{2}{3} \exp\left(\frac{2\phi}{\sqrt{6}} \right) + \frac{1}{3} \exp\left(-\frac{4\phi}{\sqrt{6}} \right) \tag{6.5.21}$$

The metric in five-dimensional gauged supergravity is then

$$\mathrm{d}s^2 = \lambda^2 w^2 \left(\frac{\mathrm{d}w^2}{\lambda^6 w^4} + \mathrm{d}x \cdot \mathrm{d}x \right) \tag{6.5.22}$$

with

$$\lambda^6 = \left(1 + \frac{\sigma^2}{w^2} \right). \tag{6.5.23}$$

Here the coordinate $w \to \infty$ at the conformal boundary and σ characterises the expectation value of the dual scalar operator. The scalar field can be expressed by the relation

$$\sigma^2 \frac{e^{\frac{2}{\sqrt{6}}\phi}}{1 - e^{\sqrt{6}\phi}} = \lambda^2 w^2. \tag{6.5.24}$$

Using the standard Fefferman-Graham coordinates near the conformal boundary:

$$\mathrm{d}s^2 = \frac{1}{\rho^2}\mathrm{d}\rho^2 + \frac{1}{\rho^2}\left(1 - \frac{1}{18}\sigma^4\rho^4 + \cdots\right)\mathrm{d}x\cdot\mathrm{d}x, \qquad \phi = \frac{1}{\sqrt{6}}\sigma^2\rho^2 + \cdots \tag{6.5.25}$$

We can then read off the expectation values of the dual stress energy tensor and scalar operator, following [152, 153]:

$$\langle T_{ij}\rangle = 0 \qquad \langle\mathcal{O}\rangle = \frac{N^2}{\sqrt{6}\pi^2}\sigma^2 \tag{6.5.26}$$

where we use the standard relation between the Newton constant and the rank of the dual gauge theory:

$$\frac{1}{16\pi G_5} = \frac{N^2}{2\pi^2}. \tag{6.5.27}$$

The vanishing of the dual stress energy tensor is required given the supersymmetry but careful holographic renormalization is required to derive this answer.

The regulated entanglement entropy of a slab domain in this geometry can be written as

$$S_{\mathrm{reg}} = \frac{V_2}{2G_5}\int_{w_0}^{\Lambda}\mathrm{d}w\lambda^3 w^3\sqrt{(x')^2 + \frac{1}{w^4\lambda^6}}. \tag{6.5.28}$$

Using the first integral of the equations of motion the width of the entangling region can be expressed in terms of the turning point of the surface w_0 as

$$L = 2\int_{w_0}^{\infty}\frac{c\,\mathrm{d}w}{w^2\lambda^3\sqrt{\lambda^6 w^6 - c^2}} \tag{6.5.29}$$

where c is an integration constant and w_0 satisfies

$$w_0^4(\sigma^2 + w_0^2) = c^2. \tag{6.5.30}$$

The regulated entanglement entropy is then

$$S_{\mathrm{reg}} = \frac{V_2}{2G_5}\int_{w_0}^{\Lambda}\mathrm{d}w\frac{w^3\sqrt{w^2+\sigma^2}}{\sqrt{w^4(w^2+\sigma^2) - c^2}} \tag{6.5.31}$$

and the required counterterm is expressed in terms of the regulated area of the boundary of the entangling surface i.e. there are counterterm contributions

$$S_{\mathrm{ct}} = -\frac{V_2}{8G_5}\Lambda^2\left(1 + \frac{\sigma^2}{\Lambda^2}\right)^{\frac{1}{3}} \tag{6.5.32}$$

at each side of the slab. (The total contribution is therefore twice this value.) Note that the counterterms in this case clearly contribute both divergent and finite parts: expanding

in powers of the cutoff Λ

$$S_{\rm ct} = -\frac{V_2}{8G_5}\Lambda^2 - \frac{V_2}{24G_5}\sigma^2 + \cdots \tag{6.5.33}$$

It is then convenient to write the entanglement entropy in terms of dimensionless quantities as

$$S_{\rm ren} = \frac{V_2\sigma^2}{4G_5}\lim_{\tilde{\Lambda}\to\infty}\left(\int_{y_0}^{\tilde{\Lambda}} {\rm d}y \frac{y\sqrt{y+1}}{\sqrt{y^2(y+1)-y_0^2(y_0+1)}} - \tilde{\Lambda} - \frac{1}{3}\right), \tag{6.5.34}$$

where $\tilde{\Lambda}$ is a rescaled dimensionless cutoff. Implicitly this expression assumes that $\sigma^2 \neq 0$ and y_0 is the turning point of the surface. Then

$$\sigma L = y_0\sqrt{y_0+1}\int_{y_0}^{\infty} \frac{{\rm d}y}{y\sqrt{(y+1)}\sqrt{y^2(y+1)-y_0^2(y_0+1)}} \tag{6.5.35}$$

These integrals can be computed numerically. There is a maximal value of L (for fixed σ) for which a connected entangling surface exists: the critical value of L is such that

$$\sigma L_{\rm crit} \approx 1.5708. \tag{6.5.36}$$

For $L > L_{\rm crit}$ there is no connected entangling surface but the disconnected entangling surface consisting of two components $x = -L/2$ and $x = L/2$ still exists. For the latter one can straightforwardly calculate the renormalized entanglement entropy as

$$S_{\rm ren} = -\frac{V_2\sigma^2}{12G_5}. \tag{6.5.37}$$

The renormalized entanglement entropy is plotted in Figure 6.5.1: it is continuous at $L = L_{\rm crit}$, and saturates for $L > L_{\rm crit}$. For small values of L, the analytic expressions (6.5.19) is valid:

$$S_{\rm ren} = \frac{V_2}{G_5}\left(-\left(\frac{2\sqrt{\pi}\Gamma(\frac{2}{3})}{\Gamma(\frac{1}{6})}\right)^2\frac{1}{8L^2} + C_1\sigma^4L^2 + \cdots\right) \tag{6.5.38}$$

and the constant C_1 can be determined as:

$$C_1 \approx -0.03137 \tag{6.5.39}$$

6.5.1.2 Coulomb branch spherical distribution

We now consider the renormalized entanglement entropy of slab domains on the Coulomb branch of $\mathcal{N} = 4$ SYM for the case of a spherical distribution of branes, preserving $SO(4) \times SO(2)$ symmetry. The equations of motion follow from (6.5.1), with the super-

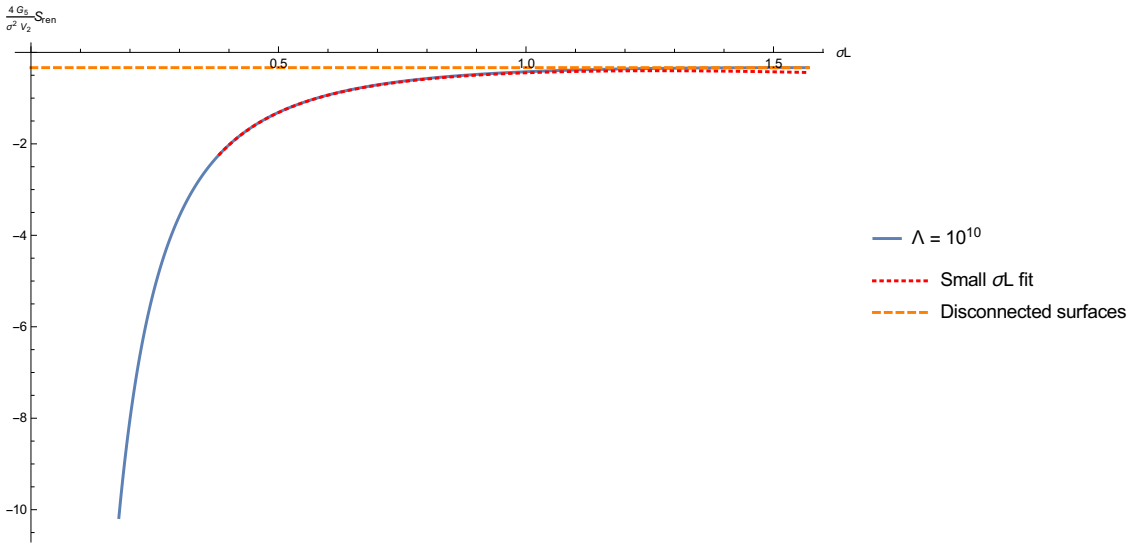

Figure 6.5.1: The renormalized entropy for Coulomb branch disk distribution. The blue line shows the numerical results for a cut-off of $\Lambda = 10^{10}$, the dotted red line shows the small σL fit of equation (6.5.38), the dashed yellow line shows the value of the renormalized entropy for disconnected surfaces.

potential being [151]

$$W(\phi) = \frac{2}{3}\exp\left(-\frac{2\phi}{\sqrt{6}}\right) + \frac{1}{3}\exp\left(\frac{4\phi}{\sqrt{6}}\right) \tag{6.5.40}$$

The metric in five-dimensional gauged supergravity is then

$$\mathrm{d}s^2 = \lambda^2 w^2\left(\frac{\mathrm{d}w^2}{\lambda^6 w^4} + \mathrm{d}x\cdot\mathrm{d}x\right) \tag{6.5.41}$$

with

$$\lambda^6 = \left(1 - \frac{\sigma^2}{w^2}\right). \tag{6.5.42}$$

Here the coordinate $w \to \infty$ at the conformal boundary and σ characterises the expectation value of the dual scalar operator. The scalar field can be expressed by the relation

$$\sigma^2\frac{e^{-\frac{2}{\sqrt{6}}\phi}}{1-e^{-\sqrt{6}\phi}} = -\lambda^2 w^2. \tag{6.5.43}$$

Using the standard Fefferman-Graham coordinates near the conformal boundary:

$$\mathrm{d}s^2 = \frac{1}{\rho^2}\mathrm{d}\rho^2 + \frac{1}{\rho^2}\left(1 - \frac{1}{18}\sigma^4\rho^4 + \cdots\right)\mathrm{d}x\cdot\mathrm{d}x, \qquad \phi = \frac{1}{\sqrt{6}}\sigma^2\rho^2 + \cdots. \tag{6.5.44}$$

We can then read off the expectation values of the dual stress energy tensor and scalar operator, following [152, 153]:

$$\langle T_{ij}\rangle = 0 \qquad \langle\mathcal{O}\rangle = \frac{N^2}{\sqrt{6}\pi^2}\sigma^2 \tag{6.5.45}$$

where we use the standard relation between the Newton constant and the rank of the dual gauge theory:

$$\frac{1}{16\pi G_5} = \frac{N^2}{2\pi^2}. \tag{6.5.46}$$

The vanishing of the dual stress energy tensor is required given the supersymmetry but again careful holographic renormalization is required to derive this answer.

The regulated entanglement entropy is then

$$S_{\rm reg} = \frac{V_2}{2G_5}\int_{w_0}^{\Lambda} {\rm d}w \frac{w^3\sqrt{w^2-\sigma^2}}{\sqrt{w^4(w^2-\sigma^2)-c^2}} \tag{6.5.47}$$

and the required counterterm is expressed in terms of the regulated area of the boundary of the entangling surface i.e. there are counterterm contributions

$$S_{\rm ct} = -\frac{V_2}{8G_5}\Lambda^2\left(1-\frac{\sigma^2}{\Lambda^2}\right)^{\frac{1}{3}} \tag{6.5.48}$$

at each side of the slab. (The total contribution is therefore twice this value.) Note that the counterterms in this case clearly contribute both divergent and finite parts: expanding in powers of the cutoff Λ

$$S_{\rm ct} = -\frac{V_2}{8G_5}\Lambda^2 + \frac{V_2}{24G_5}\sigma^2 + \cdots \tag{6.5.49}$$

It is then convenient to write the entanglement entropy in terms of dimensionless quantities as

$$S_{\rm ren} = \frac{V_2\sigma^2}{4G_5}\lim_{\tilde{\Lambda}\to\infty}\left(\int_{y_0}^{\tilde{\Lambda}} {\rm d}y \frac{y\sqrt{y^2-1}}{\sqrt{y^2(y-1)-y_0^2(y_0-1)}} - \tilde{\Lambda} + \frac{1}{3}\right), \tag{6.5.50}$$

where $\tilde{\Lambda}$ is a rescaled dimensionless cutoff. Implicitly this expression assumes that $\sigma^2 \neq 0$ and y_0 is the turning point of the surface. Then

$$\sigma L = y_0\sqrt{y_0-1}\int_{y_0}^{\infty} \frac{{\rm d}y}{y\sqrt{(y-1)}\sqrt{y^2(y-1)-y_0^2(y_0-1)}} \tag{6.5.51}$$

These integrals can again be computed numerically. As in the previous case, for fixed σ there is a maximal value of L for which a connected entangling surface exists. The critical value is

$$\sigma L_{\rm crit} \approx 0.8317 \tag{6.5.52}$$

For lengths grater than the critical length, the minimal surface is disconnected and the

renormalized entanglement entropy can be calculated analytically as

$$S_{\text{ren}} = -\frac{V_2\sigma^2}{6G_5}. \tag{6.5.53}$$

For sub-critical values, there are two possible surfaces with turning points y_0 for each width L and one must choose the surface for which the renormalized area is minimised. These two different turning points can be categorised as either $y_0 < y_{0,\text{crit}}$ or $y_0 > y_{0,\text{crit}}$ where $y_{0,\text{crit}}$ is some critical value where only one solution exists. In all cases the $y_0 > y_{0,\text{crit}}$ branch is preferred, which corresponds to entnagling surfaces that can get arbitrarily close to the conformal boundary $y \to \infty$.

The renormalized entanglement entropy is plotted in Figure 6.5.2. There is a phase transition between the connected and disconnected entangling surfaces at L_c such that

$$\sigma L_c \approx 0.75 \tag{6.5.54}$$

i.e. $L_c < L_{\text{crit}}$, and the entanglement entropy is saturated for $L \geq L_c$. In the regime of small L the analytic expressions (6.5.19) are valid:

$$S_{\text{ren}} = \frac{V_2}{G_5}\left(-\left(\frac{2\sqrt{\pi}\Gamma(\frac{2}{3})}{\Gamma(\frac{1}{6})}\right)^2\frac{1}{8L^2} + C_1\sigma^4L^2 + \cdots\right) \tag{6.5.55}$$

where the constant C_1 can be determined as:

$$C_1 \approx -0.03167 \tag{6.5.56}$$

6.5.2 Operator driven RG flow

In this section we consider the case of an operator driven RG flow, the GPPZ flow [154]. The equations of motion again follow from (6.5.1), with the superpotential being

$$W(\phi) = \frac{1}{2}\left(1 + \cosh\left(\frac{2\phi}{\sqrt{3}}\right)\right) \tag{6.5.57}$$

The metric can be expressed as

$$\mathrm{d}s^2 = \frac{\mathrm{d}\rho^2}{\rho^2} + \frac{1}{\rho^2}(1-\mu^2\rho^2)\mathrm{d}x\cdot\mathrm{d}x \tag{6.5.58}$$

while the scalar field is given by

$$\phi = \frac{\sqrt{3}}{2}\log\left(\frac{1+\mu\rho}{1-\mu\rho}\right) \tag{6.5.59}$$

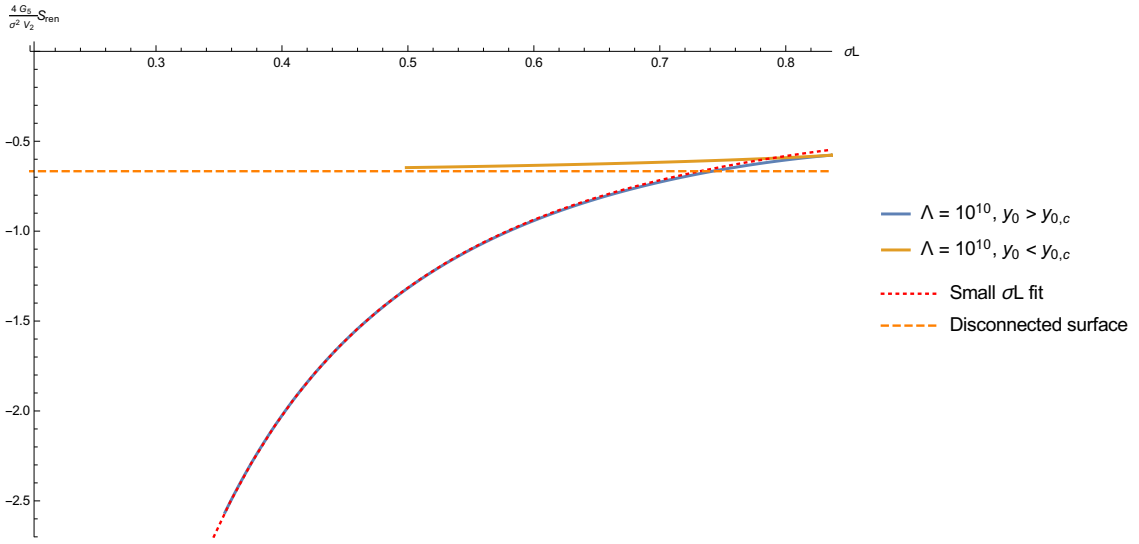

Figure 6.5.2: The renormalized entropy for Coulomb branch sphere distribution. The solid blue and solid orange lines indicate the renormalized entanglement entropy for the two possible connected minimal surfaces. The dashed orange line indicates the entanglement entropy for the disconnected surface. The dotted red line shows the small σL fit of equation (6.5.55).

The scalar ϕ is dual to a dimension three operator. By expanding near the conformal boundary and using the holographic renormalization dictionary, [152, 153] showed that the GPPZ solution is dual to a deformation (proportional to μ) of $\mathcal{N} = 4$ SYM by the dimension three scalar operator, with the expectation values of the operators being

$$\langle \mathcal{T}_{ij} \rangle = \langle \mathcal{O} \rangle = 0. \tag{6.5.60}$$

The vanishing stress energy tensor is required by supersymmetry.

Now let us consider the renormalized entanglement entropy of a strip region in this geometry. The entanglement entropy can be expressed as

$$S = \frac{V_2}{2G_5} \int \mathrm{d}\rho \frac{(1-\mu^2\rho^2)}{\rho^3} \sqrt{1 + (1-\mu^2\rho^2)(x')^2} \tag{6.5.61}$$

The overall dependence on the deformation μ can be scaled out to give

$$S = \frac{V_2\mu^2}{2G_5} \int \mathrm{d}v \frac{(1-v^2)}{v^3} \sqrt{1 + (1-v^2)(\partial_v X)^2} \tag{6.5.62}$$

where $v = \mu\rho$ and $X = \mu x$. Then the entangling surface of width L satisfies

$$\mu L = 2\lambda \int_0^{v_0} \mathrm{d}v \frac{v^3}{\sqrt{(1-v^2)^4 - v^6\lambda^2(1-v^2)}} \tag{6.5.63}$$

where the integration constant λ is related to the turning point of the surface v_0 by

$$\lambda = \frac{(1-v_0^2)^{3/2}}{v_0^3}. \tag{6.5.64}$$

As in the previous cases there is a phase transition between a connected solution for $\mu L < \mu L_{\text{crit}}$ and a disconnected solution for $\mu L > \mu L_{\text{crit}}$ where

$$\mu L_{\text{crit}} \approx 0.3008. \tag{6.5.65}$$

For $\mu L > \mu L_{\text{crit}}$ the renormalized entanglement entropy can be calculated analytically:

$$S_{ren} = \lim_{\epsilon\to 0} \frac{V_2\mu^2}{G_5}\left(\int_\epsilon^1 \mathrm{d}v \frac{1-v^2}{v^3} - \frac{1}{\epsilon^2} + 1 - 2\log\epsilon\right) = 0. \tag{6.5.66}$$

The regulated entanglement entropy is then

$$S_{\text{reg}} = \frac{V_2\mu^2}{2G_5}\int_\epsilon^{v_0} \mathrm{d}v \frac{(1-v^2)^{5/2}}{v^3\sqrt{(1-v^2)^3 - v^6\lambda^2}}. \tag{6.5.67}$$

The counterterms for the entanglement entropy can be derived from the bulk action counterterms using the replica trick:

$$S_{\text{ct}} = -\frac{1}{8G_5}\int_{\partial\Sigma_{\tilde\epsilon}} \mathrm{d}^2x\sqrt{\tilde h}\left(1 + \frac{2}{3}\phi^2\log(\epsilon)\right) \tag{6.5.68}$$

where the cutoff in the ρ coordinates is $\tilde\epsilon = \epsilon/\mu$. Evaluating this counterterm gives a contribution from each endpoint of the strip:

$$S_{\text{ct}} = -\frac{V_2}{8G_5}\left(\frac{1}{\epsilon^2} - 1 + 2\log\epsilon\right), \tag{6.5.69}$$

which indeed matches the regulated divergences of (6.5.67). Thus the total renormalized entropy is

$$S_{\text{ren}} = \frac{V_2\mu^2}{4G_5}\lim_{\epsilon\to 0}\left(2\int_\epsilon^{v_0} \mathrm{d}v \frac{(1-v^2)^{5/2}}{v^3\sqrt{(1-v^2)^3 - v^6\lambda^2}} - \frac{1}{2\epsilon^2} + \frac{1}{2} - \log\epsilon\right). \tag{6.5.70}$$

These integrals can once again be evaluated numerically, the results of which are plotted in Figure 6.5.3. As in the case of the spherical brane distribution there are two possible turning points for a given length $L < L_{\text{crit}}$ and the branch with $v_0 < v_{0,\text{crit}}$ is preferred. The entropy is strictly positive for $\mu L \lesssim \mu L_{\text{crit}}$ and so, like in the previous case, there is

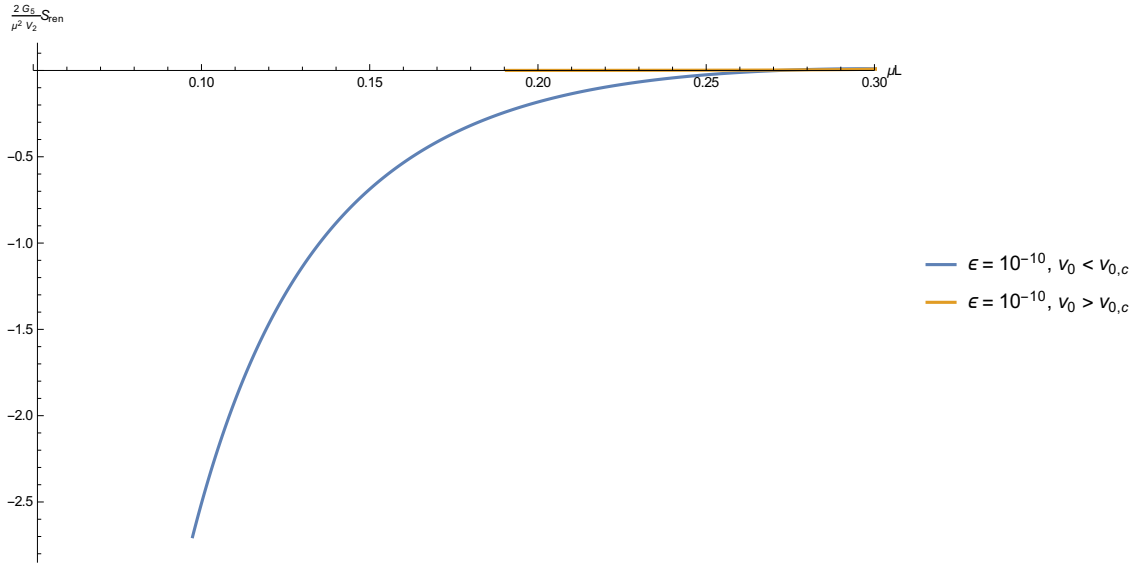

Figure 6.5.3: The renormalized entropy for the GPPZ flow. The solid blue line and solid orange lines indicate the renormalized entropy for the two possible connected minimal surfaces.

a phase transition between the connected and disconnected surface at around

$$\mu L \approx 0.275 < \mu L_{\text{crit}}. \tag{6.5.71}$$

6.6 Conclusions and outlook

In this chapter we have ivestigated a number of examples of the holographic renormalization scheme for the entanglement entropy introduced in Chapter 5. We have demonstrated that this method allows one to extract the scheme independent contributions to the entanglement entropy both analytically and numerically in a range of holographic models.

In the three RG flow models we investigated we discovered that the covariant counterterm action contained finite contributions. These contributions indicate that the renormalization is non-trivial and that naïve subtraction is not an appropriate scheme for the entanglement entropy. These finite contributions to the renormalized entanglement entropy appeared regardless of the existence of wholly finite counterterms which capture the scheme dependence, which we did not investigate in this work.

We confirmed the ability of the renormalized entanglement entropy to probe both the UV and IR of the dual theory by choosing an appropriate entangling surface. The investigation above focussed solely on infinite strip entangling regions where only one length scale is being probed. It would be interesting to understand how different entangling

regions can be used to probe different aspects of the RG flow, and what this can tell us about the dual theory.

In all of the examples considered in this chapter the renormalized entanglement entropy was found to be non-positive, a continuation of the trend that was seen in the analytic examples studied in Chapter 5. It is important to understand the significance of this and whether it is a robust feature of the renormalized entanglement entropy or if it is just an artefact of the entangling surfaces and models we have chosen to investigate.

Bibliography

[1] M. Taylor and W. Woodhead, *Inhomogeneity simplified*, *The European Physical Journal C* **C74** (June, 2014) 3176, [1406.4870].

[2] M. Taylor and W. Woodhead, *Renormalized entanglement entropy*, *Journal of High Energy Physics* **2016** (Aug., 2016) , [1604.06808].

[3] M. Taylor and W. Woodhead, *The holographic F theorem*, 1604.06809.

[4] J. D. Bekenstein, *Black holes and the second law*, *Lett. Nuovo Cim.* **4** (Aug., 1972) 737–740.

[5] S. W. Hawking, *Particle Creation by Black Holes*, *Communications In Mathematical Physics* **43** (Aug., 1975) 199–220.

[6] G. t. Hooft, *Dimensional Reduction in Quantum Gravity*, Oct., 1993.

[7] L. Susskind, *The world as a hologram*, *Journal of Mathematical Physics* **36** (Sept., 1995) 6377, [hep-th/9409089].

[8] J. M. Maldacena, *The Large N Limit of Superconformal Field Theories and Supergravity*, *International Journal of Theoretical Physics* **2:231-252,1998** (Nov., 1997) 20, [hep-th/9711200].

[9] J. McGreevy, *TASI lectures on quantum matter (with a view toward holographic duality)*, in *New Frontiers in Fields and Strings*, World Scientific Pub Co Pte Lt,

June, 2016. 1606.08953. DOI.

[10] N. Iqbal, H. Liu and M. Mezei, *Lectures on holographic non-Fermi liquids and quantum phase transitions*, in *Proceedings, Theoretical Advanced Study Institute in Elementary Particle Physics (TASI 2010). String Theory and Its Applications: From meV to the Planck Scale*, pp. 707–816, World Scientific Pub Co Pte Lt, Oct., 2011. 1110.3814. DOI.

[11] G. W. Gibbons and S. W. Hawking, *Action integrals and partition functions in quantum gravity*, *Physical Review D* **15** (May, 1977) 2752–2756.

[12] J. W. York, *Role of Conformal Three-Geometry in the Dynamics of Gravitation*, *Phys. Rev. Lett.* **28** (Apr, 1972) 1082–1085.

[13] E. Witten, *Anti-de Sitter space and holography*, *Advances in Theoretical and Mathematical Physics* **2** (1998) 253–291, [hep-th/9802150].

[14] C. Fefferman and C. R. Graham, *Conformal invariants*, *asterisque* **95** (1985) .

[15] M. Henningson and K. Skenderis, *The Holographic Weyl anomaly*, hep-th/9806087.

[16] I. R. Klebanov and E. Witten, *AdS / CFT correspondence and symmetry breaking*, hep-th/9905104.

[17] E. Witten, "Multitrace operators, boundary conditions, and AdS / CFT correspondence."

[18] I. Papadimitriou, *Non-Supersymmetric Membrane Flows from Fake Supergravity and Multi-Trace Deformations*, *Journal of High Energy Physics* **02** (Feb., 2007) 008, [hep-th/0606038].

[19] S. S. Gubser, I. R. Klebanov and A. M. Polyakov, *Gauge theory correlators from noncritical string theory*, *Physics Letters B* **B428** (May, 1998) 105–114, [hep-th/9802109].

[20] K. Skenderis and B. C. van Rees, *Real-Time Gauge/Gravity Duality*, *Physical Review Letters* **101** (Aug., 2008) 081601, [arXiv:0805.0150v2].

[21] K. Skenderis and B. C. van Rees, *Real-time gauge/gravity duality: Prescription, Renormalization and Examples*, *Journal of High Energy Physics* **05** (May, 2009) 085, [0812.2909].

[22] B. C. van Rees, *Real-time gauge/gravity duality and ingoing boundary conditions*, *Nuclear Physics B - Proceedings Supplements* **192-193** (July, 2009) 193–196, [arXiv:0902.4010v1].

[23] V. Balasubramanian and P. Kraus, *A Stress tensor for Anti-de Sitter gravity*, hep-th/9902121.

[24] S. de Haro, K. Skenderis and S. N. Solodukhin, *Holographic Reconstruction of Spacetime and Renormalization in the AdS/CFT Correspondence*, *Communications in Mathematical Physics* **217** (Mar., 2001) 595–622, [hep-th/0002230v3].

[25] K. Skenderis, *Lecture notes on holographic renormalization*, *Classical and Quantum Gravity* **19** (Nov., 2002) 5849–5876, [hep-th/0209067].

[26] P. Kovtun, D. T. Son and A. O. Starinets, *Viscosity in Strongly Interacting Quantum Field Theories from Black Hole Physics*, hep-th/0405231v2.

[27] N. Iqbal and H. Liu, *Universality of the hydrodynamic limit in AdS/CFT and the membrane paradigm*, 0809.3808v2.

[28] H. Song, *QGP viscosity at RHIC and the LHC - a 2012 status report*, 1210.5778v2.

[29] B. Batlogg and C. Varma, *The underdoped phase of cuprate superconductors*, *Physics World* **13** (Feb., 2000) 33–37.

[30] S. A. Hartnoll, C. P. Herzog and G. T. Horowitz, *Holographic Superconductors*, *Journal of High Energy Physics* **2008** (Dec., 2008) 015–015, [0810.1563v1].

[31] S. S. Gubser, C. P. Herzog, S. S. Pufu and T. Tesileanu, *Superconductors from Superstrings*, *Physical Review Letters* **103** (Sept., 2009) , [0907.3510v2].

[32] G. T. Horowitz, *Introduction to Holographic Superconductors*, vol. 828 of *Lecture Notes in Physics*. Springer Berlin Heidelberg, Berlin, Heidelberg, 2011, 10.1007/978-3-642-04864-7.

[33] M. Ammon, J. Erdmenger, M. Kaminski and P. Kerner, *Superconductivity from gauge/gravity duality with flavor*, 0810.2316v2.

[34] M. Ammon, J. Erdmenger, M. Kaminski and P. Kerner, *Flavor Superconductivity from Gauge/Gravity Duality*, 0903.1864v2.

[35] K. Peeters, J. Powell and M. Zamaklar, *Exploring colourful holographic superconductors*, 0907.1508v1.

[36] K.-Y. Kim and M. Taylor, *Holographic d-wave superconductors*, *Journal of High Energy Physics* **2013** (Aug., 2013) 112, [1304.6729].

[37] M. Taylor, *Lifshitz holography*, *Classical and Quantum Gravity* **33** (Jan., 2016) 033001, [1512.03554].

[38] W. Chemissany and I. Papadimitriou, *Lifshitz holography: The whole shebang*, *Journal of High Energy Physics* **2015** (Aug., 2014) 83, [1408.0795].

[39] T. Nishioka, S. Ryu and T. Takayanagi, *Holographic entanglement entropy: an overview*, *Journal of Physics A: Mathematical and Theoretical* **42** (Dec., 2009) 504008, [0905.0932].

[40] M. Srednicki, *Entropy and Area*, hep-th/9303048v2.

[41] S. Ryu and T. Takayanagi, *Holographic Derivation of Entanglement Entropy from AdS/CFT*, *Physical Review Letters* **96** (May, 2006) , [hep-th/0603001].

[42] S. Ryu and T. Takayanagi, *Aspects of Holographic Entanglement Entropy*, hep-th/0605073v3.

[43] M. Headrick and T. Takayanagi, *A holographic proof of the strong subadditivity of entanglement entropy*, *Physical Review D* **76** (Nov., 2007) , [0704.3719v1].

[44] A. Lewkowycz and J. Maldacena, *Generalized gravitational entropy*, *Journal of High Energy Physics* **08** (Aug., 2013) 090, [1304.4926].

[45] H. Casini and M. Huerta, *On the RG running of the entanglement entropy of a circle*, 1202.5650.

[46] S. A. Hartnoll, *Horizons, holography and condensed matter*, in *Black Holes in Higher Dimensions* (G. T. Horowitz, ed.), p. 34. Cambridge University Press (CUP), June, 2011. 1106.4324. DOI.

[47] G. T. Horowitz, J. E. Santos and D. Tong, *Optical Conductivity with Holographic Lattices*, 1204.0519.

[48] G. T. Horowitz, J. E. Santos and D. Tong, *Further Evidence for Lattice-Induced Scaling*, 1209.1098.

[49] Y. Ling, C. Niu, J.-P. Wu and Z.-Y. Xian, *Holographic Lattice in Einstein-Maxwell-Dilaton Gravity*, 1309.4580.

[50] Y. Ling, C. Niu, J. Wu, Z. Xian and H. Zhang, *Holographic Fermionic Liquid with Lattices*, *Journal of High Energy Physics* **07(2013)045** (July, 2013) 07045, [1304.2128].

[51] A. Donos and J. P. Gauntlett, *The thermoelectric properties of inhomogeneous holographic lattices*, 1409.6875v3.

[52] B. Goutéraux, *Universal scaling properties of extremal cohesive holographic phases*, 1308.2084.

[53] N. Iizuka, S. Kachru, N. Kundu, P. Narayan, N. Sircar, S. P. Trivedi et al., *Extremal Horizons with Reduced Symmetry: Hyperscaling Violation, Stripes, and a Classification for the Homogeneous Case*, 1212.1948.

[54] A. Donos and J. P. Gauntlett, *Novel metals and insulators from holography*, *Journal of High Energy Physics* **06** (June, 2014) 007, [1401.5077].

[55] A. Donos and J. P. Gauntlett, *Holographic Q-lattices*, *Journal of High Energy Physics* **04** (Apr., 2014) 040, [1311.3292].

[56] A. Donos and S. A. Hartnoll, *Interaction-driven localization in holography*, *Nature Physics* **9** (Aug., 2013) 649–655, [1212.2998].

[57] B. Goutéraux, *Charge transport in holography with momentum dissipation*, *Journal of High Energy Physics* **04** (Apr., 2014) 181, [1401.5436].

[58] E. Mefford and G. T. Horowitz, *Simple holographic insulator*, *Physical Review D* **D90** (June, 2014) 084042, [1406.4188].

[59] D. Vegh, "Holography without translational symmetry."

[60] R. A. Davison, *Momentum relaxation in holographic massive gravity*, 1306.5792.

[61] M. Blake, D. Tong and D. Vegh, *Holographic Lattices Give the Graviton an Effective Mass*, 1310.3832.

[62] A. Amoretti, A. Braggio, N. Maggiore, N. Magnoli and D. Musso, *Thermo-electric transport in gauge/gravity models with momentum dissipation*, 1406.4134.

[63] T. Andrade and B. Withers, *A simple holographic model of momentum relaxation*, *Journal of High Energy Physics* **05** (May, 2014) 101, [1311.5157].

[64] Y. Bardoux, M. M. Caldarelli and C. Charmousis, *Shaping black holes with free fields*, 1202.4458.

[65] N. Afshordi, D. J. H. Chung and G. Geshnizjani, *Cuscuton: A Causal Field Theory with an Infinite Speed of Sound*, hep-th/0609150.

[66] N. Afshordi, D. J. H. Chung, M. Doran and G. Geshnizjani, *Cuscuton Cosmology: Dark Energy meets Modified Gravity*, astro-ph/0702002.

[67] G. Compère, P. McFadden, K. Skenderis and M. Taylor, *The holographic fluid dual to vacuum Einstein gravity*, 1103.3022.

[68] G. Compère, P. McFadden, K. Skenderis and M. Taylor, *The relativistic fluid dual to vacuum Einstein gravity*, *Journal of High Energy Physics* **03** (Mar., 2012) 076, [1201.2678].

[69] D. G. Boulware and S. Deser, *Can gravitation have a finite range?*, *Physical Review D* **D6** (Dec., 1972) 3368–3382.

[70] S. Deser and A. Waldron, *Stability of massive cosmological gravitons*, hep-th/0103255.

[71] N. Arkani-Hamed, H. Georgi and M. D. Schwartz, *Effective field theory for massive gravitons and gravity in theory space*, hep-th/0210184.

[72] C. de Rham and G. Gabadadze, *Generalization of the Fierz-Pauli Action*, *Physical Review D* **D82** (Aug., 2010) 044020, [1007.0443].

[73] C. de Rham, G. Gabadadze and A. J. Tolley, *Resummation of Massive Gravity*, *Physical Review Letters* **106** (June, 2011) 231101, [1011.1232].

[74] S. F. Hassan and R. A. Rosen, *On Non-Linear Actions for Massive Gravity*, 1103.6055.

[75] S. F. Hassan, R. A. Rosen and A. Schmidt-May, *Ghost-free Massive Gravity with a General Reference Metric*, 1109.3230.

[76] S. F. Hassan and R. A. Rosen, *Resolving the Ghost Problem in non-Linear Massive Gravity*, 1106.3344.

[77] S. S. Gubser, *Curvature singularities: The Good, the bad, and the naked*, *Advances in Theoretical and Mathematical Physics* **4** (2000) 679–745, [hep-th/0002160].

[78] S. de Haro, S. N. Solodukhin and K. Skenderis, *Holographic reconstruction of space-time and renormalization in the AdS / CFT correspondence*, hep-th/0002230.

[79] M. Henningson and K. Skenderis, *Holography and the Weyl anomaly*, hep-th/9812032.

[80] G. T. Horowitz and M. M. Roberts, *Zero Temperature Limit of Holographic Superconductors*, 0908.3677.

[81] K. Goldstein, S. Kachru, S. Prakash and S. P. Trivedi, *Holography of Charged Dilaton Black Holes*, 0911.3586.

[82] C. Charmousis, B. Gouteraux, B. S. Kim, E. Kiritsis and R. Meyer, *Effective Holographic Theories for low-temperature condensed matter systems*, 1005.4690.

[83] A. Donos and S. A. Hartnoll, *Universal linear in temperature resistivity from black hole superradiance*, *Physical Review D* **D86** (Dec., 2012) 124046, [1208.4102].

[84] S. Kachru, X. Liu and M. Mulligan, *Gravity duals of Lifshitz-like fixed points*, *Physical Review D* **D78** (Nov., 2008) 106005, [0808.1725].

[85] M. Taylor, "Non-relativistic holography."

[86] L. Huijse, S. Sachdev and B. Swingle, *Hidden Fermi surfaces in compressible states of gauge-gravity duality*, 1112.0573.

[87] X. Dong, S. Harrison, S. Kachru, G. Torroba and H. Wang, *Aspects of holography for theories with hyperscaling violation*, 1201.1905.

[88] S. Harrison, S. Kachru and H. Wang, *Resolving Lifshitz Horizons*, 1202.6635.

[89] J. Bhattacharya, S. Cremonini and A. Sinkovics, *On the IR completion of geometries with hyperscaling violation*, 1208.1752.

[90] N. Kundu, P. Narayan, N. Sircar and S. P. Trivedi, *Entangled Dilaton Dyons*, 1208.2008.

[91] J. Gath, J. Hartong, R. Monteiro and N. A. Obers, *Holographic Models for Theories with Hyperscaling Violation*, 1212.3263.

[92] A. Lucas, S. Sachdev and K. Schalm, *Scale-invariant hyperscaling-violating holographic theories and the resistivity of strange metals with random-field disorder*, 1401.7993.

[93] W. Chemissany and I. Papadimitriou, *Generalized dilatation operator method for non-relativistic holography, Phys. Lett. B* **737** (May, 2014) 6, [1405.3965].

[94] D. T. Son, *Toward an AdS/cold atoms correspondence: a geometric realization of the Schroedinger symmetry*, *Physical Review D* **78:046003,2008** (Aug., 2008) , [0804.3972].

[95] E. Ardonne, P. Fendley and E. Fradkin, *Topological Order and Conformal Quantum Critical Points*, *Annals of Physics* **310** (Apr., 2004) 493–551, [cond-mat/0311466].

[96] M. Blau, J. Hartong and B. Rollier, *Geometry of Schroedinger Space-Times, Global Coordinates, and Harmonic Trapping*, 0904.3304.

[97] Y. Lei and S. F. Ross, *Extending the nonsingular hyperscaling violating spacetimes*, *Classical and Quantum Gravity* **31** (Dec., 2013) 035007, [1310.5878].

[98] M. Abramowitz and I. Stegun, *Handbook of Mathematical Functions*. Dover Publications Inc., 1965.

[99] D. L. Jafferis, I. R. Klebanov, S. S. Pufu and B. R. Safdi, *Towards the F-Theorem: N=2 Field Theories on the Three-Sphere*, 1103.1181.

[100] I. R. Klebanov, S. S. Pufu and B. R. Safdi, *F-Theorem without Supersymmetry*, 1105.4598.

[101] C. P. Herzog, I. R. Klebanov, S. S. Pufu and T. Tesileanu, *Multi-Matrix Models and Tri-Sasaki Einstein Spaces*, 1011.5487.

[102] D. L. Jafferis, *The Exact Superconformal R-Symmetry Extremizes Z*, 1012.3210.

[103] D. Martelli and J. Sparks, *The large N limit of quiver matrix models and Sasaki-Einstein manifolds*, 1102.5289.

[104] D. R. Gulotta, C. P. Herzog and S. S. Pufu, *From Necklace Quivers to the*

F-theorem, Operator Counting, and T(U(N)), 1105.2817.

[105] D. Z. Freedman and S. S. Pufu, *The holography of F-maximization*, 1302.7310.

[106] H. Casini, M. Huerta and R. C. Myers, *Towards a derivation of holographic entanglement entropy*, 1102.0440.

[107] I. R. Klebanov, S. S. Pufu, S. Sachdev and B. R. Safdi, *Entanglement Entropy of 3-d Conformal Gauge Theories with Many Flavors*, 1112.5342.

[108] I. R. Klebanov, T. Nishioka, S. S. Pufu and B. R. Safdi, *On Shape Dependence and RG Flow of Entanglement Entropy*, 1204.4160.

[109] H. Casini, M. Huerta, R. C. Myers and A. Yale, *Mutual information and the F-theorem*, 1506.06195.

[110] H. Liu and M. Mezei, *A Refinement of entanglement entropy and the number of degrees of freedom*, 1202.2070.

[111] H. Liu and M. Mezei, *Probing renormalization group flows using entanglement entropy*, 1309.6935.

[112] I. R. Klebanov, T. Nishioka, S. S. Pufu and B. R. Safdi, *Is Renormalized Entanglement Entropy Stationary at RG Fixed Points?*, *Journal of High Energy Physics* **2012** (Oct., 2012) , [1207.3360].

[113] D. Berenstein and A. Miller, *Conformal perturbation theory, dimensional regularization, and AdS/CFT correspondence*, 1406.4142.

[114] S. W. Hawking, *The Boundary Conditions for Gauged Supergravity*, *Physics Letters B* **B126** (June, 1983) 175–177.

[115] T. Nishioka, *Relevant Perturbation of Entanglement Entropy and Stationarity*, *Physical Review D* **D90** (Aug., 2014) 045006, [1405.3650].

[116] J. Gomis, P.-S. Hsin, Z. Komargodski, A. Schwimmer, N. Seiberg and S. Theisen, *Anomalies, Conformal Manifolds, and Spheres*, 1509.08511.

[117] T. Takayanagi, *Entanglement Entropy from a Holographic Viewpoint*, *Classical and Quantum Gravity* **29** (June, 2012) 153001, [1204.2450].

[118] M. Headrick, *General properties of holographic entanglement entropy*,

1312.6717.

[119] I. R. Klebanov, D. Kutasov and A. Murugan, *Entanglement as a probe of confinement*, 0709.2140.

[120] M. Henningson and K. Skenderis, *Weyl anomaly for Wilson surfaces*, hep-th/9905163.

[121] S. N. Solodukhin, *Entanglement entropy, conformal invariance and extrinsic geometry*, *Physics Letters B* **B665** (July, 2008) 305–309, [0802.3117].

[122] D. V. Fursaev, A. Patrushev and S. N. Solodukhin, *Distributional Geometry of Squashed Cones*, 1306.4000.

[123] H. Casini and M. Huerta, *Entanglement and alpha entropies for a massive scalar field in two dimensions*, cond-mat/0511014.

[124] H. Casini and M. Huerta, *Universal terms for the entanglement entropy in 2+1 dimensions*, hep-th/0606256.

[125] P. Calabrese and J. Cardy, *Entanglement entropy and conformal field theory*, 0905.4013.

[126] N. Drukker, D. J. Gross and H. Ooguri, *Wilson loops and minimal surfaces*, hep-th/9904191.

[127] T. Hirata and T. Takayanagi, *AdS/CFT and Strong Subadditivity of Entanglement Entropy*, hep-th/0608213v2.

[128] I. Papadimitriou, *Holographic renormalization as a canonical transformation*, *Journal of High Energy Physics* **11** (Nov., 2010) 014, [1007.4592].

[129] C. R. Graham and E. Witten, *Conformal anomaly of submanifold observables in AdS / CFT correspondence*, hep-th/9901021.

[130] R. C. Myers and A. Sinha, *Seeing a c-theorem with holography*, *Physical Review D* **D82** (Aug., 2010) 046006, [1006.1263].

[131] D. Z. Freedman, C. Nunez, M. Schnabl and K. Skenderis, *Fake supergravity and domain wall stability*, hep-th/0312055.

[132] P. A. R. Jones and M. Taylor, *Entanglement entropy and differential entropy for*

massive flavors, *Journal of High Energy Physics* **08** (Aug., 2015) 014, [1505.07697].

[133] H.-C. Chang and A. Karch, *Entanglement Entropy for Probe Branes*, 1307.5325.

[134] A. Karch and C. F. Uhlemann, *Generalized gravitational entropy of probe branes: flavor entanglement holographically*, 1402.4497.

[135] P. A. R. Jones and M. Taylor, *Entanglement entropy in top-down models*, *Journal of High Energy Physics* **2016** (Aug., 2016) , [1602.04825].

[136] A. Bhattacharyya, A. Kaviraj and A. Sinha, *Entanglement entropy in higher derivative holography*, 1305.6694.

[137] J. T. Liu and W. A. Sabra, *Hamilton-Jacobi Counterterms for Einstein-Gauss-Bonnet Gravity*, 0807.1256.

[138] S. Cremonini, J. T. Liu and P. Szepietowski, *Higher Derivative Corrections to R-charged Black Holes: Boundary Counterterms and the Mass-Charge Relation*, 0910.5159.

[139] V. Jahnke, A. S. Misobuchi and D. Trancanelli, *Holographic renormalization and anisotropic black branes in higher curvature gravity*, 1411.5964.

[140] K. Skenderis and P. K. Townsend, *Hidden supersymmetry of domain walls and cosmologies*, *Physical Review Letters* **96** (May, 2006) 191301, [hep-th/0602260].

[141] I. Papadimitriou, *Holographic Renormalization of general dilaton-axion gravity*, *Journal of High Energy Physics* **08** (Aug., 2011) 119, [1106.4826].

[142] I. Kanitscheider, K. Skenderis and M. Taylor, *Precision holography for non-conformal branes*, 0807.3324.

[143] V. E. Hubeny, M. Rangamani and T. Takayanagi, *A Covariant holographic entanglement entropy proposal*, 0705.0016.

[144] I. Bah, A. Faraggi, L. A. P. Zayas and C. A. Terrero-Escalante, *Holographic Entanglement Entropy at Finite Temperature*, *International Journal of Modern Physics A* **24** (jun, 2009) 2703–2728, [0710.5483v3].

[145] M. Fujita, T. Nishioka and T. Takayanagi, *Geometric Entropy and Hagedorn/Deconfinement Transition*, *Journal of High Energy Physics* **2008** (sep, 2008) 016–016, [0806.3118v2].

[146] A. Bzowski, *Dimensional renormalization in AdS/CFT*, 1612.03915v1.

[147] H. J. Boonstra, K. Skenderis and P. K. Townsend, *The domain-wall/QFT correspondence*, *Journal of High Energy Physics* **1999** (jan, 1999) 003–003, [hep-th/9807137v2].

[148] E. Witten, *Anti-de Sitter Space, Thermal Phase Transition, And Confinement In Gauge Theories*, *Advances in Theoretical and Mathematical Physics* **2** (1998) 505–532, [hep-th/9803131v2].

[149] T. Sakai and S. Sugimoto, *Low energy hadron physics in holographic QCD*, *Progress of Theoretical Physics* **113** (apr, 2005) 843–882, [hep-th/0412141v5].

[150] T. Sakai and S. Sugimoto, *More on a holographic dual of QCD*, *Progress of Theoretical Physics* **114** (nov, 2005) 1083–1118, [hep-th/0507073v4].

[151] D. Z. Freedman, S. S. Gubser, K. Pilch and N. P. Warner, *Continuous distributions of D3-branes and gauged supergravity*, *Journal of High Energy Physics* **2000** (jul, 2000) 038–038, [hep-th/9906194v3].

[152] M. Bianchi, D. Z. Freedman and K. Skenderis, *Holographic Renormalization*, *Nuclear Physics B* **631** (jun, 2002) 159–194, [hep-th/0112119v2].

[153] M. Bianchi, D. Z. Freedman and K. Skenderis, *How to go with an RG Flow*, *Journal of High Energy Physics* **2001** (aug, 2001) 041–041, [hep-th/0105276v2].

[154] L. Girardello, M. Petrini, M. Porrati and A. Zaffaroni, *The Supergravity Dual of N=1 Super Yang-Mills Theory*, *Nuclear Physics B* **569** (mar, 2000) 451–469, [hep-th/9909047v2].